Primary productivity in Arctic sea ice and ocean

Dissertation zur Erlangung des Doktorgrades der Naturwissenschaften

- Dr. rer. nat. -

dem Fachbereich 2 Biologie/Chemie der Universität Bremen

vorgelegt von

Mar Fernández-Méndez

Bremen, August 2014

Die vorliegende Arbeit wurde in der Zeit von Juni 2011 bis August 2014 am Alfred-Wegener-Institut Helmholtz-Zentrum für Polar- und Meeresforschung und dem Max Planck Institut für Marine Mikrobiologie angefertigt.

1. Gutachterin: Prof. Dr. Antje Boetius
2. Gutachterin: Prof. Dr. Anya Waite

1. Prüfer: Prof. Dr. Kai Bischof
2. Prüfer: PD Dr. Bernhard Fuchs

Tag des Promotionskolloqiums: 16. Oktober 2014

„Nature improvises as she goes along. When we marine ecologists train ourselves to read numbers as musicians read notes, we might learn to appreciate music where we have previously only sensed cacophony.“

Victor Smetacek, 1986

Summary

Primary productivity in the Arctic Ocean is heavily influenced by sea ice dynamics, which governs light and nutrient availability. Until the last decade, the permanently ice-covered Central Arctic north of 78 ºN, was considered to have very low productivity and was often neglected in estimates of primary production in the Arctic. Due to global warming, the Central Arctic is shifting from a perennial to a seasonal ice zone. The reduction in ice cover and thickness leads to an increase in the amount of light that penetrates the ice. In addition, ice melt strengthens stratification that hinders nutrient upwelling, increasing nitrate limitation.

Our knowledge about how changes in light and nutrients affect carbon and nutrient budgets in sea-ice algae and phytoplankton is limited, especially in the ice-covered oligotrophic Central Arctic. Understanding the processes that control primary productivity is crucial to predict how the Arctic ecosystem will react to further sea-ice decline.

The overall **objective** of this thesis is to better understand the physical and biological processes that affect primary productivity in the Central Arctic. Specific goals are to investigate i) the role of microbial algal aggregations in carbon and nutrient cycling, ii) the contribution of sea ice to total primary productivity and the impact of sea-ice retreat on annual productivity, and iii) the diversity of nitrogen-fixing bacteria in the Central Arctic. The methods used in this thesis included net primary productivity (NPP) measurements by radioactive carbon (^{14}C) uptake at different irradiances, an irradiance-based model to upscale measured NPP and annual production estimates from the seasonal nutrient drawdown in the mixed layer since last winter.

In **Chapters I-IV** the first specific goal was addressed. Our results showed that sub-ice algal aggregates, such as *Melosira arctica* filaments, can sink rapidly to the seafloor in early summer when the ice melts contributing to carbon export to the benthos (**Chapter I**). The aggregates that remain floating below the ice can serve as a food source for ice-associated fauna in late summer (**Chapter II**). A potential factor controlling the buoyancy of the aggregates was photosynthetic oxygen production (**Chapter III**). The distribution of aggregates was very patchy and seemed to be governed by ice topography (**Chapter IV**).

In **Chapter V** the second specific goal was examined. The NPP measurements showed that the relative contribution of sea-ice algae to total NPP was as high as 60% in late summer, when

phytoplankton below the ice was light limited. According to the nutrient ratios in the water column, nitrate and silicate were the main limiting nutrients in the Eurasian Basin. Although sea-ice cover was substantially reduced in 2012, total annual new production was similar to estimates of previous years. However, when including the contribution by algal aggregates, the estimated annual production increased. This indicates that sub-ice algae are an important component of the ice-covered Arctic.

Nitrogen fixation could increase the amount of nitrate available for new production. Corresponding to the third specific goal, in **Chapter VI** the nitrogenase coding gene, *nifH*, was amplified to examine the diversity of nitrogen fixing organisms. A wide diversity of potential nitrogen fixing bacteria was discovered, especially in sea-ice, seawater and algal aggregates. If the observed diversity corresponds to an active community, then Arctic nitrogen fixing bacteria might contribute to alleviate nitrate limitation.

In **conclusion**, the Central Arctic Ocean hosts low but significant productivity in and below the ice and should be included in primary productivity models. As sea-ice retreats further, primary productivity might increase locally due to higher light availability. However, the total amount of carbon fixed will still be constrained by the nutrients available in the surface waters during the productive season. Therefore, understanding the impacts of sea-ice retreat on nutrient replenishment mechanisms is essential to predicting Arctic primary productivity.

Zusammenfassung

Primärproduktion im Arktischen Ozean wird stark durch die Dynamik des Meereises beeinflusst, welche die Verfügbarkeit von Licht und Nährstoffen bestimmt. Bis zum letzten Jahrzehnt wurde der permanent eisbedeckte zentrale Arktische Ozean nördlich von 78 °N als Gegend mit niedriger Produktivität angesehen und wurde oft in Abschätzungen der arktischen Primärproduktion vernachlässigt. Aufgrund der weltweiten Klimaerwärmung verändert sich die zentrale Arktis von einem ganzjährig eisbedeckten Gebiet in ein Gebiet, das nur Teile des Jahres eisbedeckt ist. Der Rückgang von Meereisbedeckung und –dicke führt zu einem Anstieg der Lichtmenge, die in das Eis eindringt. Zusätzlich verstärkt die Eisschmelze die Stratifizierung der Wassersäule, was den Nährstoffaustausch mit tieferen Wasserschichten behindert und die Nitratlimitierung verstärkt.

Unser Wissen darüber, wie die Veränderungen von Licht und Nährstoffen sich auf Kohlenstoff- und Nährstoffhaushalte von Meereisalgen und Phytoplankton auswirken ist besonders in der eisbedeckten oligotrophischen Zentralen Arktis begrenzt. Um Vorhersagen treffen zu können, wie das Arktische Ökosystem auf weiteren Meereisrückgang reagieren wird, ist es notwendig die Prozesse zu verstehen, welche die Primärproduktion kontrollieren.

Das Ziel dieser Arbeit ist es daher, die physikalischen und biologischen Prozesse, welche die Primärproduktion in der Zentralen Arktis beeinflussen besser zu verstehen. Konkrete Ziele waren hierbei die Untersuchung i) der Rolle mikrobieller Algenaggregate im Kohlenstoff- und Nährstoffkreislauf, ii) des Beitrags von Meereis zur gesamten Primärproduktion und der Einfluss des Meereisrückgangs auf die jährliche Produktivität, sowie iii) der Diversität von Stickstoff fixierenden Bakterien in der Zentralen Arktis. Die in dieser Arbeit verwendeten Methoden sind die Messung der Netto-Primärproduktion (NPP) durch Aufnahme von radioaktivem Kohlenstoff (^{14}C) bei verschiedenen Lichtintensitäten, ein auf Irradianz basierendes Model zur hoch Skalierung der NPP Messungen, sowie Abschätzungen der jährlichen Produktion auf Basis des Nährstoffverbrauchs in der durchmischten Wasserschicht seit dem letzten Winter.

In den **Kapiteln I-IV** wird das erste der konkreten Ziele bearbeitet. Unsere Ergebnisse zeigen, dass Algenaggregate unter dem Eis, wie beispielsweise die Filamente von *Melosira arctica,* im Sommer wenn das Eis schmilzt schnell auf den Meeresboden absinken können, was zum Kohlenstoff-Export in das Benthos beiträgt (**Kapitel I**). Die Aggregate, die weiter unter dem Eis

treiben, können im späten Sommer als Nahrungsquelle für eis-assoziierte Fauna dienen. (**Kapitel II**). Ein möglicher Faktor, der den Auftrieb der Aggregate regelt ist Sauerstoffproduktion durch Photosynthese (**Kapitel III**). Die räumliche Verteilung der Aggregate ist sehr ungleichmäßig und wird durch die Eistopographie bestimmt (**Kapitel IV**).

In **Kapitel 5** wird das zweite konkrete Ziel untersucht. Die NPP Messungen zeigen, dass der relative Beitrag von Meereisalgen an der gesamten NPP bis zu 60% beträgt, wenn im späten Sommer das Phytoplankton unter dem Eis lichtlimitiert ist. Die Nährstoffverhältnisse in der Wassersäule zeigen, dass Nitrat und Silikat die hauptsächlichen limitierenden Nährstoffe im eurasischen Becken sind. Obwohl die Meereisbedeckung im Jahr 2012 bedeutend reduziert war, war die totale jährliche neue Produktion ähnlich zu Abschätzungen aus den Jahren zuvor. Wenn man jedoch den Beitrag von Algenaggregaten berücksichtigt ist die jährliche Produktion angestiegen. Dies weist darauf hin, dass Untereisalgen ein wichtiger Bestandteil der eisbedeckten Arktis sind.

Stickstofffixierung könnte die Menge des für neue Produktion verfügbaren Stickstoffs erhöhen. Entsprechend des dritten Arbeitsschwerpunktes, wurde in **Kapitel VI** das Nitrogenase Kodierungs-Gen, *nifH*, verstärkt um die Diversität von Stickstoff fixierenden Organismen zu untersuchen. Eine große Diversität von potentiell Stickstoff-fixierenden Bakterien wurde insbesondere in Meereis, Meerwasser und Algen-Aggregaten entdeckt. Wenn die beobachtete Diversität einer aktiven Gemeinschaft entspricht, dann könnten arktische Stickstoff-fixierende Bakterien dazu beitragen, die Nitrat-Limitierung abzuschwächen.

Im zentralen Arktischen Ozean gibt es geringe aber signifikante Produktivität in und unter dem Eis, die in Modellen der Primärproduktion berücksichtigt werden sollte. Mit einem weiteren Rückgang des Meereises könnte die Primärproduktion lokal aufgrund der höheren Verfügbarkeit von Licht ansteigen. Die gesamte Menge fixierten Kohlenstoffs wird jedoch weiterhin durch die während der produktiven Jahreszeit in den oberflächennahen Wasserschichten verfügbaren Nährstoffe begrenzt. Um arktische Primärproduktion vorhersagen zu können ist es daher unverzichtbar den Einfluss des Meereisrückgangs auf die Mechanismen des Nährstoffkreislaufs zu verstehen.

Abbreviations

ANOSIM	Analysis of similarity
ARISA	Automated Ribosomal Intergenic Spacer Analysis
CAOPP	Central Arctic Ocean Primary Productivity model
Chl *a*	Chlorophyll *a*
CO_2	Carbon dioxide
CTD	Conductivity temperature depth
DIC	Dissolved inorganic carbon
DOC	Dissolved organic carbon
FYI	First-year ice
IB	Ice bottom
INPP	Integrated net primary productivity
IT	Ice top
ITP	Ice tethered profiler
MP	Melt pond
MYI	Multi-year ice
NMDS	Non-metric multidimensional scaling
NPP	Net primary productivity
PAR	Photosynthetically active radiation
PI	Photosynthesis versus Irradiance curve
POC	Particulate organic carbon
PON	Particulate organic nitrogen
ROV	Remotely operated vehicle
rRNA	Ribosomal ribonucleic acid
SW	Surface waters
TEP	Transparent exopolymers
WUI	Water under the ice

Table of contents

1. Introduction

1.1. The Arctic Ocean in a changing world

1.1.1. The Arctic Ocean

The Arctic Ocean and its marginal seas are located in the Northern Hemisphere inside the Arctic Circle (north of 66º 34´N). The Arctic Circle is defined as the region where the sun can remain below or above the horizon for 24 hours consecutively. This means that this region experiences 24 hours of sunlight during the three summer months (June-July-August) and 24 hours of darkness during the polar winter (November-December-January). The Arctic is the smallest and shallowest of the world´s oceans, is surrounded by land and has limited exchange with the Atlantic and Pacific oceans. It is formed by a deep central basin surrounded by shallow shelves. The continental shelves cover 50% of the Arctic Oceans total extent (~14 Mio. km^2). They have an average depth of 100 m and are relevant for sea-ice formation (Michel et al., 2006). These broad coastal areas are seasonal ice zones that receive 10% of the global river runoff and can sustain high productivity (Carmack and Wassmann, 2006; Tremblay and Gagnon, 2009). In contrast, the offshore deep central basins (>4000 m depth) are perennially ice-covered and are thought to be less productive (Sakshaug et al., 2004).

The Central Arctic Ocean is divided into two deep basins, the Amerasian and the Eurasian Basins, separated by the Lomonosov Ridge (Figure 1) (Jakobsson et al., 2004). These two basins differ in the inflow of subsurface waters (Jones et al., 1998; Rudels, 1995). Low salinity, phosphate rich and nitrate depleted Pacific waters enter the Amerasian Basin through the Bering Strait. Warm, high salinity Atlantic waters with a higher nitrate to phosphate ratio enter the Eurasian Basin through the Barents Sea and the Fram Strait. The Eurasian Basin is divided by the Gakkel Ridge into the Amundsen and the Nansen Basin. Both branches of Atlantic waters enter the Nansen Basin and flow eastward along the Siberian continental slope (Rudels et al., 2004). These waters together with the river runoff that they absorb at the shelves continue until the Laptev Sea before flowing into the deeper and more central Amundsen Basin following the transpolar drift (Figure 1). Sea ice formation at the surface ejects salt concentrated water, called brine, which causes the now denser water to sink. These waters exit the Arctic through the Greenland Sea, driving the global thermohaline circulation (Aagaard et al., 1985; Rudels, 1995).

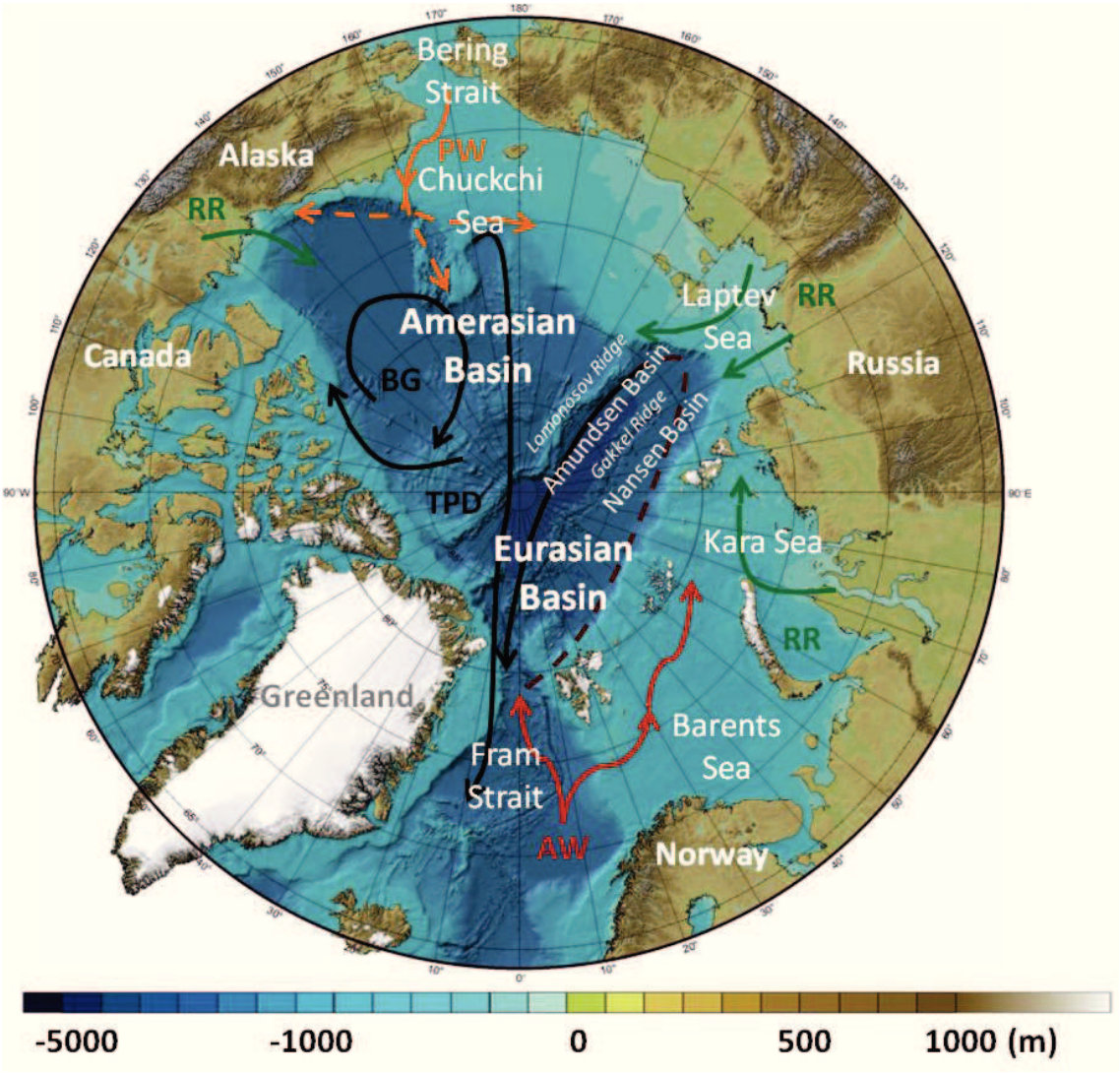

Figure 1. Bathymetry of the Arctic Ocean and its adjacent seas with superimposed surface waters circulation. Orange lines indicate waters from Pacific origin (PW), red lines indicate warm waters from Atlantic origin (AW), black lines indicate cold less saline polar water currents such as the Beaufort Gyre (BG) and the Transpolar Drift (TPD), green lines indicate river runoff inflow (RR) and the dark red dashed line indicates the formation of the polar water area. (Modified from Jakobsson et al., 2004; Rudels, 2012).

The main characteristic of the Central Arctic, north of 78 ºN, is the almost permanent ice cover. In autumn, when temperatures drop below the freezing point of seawater, sea ice starts forming at the surface. In the Eurasian Basin, pack ice forms offshore but close to the Siberian shelf, and drifts with the wind and the water currents eastward and across the Central Arctic with the transpolar drift (Pfirman et al., 1997). The sea ice that forms freshly in

winter is referred to as first-year ice (FYI) and the sea ice that remains more than one year in the Arctic is referred to as multi-year ice (MYI).

In summer, sea ice melts from below due to warmer incoming waters, forming a low salinity, less dense upper water layer that leads to strong stratification (Korhonen et al., 2013). At the same time, sea ice and its snow cover melt from above, forming freshwater ponds of diverse shapes that can eventually melt through the ice allowing saline water to enter the pond (Fetterer and Untersteiner, 1998; Lee et al., 2011; Polashenski et al., 2012). These melt ponds are common features of Arctic sea ice and cover 40-60% of the pack ice in summer (Rösel et al., 2011).

The dynamic sea-ice cover has a profound effect in shaping the life conditions of Arctic organisms because it strongly influences light and nutrient availability (Arrigo, 2014). Indeed, the Arctic Ocean is unique due to the strong seasonal forcing that makes the water column seasonally or permanently ice-covered depending on the latitude. Freezing and melting of sea ice causes changes in the surface albedo (proportion of incident light reflected) and in the temperature and salinity profiles of the upper water masses (Aagaard et al., 1981; Perovich, 1996). Therefore, sea ice regulates how much light reaches surface waters and defines the vertical transport processes that replenish surface waters with nutrients.

1.1.2. Relevance of the Arctic Ocean

Despite being the smallest of the five world´s oceans, the Arctic Ocean is of great economic and environmental importance. Arctic ecosystem services include climate regulation, carbon sequestration, biodiversity maintenance, fuel source and food production (Chapin et al., 2005). Changes in Arctic water circulation or sea ice dynamics due to recent warming can cause major perturbations in the Earth´s climate (Coumou et al., 2014; McGuire et al., 2006). Regarding the global carbon cycle, the Arctic Ocean takes up 14% of the global carbon dioxide (CO_2) from the atmosphere (Bates and Mathis, 2009). This carbon uptake partially contributes to equilibrate anthropogenic CO_2 emissions. However, the land and shallow sediments around the Arctic Ocean contain vast amounts of frozen methane (CH_4), a four times more potent greenhouse gas than carbon dioxide, which could be released upon warming (Shakhova et al., 2010). Therefore, changes in the Arctic marine and terrestrial

environment due to global warming might have consequences for the global carbon cycle (McGuire et al., 2009).

Biogenic carbon flows through the unique food web of the Arctic Ocean (Forest et al., 2011). The marine Arctic ecosystem has a complex food web formed by a great diversity of organisms. At the center of this food web are phytoplankton and ice algae, which produce organic carbon with energy from the sun. They sustain higher trophic levels such as zooplankton, benthic organisms, fish, birds, and marine mammals like polar bears, walruses, seals and whales (Bluhm and Gradinger, 2008; Michel et al., 2012). Microorganisms such as bacteria recycle nutrients making them available again for the ecosystem (Bowman, 2013). All these organisms are highly adapted to the extreme conditions of the Arctic Ocean and are responsible for the proper functioning of the ecosystem (Thomas and Dieckmann, 2010). Therefore, conserving the Arctic biodiversity is essential in order to maintain the ecosystem services that the Arctic provides.

Some of these ecosystem services are highly relevant for human activities such as fishing, transportation and mining. The extensive shelves host high productivity and are therefore important for global fisheries (Carmack et al., 2006). Changes in primary production and in the temperature and salinity of Arctic waters could influence fish populations with both local and global impacts for fisheries (Reist et al., 2006). Shipping companies have always targeted the North-West passage to reduce the transportation costs from Europe to Asia (Lasserre and Pelletier, 2011). With diminished sea-ice conditions in summer, more maritime traffic is expected to cross the Arctic Ocean increasing the risk of spills and ballast water contamination (Ho, 2010). In addition, the Arctic region is also one of the last un-exploited fossil fuels reservoirs (Gautier et al., 2009). The risks associated with drilling in the Arctic Ocean shelves are huge due to the unpredictability of sea-ice behavior. Thus oil spills might occur in the Arctic Ocean with large negative impacts on the entire ecosystem (Burek et al., 2008; Gerdes et al., 2005). Due to the relevance of the ecosystem services that the Arctic provides, both at a local and global scale, it is important to monitor how environmental changes affect the functioning of the Arctic ecosystem.

1.1.3. Impacts of climate change in the Arctic Ocean

Global mean surface temperature on land and ocean has increased by 0.89 ºC since the beginning of the 20th century due to anthropogenic release of CO_2 to the atmosphere (IPCC, 2013). The Arctic region is warming at two to three times the global average rate. This process is known as "Arctic amplification" (MacDonald, 2010). The increase in Arctic air temperatures and the observed enhanced heat transfer to the Arctic Ocean by advection of warm Atlantic waters can induce ice melt (Polyakov et al., 2010; Stroeve et al., 2012). Indeed, the summer minimum ice extent has decreased by 45% in the last 30 years (Arrigo, 2014) reaching a minimum record of 3.5 million km^2 in September 2012 (Parkinson and Comiso, 2013) (Figure 2).

This loss of ice cover is unprecedented in the past 1.5 millennia and has diverse consequences on the Arctic ecosystem (Kinnard et al., 2011). If CO_2 emissions continue increasing, a summer ice-free Arctic Ocean is predicted to occur in the next 30 years (Wang and Overland, 2012). Besides the reduction in ice extent, the proportion of thick MYI covering the Central Basins is decreasing as well (Maslanik et al., 2007). Thus, the pack ice in the Central Arctic has become thinner, less ridged, with less snow cover (Webster et al., 2014) and a higher melt pond coverage (Rösel and Kaleschke, 2012; Rothrock et al., 1999). This implies that more light is transmitted through sea-ice into the water column (Bélanger et al., 2013; Nicolaus et al., 2012). In addition, the length of the productive season might be extended due to an earlier melt onset and a later freeze up (Markus et al., 2009). This shift in the under-ice light availability could favor the productivity of photosynthetic microorganisms living in and below the ice (Arrigo et al., 2008; Tedesco et al., 2012). However, the lack of snow cover at the beginning of the growth season and the increased cloudiness due to open water evaporation, might hinder the increase in productivity (Bélanger et al., 2012; Bintanja and Selten, 2014; Juhl and Krembs, 2010). Since photosynthetic organisms are the base of the food web, cascading effects through the entire Arctic ecosystem are to be expected.

Another important factor for primary producers is nutrient availability. The way sea ice retreat will affect nutrient supply is one of the key discrepancies between general circulation models that try to predict trends in primary production (Popova et al., 2012; Vancoppenolle et al., 2013). Further consequences of ice melt are surface water freshening and increased stratification (Rabe et al., 2011). The increase in Arctic precipitations is likely to increase river discharge and therefore the amount of freshwater that will additionally strengthen

stratification (Peterson et al., 2002; Yamamoto-Kawai et al., 2009). These changes in the freshwater surface layer might prevent mixing of nutrients from deeper waters (Arrigo, 2005; Sarmiento et al., 1998). A possible increase in riverine nutrient input was hypothesized but a recent study by Le Fouest and colleagues (2012) concluded that this slight increase in nutrient input will not reach the Central Arctic Basins and will only have local influence on the shelves. An increase in wind-driven mixing in newly open waters could partially counteract the strong stratification (Mathis et al., 2012). However, in the deep Central Basins the mixing will probably not reach the nutrient-rich deep waters (Stein and Macdonald, 2004). In summary, several processes, which take place at different time and spatial scales, need to be considered to assess the impact of sea ice retreat on nutrient dynamics.

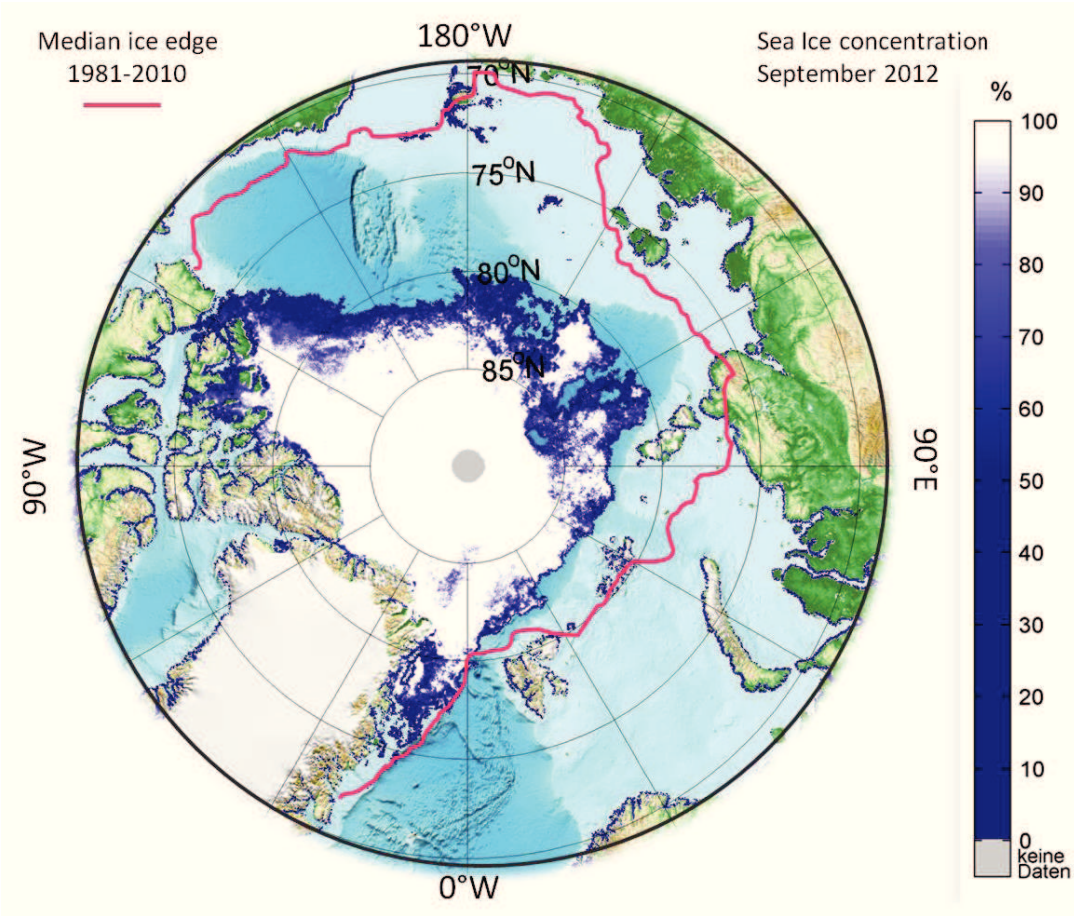

Figure 2. Sea ice concentration in September 2012 (Data source: www.meereisportal.de University of Bremen and Alfred Wegener Institute). The magenta line depicts the median sea ice edge in September from 1981-2010 (Data source: http://nsidc.org National Snow and Ice Data Center).

Finally, rising atmospheric CO_2 concentrations can also increase the pCO_2 absorbed by seawater causing ocean acidification. The fast retreat of sea ice exposes cold, fresh, pCO_2 under-saturated waters due to ice melt to the atmosphere, accelerating CO_2 absorption and consequently leading to acidification of Arctic waters (Bates et al., 2014). In the Arctic, acidification is more pronounced than in any other ocean (Steinacher et al., 2009). The effects of ocean acidification will be regionally variable and the Central Arctic will be one of the most affected regions (Popova et al., 2014). Elevated CO_2 can stimulate carbon fixation by phytoplankton and can also cause shifts in phytoplankton communities with the corresponding implications for primary production (Riebesell and Tortell, 2011). Currently, the Arctic Ocean accounts for 5-14% of total ocean carbon uptake (Anderson et al., 1998; Bates and Mathis, 2009), and it is still heavily debated if sea-ice retreat will lead to a decrease or an increase in the CO_2 uptake capacity of the Arctic Ocean (Cai et al., 2010b; Nishino et al., 2011).

1.1.4. Observed ecological changes of the Arctic marine ecosystem

The effects of climate change are already visible in the Arctic marine ecosystem. However, identifying ecological impacts and attributing them to Arctic climate change is very challenging due to the lack of reliable baseline information. Therefore, well-documented changes in the Arctic marine ecosystem are surprisingly rare (Wassmann et al., 2011).

Observed responses include a northward shift in various phytoplankton species ranges, such as the coccolithophore *Emiliania huxley* (Lalande et al., 2014; Smyth, 2004) and the Pacific diatom *Neodenticula seminae* (Reid et al., 2007). In addition, a general shift towards small picoplankton has also been observed in the Arctic Ocean due to the nutrient impoverishment of surface waters as a result of increased freshening and stratification (Ardyna et al., 2011; Li et al., 2009; Seuthe et al., 2010). These shifts in plankton composition led to rearrangements of food webs and communities. In higher trophic levels, the Atlantic amphipod *Themisto compressa* (Kraft et al., 2013) and the fish *Boreogadus saida*, commonly known as Arctic cod (Drinkwater, 2009), have also moved northward. The shift in prey will in turn also affect Arctic marine mammals, such as walruses, seals, beluga whales and polar bears, that might find new feeding grounds in the high Arctic if they are able to adapt (Bluhm and Gradinger, 2008; Moore and Huntington, 2008).

Besides the impacts on Arctic biodiversity, global warming affects the metabolism of Arctic organisms as well. Community respiration rates of Arctic planktonic communities increases steeply with warming (Holding et al., 2013; Vaquer-Sunyer et al., 2010). Furthermore, studies derived from remote sensing, report increased phytoplankton biomass and productivity due to sea-ice retreat (Arrigo et al., 2008; Brown and Arrigo, 2012). This has been confirmed by modeling simulations that indicate that total primary production in the Arctic Ocean will increase in the future (Palmer et al., 2014; Slagstad et al., 2011). However, the role of sea-ice algae in this predicted increase is unknown. There is no data including the sea-ice production from formerly ice-covered parts of the Central Arctic Basins because of the difficult access and the inability of satellites to monitor ocean color in ice-covered waters. Model results indicate that ice algal production might increase, while phytoplankton productivity would be reduced due to stratification (Tedesco et al., 2012). However, as the sea-ice habitat continues to decrease, the relative proportion of annual production contributed by ice algae will probably decrease (Johannessen and Miles, 2011). Ground truth data (information collected on location) especially from the Central Arctic is needed, to calibrate remote sensing data and to confirm model results to improve Arctic primary production predictions.

Changes in timing and quality of sea-ice production affect the pelagic food web and therefore the transfer of energy and matter to higher trophic levels (Ji et al., 2013; Leu et al., 2011), extending to the benthos (Tamelander et al., 2009). The reproductive cycle of Arctic grazers might be negatively impacted by sea-ice retreat, since the key herbivorous copepod, *Calanus glacialis,* utilizes the high-quality sea-ice algae to fuel early maturation and reproduction (Soreide et al., 2010). A mismatch between primary and seconday producers leads to an increase in the amount of algae that sink through the water column to the seafloor (Wassmann, 1998). For example, during the first sea-ice minimum record in 2007, the organic carbon flux to the seafloor increased, probably due to an increase in primary production (Lalande et al., 2009). In addition, sea-ice melt can release terrigenous particles trapped in it, increasing the carbon flux to the seafloor (Wassmann et al. 2004).

To understand how global change affects the Arctic ecosystem, the concept of tipping points needs to be clarified. Ecosystems have multiple stable states and can undergo sudden and often irreversible change in response to smaller alterations of external factors. These thresholds of environmental forcing beyond which ecosystems change abruptly are referred to as tipping points (Duarte and Wassmann, 2011). In the Arctic Ocean, the main tipping element is sea ice that responds quickly to changes in temperature. Therefore, the Central

Arctic Ocean, where the perennial sea-ice zone will be substituted by a seasonal ice zone, will most likely trespass its tipping point within the next 50 years (Wassmann and Reigstad, 2011). Furthermore, the increase in sunlight reaching the Arctic Ocean as sea-ice retreats is likely to drive another tipping point that will affect primary producers (Clark et al., 2013). This thesis focuses on Arctic primary producers at the basis of the tightly coupled marine food web, since their activity determines the amount of fixed carbon made available for the rest of the ecosystem.

1.2. Primary Production in the Central Arctic Ocean

1.2.1. Photosynthetic carbon uptake, microalgae and seasonality.

Photosynthesis is the production of organic compounds from carbon dioxide using sunlight as energy source and producing oxygen as a byproduct. The organisms responsible for this process are known as phototrophs or primary producers because they constitute the basis of the food web. There are various terms that define different aspects of primary production. Net primary production is the gross carbon uptake minus losses by respiration (Falkowski and Raven, 2007). Total primary production is comprised of new production and regenerated production, with the former being based on the availability of the limiting nutrient (usually nitrate) and the latter being based on remineralized nutrients (such as ammonium) (Dugdale and Goering, 1967). New production represents the maximum biomass that can be transferred to higher trophic levels. The amount of new production that escapes grazing and reaches the seafloor, thereby feeding the benthic community, is the vertical export carbon flux (Wassmann and Reigstad, 2011). In general, nutrient uptake for new production follows the Redfield C:N:P ratio of 106:16:1. However, in the Arctic, and especially in the Central Basins, ratios higher than Redfield have been measured in the phototrophic biomass (Frigstad et al., 2013).

In the Central Arctic Ocean, primary producers are microscopic unicellular algae, mainly diatoms, phototrophic dinoflagellates, chlorophytes and haptophytes, and other small eukaryotic protists (Kilias et al., 2014). The autotrophic community living in the sea ice is referred to as sea-ice algae, and the autotrophs living in the water column are called phytoplankton. According to their size, phytoplankton can be divided into three categories:

picoplankton (0.2-2 μm), nanoplankton (2-20 μm) and microplankton (20-200 μm). While picoplankton is often the most abundant group (Booth and Horner, 1997), it is the diatoms, included in the nano- and microplankton, that contribute the most to primary production (Gosselin et al., 1997).

The most common phytoplankton diatom species in the Arctic Ocean belong to the genera *Chaetoceros*, *Thalassiosira* and *Coscinodiscus* (Fig. 3A, B, and C). The most common sea-ice algae are pennate diatoms from the genera *Nitzschia*, *Navicula*, *Fragilariopsis* and *Entomoneis*, and the centric diatom *Melosira arctica* (Quillfeldt et al., 2009) (Fig.3 E, F and G). The latter species is known to form meter long filaments attached to the underside of the ice (Melnikov and Bondarchuk, 1987). Sea-ice algal mats, formed by *Melosira arctica* or by other species, are referred to as sub-ice algal assemblages (Horner et al., 1988). Other unicellular microorganisms found in sea ice are dinoflagellates, silicoflagellates and flagellates that can be autotroph, heterotroph or mixotroph (Fig. 3D). In addition, sympagic meiofauna such as ciliates, tintinnids, nematodes and foraminifera can be found in sea ice feeding on small unicellular protists (Fig. 3H). Furthermore, during the Arctic summer, microalgae, picoplankton and their grazers can also thrive in melt ponds (Carstens, 2002).

The Arctic receives as much daylight over a whole year as any other part in the planet, but it receives less solar radiation due to the low angle of the sun. In the Central Arctic, north of 78 ºN, the productive season, which is constrained by light availability, starts in May, almost one month later than in southern Arctic regions (Leu et al., 2011). Sea-ice algae start growing in and below the ice from May to June and reach their peak in productivity around July (Fig.4). The Central Arctic is characterized by a high percentage of MYI and complete sea-ice melt only occurs in some parts. As the ice starts to melt some sea-ice algae are released to the water column and sink to the deep sea where they provide an important food source for opportunistic benthic organisms. In July, the stronger surface layer stratification of the water column, caused by ice melt, and the increased light penetration through the thinner and ponded sea ice both create favorable conditions for phytoplankton growth (Nicolaus et al., 2012; Sakshaug et al., 2004).

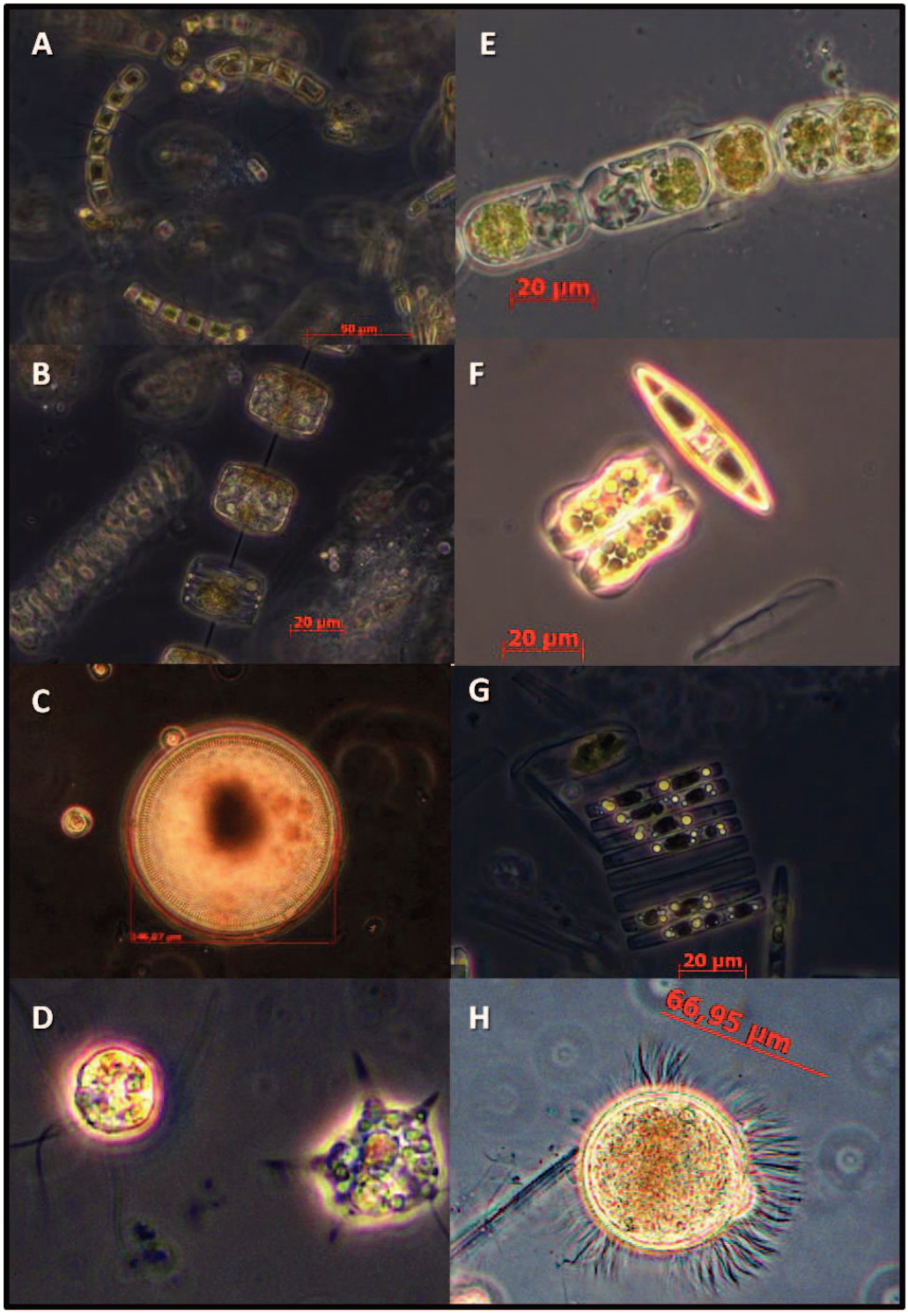

Figure 3. Light microscopy images of typical pelagic and sympagic microorganisms. Panels A, B and C correspond to phytoplankton diatom species, and panels E, F and G correspond to typical sea-ice diatoms. Panels D and H correspond to Arctic microorganisms from other groups. (A) *Chaetoceros socialis*, (B) *Thalassiosira sp.*, (C) *Coscinodiscus sp.*, (D) dinoflagellate and silicoflagellate, (E) *Melosira arctica*, (F) *Navicula sp.* and *Entomoneis sp.*, (G) *Fragilariopsis sp.* chain and, (H) ciliate.

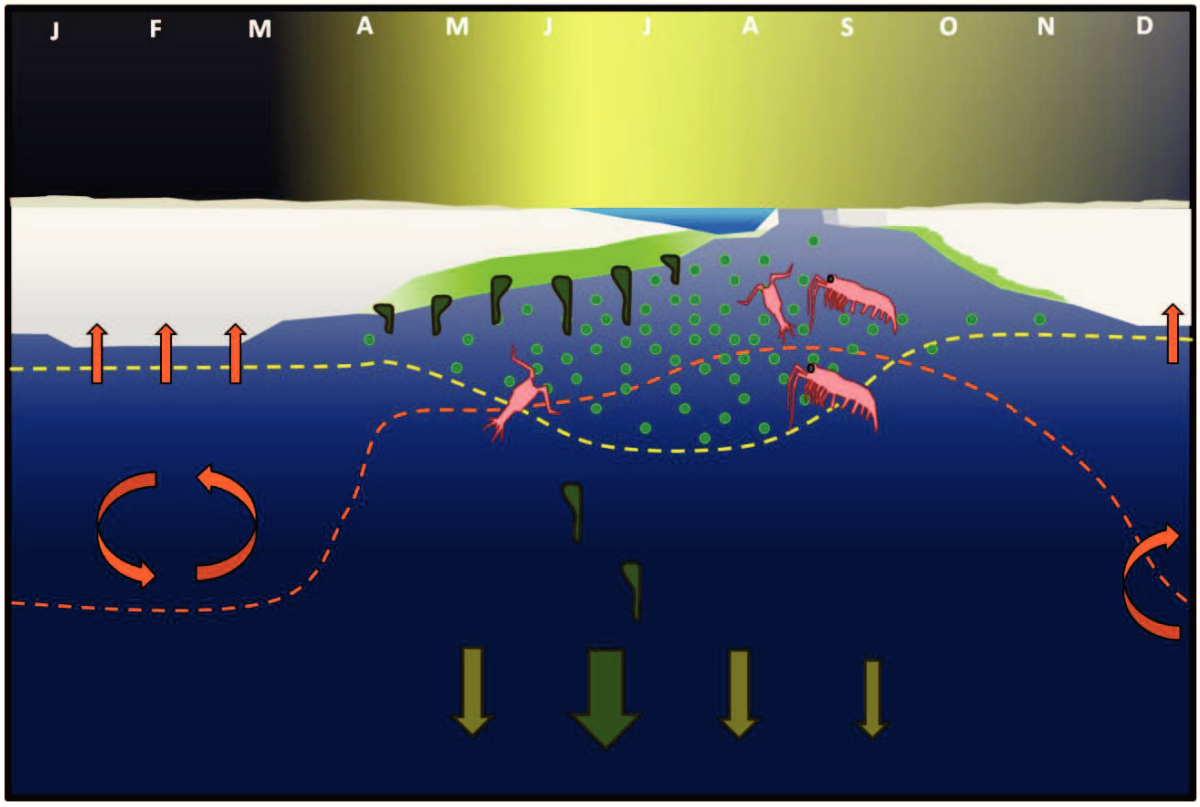

Figure 4. Conceptual model of the seasonality of the Central Arctic ecosystem from January (J left) to December (D right). Incoming irradiance is symbolized by yellow sky. The sea ice thickness is 2 m in January and decreases as the season evolves until it fully melts. Only some areas of the Central Arctic are ice-free in summer for a short period (August), the rest is permanently ice-covered. Sea-ice algae (in and below the ice as sub-ice algal filaments) start growing in the ice as soon as enough light is available in April. As the ice gets thinner and melt pond appear at the surface, more light penetrates through the ice and phytoplankton blooms occur below the ice. Different zooplankton groups feed on the ice algae and the phytoplankton. Non-grazed algae and fecal pellets from the grazers sink to the seafloor. Orange arrows indicate nutrient fluxes. Green arrows indicate carbon export to the seafloor. The bigger size and the darker color indicate fresher and higher carbon flux. The yellow dashed line represents the euphotic zone depth (1% incoming irradiance) and the orange dashed line indicates the mixed layer depth.

Photosynthesis can only occur within the layer of the water column that receives more than 1% of the incoming photosynthetically active radiation (PAR), also called the euphotic zone. As the season evolves, the euphotic zone expands to greater depths and nutrients get depleted. This leads to the formation of deep subsurface Chl *a* maxima, and a shift from new to regenerated production (Martin et al., 2012; Tremblay and Gagnon, 2009). In August sub-ice

algal communities can make up for >50% of the production in the Central Arctic (Gosselin et al., 1997). In late August, early September, heterotrophic processes dominate and only a very small amount of degraded carbon reaches the deep-sea floor since zooplankton consume most of the biomass produced (Olli et al., 2007). During the dark months from October to March, sea-ice formation leads to deep haline convection processes (50-90 m), which mix the water column. Thereby, the upper layers are replenished with nutrients (Korhonen et al., 2013), which are utilized by sea-ice algae as soon as >1 μmol photons m^{-2} s^{-1} are available in the spring (Gosselin et al., 1986; Mock and Gradinger, 1999)(Fig.4).

1.2.2. Export of organic matter to the deep Arctic Basins.

During the productive season, the food chain in the Central Arctic Ocean evolves from an export food chain, with new production taking place at the beginning of the season, to a retention food chain, with the recycling of organic matter and nutrients at the surface and only small amounts of carbon sinking to the seafloor (Wassmann, 1998). The highest biogenic flux takes place between July and August (0.07-0.1 g C m^{-2} d^{-1}) and is followed by a lithogenic flux in September-October influenced by lateral transport of sediments from the shelves (Fahl and Nöthig, 2007).

The Central Arctic Basins are >4000 m deep, therefore, the link between the pelagic realm below the ice and the seafloor is not as direct as in the shallower Arctic shelves, where a tight pelagic-benthic coupling has been observed (Wassmann et al., 2004). Due to the low productivity of MYI covered waters and the high carbon demand of the zooplankton community (Olli et al., 2007), the carbon export to the deep basins from August to September is low (0.001-0.1 g C m^{-2} d^{-1} Cai et al., 2010; Lalande et al., 2014) compared to the more productive ice margin and shelf areas (Wassmann et al., 2004). This means that the pelagic-benthic coupling in the Central Arctic is less tight than at the shelves, since most of the carbon fixed by the autotrophs is retained in the water column and transferred to higher trophic levels, rather than sinking to the deep sea and feeding the benthic community (Piepenburg, 2005). However, the role of sea-ice algal aggregations that grow below the ice and sink when the ice melts, such as those formed by *Melosira arctica*, is not well investigated yet (Ambrose et al., 2005; Fahl and Nöthig, 2007; Gutt, 1995).

The carbon to nitrogen (C:N) ratio of sinking particles in the European Arctic is higher than Redfield stoichiometry, which is more typical in algal particles during the growth season (Frigstad et al., 2013). This corresponds to the generally more degraded status of the sinking particles. This indicates that carbon export estimates performed using Redfield might have underestimated carbon export by 40% in the Central Arctic, where the C:N ratio is highest (Tamelander et al., 2013). The role of light and nutrient concentrations in carbon to nutrient uptake ratios during growth and sinking in the Arctic Ocean is not well understood.

1.2.3. Factors controlling primary production and export.

The Arctic is a poorly-lit oligotrophic (nutrient poor) ocean. Thus, both light and nutrients are bottom-up limiting factors of primary production. On an annual base, the depth of the winter mixing and the total incoming irradiance are the two factors that constrain Arctic primary productivity (Popova et al., 2010). Light determines the length of the productive season that, north of 78ºN, lasts for four months (roughly from mid-May to mid-September) (Fig.4). The low incident angle and the thick sea-ice and snow cover strongly reduce the amount of light that reaches the microalgae. Sea-ice algae living in the sea ice are low-light-adapted and can thus start growing as soon as some light starts penetrating through the ice in spring (Michel et al., 1988). Because they are low-light-adapted, snow seems to be an important factor for their initial growth and if the snow is removed at the beginning of the season sea-ice algae can be photoinhibited (Juhl and Krembs, 2010; Lund-Hansen et al., 2014). Likewise, light is the main limiting factor for phytoplankton below thick ice, especially at the beginning of the productive season (Sherr et al., 2003). Phytoplankton can start utilizing nutrients in the water column when incoming irradiance and transmittance through melting sea ice increases in summer. Indeed, massive phytoplankton blooms have been observed below thin and heavily ponded sea ice in the Chukchi Sea (Arrigo et al., 2012, 2014). As light is attenuated in the water column, the depth of the mixed layer and the rate of mixing are essential in controlling the amount of light available for phytoplankton growth (Sakshaug and Slagstad, 1991).

Nutrients are an important limiting factor for primary productivity in the Central Arctic since upwelling events are not as common as on the marginal shelf seas (Codispoti et al., 2013; Tremblay et al., 2008). Both sea-ice algae and phytoplankton use the nutrients available in

surface waters, albeit with a time shift (Matrai and Apollonio, 2013). The main mechanism for nutrient replenishment is deep haline convection (50-90 m) during winter (Carmack and Wassmann, 2006; Rudels et al., 2012). In addition, eddies can sometimes transport nutrients from the shelves to the Central Basins (Watanabe et al., 2014). Other mechanisms of nutrient replenishment for sea ice have been suggested, such as wind-driven dust deposition from the land on the shelves (Arrigo, 2014).

In the water column, nitrate is considered the main limiting nutrient for primary production in the Central Arctic (Tremblay and Gagnon, 2009). This is because most of the studies regarding nutrient limitation in Arctic waters focussed on the Amerasian Basin, that has a low N:P ratio due to denitrification processes on the shelves influenced by the Pacific inflow (Devol et al., 1997). Nitrate concentrations in surface waters (0-50 m) in the Amerasian Basin range between 0 and 10 μmol L^{-1} in winter and decrease to 0 in summer (Codispoti et al., 2013). In the Eurasian Basin, however, concentrations can be up to 20 μmol L^{-1} below the halocline in winter and decline to 2-8 μmol L^{-1} below the mixed layer (30-60m) and 0-5 μmol L^{-1} in the mixed layer (5-20 m depth) during summer (Codispoti et al., 2013; Lalande et al., 2014). Therefore, nitrate may also be the main limiting nutrient in the Eurasian Basin (Codispoti et al., 2013). In contrast, in sea ice, silicate seems to be the limiting factor in some cases, probably due to the high demand of silicate by diatoms, which use it to build their cell walls, and the low remineralization rate of silicate in the ice (Arrigo, 2014; Cota and Smith, 1991; Lee et al., 2008).

Grazing pressure also plays an important role in controlling the amount of organic matter exported to the benthos (Olli et al., 2007), but the exact magnitude of its limiting role is understudied in the Central Arctic. It is known that genera such as *Calanus* feed on sea-ice algae (Soreide et al., 2010) and amphipods have been observed feeding below the ice (Poltermann, 2001). However, grazers mainly influence the amount of carbon exported to the seafloor. The amount of new production, which equals the amount of new organic matter available for higher trophic levels, is finally constrained by nutrients, mainly nitrate. Sources of allochthonous nitrate in other oceans are rivers, deep waters and nitrogen fixation. In the Arctic, nitrate riverine input remains on the shelves, and haline convection is not very deep and only happens once a year in winter. Regarding nitrogen fixation, nothing is known about its possible role in the Central Arctic.

1.2.4. Potential role of nitrogen fixers in the Arctic.

Nitrogen can only be made available for marine organisms via atmospheric deposition or nitrogen fixation by bacteria (Gruber and Galloway, 2008). Microorganisms capable of nitrogen fixation are known as diazotrophs. In the marine environment the most conspicuous group of diazotrophs are autotrophic cyanobacteria, but several groups of marine heterotrophic bacteria can also perform nitrogen fixation and have been recently found in all oceans (Farnelid et al., 2011). Yet, nothing is known regarding nitrogen fixation in the Central Arctic Ocean.

In general, diazotroph distribution is related to areas of low nitrate concentration, with sufficient amounts of iron and phosphate and warm temperatures (Ward et al., 2013). Since cyanobacteria are very rare in Arctic waters (Vincent, 2000), it has long been assumed that nitrogen fixation does not take place in polar marine regions. The only two previous studies on diazotroph diversity in the Arctic Ocean were conducted in the Canadian Arctic close to the Mackenzie river (Blais et al., 2012), and in the Fram Strait (Díez et al., 2012). The community found in the Canadian Arctic originated from the Mackenzie River and was mainly formed by heterotrophic bacteria and some cyanobacteria (Blais et al., 2012). In Fram Strait, cyanobacterial nitrogen fixation genes could be amplified using molecular techniques, together with *Alpha* and *Gammaproteobacteria* (Díez et al., 2012).

Diazotrophs could be advected into the Central Arctic Ocean from the North Atlantic (Langlois et al., 2008; Turk et al., 2011) or drift together with sea ice from the shelves. Diazotrophs thriving in river freshwater could potentially be frozen up in the ice that forms on the shelves and then be transported to the Central Arctic. Another possibility would be wind-driven transport of diazotrophs from land to the ice top (Harding et al., 2011). Additionally, summer melt ponds would be a favorable habitat for riverine diazotrophs to develop due to their low salinity.

Pacific influenced waters enter the Arctic through the Bering Strait where high denitrification rates in the sediments reduce the nitrate concentration relative to phosphate (Devol et al., 1997). In the Atlantic influenced Arctic Ocean, nitrate concentrations are higher, but N:P concentrations are below Redfield at the end of the productive season. In addition, the strong riverine and terrestrial influence in the Arctic Ocean leads to high concentrations of dissolved iron (Klunder et al., 2012), which is a main component of the enzymes involved in nitrogen

fixation (Ward et al., 2013). Therefore, nitrogen fixation could potentially take place in summer, when nitrate is low and phosphate and iron are sufficient. According to the few measurements performed with the acetylene reduction method in the coastal Canadian Arctic, nitrogen fixation could contribute 7% to new production (Blais et al., 2012). However, it has been suggested that this method underestimates nitrogen fixation (Mohr et al., 2010). Hence, the potential role of diazotrophs in the Arctic Ocean might have been underestimated, and more studies are needed, particularly in the Central Arctic where nitrogen fixation measurements have never been performed.

1.2.5. Lack of data from the Central Arctic.

Current knowledge of the Central Arctic is based on snapshots derived from icebreaker visits, usually in summer. Due to its difficult access, the biological data from this vast area that covers 40% of the Arctic Ocean, is very reduced compared to the Arctic shelves (Wassmann, 2011). Table 1 shows a compilation of available primary productivity related data from the Central Arctic. Pan-Arctic studies of primary production that are usually based on satellite observations, assume that the ice-covered waters of the Central Arctic host no productivity (Matrai et al., 2013; Pabi et al., 2008). However, we know that the ice-covered Arctic is not a biological desert from the few measurements available (Wheeler et al., 1996). Furthermore, the recent discovery of massive phytoplankton blooms below the ice challenges this paradigm (Arrigo et al., 2014).

Areal and temporal estimates of Arctic primary production are not very accurate because they are generally based on extrapolation and interpolation using simple models and basic knowledge of algal physiology (Sakshaug et al., 2004). For example, the Chl *a* :C ratio, commonly used to transform autotrophic biomass into fixed carbon estimates, is 0.036 on average for Arctic diatoms during the growth season in the Arctic. However, ranges from 0.003 to 0.08 have been measured depending on the acclimation status of the algae (Sakshaug et al., 2004). In addition, the different methodologies to estimate PP (carbon or nutrient uptake, oxygen production and changes in Chl *a*), together with the high spatial and temporal variability result in a poorly constrained range of PP values for the Central Arctic Basins, from 1 Tg C yr^{-1}, when assuming no production in ice-covered areas (Hill et al., 2013), up to 119 Tg C yr^{-1} when taking into account the total amount of nutrients used for PP (Codispoti et al., 2013).

Besides three Arctic-wide synthesis studies (Codispoti et al., 2013; Hill et al., 2013; Matrai et al., 2013), there are only two ecological studies in the Central Arctic Ocean that include sea-ice and water-column PP and discuss nutrients, light and grazing as limiting factors. From the Arctic Ocean Sampling expedition in 1996 we know that in the Central Arctic sea-ice algae can contribute up to 57% of the net primary productivity in summer (Gosselin et al., 1997). However, their patchy distribution, especially of sub-ice algal aggregates, and the technological challenges of producing *in situ* estimates of their PP cause a high uncertainty in the overall estimates (Legendre et al., 1992; Syvertsen, 1991). The annual areal NPP estimates for the Eurasian Basin including sea-ice algae range between 10-15 g C m^{-2} yr^{-1}, double that of estimates for the Amerasian Basin (Codispoti et al., 2013; Gosselin et al., 1997; Sakshaug et al., 2004; Wheeler et al., 1996).

Primary production determines the potential amount of carbon that could be exported to the seafloor. However, the final amount of carbon that reaches the seafloor is strongly controlled by grazers at the surface and the microbial loop that remineralizes the organic matter as it sinks. Carbon export in the Central Arctic is strongly controlled by grazers such as amphipods and copepods (Olli et al., 2007). The carbon export to the deep Central Basins is generally very low (~1g C m^{-2} yr^{-1} (Sakshaug et al., 2004)), however in recent years with rapid and extensive ice melt, higher carbon export rates have been measured (Lalande et al., 2009).

In summary, the Central Arctic Ocean has been long considered an area of very low productivity but very few complete process ecosystem studies are available. There is still a lack of a comprehensive baseline to compare future Central Arctic studies with, in order to appropriately detect changes on the ecosystem caused by climate change (Wassmann et al., 2011). Despite recent efforts, biogeochemical measurements of carbon and nutrient fluxes in sea ice, melt ponds and water column of the Central Arctic are still scarce.

Table 1. Summary of biological parameters from the Central Arctic Ocean.

Parameter	Value	Units	Sea Water/Ice	Time of measurement	Reference
Primary Productivity	0.26 ± 0.24	g C m^{-2} d^{-1}	SW	August 1994	Wheeler, 1996
	0.003	g C m^{-2} d^{-1}	SI	August 1994	Wheeler, 1996
	0.03 ± 0.01	g C m^{-2} d^{-1}	SW	August 1994	Gosselin, 1997
	0.057	g C m^{-2} d^{-1}	SI	August 1994	Gosselin, 1997
	0.05-0.15	g C m^{-2} d^{-1}	SW	August 2001	Olli, 2007
Primary Production	10	g C m^{-2} yr^{-1}	SW+SI	Annual 1994	Wheeler, 1996
	15	g C m^{-2} yr^{-1}	SW+SI	Annual 1994	Gosselin, 1997
	11	g C m^{-2} yr^{-1}	SW+SI	Annual	Sakshaug, 2004
New production	1	g C m^{-2} yr^{-1}	SW+SI	Annual	Sakshaug, 2004
	15± 10	g C m^{-2} yr^{-1}	SW+SI	Annual	Codispoti, 2013
Chlorophyll *a*	0.03-0.3	mg Chl *a* m^{-3}	SW	August 2001	Olli, 2007
	1.2-50	mg Chl *a* m^{-2}	SW	August 1994	Gosselin, 1997
	0.2-14	mg Chl *a* m^{-2}	SI	August 1994	Gosselin, 1997
POC	0.002-0.05	g C m^{-3}	SW	August 1994	Gosselin, 1997
	0.003-0.08	g C m^{-3}	SI	August 1994	Gosselin, 1997
DOC	0.6-1	g C m^{-3}	SW	August 1994	Wheeler, 1997
Chl *a*:C	0.003-0.08	w:w	SI		Booth, 1997
C:N	9.7	mol:mol	SW		Tamelander, 2013
	6.6	mol:mol	SW	August 2001	Frigstad, 2013
Si:N	0.31	mol:mol	SW		Sakshaug, 2004
Carbon export	0.04-0.09	g C m^{-2} yr^{-1}	SW	August 2001	Olli, 2007
	0.07-0.1	g C m^{-2} d^{-1}	SW	July-October 1996	Fahl &Nöthig 2007
	0.001-0.1	g C m^{-2} d^{-1}	SW	September 2012	Lalande, 2014
	0.002	g C m^{-2} d^{-1}	SW	August 2007	Cai, 2010

1.3. Objectives

The Central Arctic has been covered by perennial sea ice since the early Holocene (120,000 years before present), and in the last 100 years extensive parts of it are now shifting towards seasonal ice zones due to the fast summer sea-ice retreat caused by global warming (Fahl and Stein, 2012; Miller et al., 2013; Polyakov et al., 2010). Due to the difficult accessibility for sampling of this region, very little is known about how this rapid sea-ice retreat is affecting the Central Arctic ecosystem. Microalgae living in the sea ice and in the water column comprise the base of the entire ecosystem and, therefore, changes in their productivity and export rates to the deep sea, will have cascading effects on the entire food web. Thus, studying primary production, its limiting factors and its fate in the Central Arctic is urgent in order to fill the gap of knowledge that actually exists for this vast area of the Arctic Ocean.

The **overall aim** of this thesis is to improve our understanding of the physical and biological processes regulating the amounts of carbon fixed and exported to the seafloor in the Central Arctic, including sea-ice algae and phytoplankton primary production, and to elucidate the effect of sea-ice retreat on these photosynthetic communities and on the whole ecosystem.

The **specific objectives** are i) to examine the role of sub-ice algal aggregates, ii) to determine the contribution of sea ice, melt pond and water column communities to total primary productivity and to identify the factors controlling primary productivity´s magnitude and distribution, and iii) to investigate the potential role of nitrogen fixers in the Eurasian Basin of the Central Arctic at the end of the productive season. These objectives are addressed using radioactive carbon uptake assays under different light and nutrient conditions, a simple irradiance model for up-scaling, traditional biological and oceanographic measurements of biomass and physicochemical environmental parameters and molecular nitrogen fixation gene analysis.

The main questions addressed in this thesis are:

1) What is the role of sea-ice algal aggregates in the Central Arctic? Their patchy distribution has made the quantification of sub-ice algae elusive. Although they can accumulate large biomass below the ice, their contribution to primary production in the ice-covered Central Basins may have been overlooked so far. In addition they may play an important

role by exporting nutrients and carbon to the deep sea, when the ice melts and algae sink to the seafloor (Chapters I, II, III and IV).

2) What is the relative contribution of sea-ice algae, melt-pond phototrophs and water-column phytoplankton to total primary productivity in the Central Arctic at the end of the productive season and how will sea-ice retreat impact carbon fixation at different spatial and temporal scales? Sea-ice cover and thickness are diminishing rapidly in the Arctic Ocean making the central region shift from a perennial ice zone to a seasonally ice-covered zone. Increased light irradiance transmitted through thinner ice and stronger stratification due to ice melt are some of the physical constraints for future Arctic primary productivity. Understanding which factors control the amount of carbon fixed in ice-covered areas will allow us to make predictions about future trends in primary production in the Central Arctic (Chapter V).
3) Could potential diazotrophs in the Central Arctic occur in nitrate limited waters of the Eurasian Basin, and in the pack ice? Nitrogen fixers have been detected in the Canadian Arctic and in the Fram Strait. Therefore, potential Central Arctic diazotrophs could originate from the river influenced Laptev Sea and then be transported with the ice following the transpolar drift (Chapter VI).

1.4. Methods used to measure primary productivity

Aquatic primary productivity can be measured using different approaches (Harrison, 1995). The most common and direct ways of measuring the rate of primary productivity are monitoring the uptake of carbon dioxide or the production of oxygen. Carbon uptake is measured by adding an isotopic tracer as labeled bicarbonate, with radioactive ^{14}C or with stable ^{13}C, and following its conversion into particulate organic carbon by photosynthesis (Galloway, 1969). Oxygen production can be measured with classical chemical methods (Winkler, 1888) or with chemical or optical sensors (Klimant et al., 1995).

A more indirect method of estimating primary production is measuring autotrophic biomass accumulation, usually represented by the concentration of the main photosynthetic pigment: chlorophyll *a* (Chl *a*) (de Vooys, 1979). This can be done by measuring the fluorescence of the Chl *a* molecules in a sample or by satellite with an ocean color algorithm (Westberry and Behrenfeld, 2014), which is possible only for ice-free waters in the Arctic (Pabi et al., 2008).

The rate of photosynthesis is related to the electron transport between the two photosystems and can be measured using a pulse-amplitude-modulated (PAM) fluorometer (Jakob et al., 2005; Suggett et al., 2003). However, the transformation from the rate of electron transport to primary productivity is not straight forward and algal self-shading makes the volumetric upscaling prone to error, especially in sea ice (Glud et al., 2002).

All these methods provide estimates of net or gross primary productivity, depending on the incubation time and if the amount of carbon lost by respiration was considered or not. These estimates can be normalized by volume and time, and can be used to extrapolate to larger areas and longer time scales. Nevertheless, the high variability of algal productivity reduces the accuracy of these extrapolations. A way to estimate annual production without extrapolating is to compute the seasonal draw-down of nutrients in the euphotic zone (Codispoti et al., 2013).

In the Arctic Ocean, all of these methods have been used to measure primary productivity (daily rate) and production (annual rate), both in the water column and in sea ice, except for satellite ocean color estimates that are restricted to ice-free waters. In this thesis, seawater was sampled using Niskin bottles attached to the ship's Conductivity-Temperature-Depth (CTD) rosette, while sea ice was sampled using an ice corer. The main limitation when estimating sea-ice primary productivity is that the sea-ice structure generally needs to be destroyed to perform the measurements, thus the estimated rates are only potential *in situ* rates. Some *in situ* incubators have been developed to prevent melting the ice, but then other problems, such as the lack of homogeneous distribution of the tracer, arise (Mock and Gradinger, 1999; Smith and Herman, 1991). The only two methods that do not require melting the sea ice are oxygen measurements below the ice and PAM fluorometry. However, these two methods also have disadvantages and can lead to underestimations. Oxygen measurements below the ice are affected by water column biological processes and by oxygen dynamics related to ice melting and freezing (Glud et al., 2014). Fluorometric methods only measure the first layer of algae in the ice and therefore, their volumetric upscaling is prone to error (Glud et al., 2002). Nevertheless, the greatest challenge to estimate sea-ice primary productivity correctly at larger scales is to take into account its spatial variability. The amount of Chl *a* in the ice can be inferred from the spectra of the light transmitted through the ice. Measuring under ice light transmittance with an under-ice remotely operated vehicle (ROV) that can cover wider areas than traditional ice coring might be a step forward (Mundy et al., 2007). However, this

method only provides Chl *a* concentrations, which are not easily transformed to primary productivity correctly, and it requires constant calibration.

Based on preliminary studies with sea-ice algae cultures, where different methods to measure primary productivity were compared under different environmental conditions (Fernández-Méndez, 2011), the most accurate method to measure primary productivity in the Central Arctic at the end of the productive season, when very few cells per volume are present, is the incubation with radioactive carbon isotope ^{14}C-bicarbonate due to its high sensitivity.

1.4.1. Photosynthesis versus irradiance curves using the ^{14}C method

The ^{14}C-method to measure aquatic primary productivity was introduced by Steemann Nielsen in 1952. It consists in adding a radioactive tracer to the samples (^{14}C-bicarbonate), incubating them in the laboratory under different light intensities, filtering the samples to retain the particulate carbon and measuring the amount of tracer taken up with a scintillation counter (Steemann Nielsen, 1952). Our custom-made incubator had 10 different light levels from 0 to 420 μmol photons m^{-2} s^{-1} and was connected to a Julabo cooling system to keep the temperature constant at -1.3ºC, slightly above the freezing point of seawater, which was roughly the light and temperature conditions that sea-ice related Arctic communities experience *in situ*. Plastic cell culture bottles with 20 ml of liquid sample each and 1 μCi/ml of ^{14}C-bicarbonate final concentration were incubated for 12 h (Fig.5). This incubation time is enough to take into account carbon losses by respiration and therefore net primary productivity estimates are obtained (Fernández-Méndez, 2011; Gieskes et al., 1979). After incubation, samples were filtered through 0.2 μm pore size filters in which radioactivity was measured with a scintillation counter by adding a liquid scintillation cocktail. The natural dissolved inorganic carbon (DIC) present in the sample before spiking was used to calculate the amount of labeled inorganic carbon fixed into the cells. The value of the dark bottle was subtracted from the light values. The NPP rates obtained were then normalized by Chl *a*. By plotting the NPP values against the incubation irradiances (I) and fitting the data to the equation published by Platt et al., (1980) (shown in Fig.5), a photosynthesis versus irradiance curve (PI curve) is obtained. P^b_{max} depicts the chlorophyll normalized theoretical maximum carbon fixation rate which equals P_{max} for cases with negligible photoinhibition parameter β and the initial slope is given by α. Photosynthetic parameters such as the photoacclimation

parameter (Ik) can be calculated from this curve to describe the photosynthetic community studied (Forget et al., 2007).

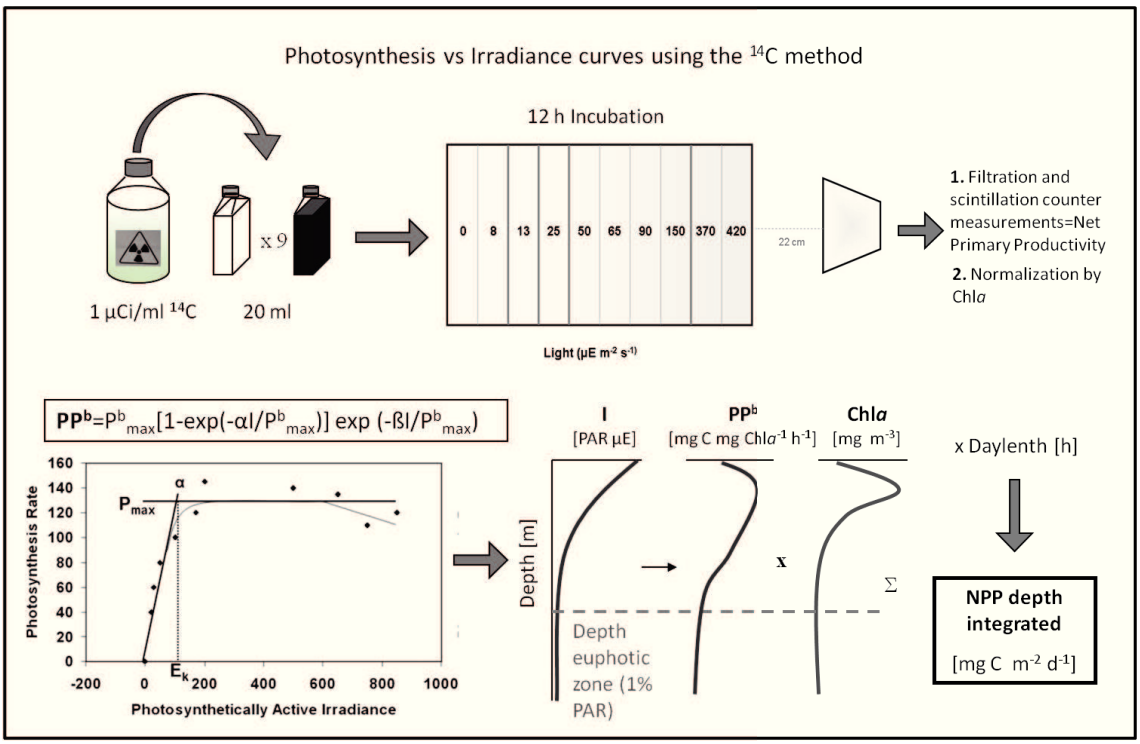

Figure 5. Workflow of the ^{14}C method to measure Net Primary Productivity (NPP) by incubating the samples under different irradiances (I). The superscript *b* means biomass normalized. The model used to fit the photosynthesis versus irradiance curve is described in (Platt et al., 1980).

The PI curve equation describes the relationship between NPP and irradiance. Therefore, by calculating the light profile through melt ponds, sea ice and water column from the measured incoming irradiance at the moment of sampling, the *in situ* NPP at each depth in each environment can be calculated. Subsequently, the NPP is multiplied by the measured Chl *a* at each depth and integrated until the euphotic zone depth (1% PAR). Finally, the areal estimate is multiplied by the day length to get a final NPP estimate in mg C m^{-2} d^{-1} (Fig.5).

1.4.2. Upscaling model

PI curves are very powerful since they can be used to upscale NPP to larger areas and longer time scales (Platt and Sathyendranath, 2007). To do this, a realistic light parameterization for each environment is required. In open waters, this is straight forward since the light

extinction coefficient of seawater is well known (0.1 m^{-1}). On the contrary, sea ice transmits light differently depending not only on its thickness but also on its internal structure determined by its formation process and age (Ehn and Mundy, 2013; Katlein et al., 2014). In collaboration with the Sea-ice physics department of the Alfred Wegener Institute, a light parameterization model was developed for the Central Arctic including sea ice and melt ponds (Arndt and Nicolaus, 2014; Nicolaus et al., 2012). Using this light parameterization together with sea-ice thickness (assumed from age) and melt-pond coverage satellite data, light profiles were calculated in and below the ice for the entire Arctic Ocean. In the same way as explained above for *in situ* estimates, depth integrated NPP can be calculated for the entire Arctic with a resolution of 10 km^2. Similar approaches have been used to calculate NPP in Arctic waters (Ardyna et al., 2013). However, prior to this thesis light parameterization for sea ice did not account for the high spatial variability of the optical properties of sea ice (Perovich, 1996).

1.4.3. New production

To estimate the total amount of new production that can be transferred to higher trophic levels, we used nutrient uptake in the euphotic zone during the productive season (Codispoti et al., 2013). This method has been previously used in the Arctic giving total estimates of annual sea-ice and phytoplankton new production based on the difference between nitrate inventories in surface waters in early spring and in late summer (Codispoti et al., 2013; Matrai and Apollonio, 2013). If no winter nutrient values are available, the initial nutrient concentration can also be calculated from the temperature and nutrient profiles at the end of the productive season. The minimum in the temperature profile at the end of the season is indicative of the depth of the winter haline convection (Korhonen et al., 2013; Rudels, 1995). Thus, assuming that there is no lateral transport through advection, the nutrient concentration at that depth was the initial concentration of nutrients in the mixed layer available for production. By assuming a constant profile in winter and depth integrating the difference with the nutrient profile at the end of the season, the total amount of nutrients used during the productive season can be calculated. Afterwards, using the carbon to nutrient ratio of the autotrophic biomass, which is generally close to Redfield during growth (Frigstad et al., 2013), the total amount of carbon taken up during the productive season can be calculated.

1.4.4. Nutrient addition experiments

Nutrient addition experiments or enrichment bioassays have been long used in marine ecology to determine the limiting nutrient for phytoplankton primary productivity in the water column (Tilman et al., 1982). The algal community's response in terms of changes in biomass or productivity to the addition of different nutrients gives indications about which nutrient limits production at the moment of sampling. In the Arctic, several enrichment bioassays have been performed in coastal areas, both with phytoplankton and sea-ice algae (Cota et al., 1996; Maestrini et al., 1986; Taylor et al., 2013). The main problem with this method in cold polar environments is the lag phase that the algae suffer when transferred to the lab. Therefore, elongated incubation times are necessary to detect changes in productivity.

In addition, the nutrient ratios present in the studied environment can also indicate which nutrient is limiting production. The Redfield ratio C:N:P:Si of 106:16:1:15 is generally assumed to be the optimal ratio for algal growth (Redfield, 1958). Deviations from this ratio usually mean nutrient limitation (Elser et al., 2009; Spilling et al., 2010). However, there is a great variability in nutrient supply and biological demand, making generalizations difficult (Moore et al., 2013).

1.4.5. Environmental parameters

Complementary to the primary productivity measurements, a range of environmental variables were measured to study the entire ecosystem from a broader perspective. It is important, when doing process studies, to include as much physical, chemical and biological variables as possible, since they are strongly interlinked and will help in interpreting the results correctly.

Through several collaborations with other teams on board, a comprehensive dataset of environmental parameters was obtained. Physical parameters included sea-ice thickness and coverage, melt-pond coverage, incoming irradiance, and temperature. Chemical parameters included salinity, inorganic nutrient concentrations, dissolved inorganic carbon, dissolved oxygen and pH. Besides primary productivity, other biological parameters such as photosynthetic pigments, particulate organic carbon and nitrogen, bacterial abundance and productivity, and transparent exopolymers concentration were obtained.

1.5. Publication outline

In the following chapters I will present evidence for sea-ice algal export to the deep sea in the Central Arctic linked to sea-ice melt, as well as a comprehensive study at different spatial scales on the abundance, composition, buoyancy regulation and role of sub-ice algal aggregates in the carbon and nitrogen cycles. Subsequently, I will present recent estimates of primary productivity in the three different Arctic environments: water column, sea ice and melt ponds, at different spatial and temporal scales, as well as the main limiting factors for primary productivity at the end of the productive season. These results are discussed in the light of current anthropogenic climate change trends in the Central Arctic Ocean. Finally, investigations of diazotroph diversity in the Central Arctic will reveal a high diversity of potential nitrogen fixers in Arctic sea ice and the water column, with potential implications for nitrate limitation in the oligotrophic Arctic Ocean.

Chapter I: Export of algal biomass from the melting Arctic sea ice.

Antje Boetius, Sebastian Albrecht, Karel Bakker, Christina Bienhold, Janine Felden, Mar Fernández-Méndez, Stefan Hendricks, Christian Katlein, Catherine Lalande, Thomas Krumpen, Marcel Nicolaus, Ilka Peeken, Benjamin Rabe, Antonina Rogacheva, Elena Rybakova, Raquel Somavilla, Frank Wenzhöfer, and RV Polarstern ARK27-3-Shipboard Science Party.

Science (2013) 339:1430-1432

This study reports the deposition of sea-ice algal aggregates to the deep sea of the Central Arctic in summer 2012. This observation supports the hypothesis that a reduction in sea ice cover enhances under-ice productivity and carbon export causing changes in our understanding of the pelagic-benthic coupling in the Arctic.

The study was designed by A. Boetius. Primary productivity measurements and microscopy analysis were performed by M. Fernández-Méndez. Sea-ice biological data was provided by I. Peeken. Sea-ice physics data was provided by S. Hendricks, C. Katlein, M. Nicolaus and T. Krumpen. Oceanographic data and nutrients were provided by B. Rabe, K. Bakker, C. Lalande and R. Somavilla. Deep-sea surveys were performed by S. Albrecht, C. Bienhold, J. Felden, A. Rogacheva, E. Rybakova and F. Wenzhöfer. The manuscript was written by A. Boetius with support of all coauthors.

Chapter II: Floating ice-algal aggregates below melting Arctic sea ice.

Philipp Assmy, Jens K. Ehn, Mar Fernández-Méndez, Haakon Hop, Christian Katlein, Arild Sundfjord, Katrin Bluhm, Malin Daase, Anja Engel, Agneta Fransson, Mats A. Granskog, Stephen R. Hudson, Svein Kristiansen, Marcel Nicolaus, Ilka Peeken, Angelika H. H. Renner, Gunnar Spreen, Agnieszka Tatarek, and Jozef Wiktor.

PLoS One (2013) 8(10): e76599

This study provides first descriptive and quantitative estimates of floating sea-ice algal aggregates below Arctic sea ice. The study shows that these aggregations originate from bottom-ice algal communities and despite their low biomass at the end of the season, the abundant grazers found in them suggest that they have an important role in the ecosystem as food source when no other algal biomass is available.

The study was conceived by P. Assmy, M. Fernández-Méndez, C. Katlein, M. Nicolaus, H. Hop, J.K. Ehn, S. Kristiansen and M.A. Granskog. Experiments and measurements were performed by P. Assmy, M. Fernández-Méndez, C. Katlein and M. Nicolaus. All other coauthors contributed with environmental data. The manuscript was written by P. Assmy with the support and input of all coauthors.

Chapter III: Composition, buoyancy regulation and fate of ice algal aggregates in the Central Arctic Ocean.

Mar Fernández-Méndez, Frank Wenzhöfer, Ilka Peeken, Heidi Louise Sørensen, Ronnie Nøhr Glud, and Antje Boetius.

(18.08.2014 Accepted for publication in PLoS One)

This study describes the composition of sub-ice algal aggregates of different types and in different degradation stages, as well as the mechanisms that regulate their buoyancy. A conceptual scheme of Arctic algal aggregate formation and degradation is presented. The study shows that algal aggregates are relevant for primary productivity, biomass and nutrient cycling at a local scale.

The study was designed by M. Fernández-Méndez and A. Boetius. Experiments were performed by M. Fernández-Méndez, F. Wenzhöfer and H.L. Sørensen. I. Peeken provided sea-ice biological data. The analysis of the data was performed by M. Fernández-Méndez and H.L. Sørensen with help from F. Wenzhöfer and R.N. Glud. The manuscript was written by

M. Fernández-Méndez with input from A. Boetius and R.N. Glud and support of all other coauthors.

Chapter IV: Distribution of algal aggregates under summer sea-ice in the Central Arctic.

Christian Katlein, Mar Fernández-Méndez, Frank Wenzhöfer and Marcel Nicolaus.

(23.06.2014 Submitted to Polar Biology)

This study shows that the floe scale distribution of sub-ice algal aggregates is determined by ice topography. It further provides large scale quantification of aggregate biomass in summer below melting ice, based on data obtained with a remotely operated vehicle (ROV). Furthermore, this study reveals that differences in the upscaling procedure can lead to several orders of magnitude differences in the final biomass estimates.

This study was designed by C. Katlein and M. Fernández-Méndez. Data analysis was performed by C. Katlein. M. Fernández-Méndez and F. Wenzhöfer provided biological environmental data from the ice ecosystem. The manuscript was written by C. Katlein with input from M. Nicolaus and support from M. Fernández-Méndez and F. Wenzhöfer.

Chapter V: Photosynthetic production in the Central Arctic during the record sea-ice minimum in 2012.

Mar Fernández-Méndez, Christian Katlein, Benjamin Rabe, Marcel Nicolaus, Ilka Peeken, Karel Bakker, Hauke Flores, and Antje Boetius.

In preparation for Biogeosciences.

This study shows that ice algae can contribute up to 60% to primary production in the Central Arctic at the end of the season due to light limitation of the water column below thick pack ice. Nitrate limitation was detected in the Siberian Seas (Laptev Sea area), while silicate was the main limiting nutrient at the ice margin influenced by Atlantic waters. In addition, the study shows that although sea-ice cover was substantially reduced in 2012, total annual new production in the Eurasian Basin was similar to estimates of previous years. However, when including the contribution by sub-ice algal filaments, the annual production for the deep Eurasian Basin (north of 78°N) was higher than estimated before. This study suggests that sub-ice algae might be responsible for potential local increases in net primary

productivity due to higher light availability under the ice, and their ability to harvest nutrients from a wider area as they drift with the ice.

The study was conceived and designed by M. Fernández-Méndez with help of A. Boetius. Experimental work on board was performed by M. Fernández-Méndez. Analysis and data assimilation was done by M. Fernández-Méndez, C. Katlein, H. Flores and B. Rabe. Environmental parameters were provided by I. Peeken, K. Bakker and M. Nicolaus. The manuscript was written by M. Fernández-Méndez with input from A. Boetius, H. Flores, B. Rabe and C. Katlein and support from all other coauthors.

Chapter VI: Diazotroph diversity in sea ice, melt ponds and water column of the Central Arctic Ocean.

Mar Fernández-Méndez, Kendra Turk-Kubo, Josephine Z. Rapp, Thomas Krumpen, Antje Boetius and Johnathan Zehr.

In preparation for Aquatic Frontiers in Microbiology

This study shows a high diversity of non-cyanobacterial diazotrophs in sea ice and waters of the Central Arctic Ocean. This is the first report of potential diazotrophs north of 78ºN. This study partially rejects the hypothesis that diazotrophs in the Central Arctic Ocean originate from the river-influenced shelves and are transported with the ice. In addition, certain nitrogen fixation phylotypes seem to be associated with specific bacterial communities.

The study was designed by A. Boetius and J. Zehr. Analysis and data assimilation were performed by M. Fernández-Méndez and K. Turk-Kubo. J.Z. Rapp performed the 16S rRNA analysis. T. Krumpen provided the ice-drift information. The manuscript was written by M. Fernández-Méndez with input from A. Boetius, K.Turk-Kubo and J. Zehr.

2. Thesis Chapters

Chapter I

Export of algal biomass from the melting Arctic sea ice.

Antje Boetius[1,2], Sebastian Albrecht[4], Karel Bakker[5], Christina Bienhold[1,2], Janine Felden[3], Mar Fernández-Méndez[1,2], Stefan Hendricks[1], Christian Katlein[1], Catherine Lalande[1], Thomas Krumpen[1], Marcel Nicolaus[1], Ilka Peeken[1,3], Benjamin Rabe[1], Antonina Rogacheva[6], Elena Rybakova[6], Raquel Somavilla[1], Frank Wenzhöfer[1,2], and RV Polarstern ARK27-3-Shipboard Science Party.

[1]Alfred Wegener Institute for Polar and Marine Research, [2]Max Planck Institute for Marine Microbiology, [3]MARUM University Bremen, [4] FIELAX Gesellschaftfürwiss.DatenverarbeitungmbH, [5]NIOZ Royal Netherlands Institute for Sea Research, [6]P.P. Shirshov Institute of Oceanology, Russian Academy of Sciences.

Science (2013) 339:1430-1432

REPORTS

Export of Algal Biomass from the Melting Arctic Sea Ice

Antje Boetius,[1,2,3]*† Sebastian Albrecht,[4]† Karel Bakker,[5]† Christina Bienhold,[1,2]† Janine Felden,[3]† Mar Fernández-Méndez,[1,2]† Stefan Hendricks,[1]† Christian Katlein,[1]† Catherine Lalande,[1]† Thomas Krumpen,[1]† Marcel Nicolaus,[1]† Ilka Peeken,[1,3]† Benjamin Rabe,[1]† Antonina Rogacheva,[6]† Elena Rybakova,[6]† Raquel Somavilla,[1]† Frank Wenzhöfer,[1]† RV Polarstern ARK27-3-Shipboard Science Party†

In the Arctic, under-ice primary production is limited to summer months and is restricted not only by ice thickness and snow cover but also by the stratification of the water column, which constrains nutrient supply for algal growth. Research Vessel Polarstern visited the ice-covered eastern-central basins between 82° to 89°N and 30° to 130°E in summer 2012, when Arctic sea ice declined to a record minimum. During this cruise, we observed a widespread deposition of ice algal biomass of on average 9 grams of carbon per square meter to the deep-sea floor of the central Arctic basins. Data from this cruise will contribute to assessing the effect of current climate change on Arctic productivity, biodiversity, and ecological function.

Primary productivity in the central Arctic is limited by light and nutrients. Photosynthetically active radiation (PAR) for under-ice primary production is only available from May to August but is locally restricted by ice thickness and snow cover (*1*–*4*). Owing to stratification (*5*, *6*), the mixed layer depth is limited to 10 to 30 m in summer (Table 1), which constrains the nutrient supply for algal growth (*7*). Hence, average estimates for primary production (PP) in the ice-covered central Arctic are low, on the order of 1 to 25 g C m^{-2} $year^{-1}$ (*8*, *9*). The contribution of ice algae is not well constrained, ranging from 0 to 80% (*10*–*13*). However, as a consequence of Arctic warming, primary productivity in and under the ice may be boosted by higher light transmission through thinning sea ice (*3*, *14*, *15*) and the increase in melt-pond coverage during summer (*4*, *16*).

Assessing the consequences of current climate change in the central Arctic regions remains difficult because reliable baselines for Arctic productivity, biodiversity, and ecological function are lacking [reviewed in (*17*)]. During the 2012 sea-ice minimum, research vessel (RV) Polarstern visited the ice-covered eastern-central basins between 82° to 89°N and 30° to 130°E (Fig. 1). In this area, thick multiyear sea ice has been largely lost as a result of melt by atmospheric heat (*18*). Our airborne electromagnetic measurements confirmed that first-year ice dominated (>95%), with an average modal thickness of less than a meter and a melt-pond cover of 30 to 40%.

Previous investigations of the underside of Arctic sea ice found that the diatom *Melosira arctica* grows meter-long filaments, anchoring in troughs and depressions under ice floes and covering up to 40 to 80% of the underside of undisturbed ice floes (*12*, *19*–*24*) (Fig. 2). Warming and melting leads to their rapid sedimentation (*20*–*23*). Deposition of *Melosira* strands had been observed on the sea floor of Arctic shelves (*12*, *21*), but their contribution to carbon export in the ice-covered basins remains unknown (*25*, *26*). Particulate organic carbon flux to the deep sea, measured by sea-floor carbon demand (*25*) and by sediment traps moored in the Amundsen Basin (*27*), was around 1 g C m^{-2} $year^{-1}$ (>1500 m) in the 1990s, with a peak contribution of sub-ice algae of up to 28% in August (*27*). Repeated measurements during the first Arctic-wide sea-ice minimum in 2005–2007 showed an increased carbon flux of 6.5 g C m^{-2} $year^{-1}$ (850 m), peaking in July (*28*).

During the expedition IceArc in summer 2012, we observed in seven out of eight regions sea-floor deposits of fresh *M. arctica* strands and other sub-ice algae at 3500- to 4400-m water depth (Fig. 1, fig. S1, and movies). Patches of algae of 1 to 50 cm in diameter covered up to 10% of the sea floor. This attracted opportunistic megafauna—such as the deep-sea holothurians *Kolga hyalina* (*29*) and *Elpidia heckeri* and the ophiurid *Ophiostriatus striatus*—which were observed to feed on the *Melosira* strands. Based on their color, chlorophyll *a* content, and chloroplast morphology, the freshest algal deposits were observed at the northernmost stations, 7 and 8 (>87°N). Stations 4 to 6 (82° to 85°N), north of the Laptev Sea margin, showed degraded algal deposits. In this area, megafauna biomass was substantially elevated, as was the pigment concentration of holothurian gut content (Table 1). The larger body sizes (>6 cm) and apparent fecundity of the *Kolga* population (based on gonad sizes) in this area suggested that sources of food had been available for at least 2 months and that the main algal flux had occurred before June. This matches observations of rapid melt and export of ice from the Laptev Sea as early as May 2012. By July, large open water areas had appeared within the ice zone up to 85°N (Fig. 1),

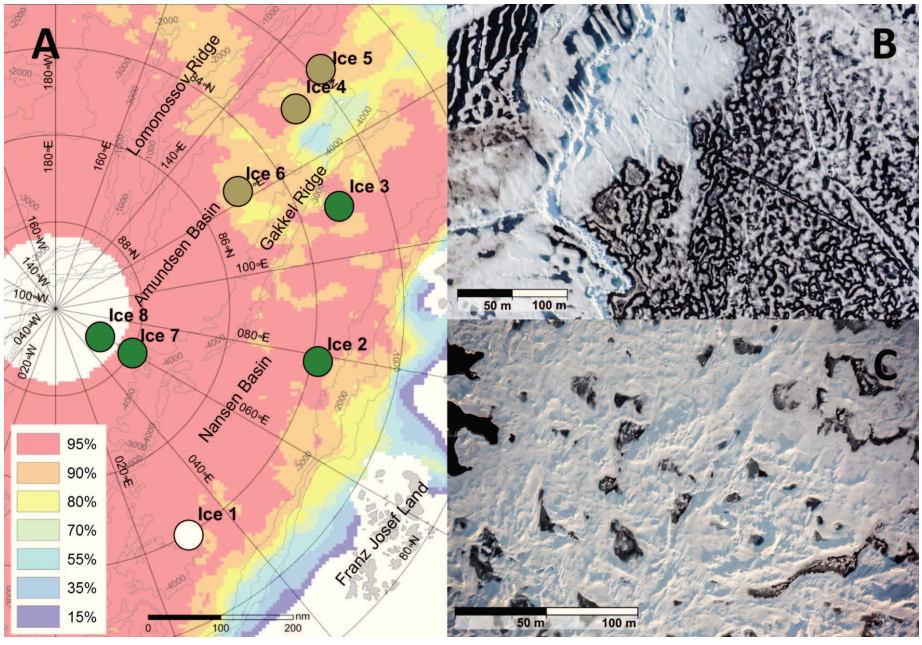

Fig. 1. Ice conditions during RV Polarstern Expedition IceArc (ARK27-3, 2 August to 8 October 2012). (**A**) Ice cover in July 2012 in percentages. Ice stations with fresh and degraded algal deposits are marked by green and brown circles, respectively. White indicates no deposits. (**B**) Aerial image of station 3 in mid-August. (**C**) Aerial image of station 6 in mid-September.

[1]Alfred Wegener Institute, Helmholtz Center for Polar and Marine Research, 27515 Bremerhaven, Germany. [2]Max Planck Institute for Marine Microbiology, 28359 Bremen, Germany. [3]MARUM, Center for Marine Environmental Sciences, University Bremen, 28334 Bremen, Germany. [4]FIELAX Gesellschaft für wissenschaftliche Datenverarbeitung mbH, 27568 Bremerhaven, Germany. [5]NIOZ Royal Netherlands Institute for Sea Research, 1790 AB Den Burg, Netherlands. [6]P. P. Shirshov Institute of Oceanology, Russian Academy of Sciences, 117997 Moscow, Russia.

*Corresponding author. E-mail: antje.boetius@awi.de
†All authors with their contributions and affiliations appear at the end of this paper, and all other contributors are listed in the supplementary materials.

causing a rapid decline of the sea-ice cover, reflected in 1 to 2 m of melt-water content above the winter thermocline (Table 1).

Our surveys showed shreds of *M. arctica* (Table 1), indicating their melt-out earlier in the season (*23*). At 3500- to 4400-m depth, deposits of coiled *Melosira* strands (diameters of 5 to 12 cm) covered 0.1 to 10% of the sea floor. The carbon deposition by sub-ice algae was estimated to be equivalent to 1 to 156 g C m^{-2} (median 9 g C m^{-2}) (Table 1). For comparison, the 2012 pelagic new production in the same regions was estimated to be 7 to 16 g C m^{-2} (median 11 g C m^{-2}) (Table 1), with a contribution by diatoms of 36% based on silicate inventories (Table 1). *Melosira* strands are not used as food in the pelagial and sink rapidly to the sea floor (*23*). This results in a contribution of at least 45% of total primary production and >85% of carbon export in 2012.

The algal deposits at the sea floor and extracts of *Kolga* gut at stations 3, 4, 7, and 8 contained living *Melosira* cells with green chloroplasts and lipid vesicles (Fig. 2). The algal deposits had variable high concentrations of chloroplast pigment equivalents (CPE) (27 ± 21 μg cm^{-3}; n = 18 aggregate samples) and a high chlorophyll *a* to total pigment ratio (51 ± 18%). In comparison, pigment contents of bare sediments next to the patches were low at 0.8 ± 0.3 μg cm^{-3}, matching concentrations found in the 1990s (*25*). The gut contents of *Kolga* specimens showed even higher pigment concentrations of, on average, 51 ± 47 μg cm^{-3} (Chl*a*/CPE ratio of 41 ± 14%; n = 15 gut samples), and algae recovered from guts were still photosynthesizing when exposed to light (*30*).

Previous investigations focusing on oligotrophic deep-sea sediments have found a direct relationship between carbon flux, benthic biomass, and remineralization rates (*31*–*35*). However, despite the widespread deposition of algae observed in the eastern-central basins, apparently only sediment bacteria (as estimated from respiration rates) (fig. S2) and large mobile megafauna had profited from the ice-algae deposition. Infauna burrows and tubes were rare, indicating an absence of the sediment-dwelling macrofauna characteristic of other deep-sea basins with seasonally sedimenting phytoplankton blooms [reviewed in (*36*)]. Furthermore, the bare sediments next to the algal deposits maintained oxygen fluxes of only 0.3 to 0.4 mmol O_2 m^{-2} day^{-1}, equivalent to a carbon demand of 1 to 2 g C m^{-2} $year^{-1}$. Such low rates are typical for oligotrophic deep-sea sediments (*37*, *38*) and match carbon export fluxes measured in the 1990s in this area (*25*, *27*). In contrast, in situ and ex situ microprofiling of diffusive oxygen fluxes into sediments covered by algal aggregates showed elevated rates of 5 to 6 mmol O_2 m^{-2} day^{-1}, equivalent to carbon fluxes of 25 g C m^{-2} $year^{-1}$ (stations 7 and 8) (fig. S2). This suggests considerable microbial respiration (13 to 60%) of the algal carbon input. Accordingly, in cores covered by *Melosira* strands, oxygen penetration in the sediment was reduced to a few

Table 1. Distribution of algal aggregates and characteristics of sea-ice stations investigated. Methods are provided in the supplementary materials. Where available, averages and standard deviations are given. FYI, first-year ice; MYI, multiyear ice; n.d., not determined.

Ice station (no.)	1	2	3	4	5	6	7	8
Event*	PS80_224	PS80_237	PS80_255	PS80_277	PS80_323	PS80_335	PS80_349	PS80_360
Date	8/9/12	8/14/12	8/20/12	8/25/12	9/4/12	9/7/12	9/18/12	9/22/12
Latitude (N)	84°3.03'	83°59.19'	82°40.24'	82°52.95'	81°55.53'	85°06.11'	87°56.01'	88°49.66'
Longitude (E)	031°6.83'	078°6.20'	109°35.37	130°7.77'	131° 7.72'	122°14.72'	61°13.04'	58°51.81'
Sea-ice cover (%)	80	80	70	80	60	50	100	100
Ice thickness (m)	1.0–1.2	1.2–2.0	0.7–1.2	0.7–0.9	1.2–1.7	0.9–1.7	1.2–1.8	1.1–1.8
First/multiyear ice	FYI	FYI	FYI	FYI	FYI	FYI/MYI	FYI/MYI	FYI/MYI
Melt-pond cover (%)	40	20	40	50	10	30	20	20
Drift (knots)	0.14 ± 0.1	0.35 ± 0.2	0.55 ± 0.2	0.24 ± 0.1	0.26 ± 0.1	0.29 ± 0.2	0.01 ± 0.0	0.17 ± 0.1
Surface radiation (W m^{-2})†	150 ± 93	97 ± 59	60 ± 38	56 ± 45	62 ± 76	26 ± 23	11 ± 6	5 ± 3
PAR under ice (W m^{-2})	33	5	9	n.d.	3	2	<1	<<1
Atmospheric temperature (°C)	−1.5	−1.2	0.3	−0.3	−3.3	−1.6	−3.9	−10.1
Seawater temperature (5 m, °C)	−1.5	−1.5	−1.6	−1.5	−1.5	−1.5	−1.8	−1.7
Salinity (5 m)	33.0	33.2	32.8	31.2	30.6	30.3	33.1	32.9
Mixed layer depth (m)	15	21	16	23	20	20	31	30
Melt water (m)‡	0.5	0.7	0.7	1.1	2.3	2.2	0.8	0.9
Nitrate concentration (μM, ‡0–2 m)	2.89	3.08	0.29	0.42	0.1	0.08	0.97	0.49
N:Si/N:P (‡0–2 m)	3/10	2/10	0.3/2	0.1/2	0.03/1	0.02/0.4	0.02/0.3	0.3/2
^{14}C-PP (mg C m^{-2} day^{-1})§	62	9	19	36	39	10	5	4
New PP (g C m^{-2} $year^{-1}$)‡	16	7	12	7	9	10	16	15
Diatom contribution (%)‡	40	28	32	24	n.a.	n.a.	41	40
Sub-ice algal cover (%)	0.04	0.19	<0.01	n.d.	0.04	0.03	0.55	0.13
Ice algae composition	dv. algae‖	div. algae‖	*Melosira*	n.d.	*Melosira*	*Melosira*	*Melosira*	*Melosira*
Sea-floor algal cover (%)	0	0.03 ± 0.04	1.3 ± 0.4	0.33 ± 0.4¶	0.5 ± 0.2¶	0.8 ± 0.6¶	2.2 ± 0.7	10.4 ± 0.5
Sediment CPE (μg cm^{-3})	0.7 ± 0.1	1.4 ± 0.3	1.0 ± 0.3	1.0 ± 0.4	0.7 ± 0.2	0.5 ± 0.1	0.6 ± 0.1	0.8 ± 0.5
Sediment Chl*a*/CPE ratio (%)	10	17	22	22	18	14	14	14
Megafauna biomass (g wet weight m^{-2})	0.42	1.01	3.36	1.07	3.19	5.49	3.46	0.33
Gut CPE (μg cm^{-3})	n.d.	n.d.	130 ± 20	41 ± 15	30 ± 2	3 ± 1	48 ± 12	n.d.
Gut Chl*a*/CPE ratio (%)	n.d.	n.d.	43	49	66	22	51	n.d.
Ice algae composition sediment/gut	n.d.	n.d.	*Melosira*	*Melosira* div. algae‖	*Melosira* div. algae‖	*Melosira* div. algae‖	*Melosira*	*Melosira* div. algae‖
Ice algae C deposition (g C m^{-2})	0	0.5	20	5	7	11	32	156
Water depth (m)	4014	3485	3569	4161	4031	4355	4380	4374

*Supplementary data available at http://doi.pangaea.de/10.1594/PANGAEA.803293. †Refers to incoming global radiation at the surface. ‡Estimates based on seasonal inventories of the mixed-layer depth of the previous freezing season (see supplementary materials). §Depth-integrated rates for the water column euphotic zone (1% PAR under the ice). ‖Diverse algae included in various ratios: *Porosira* sp., *Pleurosigma*, *Nitzschia* sp., *Fragilariopsis* sp., *Entomoneis* sp, *Chaetoceros* sp., *Navicula* sp., *Cylindrotheca*, and other chain-forming pennate diatoms. ¶Estimates include discolored patches/degraded algal patches.

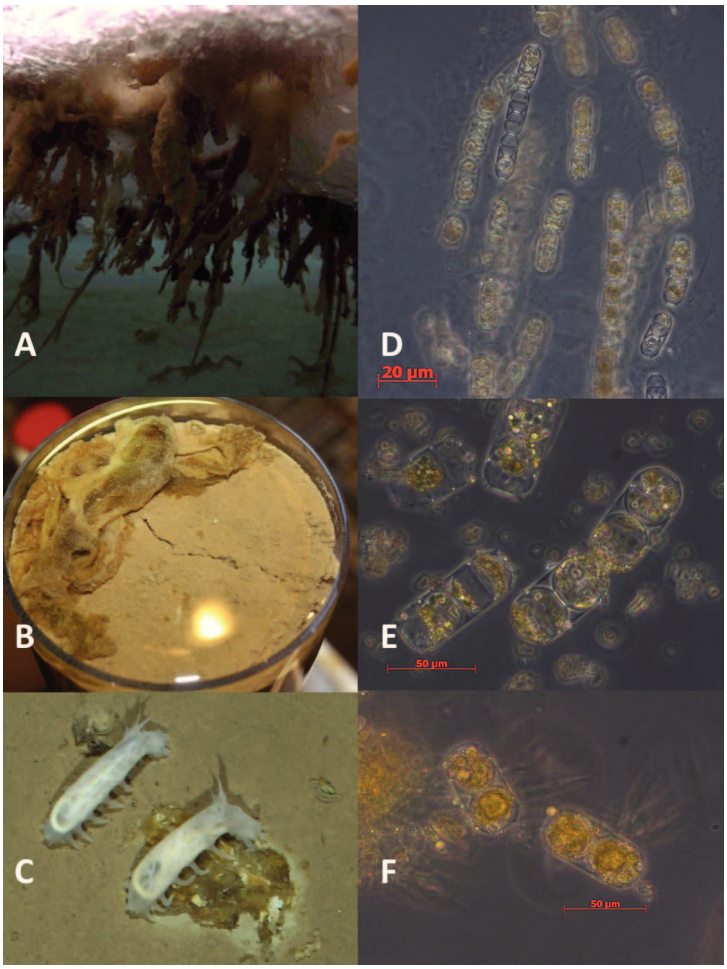

Fig. 2. *M. arctica* aggregations. Strands (~20 cm) of *Melosira* (**A**) under ice (station 7), (B) recovered from the sea floor (station 7), and (**C**) photographed in situ with *K. hyalina* grazing on deposits (station 3). (**D** to **F**) Microscopic images of *Melosira* cells from (A), (B), and (C) (extract of *Kolga* gut), respectively.

millimeters compared with the surrounding sediment, where oxygen penetrated >50 cm (fig. S1). Hence, if high exports of sea-ice algae had occurred regularly before 2012, oxygen penetration depth would have been less than observed, independent of the fresh *Melosira* deposits (*30*). Hence, we conclude that massive algal falls were rare.

Arctic climate models predict a further decline in the sea-ice cover, toward a largely ice-free summer in the Arctic in coming decades (*39*). Our observations support the hypothesis (*14*) that the current sea-ice thinning and increasing melt-pond cover may be enhancing under-ice productivity and ice-algae export, with ecological consequences from the surface ocean to the deep sea.

References and Notes

1. Cooperative Institute for Research in Environmental Sciences at the University of Colorado at Boulder, National Snow and Ice Data Center (NSIDC) Report (2012).
2. S. Rysgaard, M. Kühl, R. N. Glud, J. Würgler Hansen, *Mar. Ecol. Prog. Ser.* **223**, 15 (2001).
3. M. Nicolaus *et al.*, *J. Geophys. Res.* **115**, (C11), C11011 (2010).
4. M. Nicolaus, C. Katlein, J. A. Maslanik, S. Hendricks, *Geophys. Res. Lett.* **39**, L24501 (2012).
5. P. Bourgain, J. C. Gascard, *Deep Sea Res. Part I Oceanogr. Res. Pap.* **58**, 745 (2011).
6. B. Rabe *et al.*, *Deep Sea Res. Part I Oceanogr. Res. Pap.* **58**, 173 (2011).
7. J. E. Tremblay, J. Gagnon, in *Influence of Climate Change on the Arctic and Subarctic Conditions*, J. C. J. Nihoul, A. G. Kostianoy, Eds. (Springer Science Business Media B.V., Dordrecht, Netherlands, 2009), pp. 73–93.
8. K. R. Arrigo, G. van Dijken, S. Pabi, *Geophys. Res. Lett.* **35**, L19603 (2008).
9. P. Wassmann, D. Slagstad, I. Ellingsen, *Polar Biol.* **33**, 1641 (2010).
10. E. N. Hegseth, *Polar Res.* **17**, 113 (1998).
11. L. Legendre *et al.*, *Polar Biol.* **12**, 429 (1992).
12. P. Wassmann *et al.*, *Prog. Oceanogr.* **71**, 232 (2006).
13. M. Gosselin, M. Levasseur, P. A. Wheeler, R. A. Horner, B. C. Booth, *Deep Sea Res. Part II Top. Stud. Oceanogr.* **44**, 1623 (1997).
14. K. R. Arrigo *et al.*, *Science* **336**, 1408 (2012).
15. C. J. Mundy *et al.*, *Geophys. Res. Lett.* **36**, L17601 (2009).
16. A. Rösel, L. Kaleschke, *J. Geophys. Res.* **117**, C05018 (2012).
17. P. Wassmann, C. M. Duarte, S. A. Agustí, M. L. K. Sejr, *Glob. Change Biol.* **17**, 1235 (2011).
18. J. Maslanik, J. Stroeve, C. Fowler, W. Emery, *Geophys. Res. Lett.* **38**, L13502 (2011).
19. F. Nansen, *Northern Waters: Captain Roald Amundsen's Oceanographic Observations in the Arctic Seas in 1901* (Videnskab-Selskabets Skrifter 1, Matematisk-Naturvidenskabelig Klasse 1, Kristiania, Norway, 1906).
20. I. Melnikov, *The Arctic Sea Ice System* (Gordon and Breach Science Publishers, Amsterdam, 1997).
21. W. G. Ambrose Jr., C. Quillfeldt, L. M. Clough, P. V. R. Tilney, T. Tucker, *Polar Biol.* **28**, 784 (2005).
22. I. A. Melnikov, L. L. Bondarchuk, *Oceanology (Mosc.)* **27**, 233 (1987).
23. E. E. Syvertsen, *Polar Res.* **10**, 277 (1991).
24. J. Gutt, *Polar Biol.* **15**, 247 (1995).
25. A. Boetius, E. Damm, *Deep Sea Res. Part I Oceanogr. Res. Pap.* **45**, 239 (1998).
26. M. Klages *et al.*, in *The Arctic Organic Carbon Cycle*, R. Stein, R. W. Macdonald, Eds. (Springer, Heidelberg, 2003), pp. 139–167.
27. K. Fahl, E. Nöthig, *Deep Sea Res. Part I Oceanogr. Res. Pap.* **54**, 1256 (2007).
28. C. Lalande, S. Belanger, L. Fortier, *Geophys. Res. Lett.* **36**, L21604 (2009).
29. A. Rogacheva, *J. Mar. Biol. Assoc. U.K.* **92**, 1183 (2012).
30. Materials and methods are available as supplementary materials on *Science* Online.
31. B. D. Wigham, P. A. Tyler, D. S. M. Billett, *J. Mar. Biol. Assoc. U. K.* **83**, 175 (2003).
32. J. W. Deming, P. L. Yager, in *Deep-Sea Food Chains and the Global Carbon Cycle*, G. T. Rowe, V. Pariente, Eds. (Kluwer Academic, Dordrecht, Netherlands, 1992), pp. 11–28.
33. H. A. Ruhl, J. A. Ellena, K. L. Smith Jr., *Proc. Natl. Acad. Sci. U.S.A.* **105**, 17006 (2008).
34. C.-L. Wei *et al.*, *PLoS ONE* **5**, e15323 (2010).
35. U. Witte *et al.*, *Nature* **424**, 763 (2003).
36. A. G. Glover *et al.*, *Adv. Mar. Biol.* **58**, 1 (2010).
37. F. Wenzhöfer, R. N. Glud, *Deep Sea Res. Part I Oceanogr. Res. Pap.* **49**, 1255 (2002).
38. J. P. Fischer, T. G. Ferdelman, S. D'Hondt, H. Røy, F. Wenzhöfer, *Biogeosciences* **6**, 1467 (2009).
39. M. Y. Wang, J. E. Overland, *Geophys. Res. Lett.* **36**, L07502 (2009).

Acknowledgments: We thank the captain and crew of RV Polarstern expedition IceArc (ARK27-3) as well as our helicopter and meteorology teams for their excellent support with work at sea. This study was funded by the PACES (Polar Regions and Coasts in a Changing Earth System) program of the Helmholtz Association. Additional funds were made available to A.B. by the European Research Council Advanced Investigator grant 294757 and the Leibniz program of the Deutsche Forschungsgemeinschaft, and to B.R. for the Bundesministerium für Bildung, Wissenschaft, Forschung und Technologie project 03F0605E. Supplementary data are available at http://doi.pangaea.de/10.1594/PANGAEA.803293.

Affiliations and contributions of the RV Polarstern ARK27-3-Shipboard Science Party

Writing team: Antje Boetius[1,2,3] with all coauthors. Ice physics and remotely operated vehicle (ROV) surveys: Stefan Hendricks,[1] Christian Katlein,[1] Thomas Krumpen,[1] Marcel Nicolaus[1]; Sea-ice biology: Mar Fernández-Méndez,[1,2] Ilka Peeken[1,3]; Oceanography and nutrients: Karel Bakker,[5] Catherine Lalande,[1] Benjamin Rabe,[1] Raquel Somavilla[1]; Deep-sea surveys, sampling and measurements: Sebastian Albrecht,[4] Christina Bienhold,[1] Antje Boetius,[1] Janine Felden,[1] Antonina Rogacheva,[6] Elena Rybakova,[6] Frank Wenzhöfer

Fieldwork and scientific discussions: Shipboard Scientific Party, including other contributors listed in the supplementary materials. [1]Alfred Wegener Institute, Helmholtz Center for Polar and Marine Research, 27515 Bremerhaven, Germany. [2]Max Planck Institute for Marine Microbiology, 28359 Bremen, Germany. [3]MARUM, Center for Marine Environmental Sciences, University Bremen, 28334 Bremen, Germany. [4]FIELAX Gesellschaft für wissenschaftliche Datenverarbeitung mbH, 27568 Bremerhaven, Germany. [5]NIOZ Royal Netherlands Institute for Sea Research, 1790 AB Den Burg, Netherlands. [6]P. P. Shirshov Institute of Oceanology, Russian Academy of Sciences, 117997 Moscow, Russia.

Supplementary Materials

www.sciencemag.org/cgi/content/full/science.1231346/DC1
Materials and Methods
Figs. S1 and S2
Movies S1 and S2
References (*40*–*50*)

10 October 2012; accepted 31 January 2013
Published online 14 February 2013;
10.1126/science.1231346

Chapter II

Floating ice-algal aggregates below melting Arctic sea ice.

Philipp Assmy[1], Jens K. Ehn[2], Mar Fernández-Méndez[3,4], Haakon Hop[1], Christian Katlein[3], Arild Sundfjord[1], Katrin Bluhm[5], Malin Daase[1], Anja Engel[6], Agneta Fransson[1], Mats A. Granskog[1], Stephen R. Hudson[1], Svein Kristiansen[7], Marcel Nicolaus[3], Ilka Peeken[3,8], Angelika H. H. Renner[1], Gunnar Spreen[1], Agnieszka Tatarek[9], and Jozef Wiktor[9].

[1] Norwegian Polar Institute, Fram Centre, Tromsø, Norway, [2] University of Manitoba, Centre for Earth Observation Science, Winnipeg, Canada, [3]Alfred Wegener Institute, Helmholtz Center for Polar and Marine Research, [4]Max Planck Institute for Marine Microbiology, [5]Akvaplan-niva, Fram Centre, Tromsø, Norway, [6]GEOMAR Helmholtz Centre for Ocean Research Kiel, [7]Department of Arctic and Marine Biology, University of Tromsø [8]MARUM - Center for Marine Environmental Sciences, University of Bremen, [9]Institute of Oceanology, Polish Academy of Science, Poland.

PLoS One (2013) 8(10): e76599

OPEN ACCESS Freely available online

PLOS ONE

Floating Ice-Algal Aggregates below Melting Arctic Sea Ice

Philipp Assmy[1*], Jens K. Ehn[2], Mar Fernández-Méndez[3,4], Haakon Hop[1], Christian Katlein[3], Arild Sundfjord[1], Katrin Bluhm[5], Malin Daase[1], Anja Engel[6], Agneta Fransson[1], Mats A. Granskog[1], Stephen R. Hudson[1], Svein Kristiansen[7], Marcel Nicolaus[3], Ilka Peeken[3,8], Angelika H. H. Renner[1], Gunnar Spreen[1], Agnieszka Tatarek[9], Jozef Wiktor[9]

1 Norwegian Polar Institute, Fram Centre, Tromsø, Norway, **2** University of Manitoba, Centre for Earth Observation Science, Winnipeg, Canada, **3** Alfred-Wegener-Institut Helmholtz-Zentrum fùr Polar- und Meeresforschung, Bremerhaven, Germany, **4** Max Planck Institute for Marine Microbiology, Bremen, Germany, **5** Akvaplan-niva, Fram Centre, Tromsø, Norway, **6** GEOMAR Helmholtz Centre for Ocean Research Kiel, Kiel, Germany, **7** Department of Arctic and Marine Biology, University of Tromsø, Tromsø, Norway, **8** MARUM - Center for Marine Environmental Sciences, University of Bremen, Bremen, Germany, **9** Institute of Oceanology, Polish Academy of Science, Sopot, Poland

Abstract

During two consecutive cruises to the Eastern Central Arctic in late summer 2012, we observed floating algal aggregates in the melt-water layer below and between melting ice floes of first-year pack ice. The macroscopic (1-15 cm in diameter) aggregates had a mucous consistency and were dominated by typical ice-associated pennate diatoms embedded within the mucous matrix. Aggregates maintained buoyancy and accumulated just above a strong pycnocline that separated meltwater and seawater layers. We were able, for the first time, to obtain quantitative abundance and biomass estimates of these aggregates. Although their biomass and production on a square metre basis was small compared to ice-algal blooms, the floating ice-algal aggregates supported high levels of biological activity on the scale of the individual aggregate. In addition they constituted a food source for the ice-associated fauna as revealed by pigments indicative of zooplankton grazing, high abundance of naked ciliates, and ice amphipods associated with them. During the Arctic melt season, these floating aggregates likely play an important ecological role in an otherwise impoverished near-surface sea ice environment. Our findings provide important observations and measurements of a unique aggregate-based habitat during the 2012 record sea ice minimum year.

Citation: Assmy P, Ehn JK, Fernández-Méndez M, Hop H, Katlein C, et al. (2013) Floating Ice-Algal Aggregates below Melting Arctic Sea Ice. PLoS ONE 8(10): e76599. doi:10.1371/journal.pone.0076599

Editor: Syuhei Ban, University of Shiga Prefecture, Japan

Received April 23, 2013; **Accepted** August 26, 2013; **Published** October 16, 2013

Funding: This work was supported by the Centre for Ice, Climate and Ecosystems (ICE) at the Norwegian Polar Institute and the Alfred-Wegener-Institut Helmholtz-Zentrum für Polar- und Meeresforschung. The funders had no role in study design, data collection and analysis, decision to publish, or preparation of the manuscript.

Competing interests: The authors have declared that no competing interests exist.

* E-mail: Philipp.Assmy@npolar.no

Introduction

The ongoing thinning and loss of Arctic sea ice will lead to changes in the surface energy budget of the Arctic Ocean [1,2] and will have far-reaching ramifications for both sympagic (ice-associated) and pelagic ecosystems [3]. Nonetheless, thorough documentation of effects on Arctic marine biota in response to climate change is limited, especially for planktonic and ice-associated ecosystems [4]. Some knowledge gaps are attributable to the limited amount of quantitative data on production, consumption and biomass for Arctic marine ecosystems [5]. A recent study revealed significant changes in planktonic microbial community structure before and after the September 2007 record sea ice minimum [6]. Achieving greater understanding of these processes is important because the increased and earlier loss of Arctic sea ice will not only affect the timing of ice algal and phytoplankton blooms [7], but could also lead to trophic mismatch scenarios between primary producers and their dependant grazers [8].

Melting of summer sea ice results in habitat deterioration for ice-associated organisms and the formation of a stratified surface meltwater layer [9,10]. Ice algae, at the base of the Arctic sea ice ecosystem, have to cope with being released into freshening surface water during the melt season. Due to their inherent stickiness, they are prone to aggregation [11] and subsequent sedimentation [12]. Vertical flux and sedimentation of ice-algal material will transfer energy to pelagic and benthic ecosystems [13-16] and deprive ice-associated fauna of their food resource [9]. In order to bridge the gap between release from melting sea ice in summer and reincorporation into the ice

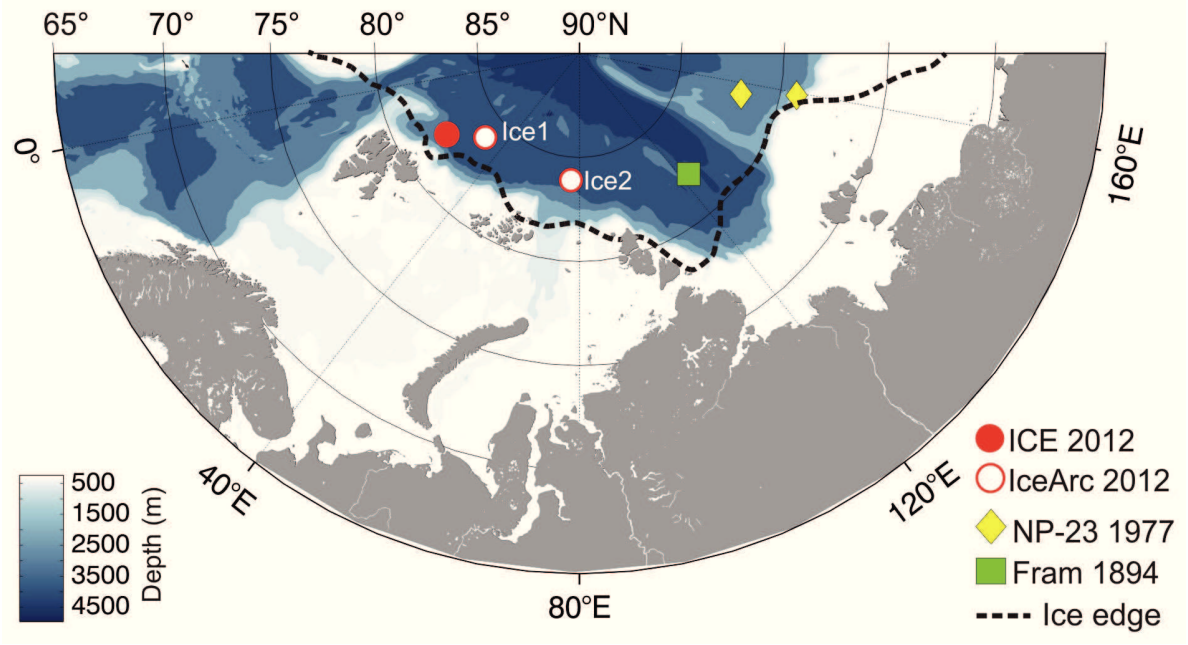

Figure 1. Ice-algal aggregate observations recorded in the Eastern Central Arctic during the Centre for Ice, Climate and Ecosystems (ICE12) cruise with RV *Lance*, IceArc expedition ARK-XXVII/3 with RV *Polarstern*, the Russian North Pole drift station NP-23 and the Fram Expedition 1893-1896. The broken line and blue colour scale indicate the approximate position of the ice edge at the end of July 2012 and the sea floor depth, respectively.

doi: 10.1371/journal.pone.0076599.g001

at the onset of freezing during autumn, ice algae must rely on other means to stay in close proximity to the sea-ice habitat, especially over the deep Central Arctic Basin. A recent study [17] suggests that progressively thinning Arctic sea ice can also lead to new ice-associated habitats. The authors propose that incorporation of algal cells in the soft ice of open melt ponds could account for the algal masses they observed at the surface of refrozen melt ponds in early autumn. Buoyant, free-floating ice-algal aggregates have previously been observed in the Arctic [18-21], but due to their patchy distribution little is known about their ecological significance during the melt season. Moreover, their potential role in seeding the next spring bloom has not been considered thus far. In addition, current models of ice algal primary production and biomass do not account for these aggregations or the metre-long mats and strands formed by the under-ice diatom *Melosira arctica* [20], and therefore underestimate the contribution of ice algae to total primary production in the Arctic Ocean [22].

Large numbers of ice-algal aggregates were encountered during two consecutive research cruises to the Eastern Central Arctic Ocean in summer 2012: (1) the Centre for Ice, Climate and Ecosystems (ICE) cruise with RV *Lance* (ICE12) and (2) IceArc expedition ARK-XXVII/3 with RV *Polarstern*. In order to elucidate the significance of these aggregates, we sampled and quantified their abundance, biomass and production using three different approaches: (i) trapping of aggregates in an ice hole ("inverted sediment trap" approach), (ii) collection by scuba divers, and (iii) under-ice video transects with a remotely operated vehicle (ROV). Combined, these different approaches enabled us to extrapolate our findings to a square metre scale and assess the significance of the floating ice-algal aggregates for the ice-associated ecosystem during the oligotrophic summer months.

Materials and Methods

Study area

The three drift ice stations were situated over the deep Arctic basin and well north of the ice edge (Figure 1). The pack ice in the area was dominated by first year ice (FYI) and featured well-developed melt ponds. The first long drift ice station was occupied from 26 July to 3 August 2012 during the ICE12 cruise and initially situated at 82.5° N, 21° E north of Svalbard while the two shorter drift ice stations, centred at 84° N, 31° E (station Ice1) and 84° N, 78° E (station Ice2) on 9–11 and 14–16 August 2012 respectively, were undertaken during the subsequent IceArc expedition.

ICE12

Sample collection and preparation. Throughout the drift ice station from 26 July to 3 August, conductivity, temperature and depth (CTD) profiles were taken daily using a rosette system (Seabird Electronics SBE911) deployed from the side of the ship. Seawater samples were collected on 26 and 30 July and daily from 1 to 3 August at five depths (surface, 10, 50, 100 m, Chl *a* maximum). Profiles of salinity, temperature,

and dissolved oxygen from the under-ice water column were obtained on 28, 30 and 31 July and 1 August using a hand-held MicroCat sensor (Seabird Electronics 37-SM) lowered through an ice hole. Subsequently, water samples from the meltwater layer underneath the sea ice were pumped through the same ice hole. Additionally video profiles (GoPro Hero2) provided information on the distribution of floating aggregates in cracks and openings in the sea ice. Three video profiles were obtained: one on 29 July at 19:30 GMT and two on 31 July at 08:30 -09:00 GMT through the ice hole used to collect the aggregates (further information below). On 29 July at 13:00 GMT, an additional video profile was obtained through an ice crevice in close proximity to the ice hole. Biological sea ice samples were collected on 28 July and 1 August using an ice corer with an inner diameter of 9 cm (Mark II coring system, KOVACS Enterprises, Inc., USA). Immediately after collection, ice cores were cut into 10-20 cm thick sections with a stainless steel saw, transferred into polyethylene zip-lock bags, stored dark and melted on board the ship at 4°C. Sea ice samples were melted directly, not in filtered seawater, because nutrient samples were taken from the same core sections. Comparison between direct melting and melting in filtered seawater at 4°C showed no significant differences in taxonomic composition of sea ice assemblages [23]. Seawater and meltwater samples as well as melted sea ice samples to be analysed for chlorophyll (Chl *a*), particulate organic carbon (POC) and nitrogen (PON) were filtered onto 25 mm Ø GF/F and pre-combusted (500°C for 4 h) GF/F filters, respectively. Between 500 and 1000 mL of seawater, and meltwater and between 150 and 500 mL of melted sea ice, were sampled for Chl *a*, POC and PON. One replicate sample per depth was collected for each parameter for seawater and meltwater, while sea ice samples were obtained from triplicate ice cores collected within 10 cm of each other. Fifty mL were sampled per analysis of ammonium. On 26 and 29 July, aggregates were collected for species identification with a coarse-meshed sieve from the side of open melt ponds and through a specially drilled ice hole also used to collect accumulated aggregates (further details below). Aggregate samples used for iodine, Chl *a*, and transparent exopolymer particle (TEP) analysis were collected directly underneath the sea ice on 31 July by divers using a slurp gun (modified 3.5 L Trident® suction gun).

Chemical and biological measurements. Ammonium was measured on fresh samples directly on board according to Solóranzo [24]. Aggregate samples for iodine speciation were filtered over polycarbonate filters (2 µm pore size) and the filtrate stored frozen (-20°C) until analysis. Iodide was determined by cathodic stripping square wave voltammetry according to the methods of Campos [25] and Luther et al. [26], with a detection limit of 0.1 to 0.2 nmol L^{-1} and a precision better than 5%. High iodide concentrations can be used as a measure of phytoplankton senescence [27].

Eight subsamples (0.5 mL each) of a diver-collected aggregate with a total volume of 38 mL were taken for Chl *a* analysis, after having removed all supernatant seawater. Chl *a* was extracted with 100% methanol at 5°C for 12 h [28] and measured fluorometrically using a Turner Fluorometer 10-AU (Turner Design, Inc.). Phaeopigments were measured after acidification with two drops of 5% HCl. Samples of POC and PON were exposed overnight to 32% HCl prior to analysis in order to remove all particulate inorganic carbon, and were thereafter folded into tin capsules. The carbon content was determined using a CHN elemental analyzer (Euro EA 3000).

For TEP analysis, two diver-collected aggregates were transferred into 15 mL centrifuge tubes and immediately frozen at -20°C. After thawing, the samples were each suspended in 169 mL of <0.2 µm filtered ISOTON (Beckmann Coulter) and divided into subsamples. Subsamples of 3-5 mL, with 4 replicates each, were filtered onto 25 mm polycarbonate filters (Nucleopore 0.4 µm pore size) and stained with Alcian Blue. TEP was measured with the colorimetric method according to Engel [29]. TEP concentrations (given in Gum Xanthan equivalents [Xeq.] L^{-1}) were converted to carbon (TEP-C, µg C L^{-1}) using a conversion factor of 0.63 [30]. In order to normalize TEP-C to bulk aggregate carbon, the POC concentration of the subsamples was also determined. POC filters were analyzed with an elemental analyser (EuroVektor EA). Measurements of TEP subsamples from samples one and two had a precision of 5 and 15 %, respectively, while measurements of POC subsamples varied by 11%.

For species identification and determination of assemblage composition, aggregates were transferred into brown glass bottles, preserved with a buffered aldehyde mixture (glutaraldehyde: 0.1% final concentration and hexamethylenetetramine-buffered formaldehyde: 1% final concentration) as suggested by Tsuji and Yanagita [31] and stored cool (5°C) and dark for subsequent counting in the home laboratory. An aggregate volume of 0.1–0.2 mL was settled in sedimentation chambers for 24 h. Cells were identified and enumerated using a Nikon Ti-U inverted light and epifluorescence microscope according to the method of Throndsen [32] and counted at 60× magnification. Each sample was examined until at least 500 cells had been counted.

Radiation measurements. Ramses-ACC-VIS hyperspectral radiometers (TriOS Mess- und Datentechnik GmbH) were used to measure incoming energy fluxes at the ice surface and transmitted fluxes at the underside of the ice. One instrument was mounted 1.5 m above the ice surface, levelled and facing upwards, while a second was swum by a diver with semi-closed rebreather (60% O_2) below the ice between two wooden bars placed through core holes and connected by a rope with marks every metre. The method was repeated three times along 30 to 35-m profiles covering a mix of bare ice, and various melt ponds. The spectral energy fluxes between 400 and 700 nm were converted to photon fluxes and integrated to get values for photosynthetically active radiation (PAR).

By identifying measurements made more than about 2 m from pond edges, typical transmittance values for PAR were determined for the various surface types (bare white ice, dark ponds and bright, blue ponds) as in Hudson et al. [1]. The investigated ice floe was then classified into these three surface types (and open water) using thresholds in the red and blue channels, and the resulting surface areas were used to calculate floe-scale transmittance [1].

"Inverted sediment trap" approach and relative under-ice current velocities. We collected all aggregates

accumulating in a 3.2 m^2 hole cut through the ice at 12 h intervals from 29 to 1 August to obtain an estimate of aggregate accumulation over time in the surface meltwater layer. We likely underestimated the amount of aggregates as not all of them would have floated up into the ice hole. The aggregate material from each sampling interval was dried at 60°C and the dry weight determined. Triplicate subsamples of 0.5-2 µg dry weight were analyzed for POC and PON. Triplicate measurements had a precision better than 7% for both POC and PON.

Relative current velocities (relative to the drifting ice floe) were measured below the ice with an ice-tethered acoustic doppler current profiler (Nortek 600 kHz Aquadopp) in the vicinity of the ice hole. The shallowest data cell was located about 1.5 m below the ice. These data (means) were extrapolated to 0.2 m below the under-ice surface through a log decay formulation (law-of-the wall approximation [33]). Mean relative current velocities for each sampling interval were then used to extrapolate the accumulated aggregate biomass to the area sampled by our "inverted sediment trap". The aggregate flux was calculated by correcting the accumulated aggregate biomass for the time between each sampling interval.

IceArc

Sample collection. Aggregates were collected together with ambient seawater using a plastic spoon or bucket. This aggregate-seawater mixture was sub-sampled for POC, PON, pigments and net primary production (NPP) analysis. In order to estimate the dilution factor with ambient seawater, individual aggregates of known volume (10-25 ml) were filtered through pre-combusted GF/F filters for POC and PON analyses as stated above. For pigment analysis including Chl *a*, 1-40 mL of aggregate-seawater mixture, 1 L of melted sea ice, 1 L of seawater and 0.5 L of melt pond water was sampled at stations Ice1 and Ice2 respectively. The ice core was cut into 10 cm sections and each section melted for 24 h in 2 L of 0.2 µm filtered seawater. The samples were filtered on GF/F filters and immediately frozen in liquid nitrogen. Sample storage prior to analysis was at -80°C. Pigments were measured with high-performance liquid chromatography as described in Taylor et al. [34].

For NPP experiments, ice-algal aggregates were collected from the same aggregate-seawater mixture sampled for POC, PON and pigment analysis; seawater was collected 0–2 m below the ice with a peristaltic pump while water from closed melt ponds (without connection to the seawater below) was sampled with a hand pump; ice cores were taken as stated above and divided in two sections: top and bottom. The aggregate mixture, seawater and melt pond samples were directly transferred into incubation bottles (cell culture bottles, Corning Inc., Corning, NY, USA). The ice core sections were melted in the dark for 24 h at 4°C prior to incubation. No filtered seawater was added during melting to avoid addition of nutrients.

Chl *a* concentrations and NPP of the aggregate-seawater mixture were corrected for dilution by a factor calculated from the POC measurements performed in the aggregate-seawater mixture and in individual aggregates in order to derive aggregate specific Chl *a* concentrations and NPP rates.

All samples were collected within 500 m of each other at both ice stations. Water and sea ice samples were taken on the same day while melt pond samples were obtained on the subsequent day but always within 24 h of the other samples.

ROV transect analysis

Detection of aggregates and their spatial distribution was monitored with an upward-looking video system (Osprey, Tritech, Aberdeen, UK) mounted onto a remotely operated vehicle (V8Sii ROV, Ocean Modules, Åtvidaberg, Sweden) navigated directly under sea ice at stations Ice1 and Ice2 [35].

Aggregates were automatically identified on the video images using a threshold algorithm. Images were extracted each 5 sec from the dive videos. All images were registered according to the distance between camera and ice given by the acoustic altimeter value and cropped leaving the central part of the image in order to remove overlays and edge effects. Images with an ROV tilt of more than 10° and those recorded deeper than 5 m were discarded. Only the green channel of the RGB image was used for analysis, as it showed the clearest aggregate signal. Pixels with a green value <100 (dark pixels, range 0 to 255) were considered as algae. Detection was verified manually. To average over the spatially unevenly distributed data (some locations were photographed several times), all records were grouped in 3×3 m cells. Means were calculated for each cell. Analysis showed that different cell size choices did not significantly change calculated numbers with the exception of total covered area. ROV video material at station Ice1 consisted of four dives covering a total area of 5184 m^2 and 3 h 52 min of dive video, while at station Ice2 five dives covered a total area of 1809 m^2 and 3 h 51 min of dive video. Due to ROV-attitude or wrong detection, 34% and 35% of the data from stations Ice1 from station Ice2, respectively, had to be discarded. For details on ROV-dive statistics and up-scaling calculations see Tables S1 and S2 respectively.

Net primary production

During the IceArc cruise NPP was measured using the ^{14}C uptake method [36] with minor modifications. All samples were spiked with 1µCi mL^{-1} of ^{14}C sodium bicarbonate. At the end of each incubation period, samples were filtered onto 0.2 µm nitrocellulose filters and the particulate radioactive carbon uptake was determined by liquid scintillation counting using Filter count (PerkinElmer) scintillation cocktail. The average of the dark values was subtracted from the light triplicates. Dissolved inorganic carbon (DIC) was estimated for each sample using the flow injection system [37] and the DIC concentration was taken into account to calculate the amount of labeled bicarbonate incorporated into the cell.

Aggregates were incubated at typical under-ice irradiances, while seawater, sea ice and melt pond samples were incubated at a range of irradiances to calculate the depth-integrated NPP. Aggregates, diluted in ambient water, were mixed well and distributed in 6 cell culture plastic bottles of 10 mL each. One set of triplicates was incubated at 50 µmol photons m^{-2} s^{-1} and the other in the dark at -1.3°C for 24 h (long enough incubation

to measure net and not gross primary production). Triplicate measurements for the aggregates had a precision of 7 and 17 % for stations Ice1 and Ice2, respectively. For direct comparison with depth-integrated seawater, melt pond and sea ice NPP, the aggregate NPP was normalized to the dilution-corrected Chl *a* concentration (see sample collection) and up-scaled based on the ROV surveys (Table S3).

Seawater, sea ice and melt pond samples were distributed in 10 cell culture plastic bottles of 20 mL each. Subsequently, they were incubated for 12 h at -1.3°C under a range of light irradiances (0–420 µmol photons m^{-2} s^{-1}). *In situ* NPP rates were inferred for each metre of water depth and for each 10 cm of sea ice and melt pond depth from the Chl *a* normalized photosynthesis-irradiance curves (P-E curves) (r^2 = 0.83-0.96) [38], as a function of the PAR available at each depth. These values were calculated from the daily average incoming PAR, measured with a pyranometer mounted on the ship, and the light attenuation coefficients of 1.5 m^{-1} for sea ice [39] and 0.1 m^{-1} for Atlantic-influenced Arctic seawater, based on data from the TransArc expedition ARK-XXVI/3 to the same area during the previous year. Subsequently, these Chl *a*-normalized rates were multiplied by the measured Chl *a* profile and summed up to give the depth-integrated NPP rates. For the water column, NPP was integrated over the euphotic zone (1% light depth).

Sea ice observations and station data from the IceArc cruise are freely available in PANGAEA, the Data Publisher for Earth & Environmental Science (http://doi.pangaea.de/10.1594/PANGAEA.803221 and http://doi.pangaea.de/10.1594/PANGAEA.803115) while aggregate NPP, TEP and species composition, "inverted sediment trap" calculations and the oxygen profiles are archived in the Marine data-base of the Norwegian Polar Institute and publicly available under http://data.npolar.no/dataset/67eede8a-fe8f-11e2-ba11-005056ad0004.

Results

ICE12 cruise

The investigated ice floe consisted of FYI and covered a total area of 0.5 km^2. The ice was characterized by a modal thickness of 0.8 m measured using an airborne electromagnetic induction device (the "EM-bird") towed above the ice by helicopter [40] and a 23% melt pond fraction based on aerial photography [1]. The average PAR transmittance of white ice, bright ponds and dark ponds was 0.17, 0.32, and 0.61, respectively. For the investigated ice floe, the calculated average transmittance for PAR was 0.25. On the three days that radiation transects were made (all within an hour of local noon under cloud cover), the incident PAR averaged 533 µmol m^{-2} s^{-1}, with a standard deviation and range of 152 µmol m^{-2} s^{-1} and 288-857 µmol m^{-2} s^{-1}, respectively. Melting was evidenced by actual thinning of the sea ice measured during the occupation of the drift ice station [1]. A roughly 0.5 m thick freshwater layer was separated from the underlying seawater by a sharp density gradient detected in cracks and openings in the ice at approximately the ice-water interface. Meltwater was also observed by scuba divers to accumulate in domes and pock holes on the ice bottom. Throughout the occupation of the drift ice station, we observed macroscopic aggregates floating within the meltwater layer beneath sea ice and accumulating in under-ice domes, open melt ponds (Figure 2A) and leads. The majority maintained buoyancy just above the sharp pycnocline that separated meltwater and seawater layers (Figure 2B).

The aggregates were relatively compact, had a mucous consistency and were light to dark brown in colour (Figure 2B-D). Whitish aggregates were frequently observed drifting at the surface of open melt ponds or settled onto the melt pond bottom. The aggregates were dominated by typical ice-associated pennate diatoms (Figure 2E, F), in particular *Navicula pelagica*, *Hantzschia weyprechtii*, *Entomoneis paludosa* and *Cylindrotheca closterium* (Table S4). The aggregates were densely packed with cells as illustrated by abundances of >2×10^5 cells mL^{-1} in case of *N. pelagica*. Centric diatoms were represented by only two species, the epiphytic *Attheya septentrionalis* and *Thalassiosira bioculata* (Table S4). Cells were embedded in a mucous matrix (Figure 2E) and a large fraction of embedded diatoms consisted of empty frustules (Figure 2F). Non-diatom protists were numerically dominated by flagellates and contributed 6-24% of the total protist abundance (Table S4). High abundances of naked ciliates were observed in the aggregates collected on 26 July (Table S4). The species could not be identified with certainty, but were possibly represented by holotrichous ciliates typically found associated with sea ice [19]. These ciliates were actively feeding within the mucous matrix of the aggregates. Larger grazers included ice amphipods, in particular *Apherusa glacialis* and *Onisimus glacialis*, feeding at the surface of the aggregates (Figure 2D). Iodide concentrations in aggregate filtrate were 2.5-fold elevated compared to ambient seawater (Figure S1), while Chl *a* concentrations of 15 ±1 mg per liter of aggregate were roughly five orders of magnitude higher than in the bottom 20 cm of sea ice (1.35 ±1.08 µg L^{-1}), the under-ice water column (0.22 ±0.11 µg L^{-1}) and melt ponds that had not melted through (0.05 µg L^{-1}). Assuming a thickness of 0.5 m for the meltwater layer (a square meter would thus correspond to 500 liter), that the majority of aggregates floated within this layer and were similar in volume to the one measured (38 mL), the Chl *a* concentration of aggregates in a random liter of seawater corrected for their square metre abundances (Table 1) would amount to 0.93 µg L^{-1} at station Ice1, 5.97 µg L^{-1} at station Ice 2 and 0.28 µg L^{-1} during ICE12. These estimates are in the range of those measured for the sea ice and under-ice water column.

TEP concentrations of the two aggregates were 4102 ±205 and 6801 ±997 µg Xeq. L^{-1}. In the case of the first aggregate, TEP concentrations normalized to aggregate carbon amounted to 0.241 ± 4.7 x10^{-5} µg Xeq. $µg^{-1}$ C, which corresponds well to earlier observations of aggregates of miscellaneous origin [41]. When converted to carbon, TEP accounted for 15% of bulk aggregate carbon. The aggregate TEP-C:POC ratio lies within the range 10-20% reported previously for seawater of the North Atlantic [30].

During the six sampling intervals between 29 July and 1 August, the ice floe drifted 64 km with a largely southward component and a mean velocity of 0.22 ±0.06 m s^{-1} (Figure 3A-C). Mean under-ice current velocities relative to the drifting ice

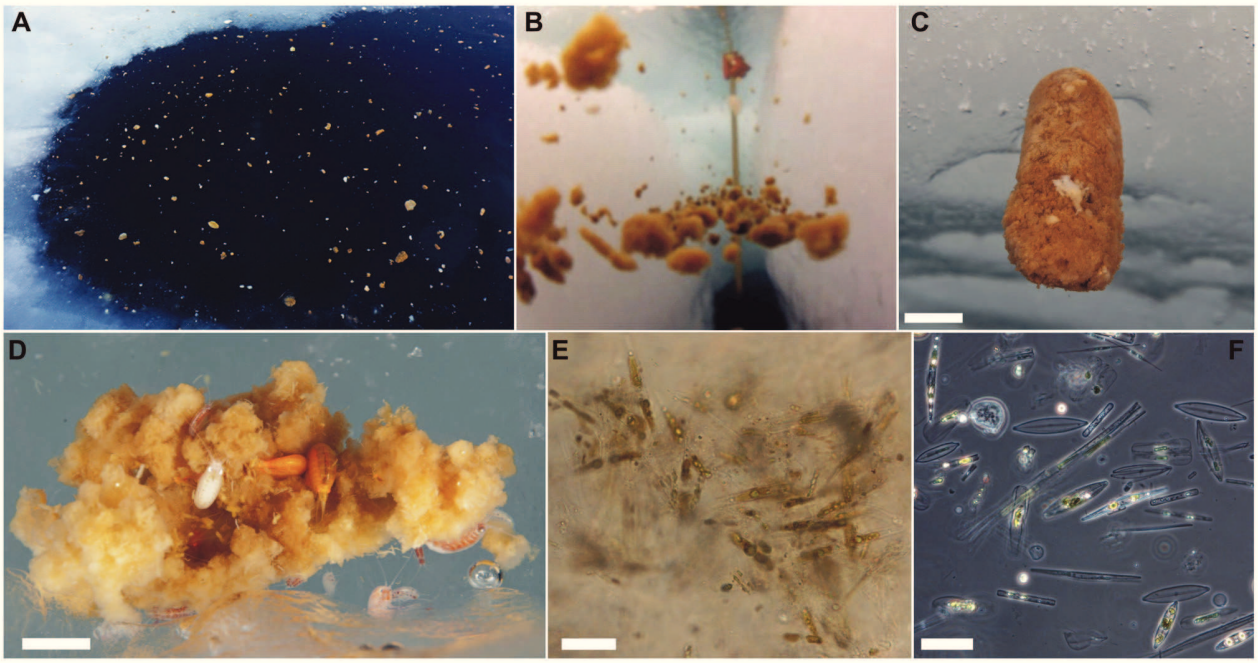

Figure 2. Distribution and composition of ice-algal aggregates. (A) Mass accumulation of aggregates in open melt pond. (B) Accumulation of aggregates at the interface between melt and seawater layers in a natural crack through the ice. (C) Composite aggregate floating beneath sea ice. (D) Porous aggregate colonized by the ice amphipod species *Apherusa glacialis* (white) and *Onisimus glacialis* (yellow). (E) Light micrograph of pennate diatoms, mainly *Hantzschia weyprechtii*, embedded in the mucous matrix. (F) Light micrograph of mainly empty frustules of different pennate diatom species. Scale bar = 0.5 m(A), 5 cm (C), 1 cm (D) and 20 µm (E and F). In panel B the measuring bar (1 m) lowered into the ice crack in the background serves as a scale for orientation. Picture A © Jenny E. Ross, pictures C and D © Peter Leopold.

doi: 10.1371/journal.pone.0076599.g002

Table 1. Aggregate parameters derived from ROV-dives and POC and PON measurements at the scale of the individual aggregate (mg L^{-1}) and up-scaled to area (mg m^{-2}) at stations Ice1 and Ice2.

	Mean	Median						
	Abundance	Diameter	POC		PON		Chl *a*	
Station	(Agg. m^{-2})	(cm)	(mg C L^{-1})	(mg C m^{-2})	(mg N L^{-1})	(mg N m^{-2})	(mg L^{-1})	(mg m^{-2})
Ice1	0.79	1.04	399	0.19	56	0.03	3.67	0.0017
Ice2	5.06	0.87	873	1.33	94	0.17	4.16	0.0063
ICE12	0.24	–	–	0.74	–	0.10	15	–

Aggregate abundance and POC and PON stocks estimated with the "inverted sediment trap" approach during cruise ICE12. See Tables S1 and S2 for details on the ROV-statistics and up-scaling calculations.

doi: 10.1371/journal.pone.0076599.t001

ranged between 0.08 and 0.19 cm s^{-1} during the sampling period and showed a slight increase with depth. Mean relative current velocity showed a linear relationship with accumulated POC, except for the highest POC value (Figure S2). The cumulative aggregate biomass over the entire sampling period amounted to 0.4 g C m^{-2}, while aggregate biomass for each sampling interval increased from initially 48 mg C m^{-2} to 200 mg C m^{-2} by 31 July and declined thereafter (Figure 3D). The aggregate flux increased from initially 104 mg C m^{-2} d^{-1} to 393 mg C m^{-2} d^{-1} by 31 July and declined thereafter to values as low as 3 mg C m^{-2} d^{-1} by 1 August. The mean (±SD) molar POC:PON ratio of the aggregates was 9.7 ±0.7. Corrected for mean relative under-ice current velocities calculated for each sampling interval, we estimated an aggregate standing stock of 0.74 mg C m^{-2} and abundance of 0.24 aggregates m^{-2} over a 499 m^2 catchment area.

In an adjacent but smaller ice hole, exceptionally high ammonium concentrations of 2.5 µmol L^{-1} were measured

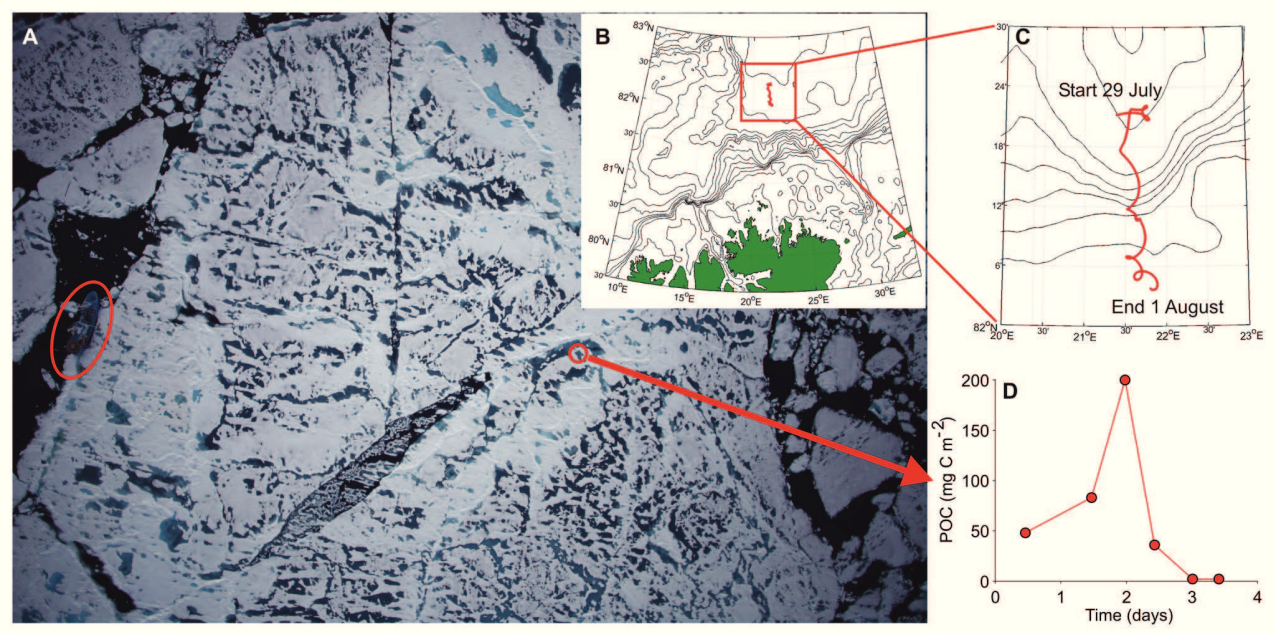

Figure 3. Aerial photograph (A) of the investigated ice floe during ICE12. Map (B) and close-up (C) of the 64 km ice floe drift trajectory north of Svalbard. "Inverted sediment trap" ice-algal aggregate POC time series covering the sampling period from 29 July-1 August (D). The red oval highlights RV *Lance* while the red circle indicates the approximate location of the ice hole. The length of RV *Lance* (60.8 m) can be used as a scale.

doi: 10.1371/journal.pone.0076599.g003

during the peak aggregate accumulation on 31 July. Oxygen profiles measured through the same ice hole showed a decrease in oxygen concentrations in the upper 3 m of the under-ice water column between the two sampling occasions on 30 and 31 July 2012 (Figure S3).

IceArc cruise

Sea ice covered 80% of the ocean surface and was dominated by FYI with a thickness of 1.0-1.2 m and a melt pond coverage of 40% at station Ice1, and a thickness of 1.2-2.0 m and a melt pond coverage of 20% at station Ice2 [42]. Different types of algal aggregates were observed at the eight ice stations occupied during the IceArc cruise. A diverse community of pennate diatoms dominated the aggregates at stations Ice1 and Ice2, while *Melosira arctica*-dominated algal aggregates were found at the remaining ice stations [42]. We will only discuss the former aggregates as the latter have been presented elsewhere [42]. The aggregates collected at stations Ice1 and Ice2 were very similar in shape, texture and species composition (dominance of pennate diatoms) to those recorded during the ICE12 cruise. Aggregate-specific Chl *a* concentrations were roughly four-times lower as compared to ICE12 and aggregate POC and PON concentrations at station Ice2 roughly twice as high as those measured at station Ice1 (Table 1). The almost-exclusive occurrence of the marker pigments fucoxanthin and chlorophyll c1+2 at station Ice1 (Figure S4C) supports the dominance of diatoms. At Ice2, the occurrence of 19-hexanoyl-oxy-fucoxanthin, chlorophyll *c* 3 as well as chlorophyll b and prasinoxanthin indicated the additional contribution of haptophytes and prasinophytes to the aggregate biomass (Figure S4D). The aggregates from Ice1 showed no chlorophyll degradation products (Figure S4A) indicating a healthy diatom population, which is further reflected in the relatively low POC: Chl *a* ratio of 109 and the near Redfield POC:PON ratio of 7.1. At Ice2, phaeophorbide *a* and pyrophaeophobide *a* indicated grazing, and the relative high proportion of phaeophythin *a* and high POC: Chl a (210) and POC:PON (9.3) ratios further suggested the occurrence of senescent algae in the aggregates (Figure S4B).

Ice-algal aggregates exhibited a patchy distribution underneath the sea ice, with maximum abundances of >10 aggregates m^{-2} (Figure 4). Mean aggregate abundances at stations Ice1 and Ice2 (Table 1) were higher than those recorded during the ICE12 cruise. The aggregates covered on average 0.01 and 0.03% of the area sampled during the ROV surveys at stations Ice1 and Ice2 respectively. The vast majority of aggregates ranged from <1 cm to 15 cm in diameter and those between 3 and 12 cm in diameter accounted for 80 to 90% of the cumulative aggregate volume. Aggregates >15 cm were occasionally observed, but due to the limited number of observations were not included in the statistical analysis. Furthermore, the assumption of a spherical shape did not apply to these large aggregates as they were more likely to represent patches of individual aggregates closely aligned or stuck to each other.

Aggregate NPP rates per volume exceeded those measured in melt ponds, sea ice and the water column by 2-4 orders of

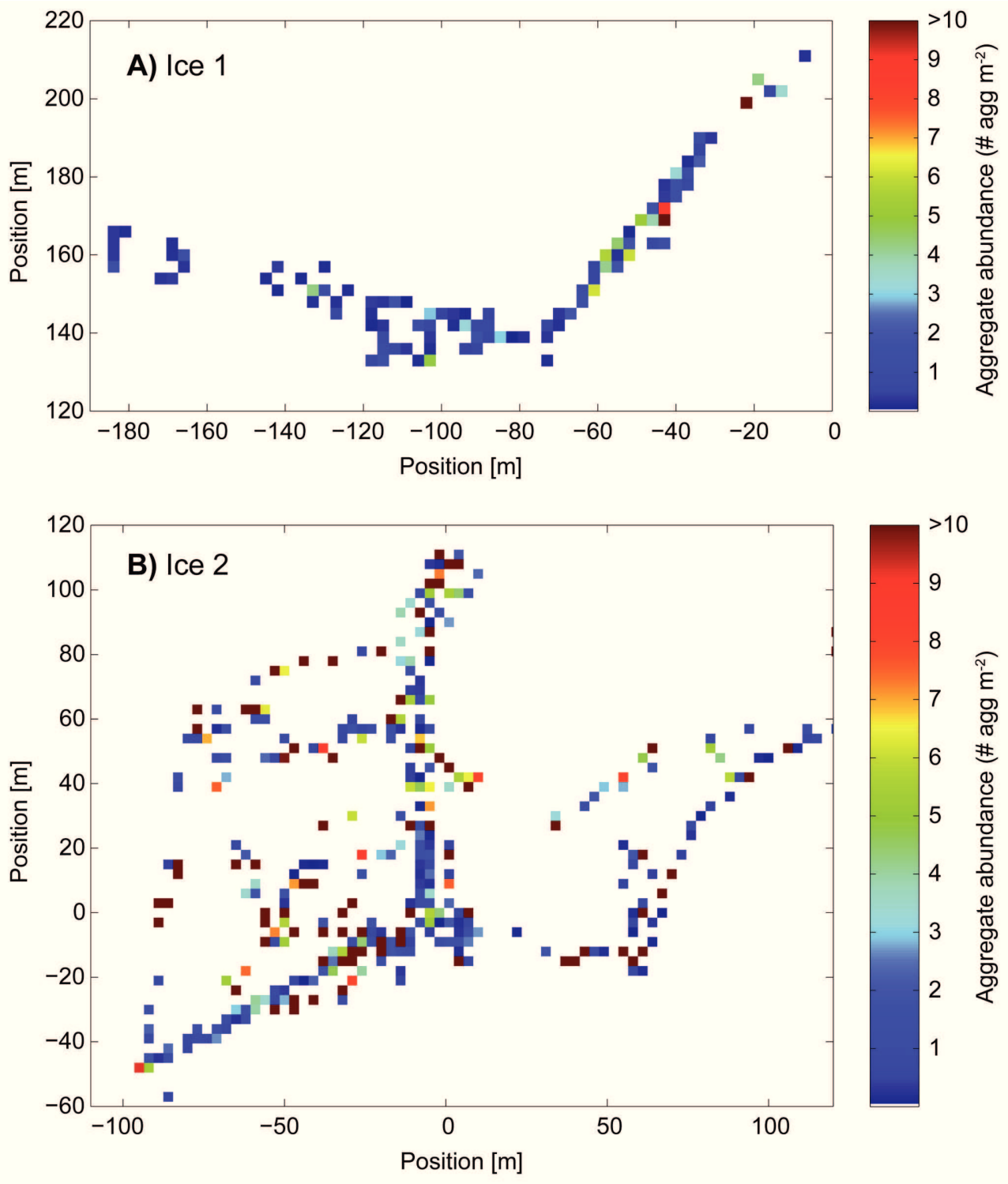

Figure 4. Abundance distribution of ice-algal aggregates at stations (A) Ice1 and (B) Ice2 measured with an upward looking camera mounted onto a remotely operated vehicle. The positions are coordinates (in m) within a floe fixed coordinate system, which was established on both stations.

doi: 10.1371/journal.pone.0076599.g004

Table 2. Net primary productivity (NPP) at the scale of the individual aggregate (mg C m^{-3} d^{-1}) and up-scaled to a square-metre area (mg C m^{-2} d^{-1}).

	NPP		Up-scaling NPP	
	(mg C m^{-3} d^{-1})		(mg C m^{-2} d^{-1})	
	Ice1	Ice2	Ice1	Ice2
Aggregate	3636	10304	0.002	0.02
Melt pond	8.6	0.2	8.4	0.04
Sea ice	4.4	2.0	9.2	1.0
Water column	2.1	1.1	19.4	2.0

Depth-integrated water column NPP was calculated for the euphotic zone (1% light depth). Depth-integrated melt pond and sea ice NPP was calculated for the entire pond depth and ice thickness, respectively. See Table S3 for details on the NPP up-scaling calculations.

doi: 10.1371/journal.pone.0076599.t002

magnitude (Table 2). ROV-derived aggregate abundances and areal percentage of aggregate cover allowed us to upscale our measurements of individual aggregates to a square-metre basis. Carbon standing stocks differed by almost one order of magnitude between station Ice1 (0.19 mg C m^{-2}) and Ice2 (1.33 mg C m^{-2}) (Table 1). The mean value derived from the "inverted sediment trap" approach during ICE12 (0.74 mg C m^{-2}) falls in between these two estimates (Table 1). Areal aggregate NPP at station Ice2 was an order of magnitude higher than at station Ice1 and in the same range as depth-integrated melt pond NPP (Table 2). However, the remaining depth-integrated melt pond, sea ice and the under-ice water column NPP rates were 2-3 orders of magnitude higher than those measured for the aggregates (Table 2).

Discussion

Formation, source and properties of ice-algal aggregates

The FYI encountered during this study was in a late stage of melt as indicated by a low modal ice thickness, high PAR transmittance, well-developed melt ponds and a freshwater layer below the ice [1]. Chl *a* concentrations were low both in sea ice and the underlying water column. As we did not observe the formation of the floating ice-algal aggregates described herein, the conditions conducive to their formation had already been established prior to our investigation period. Interestingly, all previous observations [18-21] were made during the melt season, which in itself indicates that the aggregates originated from the melting sea ice. Strong supportive evidence of this is provided by the observed species composition of the aggregates. Indeed, ice-associated diatoms dominated within the aggregates while pelagic species were conspicuously rare. We cannot rule out that the abundance of flagellates and naked ciliates within the aggregates was underestimated due to the aldehyde mixture used; however, we chose this preservation method precisely because in previous studies it resulted in no significant loss of fragile flagellates [31,43]. The holotrichous ciliate species living within the aggregate matrix were rare in the water column, implying that the aggregate matrix provided an optimal food supply and possibly some protection from pelagic grazers. These ciliates are usually predominantly bacterivorous, and were probably feeding on bacteria fuelled by dissolved organic carbon and TEP released from senescent diatoms [44].

The species composition clearly distinguished our aggregates from the metre-long filaments or strand-like aggregates formed by the centric sea ice diatom *Melosira arctica* [17,42,45-47] and those formed after phytoplankton blooms [48]. The ice-algal aggregates and those formed by *M. arctica* have been summarized under sub-ice assemblages [49] and further categorized by Melnikov [20] as plankto-benthic and benthic types respectively. Strand-like aggregates formed predominantly by *M. arctica* are attached to the underside of the ice, but grow in the underlying water column. The floating ice-algal aggregates we observed originated from the interstitial assemblage dominated by pennate diatoms that grow in the bottom of sea ice and are embedded in a mucous matrix, reminiscent of a biofilm. This continuous, inter-connected community likely already sloughed off from the bottom of the sea ice during the initial stages of melting as the darker ice-algal patches on the underside of sea ice accelerate bottom ablation. Extensive flushing of sea ice through melt pond drainage and higher light availability under thinning ice [1,50-52] likely further facilitated the formation of the floating ice-algal aggregates.

Extracellular polymeric substances (EPS) have been proposed as a binding agent of aggregates [53] and an adaptation employed by sea ice diatoms to survive the cold and saline conditions characteristic of sea ice brine channels [54]. Indeed, EPS made up >68% of dissolved carbohydrates in different sea ice habitats encountered in the Weddell Sea in 2005 and 2006 [55]. Some researchers have addressed the potential buoyancy of microorganisms upon release from melting sea ice as a result of EPS produced by ice algae [56]. Ice-algal EPS may even contribute to the release of ice-algae into the under-ice water column, as it has been suggested that EPS alter the melting rate of Arctic sea ice [57]. Interestingly, a considerable fraction of the EPS network seems to remain attached to the ice bottom even after the loss of the algae and could explain the carbon pools found in sea ice after the termination of the ice-algal bloom [58]. TEPs constitute a special type of sticky mucopolysaccharide gels, a subcategory of EPS [30] that are formed from dissolved precursors released from actively-growing or senescent phytoplankton and facilitate the aggregation of solid, non-sticky particles [59]. In the Arctic, it has been shown that the majority of TEP underneath first-year summer pack ice is produced by diatoms [60]. Once algal material is dislodged from melting sea ice, the sticky nature of TEP and collision of individual particles, when they collect in domes and crevices in the ice, will favour coagulation of the free-floating algal material into larger composite aggregates.

Distribution and ecological significance

The distribution of ice-algal aggregates underneath sea ice was very patchy as evidenced by the large temporal variability in accumulated aggregate biomass inside our ice hole, and

during diver observations and spatial ROV surveys. The skewed size-frequency distribution illustrates that the majority of ROV-detected aggregates were smaller <15 cm and likely represent individual aggregates. This is supported by the ICE12 drift station observations. However, occasional detections of patches >15 cm represent accumulations of individual aggregates that concentrate in under-ice domes, open melt ponds or leads as observed by divers and when surface sampling during ICE12. The lower aggregate abundance estimated with the "inverted sediment trap" approach, as compared to the ROV surveys, indicates that aggregates are easily transported below the ice before they settle in domes or crevices. This was also observed by divers, since exhaled air or fin movements rapidly dislodged and often dismantled the floating aggregates. Our "inverted sediment trap" estimate of aggregate abundance is therefore conservative because not every passing aggregate got trapped. Nevertheless, it lies in the range reported from an earlier study based on dive transects [20]. Changes in current speed and direction also influenced the sampling by our "inverted sediment trap", as reflected in the positive, linear relationship between mean relative current velocity and aggregate flux. The fact that this relationship did not apply for the highest accumulated aggregate biomass on 31 July was likely due to the very patchy distribution of the aggregates or changes in current direction. On that day, our "inverted sediment trap" might have sampled an area with exceptionally high aggregate abundance. Despite lower abundances overall, aggregate standing stock extrapolated to the catchment area of our "inverted sediment trap" lies within the range calculated from the ROV surveys. This is because the aggregates were generally larger than those measured during the ROV transects. In addition to the differences in methodology, comparisons are further complicated by differences in spatial coverage and duration between the "inverted sediment trap" approach and the ROV surveys. The ROV surveys covered, within a few hours, a three to 10-fold larger area as compared to the area sampled for 3.5 days by the "inverted sediment trap". Given the characteristically patchy nature of sea-ice habitats, many of the differences (or similarities) in the data may therefore simply be due to differences in location and/or sampling duration.

Aggregate NPP and standing stocks m^{-2} are small when compared to depth-integrated ice-algal biomass and primary production rates reported for the Arctic, which range from 1-340 mg C m^{-2} in the former and <1-463 mg C m^{-2} d^{-1} in the latter [61]. However, in locations where they accumulate, they constitute a highly concentrated food source for the ice-associated fauna during the oligotrophic summer months, as revealed by high abundances of ice amphipods and ciliates associated with them. Ice amphipods, such as *Apherusa glacialis*, are able to swim in the boundary layer below the ice and adapted to exploit patchy food sources [62]. Furthermore the feeding mode of herbivorous, ice-associated amphipods is not well-suited to efficiently feed on highly diluted and small-sized suspended particles typical of the summer phytoplankton community [63]. Such aggregations could thus constitute an important trophic baseline for specialized sympagic fauna during the melt season, when many organisms, such as ice amphipods, need to rely on degraded material or detritus as a food source [62]. In cases when aggregates are refrozen into the ice during autumn they could also extend food availability into the winter months [17,64] and act as a seeding stock for the next spring. Frozen-in algal aggregates have been observed by divers, particularly during spring (H. Hop, diving obs.). However, this fraction appears to be small compared to the fraction that sinks once the aggregates have lost buoyancy control. This has been shown for *Melosira arctica* dominated aggregates [42,47]. The aggregates found on the sea floor in 3485 m depth at station Ice2 were dominated by pennate diatoms [42] similar to those described herein which indicates that a significant fraction of the floating aggregates eventually lost buoyancy control and sank to the sea floor.

The algal aggregates supported high levels of biological activity on the scale of individual aggregates as revealed by Chl *a* concentrations and NPP several orders of magnitude higher than in the surrounding water column and sea ice. High POC:PON and POC: Chl *a* ratios inside the aggregates during ICE12 and at station Ice2 were likely mediated by preferential bacterial degradation of labile organic matter, in particular PON, and could explain oxygen consumption and elevated ammonium concentrations in surface waters where aggregates accumulated. The occurrence of the Chl *a* degradation products phaeophorbide *a* and pyrophaeophorbide *a* at station Ice2 indicated increased grazing [65]. Older aggregates further seem to accumulate prasinophytes and haptophytes while floating through the under-ice water column because these taxa are usually not prominent in sea ice biota. The high proportion of phaeophythin *a* indicates a high fraction of senescent algae [66] within the aggregates. This is corroborated by the frequent occurrence of bleached aggregates and elevated levels of iodide [27] within the aggregates, indicating that a considerable fraction of embedded algae was either in senescent condition or dead, possibly due to photo-oxidative stress induced by high light levels near the surface. Indeed, the majority of bleached ice-algal aggregates were observed in open melt ponds and sea ice crevices where they were exposed to high levels of incident radiation.

Historical context

The aggregates studied herein are reminiscent in shape, colour, dominance of pennate diatoms and association with the meltwater layer of the aggregates reported from the Norwegian Fram Expedition in 1894 [18,19] and the Russian North Pole drift ice station NP-23 [20] in 1977 (Figure 1), indicating that the floating ice-algal aggregates described herein are not a new phenomenon. Free-floating algal masses were also observed during the SHEBA (Surface Heat Budget of the Arctic Ocean) ice camp drift in the Canadian Basin, but the aggregations were dominated by two centric diatoms, *Chaetoceros socialis* and *Melosira arctica*, and the epiphytic diatom *Synedropsis hyperborea* [21], representing a different type of algal aggregation. Common to all previous observations is that they were made during drift ice stations that were occupied for at least one full seasonal cycle and thus covered the critical time

window during the melt season. Although intensively looked for during a summer cruise to the Arctic Ocean in 2013, we did not observe floating macroscopic aggregates in the same general area and during the same time of the year as the ICE12 drift-ice study. Also during the Fram Expedition, floating ice-algal aggregates were observed in the summer of 1894 but not in the following summer despite intensive efforts to find them [18], suggesting that the occurrence of such events is likely ephemeral and restricted to the melt season.

Conclusions

Although the biomass associated with the floating ice-algal aggregates was low compared to ice-algal blooms, they sustained high rates of biological activity at the scale of the individual aggregate and provided a concentrated food source for the ice-associated fauna during the oligotrophic Arctic summer months. This type of aggregate-based habitat is likely to be fairly unique because it constitutes an extension of the sea ice community into the under-ice water column during the Arctic summer melt season. The potential significance of the ice-algal aggregates for surface consumption, energy transfer to the benthos and seeding of the next spring bloom remains an interesting topic for future studies, and is an urgent reminder to improve our understanding of the rapidly changing Arctic sea ice ecosystem.

Supporting Information

Table S1. Results of aggregate extraction from ROV video transects at stations Ice1 (five dives) and Ice2 (four dives).
(DOCX)

Table S2. Up-scaling of aggregate biomass.
(DOCX)

Table S3. Up-scaling of Chl *a* normalized aggregate net primary production (NPP).
(DOCX)

Table S4. Composition of ice-algal aggregates.
(DOCX)

Figure S1. Iodide concentrations measured in aggregate filtrate and ambient surface seawater during cruise ICE12, July-August 2012. (SD = ±1.8 nM and ±2.4 nM for aggregate sample and surface water samples respectively; n = 3).
(TIF)

Figure S2. Relationship between mean relative under-ice current velocities (exemplified here for 3.5 m below the ice) and accumulated POC at each sampling interval between 29 July and 1 August, 2012.
(TIF)

Figure S3. Oxygen profiles from the upper 5.5 m of the under-ice water column measured with a MicroCat oxygen sensor on 30 and 31 July, 2012.
(TIF)

Figure S4. Pigment composition of ice-algal aggregates. Marker pigments and chlorophyll and its degradation products at stations Ice1 (A, C) and Ice2 (B, D). Chl *c* 3 = chlorophyll *c* 3, Chl *c1+2* = chlorophyll c1+*2*, 19-hex = 19-hexanoyloxyfucoxanthin, Fuco = fucoxanthin, Prasino = prasinoxanthin, Chl *b* = chlorophyll b, Phorbid *a* = phaeophorbide *a*, PyroPhorbid = pyrophaeophorbide *a*, Chl *a* = chlorophyll *a*, Phythin *a* = phaeophythin *a*.
(TIF)

Acknowledgements

Our research was approved and conducted as part of the ICE-Centre program of the Norwegian Polar Institute, which reports to the Ministry of Environment in Norway. There are no requirements for permits to conduct this type of research in Svalbard waters and the Arctic Ocean. Such permits only apply to harvesting of resources and work in protected areas in Svalbard, and our work did not involve any of these. The work on ice algae and plankton did not involve any protected species.

We gratefully acknowledge the support of chief scientists H. Steen and A. Boetius and the captain and crew of RV *Lance* and RV *Polarstern*. C.A. Pedersen provided valuable information on sea ice properties. We thank S. Audritz and C. Lorenzen for support with the POC and PON analysis. We also thank R. Flerus, K. Schmidt and R. Wysocki for technical assistance with the aggregate TEP analysis. We are grateful to J.E. Ross for language-editing. We kindly acknowledge two anonymous reviewers for valuable comments on the manuscript.

Author Contributions

Conceived and designed the experiments: PA HH JKE SK MAG MFM CK MN. Performed the experiments: PA MFM CK MN. Analyzed the data: PA MFM CK AS KB AE MD AF SRH SK MN IP AHHR GS AT JW. Contributed reagents/materials/ analysis tools: PA JKE MFM HH CK AS KB AE AF SRH SK MN IP AT JW. Wrote the manuscript: PA.

References

1. Hudson SR, Granskog MA, Sundfjord A, Randelhoff A, Renner AHH et al. (2013) Energy budget of first-year Arctic sea ice in advanced stages of melt. Geophys Res Lett 40: L050517.
2. Nicolaus M, Katlein C, Maslanik J, Hendricks S (2012) Changes in Arctic sea ice result in increasing light transmittance and absorption. Geophys Res Lett 39: L053738.
3. Smetacek V, Nicol S (2005) Polar Ocean ecosystems in a changing world. Nature 437: 362-368. doi:10.1038/nature04161. PubMed: 16163347.
4. Wassmann P, Duarte CM, Agusti S, Sejr MK (2011) Footprints of climate change in the Arctic marine ecosystem. Glob Change Biol 17: 1235-1249. doi:10.1111/j.1365-2486.2010.02311.x.
5. Hop H, Falk-Petersen S, Svendsen H, Kwasniewski S, Pavlov V et al. (2006) Physical and biological characteristics of the pelagic system across Fram Strait to Kongsfjorden. Prog Oceanogr 71: 182-231. doi: 10.1016/j.pocean.2006.09.007.
6. Comeau AM, Li WKW, Tremblay J-E, Carmack EC, Lovejoy C (2011) Arctic Ocean microbial community structure before and after the 2007 record sea ice minimum. PLOS ONE 6: e2749210. PubMed: 22096583.
7. Ji R, Jin M, Varpe Ø (2013) Sea ice phenology and timing of primary production pulses in the Arctic Ocean. Glob Change Biol 19: 734-741. doi:10.1111/gcb.12074.
8. Søreide JE, Leu E, Berge J, Graeve M, Falk-Petersen S (2010) Timing in blooms, algal food quality and *Calanus glacialis* reproduction and growth in a changing Arctic. Glob Change Biol 16: 3154-3163.
9. Hop H, Mundy CJ, Gosselin M, Rossnagel AL, Barber DG (2011) Zooplankton boom and ice amphipod bust below melting sea ice in the Amundsen Gulf, Arctic Canada. Polar Biol 34: 1947-1958. doi:10.1007/s00300-011-0991-4.
10. Mundy CJ, Gosselin M, Ehn JK, Belzile C, Poulin M et al. (2011) Characteristics of two distinct high-light acclimated microbial communities during advanced stages of sea ice melt. Polar Biol 34: 1869-1886. doi:10.1007/s00300-011-0998-x.
11. Riebesell U, Schloss I, Smetacek V (1991) Aggregation of algae released from melting sea ice - implications for seeding and sedimentation. Polar Biol 11: 239-248.
12. Michel C, Nielsen TG, Nozais C, Gosselin M (2002) Significance of sedimentation and grazing by ice micro- and meiofauna for carbon cycling in annual sea ice (northern Baffin Bay). Aquat Microb Ecol 30: 57-68. doi:10.3354/ame030057.
13. Tamelander T, Renaud PE, Hop H, Carroll ML, Ambrose WG Jr et al. (2006) Trophic relationships and pelagic-benthic coupling during summer in the Barents Sea Marginal Ice Zone, revealed by stable carbon and nitrogen isotope measurements. Mar Ecol Prog Ser 310: 33-46. doi:10.3354/meps310033.
14. Tamelander T, Reigstad M, Hop H, Ratkova T (2009) Ice algal assemblages and vertical export of organic matter from sea ice in the Barents Sea and Nansen Basin (Arctic Ocean). Polar Biol 32: 1261-1273. doi:10.1007/s00300-009-0622-5.
15. Renaud PE, Riedel A, Michel C, Morata N, Gosselin M et al. (2007) Seasonal variation in benthic community oxygen demand: A response to an ice algal bloom in the Beaufort Sea, Canadian Arctic? J Mar Syst 67: 1-12. doi:10.1016/j.jmarsys.2006.07.006.
16. Wassmann P, Reigstad M, Haug T, Rudels B, Carroll ML et al. (2006) Food webs and carbon flux in the Barents Sea. Prog Oceanogr 71: 232-287. doi:10.1016/j.pocean.2006.10.003.
17. Lee SH, McRoy CP, Joo HM, Gradinger R, Cui XH et al. (2011) Holes in progressively thinning Arctic sea ice lead to new ice algae habitat. Oceanography 24: 302-308. doi:10.5670/oceanog.2011.81.
18. Gran HH (1904) Diatomaceae from the ice-floes and plankton of the Arctic Ocean. Sci Res Norw North Polar Exped: 11-1896 1-74
19. Nansen F (1906) Protozoa on the ice-floes of the North Polar Sea. Sci Res Norw North Polar Exped: 1893-1896 1-22
20. Melnikov IA (1997) The Arctic sea ice ecosystem. Amsterdam: Gordon and Breach Science Publishers. 204pp.
21. Melnikov IA, Kolosova EG, Welch HE, Zhitina LS (2002) Sea ice biological communities and nutrient dynamics in the Canada Basin of the Arctic Ocean. Deep Sea Res I 49: 1623-1649. doi:10.1016/S0967-0637(02)00042-0.
22. Deal C, Jin MB, Elliott S, Hunke E, Maltrud M et al. (2011) Large-scale modelling of primary production and ice algal biomass within arctic sea ice in 1992. J Geophys Res 116: C0700410
23. Mikkelsen D, Witkowski A (2010) Melting sea ice for taxonomic analysis: a comparison of four melting procedures. Polar Res 29: 451-454. doi:10.1111/j.1751-8369.2010.00162.x.
24. Solórzano L (1969) Determination of ammonium in natural waters by the phenolhypochlorite method. Limnol Oceanogr 14: 799-801. doi: 10.4319/lo.1969.14.5.0799.
25. Campos M (1997) New approach to evaluating dissolved iodine speciation in natural waters using cathodic stripping voltammetry and a storage study for preserving iodine species. Mar Chem 57: 107-117. doi:10.1016/S0304-4203(96)00093-X.
26. Luther GW, Swartz CB, Ullman WJ (1988) Direct determination of iodide in seawater by cathodic stripping square wave voltammetry. Anal Chem 60: 1721-1724. doi:10.1021/ac00168a017.
27. Bluhm K, Croot P, Wuttig K, Lochte K (2010) Transformation of iodate to iodide in marine phytoplankton driven by cell senescence. Aquat Biol 11: 1-15. doi:10.3354/ab00284.
28. Holm-Hansen O, Riemann B (1978) Chlorophyll a determination: Improvement of the methodology. Oikos 30: 438-447. doi: 10.2307/3543338.
29. Engel A (2009) Determination of marine gel particles. In: O Wurl. Practical Guidelines for the Analysis of Seawater. CRC Press. pp. 125-142.
30. Engel A (2004) Distribution of transparent exopolymer particles (TEP) in the northeast Atlantic Ocean and their potential significance for aggregation processes. Deep Sea Res I 51: 83-92. doi:10.1016/j.dsr.2003.09.001.
31. Tsuji T, Yanagita T (1981) Improved fluorescent microscopy for measuring the standing stock of phytoplankton including fragile components. Mar Biol 64: 207-211. doi:10.1007/BF00397110.
32. Throndsen J (1995) Estimating cell numbers. In: GM HallegraeffDM AndersonAD Cembella. Manual on Harmful Marine Microalgae. Paris: UNESCO. pp. 63-80.
33. von Kármán T (1930) Mechanische. Ähnlichkeit Turbulenz Nachrichten Gesellschaft Wiss Göttingen Fachgruppe 1 (Mathematik) 5: 58-76
34. Taylor BB, Torrecilla E, Bernhardt A, Taylor MH, Peeken I et al. (2011) Bio-optical provinces in the eastern Atlantic Ocean and their biogeographical relevance. Biogeosciences 8: 3609-3629. doi:10.5194/bg-8-3609-2011.
35. Nicolaus M, Katlein C (2013) Mapping radiation transfer through sea ice using a remotely operated vehicle (ROV), The Cryosphere 7: 763-777
36. Steenmann-Nielsen E (1952) The use of radioactive carbon (C14) for measuring organic production in the sea. J Cons Int Explor Mer 18: 117-140.
37. Hall OJ, Robert C (1992) Rapid, small-volume, flow injection analysis for Σ CO2 and NH4+ in marine and freshwaters. Limnol Oceanogr 37: 1113-1119. doi:10.4319/lo.1992.37.5.1113.
38. Platt T, Gallegos CL, Harrison WG (1980) Photoinhibition and photosynthesis in natural assemblages of marine phytoplankton. J Mar Res 38: 687-701.
39. Perovich DK (1996). The optical properties of sea ice. Monograph 96-1 Hanover, NH: Cold Regions Research and Engineering Laboratory, US Army Corps of Engineers.
40. Haas C, Hendricks S, Doble M (2006) Comparison of the sea-ice thickness distribution in the Lincoln Sea and adjacent Arctic Ocean in 2004 and 2005. Ann Glaciol 44: 247-252. doi: 10.3189/172756406781811781.
41. Alldredge AL, Passow U, Haddock SHD (1998) The characteristics and transparent exopolymer particle (TEP) content of marine snow formed from thecate dinoflagellates. J Plankton Res 20: 393-406. doi:10.1093/plankt/20.3.393.
42. Boetius A, Albrecht S, Bakker K, Bienhold C, Felden J et al. (2013) Export of algal biomass from the melting Arctic sea ice. Science 339: 1430-1432. doi:10.1126/science.1231346. PubMed: 23413190.
43. Lovejoy C, Legendre L, Martineau MJ, Bacle J, von Quillfeldt CH (2002) Distribution of phytoplankton and other protists in the North Water. Deep Sea Res II 49: 5027-5047. doi:10.1016/S0967-0645(02)00176-5.
44. Meiners K, Krembs C, Gradinger R (2008) Exopolymer particles: microbial hotspots of enhanced bacterial activity in Arctic fast ice (Chukchi Sea). Aquat Microb Ecol 52: 195-207. doi:10.3354/ame01214.
45. Syvertsen EE (1991) Ice algae in the Barents Sea – types of assemblages, origin, fate and role in the ice-edge phytoplankton bloom. Polar Res 10: 277-287. doi:10.1111/j.1751-8369.1991.tb00653.x.
46. Gutt J (1995) The occurrence of sub-ice algae aggregations off northeast Greenland. Polar Biol 15: 247-252.
47. Ambrose WG Jr, von Quillfeldt C, Clough LM, Tilney PVR, Tucker T (2005) The sub-ice algal community in the Chukchi sea: large- and small-scale patterns of abundance based on images from a remotely operated vehicle. Polar Biol 28: 1-12.

48. Alldredge AL, Gotschalk CC (1989) Direct observations of the mass flocculation of diatom blooms: characteristics, settling velocities and formation of diatom aggregates. Deep Sea Res 36: 159-171. doi: 10.1016/0198-0149(89)90131-3.
49. Horner RA, Syvertsen EE, Thomas DP, Lange C (1988) Proposed terminology and reporting units for sea ice-algal assemblages. Polar Biol 8: 249-225. doi:10.1007/BF00263173.
50. Eicken H, Krouse HR, Kadko D, Perovich DK (2002) Tracer studies of pathways and rates of meltwater transport through Arctic summer sea ice. J Geophys Res 107: C000583.
51. Nicolaus M, Gerland S, Hudson SR, Hanson S, Haapala J et al. (2010) Seasonality of spectral albedo and transmittance as observed in the Arctic Transpolar Drift in 2007. J Geophys Res, 115: C03021: C1101110 PubMed: 20463844.
52. Ehn JK, Mundy CJ, Barber DG, Hop H, Rossnagel A et al. (2011) Impact of horizontal spreading on light propagation in melt pond covered seasonal sea ice in the Canadian Arctic. J Geophys Res, 116: C006908.
53. Søreide JE, Hop H, Carroll ML, Falk-Petersen S, Hegseth EN (2006) Seasonal food web structures and sympagic-pelagic coupling in the European Arctic revealed by stable isotopes and a two-source food web model. Prog Oceanogr 71: 59-87. Søreide et al. (2007) Corrigendum. Prog Oceanogr 73: 96-98 doi:10.1016/j.pocean. 2006.06.001.
54. Aslam SN, Cresswell-Maynard T, Thomas DN, Underwood GJC (2012) Production and characterization of the intra- and extracellular carbohydrates and polymeric substances (EPS) of three sea-ice diatom species, and evidence for a cryoprotective role for EPS. J Phycol 48: 1494-1509. doi:10.1111/jpy.12004.
55. Underwood GJC, Fietz S, Papadimitriou S, Thomas DN, Dieckmann GS (2010) Distribution and composition of dissolved extracellular polymeric substances (EPS) in Antarctic sea ice. Mar Ecol Prog Ser 404: 1-19. doi:10.3354/meps08557.
56. Riedel A, Michel C, Gosselin M (2006) Seasonal study of sea-ice exopolymeric substances on the Mackenzie shelf: implications for transport of sea-ice bacteria and algae. Aquat Microb Ecol 45: 195-206. doi:10.3354/ame045195.
57. Krembs C, Eicken H, Junge K, Deming JW (2002) High concentrations of exopolymeric substances in Arctic winter sea ice: implications for the polar ocean carbon cycle and cryoprotection of diatoms. Deep Sea Res I 49: 2163-2181. doi:10.1016/S0967-0637(02)00122-X.
58. Juhl AR, Krembs C, Meiners KM (2011) Seasonal development and differential retention of ice algae and other organic fractions in first-year Arctic sea ice. Mar Ecol Prog Ser 436: 1-16. doi:10.3354/meps09277.
59. Passow U (2002) Transparent exopolymer particles (TEP) in aquatic environments. Prog Oceanogr 55: 287-333.
60. Krembs C, Engel A (2001) Abundance and variability of microorganisms and transparent exopolymer particles across the ice-water interface of melting first-year sea ice in the Laptev Sea (Arctic). Mar Biol 138: 173-185. doi:10.1007/s002270000396.
61. Arrigo KR, Mock T, Lizotte MP (2010) Primary producers and sea ice. In: DN ThomasGS Dieckmann. Sea ice. Oxford: Wiley-Blackwell. pp. 283-325.
62. Poltermann M (2001) Arctic sea ice as feeding ground for amphipods – food sources and strategies. Polar Biol 24: 89-96. doi:10.1007/ s003000000177.
63. Arndt CE, Berge J, Brandt A (2005) Mouthpart-atlas of Arctic sympagic amphipods – trophic niche separation based on mouthpart morphology and feeding ecology. J Crustac Biol 25: 401-412. doi:10.1651/C-2544.
64. Werner I, Auel H (2005) Seasonal variability in abundance, respiration and lipid composition of Arctic under-ice amphipods. Mar Ecol Prog Ser 292: 251-262. doi:10.3354/meps292251.
65. Head EJH, Harris LR (1992) Chlorophyll and carotenoid transformation and destruction by *Calanus* spp. grazing on diatoms. Mar Ecol Prog Ser 86: 229-238. doi:10.3354/meps086229.
66. Owens TG, Falkowski PG (1982) Enzymatic degradation of chlorophyll a by marine phytoplankton in vitro. Phytochemistry 21: 979-984. doi: 10.1016/S0031-9422(00)82401-2.

Chapter III

Composition, buoyancy regulation and fate of ice algal aggregates in the Central Arctic Ocean

Mar Fernández-Méndez [1,2*], Frank Wenzhöfer [1,2], Ilka Peeken [3,4], Heidi L. Sørensen [5,6] , Ronnie N. Glud [5,6,7,8] , and Antje Boetius [1,2,4].

[1] Alfred-Wegener-Institut Helmholtz-Zentrum für Polar- und Meeresforschung, [2] Max Planck Institute for Marine Microbiology, Bremen, Germany, [3] Polar Biological Oceanography, Alfred-Wegener-Institut Helmholtz-Zentrum für Polar- und Meeresforschung, Bremerhaven, Germany, [4] MARUM, Center for Marine Environmental Sciences, University of Bremen, Germany, [5] Nordic Centre for Earth Evolution, University of Southern Denmark, Denmark, [6] Greenland Climate Research Centre, Greenland, [7] Scottish Association for Marine Science, UK, [8] University of Aarhus, Arctic Research Centre, Denmark

Accepted for publication in PLoS One (Available online September 2014)

Abstract

Sea-ice diatoms are known to accumulate in large aggregates in and under sea ice and in melt ponds. There is recent evidence from the Arctic that such aggregates can contribute substantially to particle export when sinking from the ice. The role and regulation of microbial aggregation in the highly seasonal, nutrient- and light-limited Arctic sea-ice ecosystem is not well understood. To elucidate the mechanisms controlling the formation and export of algal aggregates from sea ice, we investigated samples taken in late summer 2011 and 2012, during two cruises to the Eurasian Basin of the Central Arctic Ocean. Spherical aggregates densely packed with pennate diatoms, as well as filamentous aggregates formed by *Melosira arctica* showed sign of different stages of degradation and physiological stoichiometries, with carbon to chlorophyll *a* ratios ranging from 110 to 66700, and carbon to nitrogen molar ratios of 8–35 and 9–40, respectively. Sub-ice algal aggregate densities ranged between 1 and 17 aggregates m^{-2}, maintaining an estimated net primary production of 0.4–40 mg C m^{-2} d^{-1}, and accounted for 3–80% of total phototrophic biomass and up to 94% of local net primary production. A potential factor controlling the buoyancy of the aggregates was light intensity, regulating photosynthetic oxygen production and the amount of gas bubbles trapped within the mucous matrix, even at low ambient nutrient concentrations. Our data-set was used to evaluate the distribution and importance of Arctic algal aggregates as carbon source for pelagic and benthic communities.

Keywords: Arctic, sea-ice algae, aggregates, diatoms, *Melosira arctica*, oxygen, buoyancy, carbon export, nitrogen.

Introduction

In the Arctic Ocean, sea ice and water column microbial communities both contribute to photosynthetic production, but the relative importance of the pelagic versus the sympagic communities depends on season and geographical region [1]. Depending on light availability, the ice-algal growth season begins in April, and ends in September [2]. The total amount of productivity and standing stock formed seasonally in the water below the ice in the Central Arctic is constrained by light, as well as nutrient availability in the euphotic zone. Annual production in the ice-covered Central Arctic is estimated to be 9–10 g C m^{-2} yr^{-1}, which is very low even compared to other oligotrophic oceans [3,4]. Previous investigations before 1997 have indicated a significant annual contribution by sea-ice algae to total photosynthetic productivity, on the order of 4–57% [3, 5, 6]. The wide range (0–10 g C m^{-2} yr^{-1}) of sea ice primary production rates including the Arctic shelves is due to a very high spatial variability [3].

Sub-ice algae can accumulate substantial biomass in the Central Arctic basins, at times exceeding 80% of the standing stock [5]. They offer an additional food source to planktonic grazers in early spring [6] and in late autumn when other food sources are scarce [7,8]. Also their contribution to carbon export from surface waters can be substantial (1–9 g C m^{-2} yr^{-1}) [9,10]. Ice algae comprise pennate diatoms such as *Nitzschia* sp., *Pseudonitzschia* sp., *Cylindrotheca* sp., *Entomoneis* sp., and *Navicula* sp., which inhabit the ice pores and brine channels of first year (FYI) and multiyear ice (MYI) (e.g., [11–13]). The endemic sub-ice diatom, *Melosira arctica*, has a hybrid strategy, growing attached to the underside of ice-floes, of both FYI and MYI, forming filamentous strands of several meters length below the ice [14–17]. Different types of large sub-ice algal aggregates (up to 15 cm in diameter) have been observed in the Central Arctic since its first exploration in the 19th century, but due to sampling difficulties still little is known about their physiology, traits and adaptations [18–21]. More recently, floating algal aggregations formed mainly by sea-ice pennate diatoms have been observed in melting FYI north of Svalbard and in the Fram Strait [8,22].

Planktonic diatoms tend to collide and aggregate in nutrient depleted waters after a bloom due to mucus secretion during senescence [23,24] and in general, sedimenting diatom aggregates contribute significantly to the marine biological carbon pump [25,26]. Sea-ice algae are known to produce large amounts of extracellular polymeric substances for attachment and cryoprotection [27–29]. This may support their aggregation in summer when the ice cracks and melts, and when nutrients become limiting [23]. Algal aggregates eventually sink into deeper water column layers as a consequence of ice break up and melting [9,15]. Freshly deposited algal aggregates have been

observed at the seafloor of the shelves [30] and central deep basins of the Arctic [9], indicating their rapid sedimentation at the end of the summer along the receding ice edge and in the event of substantial under-ice melt.

Many questions remain about aggregate formation, decay, grazing and sinking, as well as their contribution to carbon fluxes in the Central Arctic. Due to the rapid warming of the Arctic leading to a decrease in sea-ice extent and thickness [31,32] and an increase in the amount of light transmitted through the ice [33], both sea-ice and pelagic phototrophic communities are expected to change with respect to composition and distribution [34,35], productivity [36,37], and life cycle [2,9,38]. A better understanding of the factors regulating sea-ice productivity, aggregate formation and sinking of sea-ice algae is important for future estimates of the Arctic carbon and nitrogen cycling. By combining field observations with simple experiments, this study examines the relevance of sea-ice algal aggregation for carbon and nitrogen turnover and reservoirs, as well as the processes regulating buoyancy versus sinking. Our data are used to assess the potential importance of algal aggregates for the export of organic matter from the surface ocean to the deep sea.

Materials and methods

Sampling area

Samples were collected during two cruises to international waters of the Central Arctic Ocean with RV Polarstern in August-September 2011 and 2012 (PS78/3 and PS80/3 respectively) between 81°55´-87°56´N and 31°7´-131°7´E (Fig.1). Six stations were in international waters and no specific permissions were required for these locations. For the two stations in the Russian exclusive economic zone, the diplomatic permissions for sampling were obtained from the responsible authorities. The field study did not involve endangered or protected species. Data was submitted to PANGAEA (http://doi.pangaea.de/10.1594/PANGAEA.832345).

Replicates of two different algal aggregate types dominated either by pennate diatoms or by *Melosira* were sampled at eight ice stations (Fig.1). For each station the ice type (MYI or FYI) and the melt pond coverage were assessed [39]. Temperature and salinity of melt ponds containing aggregates were measured *in situ* using a hand-held conductivity meter (315i with TetraCon electrode cell, WTW GmbH, Weilheim in Oberbayern, Germany). Irradiance reaching the aggregates was calculated using the light attenuation coefficients of 1.5 m^{-1} for sea ice, 10 m^{-1} for snow [40] and 0.1 m^{-1} for Atlantic influenced Arctic seawater (based on data from the first expedition, PS78/3), and the daily average total incoming photosynthetically active radiation (PAR) measured with a pyranometer (Kipp&Zonen, Delft, Netherland) mounted on the ship.

Chemical composition of aggregates

Several aggregates (between 2 and 20) were sampled at each station together with some ambient water using a manually operated vacuum pump, when found in melt ponds (Fig.2A), or a plastic ladle, when found in ice cracks. In general aggregates were pooled and homogenized to be able to measure a wide range of biological parameters on standardized subsamples. On two occasions individual aggregates were sampled at stations PS80/3_224 and PS80/3_349 for specific experiments. When classified according to their species composition, pennate diatom aggregates where sampled 6 times and *Melosira arctica* filaments 5 times (Table 1). Aggregate slurry was filtered through a pre-combusted GF/F filter (0.7 μm pore size, Whatman, Kent, United Kingdom) and analyzed with an elemental analyzer (EA3024-IRMS, EuroVetorSpA, Milan, Italy) to determine particulate organic carbon (POC) and particulate organic nitrogen (PON). POC was

used to normalize all parameters to carbon mass. For pigment analysis 1-200 ml of the algal slurry (equivalent to 0.1–3 mg C) were filtered through GF/F filters, immediately frozen in liquid nitrogen, and stored at -80°C. Chlorophyll *a* and phaeopigments were measured using high-performance liquid chromatography (HPLC) as described in [41]. The analytical error for the POC, PON and Chl *a* measurements was generally below 2%. For transparent exopolymers (TEP), 1–20 ml of the algal slurry (equivalent to 0.01–2.6 mg C) were filtered in triplicate on to 0.4 □ m pore size polycarbonate filters (Nuclepore, Whatman, Kent, United Kingdom), stained with Alcian Blue and stored at -20°C. TEP concentration was measured with the colorimetric method according to [42] and transformed to carbon equivalents as described in [43]. Occasional dilution prior to filtration was accounted for using measured blank values of the dilution water. For dissolved organic carbon (DOC) 10 ml of the algal slurry (equivalent to 0.07–1.3 mg C) were filtered in triplicate through pre-combusted GF/F filters and the filtrate collected in pre-combusted glass vials. The DOC concentration was determined by high temperature catalytic oxidation with a Shimadzu TOC-VCPN analyzer (Shimadzu Scientific Instruments, Kyoto, Japan). Samples were acidified in the auto-sampler and analyzed directly. Nutrients (phosphate, silicate, and nitrate) were measured in seawater, ice and aggregate slurries in an air-conditioned lab container with standard photometric method using a Technicon TRAACS 800 continuous flow auto analyzer (Technicon Corporation) according to established methods [44].

Microscopy of aggregates

The qualitative algal aggregate composition was studied directly on board of the ship with a plankton chamber (Hydro-Bios, Altenholz, Germany) and an inverted light microscope with phase contrast optics (Axiovert 40C, Carl Zeiss, Jena, Germany) and an integrated camera (AxioCamMRc, Carl Zeiss, Jena, Germany). The condition of the diatoms in each sample was defined according to the color and shape of the chloroplasts visible in the interior of the frustules. Green-brownish aggregates contained mostly healthy cells with bright green chloroplasts occupying the entire cytoplasm, while white-yellowish aggregates contained many dead cells with empty frustules or reduced yellowish chloroplasts. To determine bacterial abundance with Acridine Orange direct counts (AODC), sub-samples of the algal slurry were preserved with 2% formalin and sonicated (1 × 90 s). One milliliter was filtered on to a 0.2 μm pore size polycarbonate filter (Nuclepore, Whatman, Kent, United Kingdom) previously stained with Irgalan black to eliminate autofluorescence [45]. Subsequently the filter was stained with a 0.01%

Acridine Orange solution as described in Meyer-Reil (1983) [46]. At least 1000 bacterial cells were counted per filter, using an Axiophot HBO50 (Carl Zeiss, Jena, Germany) microscope. Triplicate filters were counted per sample and the average error was 15%. The percentage of POC contained in the prokaryotic biomass was calculated using the carbon conversion factor of 0.03 pg C per cell specific for Arctic bacteria [47].

Biomass and primary production in water column, sea ice and aggregates

Although green-brownish sub-ice algal aggregates were observed at all ice stations [9], for logistic reasons we were only able to sample sufficient material at three stations. Here depth-integrated biomass and net primary production (NPP) were calculated for sea ice and water column (PS80/3_224, PS80/3_237 and PS80/3_349) and compared to the integrated sub-ice algal aggregates per m^{-2}.

Sea-ice algal biomass was determined by cutting a representative ice core at each station in 10–20 cm slices, melting them in filtered seawater (200 mL of 0.2 μm filtered seawater were added per cm of ice [48]) and filtering them through GFF filters to determine Chl *a* and POC as for the aggregate slurry. For the phytoplankton community in the water below the ice, samples were taken with Niskin bottles disposed in a rosette attached to the Conductivity-Temperature-Depth sensor (CTD) at discrete depths, the water was filtered, and Chl *a* and POC was analyzed as above. Water column phytoplankton biomass was integrated over the euphotic zone (1% incoming irradiance) while sea-ice algal biomass accounted for the ice thickness (Table 2).
Depth-integrated NPP was estimated from ^{14}C uptake rates [8,49]. All aggregate samples were homogenized before spiking the slurry with ^{14}C bicarbonate 0.1 μCi ml^{-1} final concentration ($NaH^{14}CO_3$ solution 52 mCi $mmoL^{-1}$ specific activity, Moravek Biochemicals, Brea, California, USA). Temperature was maintained stable at -1.3°C with a thermo bath (Julabo GmbH, Seelbach, Germany). Three clear bottles with 10 mL each were incubated in the light and one in the dark. The estimated error of the method from the triplicates incubated in the light was 15% on average. Floating aggregate slurries collected at station PS80/3_224 and PS80/3_237 were incubated at 50 μmol photons m^{-2} s^{-1}, which was a typical mid-day *in situ* value. Aggregate slurries from station PS80/3_349, as well as sea ice and water column of all stations were incubated under a range of irradiances (0, 8, 25, 50 and 90 μmol photons m^{-2} s^{-1}) during 24 hours to calculate the *in situ* NPP from photosynthesis vs irradiance curves (PI curves). Using this incubation time NPP is assessed (gross PP minus respiration) [50]. The PI curve was obtained after fitting the data with the

equation from [51] using MATLAB®. Only regressions with $R^2 > 0.5$ were retained. *In situ* NPP was calculated applying the irradiance measurements at the ice station to the PI curve equation.

To quantify the aggregated biomass and calculate NPP per area, aggregate abundance was quantified from scaled images. At stations PS80/3_224 (Aggregate P4) and PS80/3_237 (Aggregate P5) mean aggregate abundance under the ice was estimated from images taken by the upward looking camera of a Remotely Operated Vehicle (ROV) as described in [8]. At station PS80/3_349, *Melosira* filamentous biomass (Aggregate M5) was estimated from scaled images of the open melt pond (Fig. 2B). The aggregates were photographed with a waterproof camera (Lumix DMC-TS1). The diameter size range used to calculate the aggregate volume, assuming spherical shape, was determined from *in situ* observations of ~10 aggregates per station before mixing them to form slurry. Thus, the up scaled values in this study represent local estimates for spatial scales of 1–10 m. This approach is different from that of [8] where the mean aggregate diameter was calculated from the ROV dives and used for up scaling to the dimensions of the ice floe. For spherical aggregates, the *in situ* measured diameter size range used in this study was 3–10 cm, while in [8] the mean diameter for the floe scale used was determined to be 0.8–1 cm. For the filamentous aggregates the measured length was 10–30 cm and the observed shape was cylindrical. The minimum and the maximum aggregated biomass per m^2 was calculated by multiplying the average volume of aggregates (n = 10) by the number of aggregates observed per m^2 and by the carbon concentration of the aggregate per volume (mg C m^{-3}). The aggregate NPP per m^2 was calculated similarly, by multiplying the total aggregate volume per m^2 by the measured carbon fixation rate. Chl *a* was estimated from the C:Chl *a* ratio measured in the algal slurry from the same aggregate type. A similar procedure was used for the C:N ratios. Since aggregates showed a very patchy distribution, these calculations reflect local estimates at the sampling spot and cannot be directly up scaled to the Arctic-wide ice-cover.

Oxygen, carbon and nitrogen turnover of Melosira arctica aggregates

On 18 September 2012, station PS80/3_349 (87° 56.01' N, 61° 13.04' E), a piece of ice from the frozen surface of an open melt pond was retrieved with algal aggregates attached (Fig. 2B). These were kept in a glass beaker with 800 mL of ambient seawater, at simulated *in situ* conditions: low light (8 μmol photons m^{-2} s^{-1}) and cold temperature (0°C). The initial temperature of the melt pond water collected for the experiment was -1°C. After 12 h in the cold lab-container (0°C) under low light intensity (8 μmol photons m^{-2} s^{-1}), the water reached 0°C and the piece of ice

started melting. The vertical position of the aggregates was followed over time and as a function of the salinity gradient and the light intensity, to assess their buoyancy at different environmental conditions. In parallel, sub-samples of the algal slurry from the same type of aggregate were incubated under different conditions to assess oxygen, carbon and nitrogen fluxes.

Five sub-samples were incubated under different light intensities to estimate NPP from ^{14}C uptake rates, as described above. In addition, oxygen concentration was followed in the same vials using fiber optic oxygen sensors (FireStingO2, PyroScience GmbH, Aachen, Germany). Oxygen sensitive sensor spots were glued to the interior of the glass vials previous to the experiment. The sensor spots contain an oxygen quenchable fluorophore (oxygen sensitive dye) which changes its fluorescence properties according to the oxygen concentration [52]. After a two point calibration at the temperature of the experiment, in air saturated and oxygen free seawater, oxygen concentration was measured in each vial prior to the experiment, after 2, 7, 17 and 28 h of incubation. NPP was calculated from the slope between oxygen concentration at each time point (regression $R^2 > 0.93$) and a photosynthetic quotient of 1.25 was used to convert the oxygen exchange to carbon equivalents [53].

To measure the nitrate uptake, a 50 mL slurry sub-sample was incubated at 50 μmol photons m^{-2} s^{-1} and nitrate was measured initially and after 1 and 4 days. In parallel, 18 subsamples of the algal slurry were incubated in 12 mL exetainers (Labco Inc., Buckinghamshire, England) to measure the denitrification and nitrification potential. Subsamples of the slurries were spiked either with $^{15}NO_3$, with $^{15}NH_4^+$ or with a mixture of $^{14}NO_3$ and $^{15}NH_4^+$ (final concentration 50 μmol L^{-1}), using a modified version of the method described in [54]. One sub-sample of each treatment was placed at 50 μmol photons m^{-2} s^{-1}, while the remaining sub-samples were placed in darkness. The gradual O_2 consumption was followed in both set ups using the optode system described above. Anoxic conditions were reached after two days in the dark. The first time series was ended immediately by injecting 100 μL $ZnCl_2$ into the exetainers, while the remaining samples were terminated as the oxygen level reached 67, 35, and 0%, after 0.8, 1.2 and 2 days respectively. The isotopic composition of the N_2 was measured using a gas chromatograph coupled to an isotope ratio mass spectrometer through a ConFlo-III interphase [55]. Calculations for denitrification rates were done according to [56]. The remaining sample volume was subsequently filtered through disposable, 0.45 μm filters and concentrations of ammonium, nitrate and nitrite (NO_x) were determined [57,58].

Results

Sea ice and melt pond observations

During August and September 2011 and 2012, FYI in a late melting stage was the dominant ice type at seven of the eight ice stations investigated (Table S1 and S2). Sea-ice thickness was between 0.7 and 2 m and melt pond coverage ranged between 10 and 50%. Only one MYI floe could be sampled during both cruises. The melt ponds sampled along the eight ice stations, had different depths (0.3–1 m), salinities (0–32), were open or closed to the seawater below them, and varied in ice cover. In partially open melt ponds at stations PS78/3_212 (Fig.2A) and PS80/3_224 (Fig.2D), a steep salinity gradient with 0 at the surface and values of 28–30 at the bottom (~0.4 m depth) was measured. Closed melt ponds at stations PS78_203, PS78/3_209, PS80/3_224 and PS80/3_255 had a steep salinity gradient too, but the maximum salinity at the bottom (0.3–0.6 m depth) was generally lower than in open melt ponds (Table S1 and S2). Aggregates were located either at the bottom of the melt pond where the salinity was highest or frozen within the ice cover (Fig. 2B).

Types of algal aggregates and their degradation stages

By macroscopic and microscopic observations of the diatom composition (Fig. 3), two different types of algal aggregates were identified: (1) spherical aggregates floating under the ice or trapped in melt ponds, mainly composed of pennate diatoms (*Nitzschia* sp.*, Navicula* sp.*, Fragilariopsis* sp., and *Entomoneis* sp.) (Table S1), and (2) hanging filamentous strings, mainly composed of the centric diatom *Melosira arctica* (Table S2).

Both the pennate and centric diatom aggregates were present in different degradation stages (Fig. 3). Their characteristics are summarized in Table 1. Fresh, green-brownish aggregates of both types were found below the sea ice, either floating or attached to the ice (Fig. 2B), while degraded, yellow-whitish aggregates were usually found at the bottom of melt ponds in cryoconite holes (Fig. 2A). Microscopic observations confirmed that the green-brownish aggregates were formed by diatoms with healthy-looking chloroplasts in their cytoplasm (bright green under the light microscope and occupying almost the entire cytoplasm), while the yellow and white aggregates contained a high proportion of empty frustules (Fig. 2). Green-brownish aggregates generally

occurred where nutrient concentrations were above 2 μmol L^{-1} nitrate, 0.2 μmol L^{-1} phosphate, and 2 μmol L^{-1} silicate at the bottom of melt ponds or below the ice.

White-yellowish aggregates had higher C:N molar and C:Chl *a* mass ratios than green-brownish aggregates (Table 1). The highest Chl *a* values were encountered in dark green-brown aggregates (Fig. 3A), and the lowest values were observed in aggregates with white coloration (Fig. 3B). The stickiness of the aggregates is reflected in the TEP:POC ratio (0.001–0.17), that was highest in aggregates found in melt ponds where the nutrients were low (nitrate < 0.2 μmol L^{-1}, phosphate < 0.02 μmol $L^{-1}$and silicate < 2 μmol L^{-1}) (M1 and M4, Table S2). In general, degraded aggregates contained more TEP than fresh aggregates (Table 1).

Bacterial abundance in the aggregate slurries spanned two orders of magnitude, from 6.3×10^7 to 1.5×10^9 cells mg POC^{-1}, making up 0.2–20% (Median of 1.2%) of the POC. Greenish-brownish aggregates hosted one order of magnitude more bacteria than white-yellowish aggregates. The DOC concentrations of the algal aggregates ranged between 5 and 35 μmol DOC mg POC^{-1} (Table 1), making up 4–30% of the total carbon (sum of POC and DOC). This corresponds to an average of 295 μmol L^{-1} DOC in the algal slurries, which is higher than the average DOC concentration in Central Arctic surface waters (58 μmol L^{-1} DOC [59]). White-yellowish *Melosira* filaments had slightly higher DOC concentrations than green-brownish filaments, although the difference was not statistically significant. Even though no quantification of grazing rates was performed, the observation of active ciliates, particularly in degraded aggregates and in some fresh aggregates, suggests that aggregates served as food source for sympagic meiofauna. In addition, grazing copepods and amphipods were observed in some spherical pennate aggregates. However, no such grazers were observed on green-brownish *Melosira arctica* filaments.

Contribution of algal aggregates to system scale phototrophic biomass and primary production

Due to their patchy distribution and inaccessibility, green-brownish sub-ice aggregates could only be sampled at three stations although they were observed with the ROV at all eight stations investigated. Yellow-whitish aggregates reached highest abundances in melt ponds (stations PS78/3_212 (Fig. 2A) and PS80/3_224 (Fig. 2D)).

Table 2 compares the integrated phototrophic biomass of sea ice (1.2–1.4 m thickness), water column euphotic zone (12–18 m depth), and the two different types of aggregates investigated,

including previous observations on pennate diatom [8,22] and *Melosira* based aggregates [5,14]. Under-ice ROV surveys revealed a high degree of horizontal patchiness in aggregate abundance below the ice (Fig. 2C). Locally, spherical floating aggregates reached an abundance of 0.8–5.1 aggregates m^{-2} and a diameter of 3–10 cm, containing 0.1–3.7 mg Chl *a* m^{-2}, which corresponded to 3–38 % of total phototrophic biomass. *Melosira arctica* filaments observed in autumn 2012 were 10–30 cm long and reached abundances of 17 aggregates m^{-2} with 14–44 mg Chl *a* m^{-2}, corresponding to 57–80% of total phototrophic biomass.

At the sampled sites, floating aggregates contributed with 0.5–26% (pennate), and 55–78% (*Melosira)* to the particulate organic carbon pool of the integrated euphotic zone (Table 2). Pennate-diatom aggregates showed Chl *a*/CPE values similar to the sea-ice algae at the same station, while *Melosira* filaments showed Chl *a*/CPE values similar to the pelagic communities. In general the C:N ratios of green-brownish aggregates (8–28) were higher than the values for the phytoplankton (~5) and the sea-ice algae (6–8). Green-brownish *Melosira* aggregates showed higher C:N ratios (9–28) than all pennate aggregates (8–11). In white-yellowish aggregates C:N ratios were generally higher (11–35 in pennate and 10–40 in *Melosira* aggregates).

Regarding *in situ* NPP per m^2, spherical floating aggregates showed similar NPP as the corresponding integrated value for sea ice, and 50% of the value for the depth-integrated water columns euphotic zone (15–18 m) (Table 2). In contrast, up scaled *Melosira arctica* filaments reached NPP rates one order of magnitude higher than the values of the integrated water columns euphotic zone (12 m) and the sea ice in late September (Table 2). The daily average irradiance received below the ice *in situ* at stations PS80/3_224 and 237, where pennate aggregates were found, was 99 and 52 μmol photons m^{-2} s^{-1}, respectively. Hence, *in situ* NPP of aggregates at station 224 may be underestimated, since the incubation performed at 50 μmol photons m^{-2} s^{-1}.

For the *Melosira arctica* filaments found at station PS80/3_349, both carbon uptake and oxygen production were monitored in homogenized algal slurries at different light intensities. The fitted PI curve of the carbon uptake (R^2 = 0.986), showed a photosynthetic maximum (P_{max}) of 3.7 mg C L^{-1} d^{-1}, an initial slope of 120 μg C L^{-1} d^{-1} (μmol photons m^{-2} s^{-1})$^{-1}$ and no photoinhibition at irradiances lower than 90 μmol photons m^{-2} s^{-1} (Fig. 4). Carbon uptake could be quantified even at the lowest irradiance (8 μmol photons m^{-2} s^{-1}). However, no net oxygen production took place at this irradiance, rather oxygen was consumed (Fig. 4). At light levels above 20 μmol photons m^{-2} s^{-1}, oxygen production was detected.

Buoyancy test

Besides the observations of floating aggregates in the laboratory, some aggregates were observed floating below the ice, others at the pycnocline in open melt ponds and also coming up to the surface through bore holes in the ice. To investigate the causes of buoyancy, a simple test was performed with intact aggregates (n = 4) anchored to newly formed ice from station PS80/3_349, composed of a mixture of *Melosira arctica*, *Cylindrotheca* sp., and *Nitzschia* sp. (Fig. 3C and G, Fig. 5A) (M5 in Table S2). Once the ice had melted, the four intact algal aggregates remained floating at the surface (Fig. 5B). It was then observed that air bubbles of different sizes (0.01 to 0.7 cm) were trapped in the mucous matrix of the floating aggregates (Fig. 5B bottom). To test if these air bubbles were responsible for the aggregates buoyancy, the bubbles of one aggregate were physically removed. The aggregate devoid of bubbles sunk to the bottom of the beaker, regardless of the stable salinity gradient formed due to the ice melt (Fig. 5C). After 24 hours, the remaining aggregates also sank to the bottom of the beaker (Fig. 5D). To test if photosynthetically produced oxygen was the source of the aggregate bubbles, we increased the light intensity reaching the sunken aggregates in the beaker. After increasing the irradiance to 50 µmol photons m^{-2} s^{-1} for 48 h, the sunken aggregates formed bubbles and regained their buoyancy (Fig. 5E), indicating that photosynthetically produced oxygen might be responsible for the gas bubble formation.

Oxygen and carbon turnover in algal aggregates

The *Melosira* slurry showed a bulk oxygen consumption rate of 0.13 ± 0.02 mmol O_2 L^{-1} d^{-1} at low irradiance (8 µmol photons m^{-2} s^{-1}). Non-invasive measurements with microsensors on one pennate-diatom also showed net oxygen consumption with almost anoxic conditions (10-120 µmol L^{-1} Oxygen) in the center of the aggregate (see supplementary information and Fig. S1).

Assuming a 1:1.25 ratio of CO_2 production to O_2 respiration, we transformed the oxygen consumption rate mentioned above into carbon respiration rate. Dividing the POC measured in each sample (Table S2) by the carbon respiration rate, we estimated the carbon turnover in the *Melosira* slurry. The turnover of particulate carbon at low irradiance (8 µmol photons m^{-2} s^{-1}) would be 8–11 days. Net oxygen consumption and carbon remineralization occurred at lower light intensities in the *Melosira* algal slurry than in the compact pennate-diatom aggregate. Floating

green-brownish aggregates incubated for 4–5 days at low irradiances lost their buoyancy and became net heterotrophic. Oxygen production in both aggregate types was probably light regulated. However, this observation is based on single measurements, with the two respective types of aggregates. Further experiments are needed to fully conclude that light-regulated oxygen production is responsible for aggregate buoyancy.

Nitrogen cycling in Melosira *aggregates*

Nitrate and ammonium concentrations were monitored in parallel in the *Melosira* algal slurry sample incubated under *in situ* representative light conditions (50 μmol photons m^{-2} s^{-1}). During the first 24 h, the nitrate consumption rate was 0.94 μmol N L^{-1} and the ammonium consumption 2.47 μmol N L^{-1}. Denitrification and nitrification potential was measured in slurry samples spiked with labeled nitrate and ammonium, respectively ($^{15}NO_3$ and $^{15}NH_4^+$). During light, nitrate was produced at a rate of 1.7 ± 0.001 μmol L^{-1} d^{-1} and ammonium was consumed at a rate of 1.6 ± 0.003 μmol L^{-1} d^{-1}. In the dark, nitrate was produced at lower rates (0.4–0.5 μmol L^{-1} d^{-1}) and high net ammonification rates were measured (1.5–5.8 μmol L^{-1} d^{-1}). A potential for denitrification could be detected (2–5 nmol L^{-1} d^{-1}) under anoxic conditions. Aggregates appeared to be hot spots for nitrogen cycling with potential for ammonification, nitrification and denitrification, and the rates seemed to be regulated by ambient light availability.

Discussion

Aggregate formation, distribution and degradation

Different types of aggregations of algae have been described in Arctic sea ice, mostly by observations made during summer, below pack ice [8,14,15,21,22]. At the end of the productive season, floating sub-ice algal aggregates tend to accumulate in dom-shape structures below the ice or in half open melts ponds or cracks. They have a very patchy distribution that seems to be governed by ice topography.

Based on our measurements and a synthesis of previous studies, we propose a conceptual model for aggregate formation and degradation in the Arctic (Fig. 6). This concept is based on the current trends of thinning sea-ice and higher melt pond coverage [60,61], but it only applies to the current situation and not to the Arctic ecosystem of three decades ago and it remains unclear if and for how long it can be projected into the future. Considering an average ice thickness of 1–2 m, light for photosynthesis is available to ice algae already in April-May, and single cells of sea-ice algae that have survived the winter darkness [62,63] can grow in the brine channels of the ice matrix [3] (Fig. 6.1). In summer, ice melting from the top and the bottom releases diatoms into ice cracks, melt ponds and the water column, respectively [8,21,22] (Fig. 6.2). Since sea-ice diatoms produce high concentrations of transparent exopolymers in the ice [27,64] they tend to aggregate under moderate turbulence and shear, creating algal flocs [65,66].

Newly formed melt ponds are usually shallow, light blue, have low salinity, and contain little visible life [67,68]. As melt ponds grow in depth during summer, the freshwater pool increases and sea-ice algae living at the bottom of the ponds or in pond water are gradually exposed to higher irradiances, lower salinity, and less nutrients (Fig. 6.3). Since sea-ice algae are adapted to low light [69,70], low temperature and high salinity [48,71], these new conditions could trigger the exudation of polysaccharides that create a mucous matrix around the cells [72], thereby increasing their stickiness and their predisposition to aggregation. This is probably the case for pennate diatom species growing in the ice as single cells and aggregating after their release during ice melt. However, the centric diatom *Melosira arctica*, grows forming chains and excretes high amounts of mucus that contribute to the formation of filament-shaped aggregates [73]. Nutrient depletion can also increase diatom exopolymer exudation [23,28,74], contributing to aggregation. In autumn 2011, we observed many previous ponds, which had opened to the underlying seawater, allowing an exchange of phytoplankton species between seawater and the sea ice habitat (Fig.

6.4A), for example at station PS78/3_212 (Fig. 2A, Table S1). Around mid-September ice-melt stops and melt ponds close again when their surface and bottom refreezes (Fig. 6.4B). Mostly white-yellowish, apparently degraded aggregates were found in this type of closed melt pond in late autumn (Fig. 3B). Some diatoms, such as *Melosira arctica*, build up dense biomass accumulations despite nutrient constrains, that can be exported to the deep sea upon rapid melting of the sea ice [9,75]. Probably the attachment to the lower part of the ice enables them to harvest nutrients from a wider area while drifting over large distances. Some of them can maintain buoyancy throughout summer and can then be refrozen into the newly formed ice in early autumn (Fig. 6.5) [68].

Relevance of sea-ice algal aggregates for Arctic carbon and nitrogen fluxes

The spatial and temporal patchiness remains a challenge when estimating the importance of algal aggregates for ecosystem productivity and carbon flux [8,30]. Assmy et al., 2013 measured rather small Chl *a* concentrations (2–6 μg Chl *a* m^{-2}) when up scaling the contribution of the observed aggregates to the area of the entire ice floe. Here we assessed the standing stock and productivity at a local scale, for two different types of sea-ice algal aggregates. Our study took place at the end of the summer, when nutrient depletion limits pelagic productivity. During this period, we found that algal aggregates contributed significantly to total biomass at a local scale in and below the sea-ice.

The estimates of Chl *a* reported here for spherical aggregates formed by pennate diatoms (Table 2) is within the range of values reported earlier (2.9 ± 1.2 mg Chl *a* m^{-2}; Fram Strait, [22]). Locally, higher Chl *a* values were reached by *Melosira arctica* filamentous aggregates in late September, contributing 57–80% to total phototrophic biomass when phytoplankton activity is reduced in the water column (Table 2). Also these values fall in the range of values previously reported for this type of *Melosira* sub-ice assemblage associated with MYI (22 mg Chl *a* m^{-2} [14]) or FYI (52–200 mg Chl *a* m^{-2} [5]). This suggests that ice algal aggregations could be a relevant food source in a wider area partly for under-ice zooplankton and for nekton at the end of the season and potentially also in winter, before the aggregates freeze into the ice [8,76,77]. In contrast, for *Melosira* aggregates, grazing has only rarely been observed [13] and much of their biomass may sink out earlier in the season [9,15,30]. Observations of regionally widespread algal falls to the seafloor indicate that algal aggregates are not only locally relevant as hot spots of microbial activity, but may also contribute substantially to total carbon export [9].

Similar conclusions as to the relative contribution to biomass are reached using the POC values of the aggregates compared to the total sympagic or pelagic community. The contribution to total PON at a local scale was lower (0.3–18%) for pennate aggregates than for *Melosira* filaments (23–47%). The overall relatively low mass ratios of C:Chl *a* of 110 and 212 for green-brownish pennate and centric diatom aggregates, respectively, indicate a healthy algal community. However, compared to the water column C:N ratio of 5–6, the green-brownish aggregates had an elevated C:N ratio (8–11 and 9–28 for green-brownish pennate and centric diatom aggregates, respectively). The white-yellowish aggregates containing many empty frustules even reached ratios of 40. This suggests an important contribution of exudate-carbon to the aggregates.

Pennate aggregates can contribute 1–23% to total *in situ* integrated NPP at a local scale, and *Melosira arctica* filaments as much as 83–94% of the total NPP north of 80ºN in mid-September, when very little production is taking place in the water column or in the sea-ice. *Melosira* filaments can be more productive than the integrated euphotic zone in and below the ice in the Central Arctic (Table 2). However, aggregate slurries may overestimate NPP, due to the reduction of light adsorption by dilution compared to the naturally densely packed aggregates, hence the total contribution of intact aggregates is likely lower [22]. Indeed, intact spherical aggregates incubated for some days in the laboratory under low light conditions appear to be net heterotrophic (Fig. S1).

Another aspect of the contribution of sea-ice algal aggregates to carbon fluxes in the Arctic Ocean is the contribution to particle export. Diatom aggregates can substantially enhance carbon flux from the pelagic realm to the benthos [24–26]. In the Arctic, sea-ice algae are main contributors of the vertical export flux in summer [10,78]. In 2012 the direct export of sea-ice algal aggregates was observed in relation to sea ice melt [9]. It was estimated that their contribution to the total carbon flux could reach 85% and from our results we can estimate that their contribution to the particulate nitrogen sinking flux potentially would be around 47% of the PON present at the end of the productive season. Considering the already low nutrient concentrations of the Central Arctic surface waters, such an export could only be sustained on decadal scales, if more nutrients would be mixed in, e.g. by increasing wind mixing, or by increasing transport from the Arctic shelves [79]. Due to their relevance at least for standing stock and export flux, it is important to better understand the mechanisms of sea-ice aggregate formation, buoyancy regulation and sedimentation.

Buoyancy regulation

Adaptations of phytoplankton cells to control buoyancy include the formation of gas vacuoles, lipid accumulation, ion exchange and morphological features like hairs and spines [24,80,81]. In the Arctic Ocean, the observation of algal aggregates floating below the pycnocline was previously explained by accumulation at vertical density gradients [8,19,21]. However, in our experiment the aggregates sank after physical removal of air bubbles trapped in the mucous matrix (Fig. 5). The salinity gradients might determine where aggregates accumulate, but density gradients were not the buoyancy regulating mechanisms *per se*. Both pennate and centric diatom-formed aggregates studied here showed gas bubbles trapped in the aggregates mucous matrix, which seem to be a relevant mechanism for aggregates to stay afloat. Previous physiological studies with another centric diatom have shown a correlation between increased light input and reduced sinking rates [81]. The results from our experiment that the sunken aggregates can regain buoyancy in situations favorable for photosynthesis, i.e. by increased light intensity, suggests that the balance between oxygen production by photosynthesis and consumption by respiration was the key factor for buoyancy regulation in the aggregates we investigated. Since aggregates are not closed systems, the rate of oxygen production plus the impeded diffusion across the mucus matrix of the aggregate minus oxygen consumption by the sea-ice algae themselves, bacteria and zooplankton, will determine the amount of gas available to maintain buoyancy [22]. However, further experiments are needed to confirm this hypothesis.

Other factors affecting buoyancy are the density of the aggregate. Diatoms exudates have been observed to be positively buoyant and to facilitate the attachment of bacteria to the aggregate [82]. Therefore, TEP do not only play an important role in aggregation but could also be important in buoyancy regulation. The TEP:POC ratios presented in this study (0.001–0.2) were generally lower than the ones reported for land fast sea ice in spring (0.08–0.72) [82], but in the same range reported for other marine diatom aggregates (~0.25; [83]) and higher than the TEP:POC ratios measured in the water column surrounding the aggregates.

Fate of the sea ice algal aggregates

Detrimental conditions to the aggregate community such as very low salinity from melt water, seawater warming, high grazing pressure, or nutrient depletion will eventually lead to buoyancy loss, degradation and sinking [9,15]. This could result in their accumulation at the bottom of melt ponds, or export to the sea floor [9,30]. White-yellowish aggregates of high TEP:POC, C:Chl *a*

and C:N ratios indicating substantial degradation of algal cells [43] were often found trapped in melt ponds where nutrients were depleted. Green-brownish aggregates contained more bacteria than white-yellowish, degraded aggregates, following the general correlation between bacterial abundance and Chl *a* observed in the ocean [84], suggesting that labile carbon supplies from the algae to the bacteria are still present in green-brownish aggregates at the end of the season. Despite the fact that bacterial abundances per carbon weight were in the lower range of values published for Antarctic sea-ice [82], they were still two orders of magnitude higher (10^7–10^9 cells mg POC^{-1}) than in the ambient water (10^5–10^7 cells mg POC^{-1}) suggesting that aggregates are a rich substrate for bacteria. The higher concentrations of DOC in the aggregates compared to the average DOC concentrations of Arctic surface seawater [59] indicate that algal aggregates might be a source of DOC, in which carbon is rapidly remineralized.

Net heterotrophic conditions were measured in floating sea-ice algal aggregates during summer indicating a rapid decomposition of the algal biomass in the aggregates ([22] and this study, also see supplementary information). Moreover, observations of photosynthetically active diatom cells in aggregates exported to the deep-sea [9] and subsequent oxygen depletion in the seafloor suggest rapid sedimentation and microbial remineralization of the aggregates. Nitrate production matched the ammonium consumption in the *Melosira* aggregate slurry, suggesting that nitrification might take place as well under photosynthetic conditions at high light intensities. This means that decaying algal aggregates could be sources of nitrate to the surrounding seawater in an otherwise nitrogen-limited system. Previously it has been speculated that internal nutrient regeneration by bacterial remineralization inside aggregates can support growth of at least a fraction of the algal population [85,86]. Denitrification, revealed by N_2 production, may occur in the anoxic center of intact aggregates [87], but the potentials encountered in *Melosira* algal slurry were low (0.002–0.005 μmol L^{-1} d^{-1}). This could indicate that the aggregates might remove considerable amounts of carbon and nitrogen from surface waters by export. Using the aggregate carbon export of 9 g C m^{-2} estimated previously for 2012 (Boetius et al. 2013), and the median C:N ratio of 10 of the fresh aggregates (n = 4), approximately 45% of carbon fixed as new production since last winter and 36% of surface nitrogen consumed by sea-ice algae and surface water phytoplankton was exported to depths >4000 m.

In conclusion, we suggest that pennate diatom and *Melosira arctica*-based ice-algal aggregates contribute substantially to nutrient and carbon cycling and export in the Arctic. Preliminary experiments suggest that their buoyancy is regulated by photosynthetically-produced oxygen. With the current trend of warming of the Arctic causing sea ice retreat as well as thinning of the

ice cover that increases drift speed, it is likely that sea-ice algae can grow faster and earlier in the season harvesting nutrients from a wider area of surface waters, but will more often meet unfavorable conditions during summer, e.g. nutrient limitation, freshening and melting of their habitat favoring aggregate formation and degradation. The advantages of the formation of aggregates compared to the single-cell or short-chain life style of pelagic sea ice algae is uncertain. Aggregation into large clumps and filaments may protect diatom species such as *Melosira arctica* from high irradiances. Trapping of gas bubbles in the aggregates enhancing floatation and eventually serving entrapment into the ice in late autumn might be another advantage. The intense nitrogen cycling observed in the aggregates indicates that they could play a role in nutrient cycling in the oligotrophic Arctic Ocean. It remains methodologically difficult, but important for a better understanding of carbon and nutrient budgets as well as for the ecology of the Arctic Ocean, to quantify temporal and regional variations in aggregate formation, distribution and fate on the ecosystem scale.

Acknowledgements

We are most grateful to the crew of RV Polarstern and to our colleagues on board for their excellent cooperation during both Arctic cruises (PS78/3 and PS80/3). In particular we would like to thank Christian Katlein and Marcel Nicolaus for their under-ice images of the aggregates, and Christiane Uhlig, Anique Stecher, Hauke Flores, Catherine Lalande, Karl Attard and Judith Piontek for their help during the sampling. We also thank Karel Bakker for the nutrient measurements and Dieter Janssen, Claudia Burau and Boris Koch for the DOC measurements. The technical support of Erika Allhusen, Christiane Lorenzen, Sandra Murawski and Mirja Meiners is also greatly appreciated. We are as well grateful to Eva-Maria Nöthig for the water column particulate carbon values and Kristin Hardge for help with microscopic identification. Fruitful discussions with Philipp Assmy and Victor Smetacek contributed to the development of the ideas presented in this study.

References

1. Stein R, Macdonald RW (2004) The Organic Carbon Cycle in the Arctic Ocean. 1st ed. Springer-Verlag Berlin Heidelberg GmbH.

2. Leu E, Søreide JEE, Hessen DOO, Falk-Petersen S, Berge J (2011) Consequences of changing sea-ice cover for primary and secondary producers in the European Arctic shelf seas: Timing, quantity, and quality. Prog Oceanogr 90: 18–32. doi:10.1016/j.pocean.2011.02.004.

3. Legendre L, Horner R, Ackley SF, Dieckmann GS, Gulliksen B, et al. (1992) Ecology of sea ice biota: 2. Global significance. Polar Biol 12: 429–444. doi:10.1007/BF00243113.

4. Hill VJ, Matrai PA, Olson E, Suttles S, Steele M, et al. (2013) Synthesis of integrated primary production in the Arctic Ocean: II. In situ and remotely sensed estimates. Prog Oceanogr 110: 107–125. doi:10.1016/j.pocean.2012.11.005.

5. Gosselin M, Levasseur M, Wheeler PA, Horner RA, Boothg BC (1997) New measurements of phytoplankton and ice algal production in the Arctic Ocean. Deep Sea Res Part II 44: 1623–1644. doi:10.1016/S0967-0645(97)00054-4.

6. Soreide J, Leu E, Berge J, Graeve M, Falk-Petersen S, et al. (2010) Timing of blooms, algal food quality and *Calanus glacialis* reproduction and growth in a changing Arctic. Glob Chang Biol 16: 3154–3163. doi:10.1111/j.1365-2486.2010.02175.x.

7. Bradstreet MSW, Cross WE (1982) Trophic relationships at high Arctic ice edges. Arctic 35: 1–12.

8. Assmy P, Ehn JK, Fernández-Méndez M, Hop H, Katlein C, et al. (2013) Floating ice-algal aggregates below melting Arctic sea ice. PLoS One 8: e76599. doi:10.1371/journal.pone.0076599.

9. Boetius A, Albrecht S, Bakker K, Bienhold C, Felden J, et al. (2013) Export of algal biomass from the melting Arctic sea ice. Science 339: 1430–1432. doi:10.1126/science.1231346.

10. Fahl K, Nöthig E-M (2007) Lithogenic and biogenic particle fluxes on the Lomonosov Ridge (central Arctic Ocean) and their relevance for sediment accumulation: Vertical vs. lateral transport. Deep Sea Res Part I 54: 1256–1272. doi:10.1016/j.dsr.2007.04.014.

11. Riedel A, Michel C, Poulin M, Lessard S (2003) Taxonomy and abundance of microalgae and protists at a first-year sea ice station near Resolute Bay, Nunavut Spring to Early Summer 2001.

12. Michel C, Ingram R, Harris L (2006) Variability in oceanographic and ecological processes in the Canadian Arctic Archipelago. Prog Oceanogr 71: 379–401. doi:10.1016/j.pocean.2006.09.006.

13. Quillfeldt C Von, Hegseth EN, Sakshaug E, Johnsen G, Syvertsen EE (2009) Ice algae. In: Sakshaug E, Johnsen G, Kovacs KM, editors. Ecosystem Barents Sea. Trondheim, Norway: Tapir Aacademic Press. pp. 285–302.

14. Melnikov IA (1977) The Arctic Sea Ice ecosystem. Amsterdam: Gordon and Breach Science Publishers.

15. Gutt J (1995) The occurrence of sub-ice algal aggregations off northeast Greenland. Polar Biol 15: 247–252. doi:10.1007/BF00239844.

16. Melnikov IA, Kolosova EG, Welch HE, Zhitina LS (2002) Sea ice biological communities and nutrient dynamics in the Canada Basin of the Arctic Ocean. Deep Sea Res Part I Oceanogr Res Pap 49: 1623–1649. doi:10.1016/S0967-0637(02)00042-0.

17. Poulin M, Underwood GJC, Michel C (2014) Sub-ice colonial *Melosira arctica* in Arctic first-year ice. Diatom Res 29: 1–9. doi:10.1080/0269249X.2013.877085.

18. Gran H (1904) Diatomaceae from the ice-floes and plankton of the Arctic Ocean. Sci Res North Polar Exped 11: 1–74.

19. Nansen F (1906) Protozoa on the ice-floes of the North Polar Sea. Sci Res Norw North Polar Exped 1893-1896 5: 1–22.

20. Horner RA, Syvertsen EE, Thomas DP, Lange C (1988) Proposed Terminology and Reporting Units for Sea Ice Algal Assemblages. Polar Biol 8: 249–253. doi:10.1007/BF00263173.

21. Syvertsen EE (1991) Ice algae in the Barents Sea: types of assemblages, origin, fate and role in the ice-edge phytoplankton bloom. Proc Pro Mare Symp Polar Mar Ecol: 277–287.

22. Glud RN, Rysgaard S, Turner G, McGinnis DF, Leakey RJ (2014) Biological and physical induced oxygen dynamics in melting sea-ice of the Fram Strait. Limnol Oceanogr 59: 1097–1111. doi:10.4319/lo.2014.59.4.1097.

23. Kiorboe T, Andersen K., Dam H. (1990) Coagulation efficiency and aggregate formation in marine phytoplankton. Mar Biol 107: 235–245. doi:10.1007/BF01319822.

24. Smetacek VS (1985) Role of sinking in diatom life-history cycles: ecological , evolutionary and geological significance. Mar Biol 84: 239–251. doi:10.1007/BF00392493.

25. Alldredge AL, Silver MW (1988) Characteristics, dynamics and significance of marine snow. Prog Oceanogr 20: 41–82. doi:10.1016/0079-6611(88)90053-5.

26. Jackson GA, Waite AM, Boyd PW (2005) Role of algal aggregation in vertical carbon export during SOIREE and in other low biomass environments. Geophys Res Lett 32: L13607. doi:10.1029/2005GL023180.

27. Krembs C, Eicken H, Junge K, Deming J. W (2002) High concentrations of exopolymeric substances in Arctic winter sea ice: implications for the polar ocean carbon cycle and cryoprotection of diatoms. Deep Sea Res Part I 49: 2163–2181. doi:10.1016/S0967-0637(02)00122-X.

28. Abdullahi AS, Underwood GJC, Gretz MR (2006) Extracellular matrix assembly in Diatoms (Bacillariophyceae). Environmental effects on polysaccharide synthesis in the model diatom, *Phaeodactylum tricornutum*. J Phycol 42: 363–378. doi:10.1111/j.1529-8817.2006.00193.x.

29. Aslam SN, Cresswell-Maynard T, Thomas DN, Underwood GJC (2012) Production and characterization of the intra- and extracelullar carbohydrates and polymeric substances (EPS) of three sea-ice diatom species, and evidence for a cryoprotective role for EPS. J Phycol 48: 1494–1509. doi:10.1111/jpy.12004.

30. Ambrose WG, Quillfeldt C Von, Clough LM, Tilney PVR, Tucker T (2005) The sub-ice algal community in the Chukchi sea: large- and small-scale patterns of abundance based on

images from a remotely operated vehicle. Polar Biol 28: 784–795. doi:10.1007/s00300-005-0002-8.

31. Rothrock DA, Yu Y, Maykut GA (1999) Thinning of the Arctic sea-ice cover. Geophys Res Lett 26: 3469–3472. doi:10.1029/1999GL010863.

32. Stroeve JC, Serreze MC, Holland MM, Kay JE, Malanik J, et al. (2012) The Arctic's rapidly shrinking sea ice cover: a research synthesis. Clim Change 110: 1005–1027. doi:10.1007/s10584-011-0101-1.

33. Nicolaus M, Katlein C, Maslanik J, Hendricks S (2012) Changes in Arctic sea ice result in increasing light transmittance and absorption. Geophys Res Lett 39: 1–6. doi:10.1029/2012GL053738.

34. Li WKW, McLaughlin FA, Lovejoy C, Carmack EC (2009) Smallest algae thrive as the Arctic Ocean freshens. Science 326: 539. doi:10.1126/science.1179798.

35. Carmack EC, Lovejoy C, Comeau M, Li WKW (2011) Arctic Ocean microbial community structure before and after the 2007 record sea ice minimum. PLoS One 6: e27492. doi:10.1371/journal.pone.0027492.

36. Slagstad D, Ellingsen IHH, Wassmann P (2011) Evaluating primary and secondary production in an Arctic Ocean void of summer sea ice: an experimental simulation approach. Prog Oceanogr 90: 117–131. doi:10.1016/j.pocean.2011.02.009.

37. Brown ZW, Arrigo KR (2012) Contrasting trends in sea ice and primary production in the Bering Sea and Arctic Ocean. ICES J Mar Sci 69: 1180–1193. doi:10.1093/icesjms/fss113.

38. Ji R, Jin M, Varpe Ø, Jil R, Varpe O (2013) Sea ice phenology and timing of primary production pulses in the Arctic Ocean. Glob Chang Biol 19: 734–741. doi:10.1111/gcb.12074.

39. Nicolaus M, Katlein C, Maslanik JA, Hendricks S (2012) Sea ice conditions during the POLARSTERN cruise ARK-XXVI/3 (TransArc) in 2011. PANGAEA. doi:doi:10.1594/PANGAEA.803312.

40. Perovich DK (1996) The Optical Properties of Sea Ice. Cold Reg Res Eng Lab Monograph : 1–31.

41. Tran S, Bonsang B, Gros V, Peeken I, Sarda-Esteve R, et al. (2013) A survey of carbon monoxide and non-methane hydrocarbons in the Arctic Ocean during summer 2010. Biogeosciences 10: 1909–1935. doi:10.5194/bg-10-1909-2013.

42. Engel A (2009) Determination of marine gel particles. In: Wurl O, editor. Practical Guidelines for the Analysis of Seawater. CRC Press. p. 18.

43. Engel A, Passow U (2001) Carbon and nitrogen content of transparent exopolymer particles (TEP) in relation to their Alcian Blue adsorption. Mar Ecol Prog Ser 219: 1–10. doi:10.3354/meps219001.

44. Damm E, Helmke E, Thoms S, Schauer U, Nöthig E-M, et al. (2010) Methane production in aerobic oligotrophic surface water in the central Arctic Ocean. Biogeosciences 7: 1099–1108. doi:10.5194/bg-7-1099-2010.

45. Hobbie JE, Daley RJ, Jasper S (1977) Use of nuclepore filters for counting bacteria by fluorescence microscopy. Appl Environ Microbiol 33: 1225–1228.

46. Meyer-Riel L. (1983) Benthic response to sedimentation events during autumn to spring at a shallow water station in the Western Kiel Bight. Mar Biol 77: 247–256. doi:10.1007/BF00395813.

47. Gradinger R, Friedrich C, Spindler M (1999) Abundance, biomass and composition of the sea ice biota of the Greenland Sea pack ice. Deep Sea Res Part II 46: 1457–1472. doi:10.1016/S0967-0645(99)00030-2.

48. Thomas DN, Dieckmann GS (2010) Sea Ice. Thomas DN, Dieckmann GS, editors West Sussex: Wiley-Blackwell.

49. Steemann Nielsen E (1952) The use of radio-active carbon (C14) for measuring organic production in the sea. J Cons Int Explor Mer 18: 117–140.

50. Peterson BJ (1980) Aquatic primary productivity and the ^{14}C-CO_2 method: a history of the productivity problem. Ecology 11: 359–385. doi:10.1146/annurev.es.11.110180.002043.

51. Gallegos CL, Platt T, Harrison WG, Irwin B (1983) Photosynthetic parameters of arctic marine phytoplankton: vertical variations and time scales of adaptation. Limnol Oceanogr 28: 698–708.

52. Klimant I, Kühl M, Glud RNN, Holst G (1997) Optical measurement of oxygen and temperature in microscale: strategies and biological applications. Sensors Actuators B 39: 29–37. doi:10.1016/S0925-4005(97)80168-2.

53. McMinn A, Hegseth EN (2006) Sea ice primary productivity in the northern Barents Sea, spring 2004. Polar Biol 30: 289–294. doi:10.1007/s00300-006-0182-x.

54. Rysgaard S, Glud RN (2004) Anaerobic N_2 production in Arctic sea ice. Limnol Oceanogr 49: 86–94.

55. Dalsgaard T, Thamdrup B, Farías L, Peter Revsbech N (2012) Anammox and denitrification in the oxygen minimum zone of the eastern South Pacific. Limnol Oceanogr 57: 1331–1346. doi:10.4319/lo.2012.57.5.133.

56. Thamdrup B, Dalsgaard T (2002) Production of N_2 through anaerobic ammonium oxidation coupled to nitrate reduction in marine sediments. Appl Environ Microbiol 68: 1312–1318. doi:10.1128/AEM.68.3.1312-1318.2002.

57. Bower C, Holm-Hansen T (1980) A salicylate-hypochlorite method for determining ammonia in seawater. Can J Fish Aquat Sci 37: 794–798.

58. Braman RS, Hendrix SA (1989) Nanogram nitrite and nitrate determination in environmental and biological materials by vanadiumv(III) reduction with chemiluminescence detection. Anal Chem 91: 2715–2718.

59. Wheeler PA, Gosselin M, Sherr E, Thibault D, Kirchman DL, et al. (1996) Active cycling or organic carbon in the central Arctic Ocean. Nature 380: 697–699. doi:10.1038/380697a0.

60. Maslanik JA, Fowler C, Stroeve J, Drobot S, Zwally J, et al. (2007) A younger, thinner Arctic ice cover: increased potential for rapid, extensive sea-ice loss. Geophys Res Lett 34: L24501. doi:10.1029/2007GL032043.

61. Rösel A, Kaleschke L (2012) Exceptional melt pond occurrence in the years 2007 and 2011 on the Arctic sea ice revealed from MODIS satellite data. J Geophys Res 117: 1–8. doi:10.1029/2011JC007869.

62. Sherr EB, Sherr BF, Wheeler PA, Thompson K (2003) Temporal and spatial variation in stocks of autotrophic and heterotrophic microbes in the upper water column of the central Arctic Ocean. Deep Sea Res Part I Oceanogr Res Pap 50: 557–571. doi:10.1016/S0967-0637(03)00031-1.

63. Bachy C, López-García P, Vereshchaka A, Moreira D (2011) Diversity and vertical distribution of microbial eukaryotes in the snow, sea ice and seawater near the north pole at the end of the polar night. Front Microbiol 2: 1–12. doi:10.3389/fmicb.2011.00106.

64. Juhl AR, Krembs C, Meiners KM (2011) Seasonal development and differential retention of ice algae and other organic fractions in first-year Arctic sea ice. Mar Ecol Prog Ser 436: 1–16. doi:10.3354/meps09277.

65. Riebesell U, Schloss I, Smetacek V (1991) Aggregation of algae released from melting sea ice: implications for seeding and sedimentation. Polar Biol 11: 239–248. doi:10.1007/BF00238457.

66. Kiorboe T, Hansen JLS (1993) Phytoplankton aggregate formation: observations of patterns and mechanisms of cell sticking and the significance of exopolymeric material. J Plankton Res 15: 993–1018. doi:10.1093/plankt/15.9.993.

67. Eicken H, Krouse HR, Kadko D, Perovich DK (2002) Tracer studies of pathways and rates of meltwater transport through Arctic summer sea ice. J Geophys Res 107: 8046. doi:10.1029/2000JC000583.

68. Lee SH, McRoy CPP, Joo HM, Gradinger R, Cui X, et al. (2011) Holes in progressively thinning Arctic sea ice lead to new ice algae habitat. Oceanography 24: 302–308. doi:10.5670/oceanog.2011.81.

69. Cota GF (1985) Photoadaptation of high Arctic ice algae. Nature 315: 219–222.

70. Manes SS, Gradinger R (2009) Small scale vertical gradients of Arctic ice algal photophysiological properties. Photosynth Res 102: 53–66. doi:10.1007/s11120-009-9489-0.

71. Arrigo K, Sullivan CW (1992) The influence of salinity and temperature covariation on the photophysiological characteristics of antarctic sea ice microalgae. J Phycol 28: 746–756. doi:10.1111/j.0022-3646.1992.00746.x.

72. Mari X, Burd A (1998) Seasonal size spectra of transparent exopolymeric particles (TEP) in a coastal sea and comparison with those predicted using coagulation theory. Mar Ecol Prog Ser 163: 63–76. doi:doi:10.3354/meps163063.

73. Dickie G (1852) Notes on the algae. In: Sutherland PC, editor. Journal of a Voyage in Baffin's Bay and Barrow Straits in the years 1850–1851. (Longman, Brown, Green, and Longmans, London), Vol. II. pp. cxci–cc.

74. Wood MA, Van Valen LM (1990) Paradox lost? On the release of energy rich compounds by phytoplankton. Mar Microb Food Webs 4: 103–116.

75. Lalande C, Bauerfeind E, Nöthig E-M, Beszczynska-Möller A (2013) Impact of a warm anomaly on export fluxes of biogenic matter in the eastern Fram Strait. Prog Oceanogr 109: 70–77. doi:10.1016/j.pocean.2012.09.006.

76. Poltermann M (2001) Arctic sea ice as feeding ground for amphipods – food sources and strategies. Polar Biol 24: 89–96. doi:10.1007/s003000000177.

77. Mundy C, Michel G, Jens KE, Claude B, Poulin M, et al. (2011) Characteristics of two distinct high-light acclimated algal communities during advanced stages of sea ice melt. Polar Biol 34: 1869–1886. doi:10.1007/s00300-011-0998-x.

78. Zernova VV, Nöthig E-M, Shevchenko VP, Schevschenko VP (2000) Vertical microalga flux in the northern Laptev Sea (From the data collected by the yearlong sediment trap). Oceanology 40: 850–858.

79. Watanabe E, Onodera J, Harada N, Honda MC, Kimoto K, et al. (2014) Enhanced role of eddies in the Arctic marine biological pump. Nature 5: 3950. doi:10.1038/ncomms4950.

80. Smayda TJ (1970) The suspension and sinking of phytoplankton in the sea. Oceanogr Mar Biol Annu Rev 8: 353–414.

81. Waite AM, Thompson P a., Harrison PJ (1992) Does energy control the sinking rates of marine diatoms? Limnol Oceanogr 37: 468–477. doi:10.4319/lo.1992.37.3.0468.

82. Riedel A, Michel C, Gosselin M (2006) Seasonal study of sea-ice exopolymeric substances on the Mackenzie shelf: implications for transport of sea-ice bacteria and algae. Aquat Microb Ecol 45: 195–206. doi:10.3354/ame045195.

83. Piontek J, Händel N, Langer G, Wohlers J, Riebesell U, et al. (2009) Effects of rising temperature on the formation and microbial degradation of marine diatom aggregates. Aquat Microb Ecol 54: 305–318. doi:10.3354/ame01273.

84. Li WKH, Head EJH, Harrison WG (2004) Macroecological limits of heterotrophic bacterial abundance in the ocean. Deep Sea Res I 51: 1529–1540. doi:10.1016/j.dsr.2004.06.012.

85. Simon M, Grossart H-P, Schweitzer B, Ploug H (2002) Microbial ecology of organic aggregates in aquatic ecosystems. Aquat Microb Ecol 28: 175–211. doi:10.3354/ame028175.

86. Huston AL, Deming JW (2002) Relationships between microbial extra–cellular enzymatic activity and suspended and sinking particulate organic matter: seasonal transformations in the North Water. Deep Sea Res I 49: 22–23. doi:10.1016/S0967-0645(02)00186-8.

87. Lehto N, Glud R, Nordi G, Zang H, Davison W (2014) Anoxic microniches in marine sediments induced by aggregate settlement: Biogeochemical dynamics and implications. Biogeochemistry 119: 307–327. doi:10.1007/s10533-014-9967-0.

88. Iversen MH, Ploug H (2010) Ballast minerals and the sinking carbon flux in the ocean: carbon-specific respiration rates and sinking velocity of marine snow aggregates. Biogeosciences 7: 2613–2624. doi:10.5194/bg-7-2613-2010.

Figure 1. Map of the Arctic Eurasian Basin with sampling stations.

Yellow dots represent ice stations where algal aggregates were observed (Expedition PS78/3 took place in summer 2011 and PS80/3 in summer 2012). The purple line corresponds to the September monthly average sea ice extent in 2011 and the pink line in 2012 (Source: http://nsidc.org/data/seaice_index/).

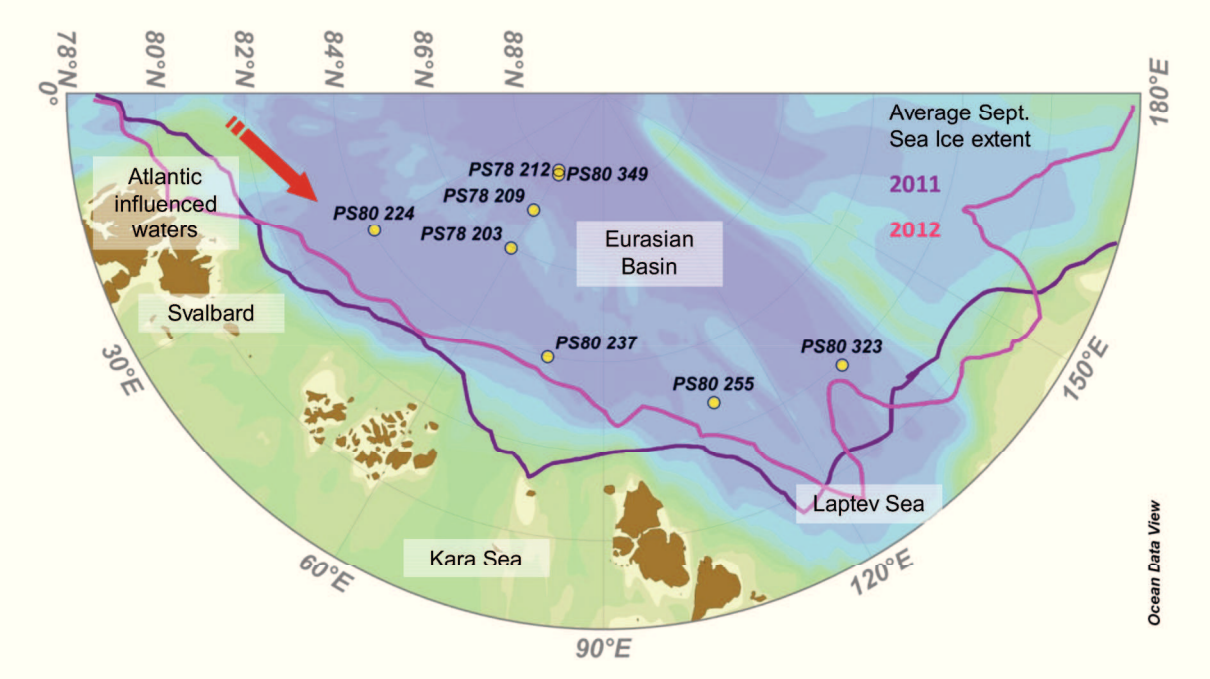

Figure 2. Distribution of aggregates in melt ponds.

Degraded pennate aggregates in cryoconite holes at the bottom of a partially open melt pond at station PS78/3_212 (A). *Melosira* filaments hanging from newly formed ice covering an open melt pond at station PS80/3_349 (B). Spherical floating aggregates below sea ice at station PS80/3_237 (Image taken with the ROV Ronja (Courtesy Alfred Wegener Institute Helmholtz Center for Marine and Polar Research (AWI)) (C). Degraded *Melosira* filaments trapped at the bottom of a partially open melt pond at station PS80/3_224 (D). Scale bar = 20 cm.

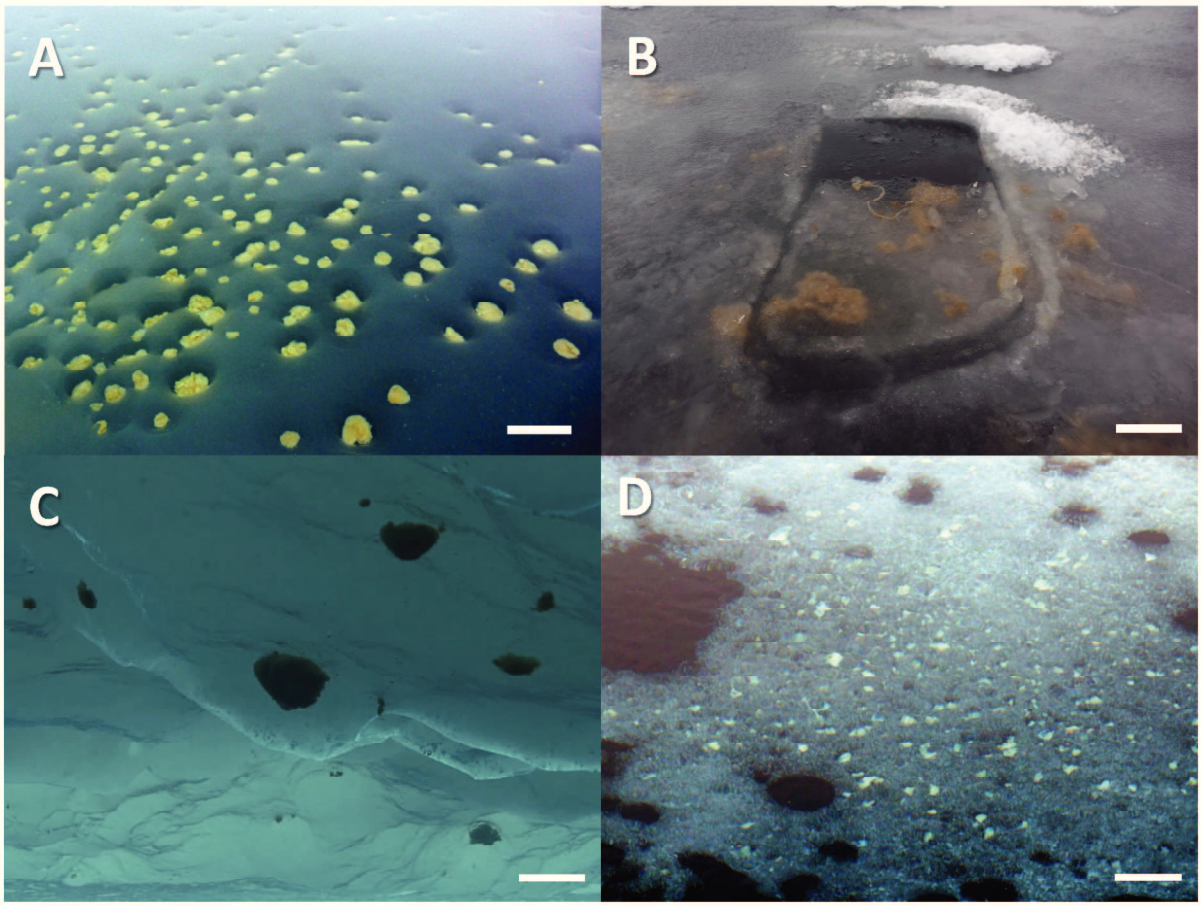

Figure 3. Representative types of aggregates observed.

Macroscopic images of the aggregates (A-D) and their microscopic composition (E-H). Fresh spherical floating aggregates below the ice formed by pennate diatoms (A and E). Degraded aggregate trapped in a closed melt pond formed by dead pennate diatoms with empty frustules (B and F). Filaments hanging from newly formed ice over an open melt pond formed by *Melosira arctica* cells that contain green chloroplasts (C and G). Degraded aggregate formed mainly by dead *Melosira arctica* cells trapped at the bottom of a partially open melt pond (D and H). Scale bar = 5 cm (A), 2 cm (B), 10 cm (C and D), and 20 μm (E-H).

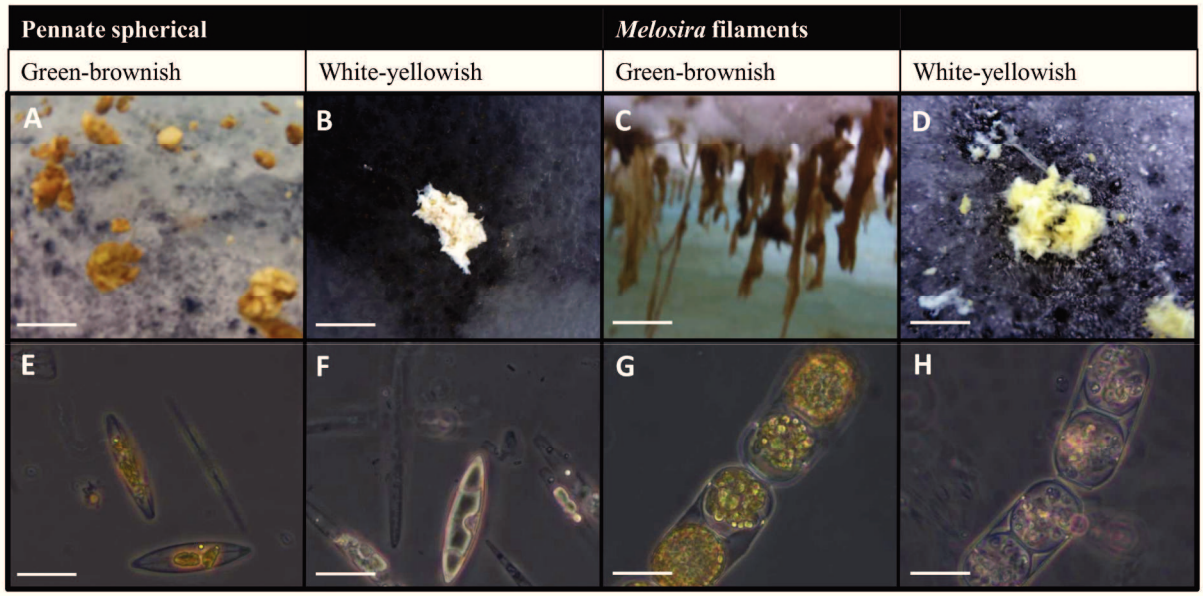

Figure 4. Photosynthesis vs Irradiance curve of *Melosira arctica* algal slurry (M5).

Carbon uptake measured with the ^{14}C radioactive isotope method (green circles) and oxygen production or consumption using optodes (purple diamonds) of the algal aggregate slurry from the *Melosira arctica* aggregate used for the buoyancy experiment (Fig. 5). The threshold irradiance for oxygen production is around 20 µmol photons m^{-2} s^{-1}. Oxygen rates have been transformed to carbon equivalents using the photosynthetic quotient of 1.25 to improve the visualization of the two different methods used to measure NPP.

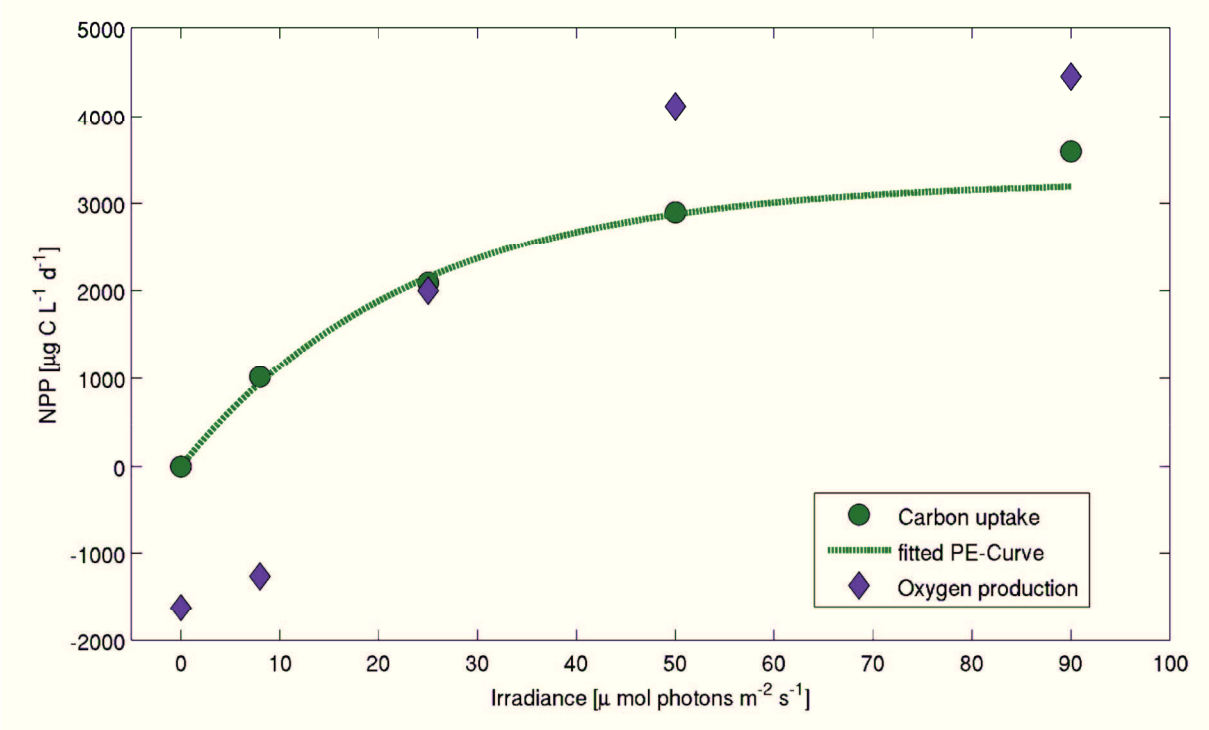

Figure 5. Buoyancy test.

(A) A piece of ice with several attached filamentous algal aggregates (Fig. 2C) was kept in a glass beaker at simulated *in situ* conditions. (B) Once the ice disappeared it was observed that air bubbles were trapped in the mucous matrix of the floating aggregates. (C) Despite the salinity gradient, one of the aggregates sank when the air bubbles were removed. (D) 24 h later all algal aggregates had sunk. (E) Only when increasing the light intensity, some of the algal aggregates were able to produce enough oxygen to regain buoyancy. Scale bar = 2 cm.

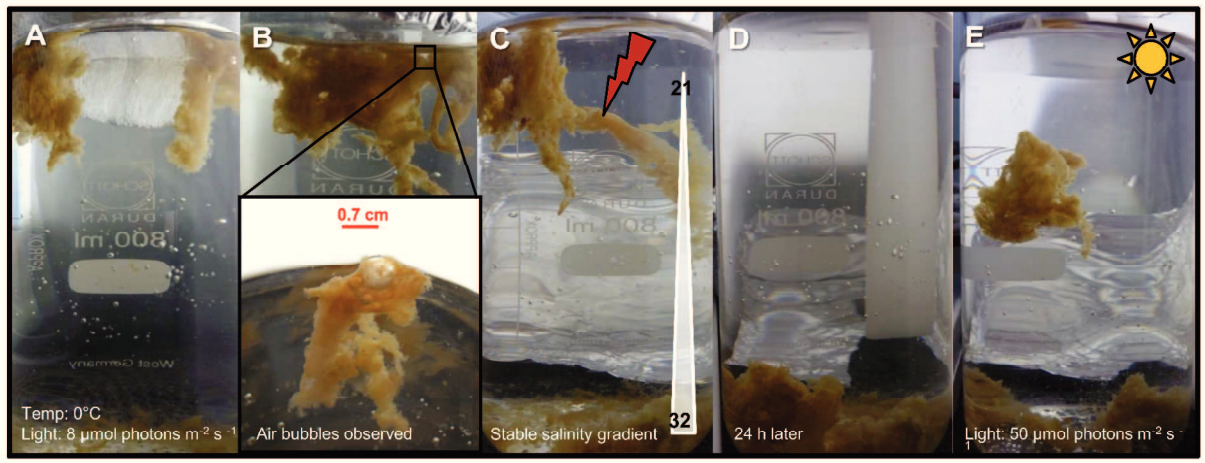

Figure 6. Conceptual model of the mechanisms responsible for the formation and fate of the different types of algal aggregates.

(1) In early spring sea-ice algal growth starts before that of phytoplankton. (2) In summer as the sea ice melts and nutrients become limiting, some sea-ice algae are released to the water column or grow into the water column. Due to their stickiness and the under-ice turbulence they form aggregates. (3) In late summer melt ponds grow in depth and the sea-ice algae that are still in the ice are gradually exposed to very low salinities, high irradiances, and nutrient depletion making them accumulate and degrade in the pond. Depending on the environmental conditions, some sub-ice aggregates sink and others remain floating. (4) In early autumn, the melt ponds can either open completely allowing some phytoplankton species to come into the melt pond, or they can refreeze again, becoming second year ice. (5) In autumn those melt ponds that were open to the seawater freeze again, trapping the floating aggregates that were not grazed in the newly formed ice.

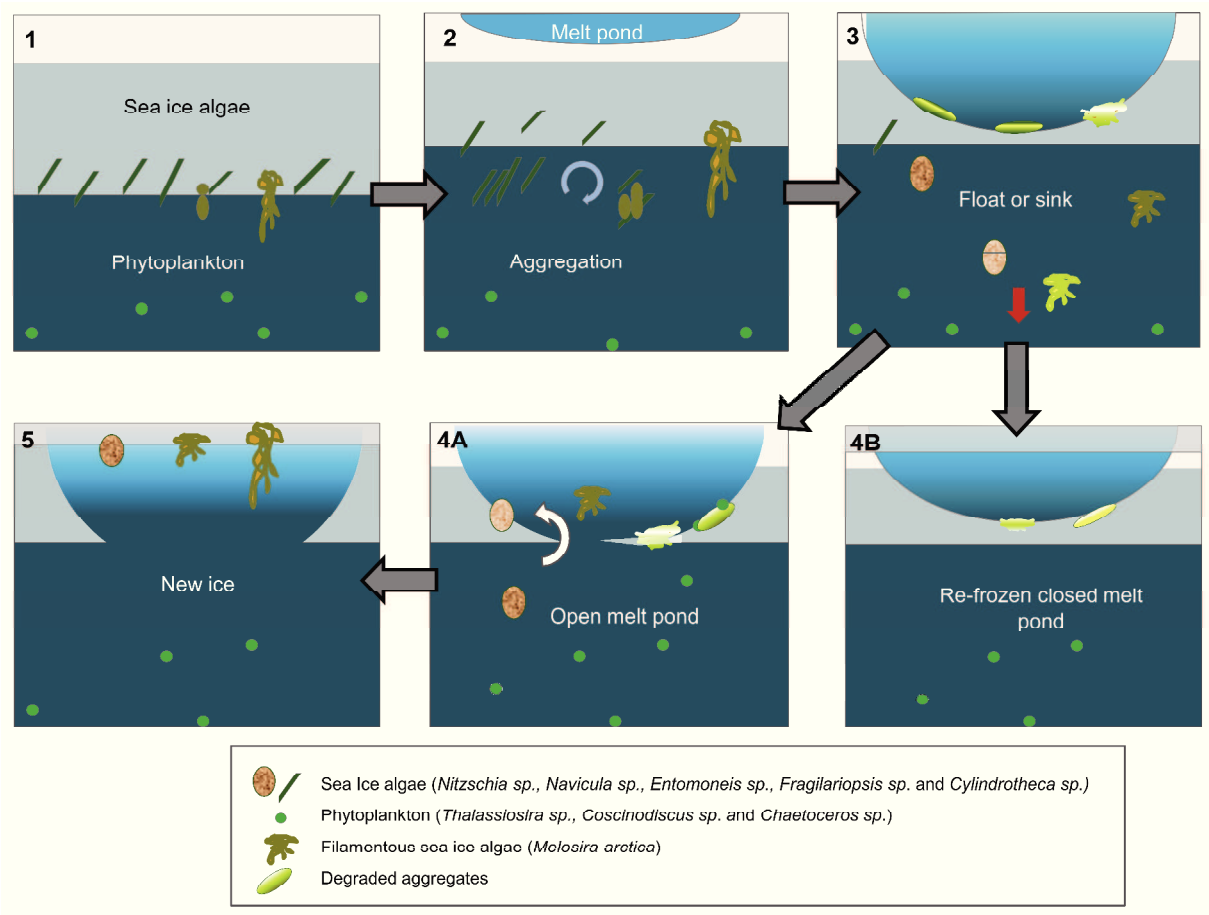

Table 1. Algal aggregate types and their degradation stages.

Aggregate type	Pennate spherical		*Melosira* filaments	
Environment	Below ice	Melt Pond	Below ice	Melt Pond
Number of samples	n = 2	n = 4	n = 2	n = 3
Size (cm)	3–15	1–15	1–30	2–15
Abundance (Agg m^{-2})	0.8–5.1	0.1–600	17	9–200
Color	Green-brownish	White-yellowish	Green-brownish	White-yellowish
POC (mg C L^{-1})*	24–110	9–86	11–130	7–49
PON (µmol N mg POC^{-1})	8–10	2–8	3–9	2–9
C:N molar	8–11	11–35	9–28	10–40
Chl*a* (µg Chl*a* mg POC^{-1})	5–9	0.01–2	3–5	0.2–1.2
C:Chl*a*	110–210	500–66700	200–340	850–4600
DOC (µmol DOC mg POC^{-1})	7–9	7–11	5–17	7–35
TEP (µg C mg POC^{-1})	0.5–2.5	4–170	2–8	4–17
TEP:POC	0.0005–0.002	0.004–0.17	0.002–0.008	0.004–0.02
NPP (mg C (mg $POC)^{-1}$ d^{-1})	0.001–0.01	0.001	0.002–0.155	0.002–0.014
Bacteria (cells mg POC^{-1})	3.9E+08–1.5E+09	6.3E+07–6.0E+08	5.6E+08	7.36E+07–6.1E+08

All chemical variables were measured from a homogeneous algal slurry prepared with the aggregates. Units presented are normalized by the POC content of the slurry expressed in mg C per volume of slurry*. The carbon normalized NPP represents a carbon turnover estimate for the algae in the aggregate at 50 µmol photons m^{-2} s^{-1}.

Table 2. Local areal estimates of fresh sub-ice algal aggregates per aggregate type compared to sea ice and water column at the same location and other studies.

		This Study		Other studies			
Number of stations Literature reference		2	1	Glud et al. 2014	Assmy et al. 2013	Melnikov et al. 1997	Gosselin et al. 1997
Algal type		Pennate spherical	*Melosira* filaments	Pennate spherical		*Melosira* filaments	
Chl *a* (mg m^{-2})	Sea Ice	1.2 - 1.7	7.7	0.46 ± 0.29			0.1-14
	Water	2.3 - 4.3	2.7	59-260			1-445
	Aggregate	0.1 - 3.7	14 - 44	2.94±1.21	0.0017-0.0063	22	52-200
	% contribution aggregates	3 - 38	57 - 80	0.6-6.5			
POC (mg m^{-2})	Sea Ice	691 - 896	853				
	Water	1380 - 1563	1614				
	Aggregate	11 - 793	3020 - 9094		0.2-1.3		
	% contribution aggregates	0.5 - 26	55 - 78				
PON (mg m^{-2})	Sea Ice	72 - 91	95				
	Water	229 - 231	267				
	Aggregate	1 - 72	108 - 324		0.03-0.17		
	% contribution aggregates	0.3 - 18	23-47				
NPP (mg C m^{-2} d^{-1})	Sea Ice	1-13	1.5	1.32			57 ± 43
	Water	25-31	1	60-204			30 ± 10
	Aggregate	0.4 - 9.7	13-40	-3.72	0.002-0.02		included in ice
	% contribution aggregates	1-23	83-94				
Integration parameters	Ice thickness (m)	1.2 - 1.4	1.4				
	Euphotic zone depth (m)	15 - 18	12	50			
	Aggregate coverage (%)	0.01 - 0.03	0.5		0.01-0.03	0.53	
	Aggregate abundance (Agg m^{-2})	0.8 - 5.1	17				
	Aggregate diameter or length (cm)	3 - 10	10-30 (length)		0.8-1	40-50 (length)	

Supplementary material

Table S1. Characteristics of pennate algal aggregates and sea ice stations investigated.
All variables except nutrients were measured from an homogeneous algal slurry and normalized by POC. Nutrients were measured in the water surrounding the aggregates and are presented per volume of water.
Individual aggregate samples (a total of 11) for each aggregate type are labeled with P for pennate diatom aggregate and M for *Melosira* aggregates.
¥ Partially open melt pond.

Pennate Aggregates	**P1**	**P2**	**P3**	**P4**	**P5**	**P6**
Station	PS78/3_203	PS78/3_209	PS78/3_212	PS80/3_224	PS80/3_237	PS80/3_323
Date (DD/MM/YYYY)	14.08.2011	17.08.2011	19.08.2011	09.08.2012	14.08.2012	04.09.2012
Latitude	85° 58.56' N	86° 59.24' N	88° 1.11' N	84° 3.03' N	83° 59.19' N	81° 55.53' N
Longitude	59° 25.16' E	58° 29.37' E	59° 58.53' E	31° 6.83' E	78° 6.20' E	131° 7.72' E
Size (cm)	1	5	10±5	10±5	7±5	2±1
Color	White-yellowish	White-yellowish	White-yellowish	Green-brownish	Green-brownish	White-yellowish
Environment	Melt Pond	Melt Pond	Melt Pond	Below ice	Below ice	Melt Pond
Sea Ice type	FYI	FYI	FYI	FYI	FYI	FYI
Melt Pond depth (m)	1	n.d.	n.d.¥	-	-	0.35
Floating	No	No	No	Yes	Yes	No
Melt Pond coverage	50%	50%	50%	40%	20%	10%
Salinity (aggregate)	0-11 (11)	9.6	1.9-5 (4.2)	29.7	0.1-32(32)	3.7-30.1 (28)
Temperature (°C)	-0.5	n.d.	n.d.	0.5	n.d.	-1
Irradiance (µmol photons m^{-2} s^{-1})	160	211	130	99	52	78
Diatom species	*Nitzschia, Pseudonitzschia, Navicula, Fragilariopsis, Chaetoceros, Coccolithophores*	*Chaetoceros, Fragilariopsis, Thalassiosira, Nitzschia,*	*Chaetoceros, Thalassiosira/Coscinodiscus, Nitzschia, Navicula, Fragilariopsis*	*Nitzschia, Navicula, Entomoneis, Fragilariopsis, Thalassiosira, Pleurosigma, Cylindrotheca*	*Nitzschia, Pseudonitzschia, Fossula arctica, Melosira arctica, Navicula, Entomoneis*	*Fragilariopsis, Navicula, Nitzschia*
Grazing observed	Ciliates	Ciliates	No	Amphipods and copepods	No	Ciliates
POC (mg C L^{-1}	86	9	66	112	24	27

slurry)						
PON (µmol N mg POC^{-1})	8	5	5	10	8	2
C:N molar ratio	11	17	17	8	11	35
Chl *a* (µg Chl*a* mg POC^{-1})	2	0.6	0.3	9	5	0
C:Chl *a* ratio	505	1609	3306	110	212	66755
Chl*a*/CPE (%)	62	95	89	92	33	26
DOC (µmol C mg POC^{-1})	n.d.	7.4	n.d.	4.2	5.8	11.2
TEP (µg C mg POC^{-1})	8±8	171±115	10±16	1.5±0.3	1.5±1	4±1
TEP:POC	0.008±0.008	0.17±0.11	0.01±0.01	0.001±0.0003	0.001±0.001	0.004±0.001
NPP at 50µE (µg C mg POC^{-1} d^{-1})	n.d.	n.d.	n.d.	9.6	1.2	1.3
Bacterial counts (cells 10^{9} mg POC^{-1})	0.6	0.06	0.1	1.5	0.4	0.1
Bacterial POC (%)	1.8	0.2	0.3	4.4	1.2	0.2
Nitrate (µmol L^{-1})	n.d.	n.d.	n.d.	2.9	2.6	3.1
Phosphate (µmol L^{-1})	n.d.	n.d.	n.d.	0.3	0.2	0.01
Silicate (µmol L^{-1})	n.d.	n.d.	n.d.	1.2	1.3	0.0

Table S2. Characteristics of *Melosira* algal aggregates and sea ice stations investigated.

***Melosira* Aggregates**	**M1**	**M2**	**M3**	**M4**	**M5**
Station	PS80/3_224	PS80/3_224	PS80/3_224	PS80/3_255	PS80/3_349
Date (DD/MM/YYYY)	09.08.2012	09.08.2012	09.08.2012	20.08.2012	18.09.2012
Latitude	84° 3.03' N	84° 3.03' N	84° 3.03' N	82° 40.24' N	87° 56.01' N
Longitude	31° 6.83' E	31° 6.83' E	31° 6.83' E	109° 35.37' E	61° 13.04' E
Size (cm)	5 (filamentous)	5±3	2±1	10±5	15±10
Color	White-yellowish	White-yellowish	Green-brownish	White-yellowish	Green-brownish
Environment	Melt Pond	Melt Pond	Melt Pond	Melt Pond	Frozen in ice
Sea Ice type	FYI	FYI	FYI	FYI	MYI
Melt Pond depth (m)	0.3¥	0.63	0.5 ¥	0.3	Open
Floating	Yes	No	No	No	Yes
Melt Pond coverage	40%	40%	40%	40%	20%
Salinity (aggregate)	1.5-20.3 (6.9)	0-32 (31.9)	0.1-31(31)	0.2-0.5 (0.5)	31
Temperature (°C)	0.1	-1.5	0.1	0.2	0.1
Irradiance (µmol photons m^{-2} s^{-1})	260	252	255	101	24
Diatom species	*Melosira arctica, Nitzschia, Dinocysts*	*Melosira arctica, Nitzschia, Dinocysts*	*Melosira arctica, Nitzschia, Navicula, Fragilariopsis*	*Melosira arctica, Navicula, Nitzschia*	*Melosira arctica, Fragilariopsis, Cylindrotheca*
Grazing observed	Ciliates	Ciliates	No	Ciliates	Ciliates
POC (mg C $L^{-1\ slurry}$)	7	49	132	16	11
PON (µmol N mg POC^{-1})	9	9	9	2	3
C:N molar ratio	10	10	9	40	28
Chl *a* (µg Chl*a* mg POC^{-1})	1.2	0.2	3	0.4	5
C:Chl *a* ratio	848	4623	337	2198	207
Chla/CPE (%)	82	96	98	94	77
DOC (µmol C mg POC^{-1})	23.3	7.2	4.6	35.4	17.3
TEP (µg C mg POC^{-1})	17±16	4±0.6	2±0.02	16±4	8±3
TEP:POC	0.02±0.01	0.004±0.001	0.002±0.0001	0.015±0.004	0.008±0.002
NPP at 50µE (µmg C mg POC^{-1} d^{-1})	0.013.3	0.014.1	0.001.5	0.002.2	0.154.9
Bacterial counts (cells 10^9 mg POC^{-1})	0.6	0.1	0.5	0.1	n.d.
Bacterial POC (%)	1.8	0.4	1.7	0.2	n.d.
Nitrate (µmol L^{-1})	0.4	1.3	2.2	0.3	0.9
Phosphate (µmol L^{-1})	0.005	0.2	0.4	6.0	0.3
Silicate (µmol L^{-1})	1.6	2.6	20.7	0.7	1.4

Figure S1. Oxygen profile inside degrading pennate diatom aggregate (P5).

Oxygen microprofiles (n=3) measured using an oxygen microoptode (FireStingO2, PyroScience GmbH, Aachen, Germany) in a 5 cm diameter spherical pennate-diatom aggregate incubated in a beaker in the lab for 3 days at 50 µmol photons m^{-2} s^{-1} and -1.3°C. Oxygen microprofiles across the water-aggregate interface were measured with steps of 0.5 mm and since the original spherical diatom aggregate started to flatten the diffusive oxygen uptake (DOU, mmol m^{-2} d^{-1}) was calculated using Fick's first law of diffusion DOU = D_0 (dC/dz), where D_0 (cm^{-2} s^{-1}) is the molecular diffusion coefficient in water, C (µmol L^{-1}) is the solute concentration, and z (cm) is the depth within the aggregate. The total oxygen consumption rate of the aggregate was calculated integrating the diffusive flux over the entire aggregate surface area [88]. Using a typical pennate-diatom aggregate size of 5 cm in diameter and a spherical shape (Volume of one aggregate = 0.06 L) the corresponding O_2 consumption rate of a degrading pennate aggregate is 1.8 ± 0.2 mmol O_2 L^{-1} d^{-1} (n = 3).

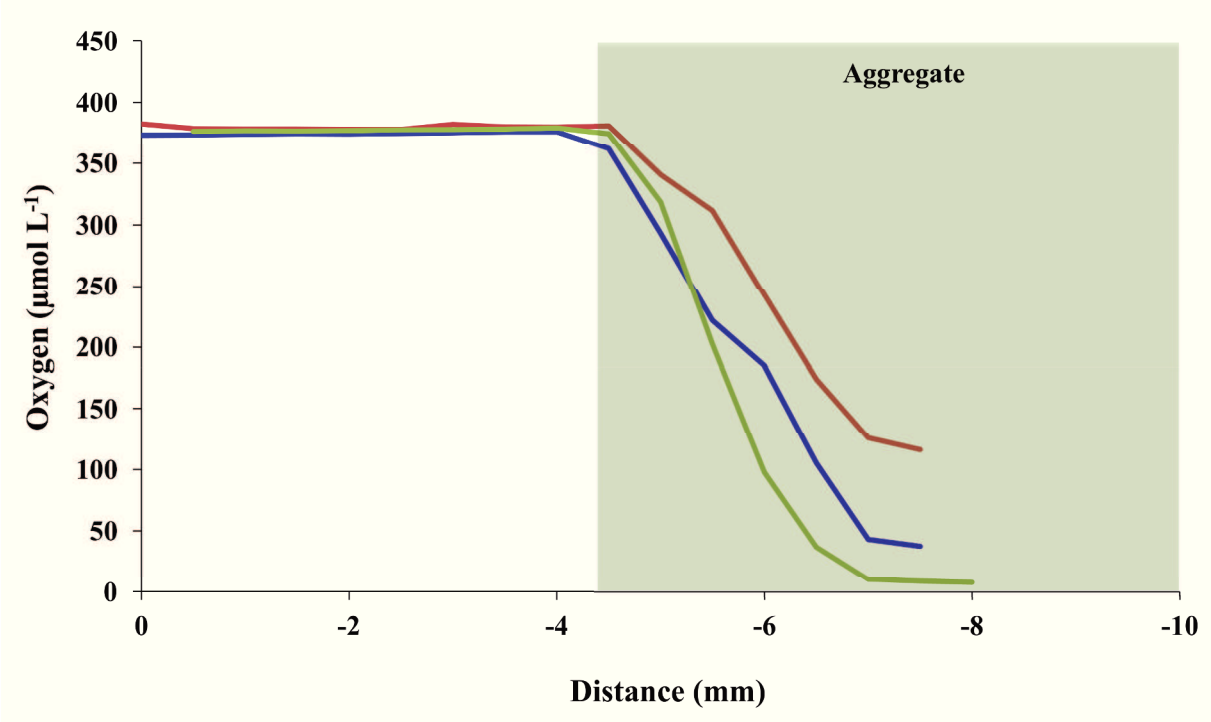

Chapter IV

Distribution of algal aggregates under summer sea ice in the Central Arctic

Christian Katlein[1], Mar Fernández-Méndez[1,2], Frank Wenzhöfer[1,2], Marcel Nicolaus[1]

[1]Alfred-Wegener-Institut Helmholtz-Zentrum für Polar- und Meeresforschung, Bremerhaven, Germany

[2]Max Planck Institute for Marine Microbiology, Bremen, Germany

Submitted to Polar Biology (June 2014)

Abstract

The sea ice cover of the Arctic Ocean has been changing dramatically in the last decades and the consequences for the sea-ice associated ecosystem remain difficult to assess. Algal aggregates underneath sea ice are known to be of great importance for the ice associated ecosystem and the coupling to benthic communities. However, their frequency but the frequency and distribution of their occurrence is not well quantified. We used upward looking images obtained by a remotely operated vehicle (ROV) to quantify ice algal aggregate biomass and to investigate their spatial distribution. During the IceArc expedition (ARK-27/3) of RV Polarstern in late summer 2012, different types of algal aggregates were observed floating underneath various ice types in the Central Arctic basins. On the large scale, filamentous aggregates of *Melosira arctica* dominate the inner part of the Central Arctic pack-ice, while closer to the ice edge under melting sea ice round aggregates mainly formed by pennate diatoms dominate. Our results show that the floe scale distribution of algal aggregates in late summer is determined by the topography of the ice underside, with aggregates collecting in dome shaped structures and at the edges of pressure ridges. The buoyancy of the aggregates was also evident from analysis of the aggregate size distribution. Depending on the approach, differences in orders of magnitude result for biomass estimates. This highlights the difficulties of upscaling observations and comparing results from surveys conducted using different methods or on different spatial scales.

Keywords: Sea Ice algae, algal assemblages, size distribution, *Melosira arctica* filaments, image processing, remotely operated vehicle.

Introduction

The Arctic Ocean has changed dramatically in the last decades. Changes of physical processes in the climate system such as decreased sea-ice extent (Serreze et al. 2007) and thickness (Haas et al. 2008; Kwok and Rothrock 2009), the trend from multiyear to younger first year sea ice (Maslanik et al. 2007), a longer melt season (Markus et al. 2009), increased melt-pond coverage (Roesel and Kaleschke 2012) and increased light transmittance through the ice (Nicolaus et al. 2012) will also affect the sea ice ecosystem (Arrigo et al. 2008; Lee et al. 2011; Arrigo 2014). Assessing the consequences of these changes in the ecosystem is difficult, as observations in the ice covered Arctic Ocean are challenging and very little baseline data is available for comparison especially in the central basins.

Sea ice harbors a complex diversity of life in and associated to its ice-water interface strongly influenced by the physical conditions present (Horner et al. 1992; Legendre et al. 1992). Changed melting conditions and increased light availability are expected to affect the life conditions of sea ice algae (Lee et al. 2011). The presence of Aggregates formed by sea-ice algae floating or hanging underneath sea ice has been described throughout the last century, however, little is known about factors controlling their distribution. In this paper, the term algal aggregates refers to macroscopic (>1 cm) mostly free-floating aggregations mainly formed by typical sea-ice associated algae such as those described by Boetius et al. (2013) and Assmy et al. (2013). These aggregates have previously been described in the literature using various names such as sub-ice assemblages, algal filaments or aggregations (Melnikov and Bondarchuk 1987; Horner et al. 1988; Horner et al. 1992; Gutt 1995). Already at the beginning of the last century algal aggregates were observed during the drift of *Fram* (Nansen 1906) in the Central Arctic. Observations are sparse and usually only cover a small spatial range due to the limits of diving operations in icy waters (Melnikov and Bondarchuk 1987; Syvertsen 1991; Melnikov 1997; Poulin et al. 2014; Glud et al. 2014). In general it is a great challenge to gather spatial datasets underneath sea ice. Only in the last decades, the technological advance of remotely operated vehicles (ROV) and digital underwater imaging enabled detailed research under polar sea ice on a larger spatial scale (Gutt 1995; Werner and Lindemann 1997; Perovich et al. 1998; Ambrose et al. 2005; Gradinger and Bluhm 2010; Nicolaus and Katlein 2013).

However, it is known that sea–ice algae play an important role in the sea-ice ecosystem supporting a substantial fraction of total primary productivity (Gosselin et al. 1997), seeding the under-ice phytoplankton bloom in spring (Wassmann and Reigstad 2011) and providing an

important food source for zooplankton (Leu et al. 2010; Leu et al. 2011). When ice algae are released to the water column due to ice melt, they are inherently prone to aggregation due to a high production of transparent exopolymers (Riebesell et al. 1991; Krembs et al. 2011). Aggregation can both lead to rapid sedimentation of biomass (Boetius et al. 2013) as well as prolonged suspension underneath the ice (Assmy et al. 2013) due to oxygen entrapment within the aggregates (Fernandez-Méndez et al. submitted 2014; Glud et al. 2014). Despite this long history of observations of algal aggregates under Arctic sea ice, little is known about their spatial distribution on both floe and basin scale.

The objective of this paper is to quantify the amount and distribution of algal aggregates underneath Arctic summer sea ice on floe scale using ROV surveys. This includes an analysis of the spatial distribution of aggregate abundance as a function of the physical properties of the habitat. In addition geometric properties of under-ice aggregates are investigated and different approaches for estimation of aggregate biomass assessed and compared to evaluate uncertainties and recommend procedures for future work.

Materials and Methods

ROV observations

Observations were carried out during the IceArc cruise (ARK-XXVII/3) of the German research icebreaker RV Polarstern to the Central Arctic in August and September 2012. Figure 1 shows the cruise track and the positions of the investigated ice stations. Algal aggregate observations were performed on eight ice stations with an average duration of two days. Ice stations were selected along the retreating sea-ice edge as well as within the Central Arctic pack ice close to the geographic North Pole. The ice floe of the first ice station was revisited at the end of the cruise, enabling repeated sampling of the same ice floe after its transition from summer melting to autumn freeze-up conditions.

We used a V8Sii-ROV (Ocean Modules, Åtvidaberg, Sweden) launched through a hole in the ice and operated from a tent directly on the ice floe. On each ice station the ROV achieved a diving time between six and eight hours. The setup and operation procedure was very similar to the one used in Nicolaus and Katlein (2013) with minor modifications: A Micron Nav (Tritech, Aberdeen, UK) ultra-short baseline (USBL) positioning system was providing precise ROV location in a floe fixed coordinate system, while the rear facing Ospray SD-camera (Tritech, Aberdeen, UK) was repositioned to provide upward looking imagery.

Several additional sensors complemented the observations with measurements of the physical properties of the under-ice habitat. Ice draft was calculated as difference between the ROV depth and its distance to the ice measured by the upward looking DST micron echosounder (Tritech, Aberdeen, UK) altimeter. Spectral light transmittance (320-950 nm) was calculated from continuous synchronous measurements of downwelling irradiance using two RAMSES-ACC spectroradiometers (TriOS GmbH, Rastede, Germany). While one sensor was mounted on the ROV, a reference sensor was placed on a tripod on the ice close to the ROV launch hole. Data processing, calibration and measurement uncertainties were described previously (Nicolaus et al. 2010; Nicolaus and Katlein 2013; Katlein et al. 2014).

At station ICE-7, under-ice aggregates could be sampled with the ROV using a custom built sampling device. Samples were analyzed for particulate organic carbon (POC) and species composition as described in Assmy et al. (2013).

Image classification

To quantify the spatial distribution of under-ice algal aggregates from the acquired ROV imagery, we applied a simple threshold algorithm implemented in MATLAB. We extracted still images (384 x 288 pixels) each five seconds from the videos of the upward looking camera using the command line tool *ffmpeg*. Extracting the images each five seconds from the video overcomes problems with multiple detection of the same aggregates for most of the cases. To overcome problems with inconsistent lighting of the entire image area and to mask out the overlay data display, we cropped the image edges to obtain undisturbed RGB-images of 250x200 pixels. Analysis of image histograms showed that aggregates could be detected well with a threshold value, by selecting all pixels with a value between 0 and 100 (out of maximal 255) in the green channel as aggregates. Thus images were converted into binary images for further analyses.

Two dimensional aggregate properties like perimeter and area as well as minor and major axis of a fitted ellipse were calculated for each individual aggregate. For all aggregates covering more than 10 pixels of the image we derived shape parameters, such as eccentricity, circularity and the equivalent circular diameter. The measurements were transformed from pixel units to real units using the distance to the ice measured by the altimeter and a laboratory calibration of the camera. Uncertainties in the distance to the ice, ROV-tilt and lens distortion result in less than 15% uncertainty in size measurements. This image registration to true geometric units also enabled us

to determine aggregate abundance per square meter as the number of aggregates in the image divided by the area surveyed by the image.

All images taken at a depth greater than 5m and at ROV tilts greater than 10° were discarded automatically. All other images were verified manually. Images where the algorithm detected aggregates, which were in reality ice structures or other objects and images where clearly identifiable aggregates where not detected by the algorithm were discarded. In the case that several close lying aggregates were mistaken as a larger one, the image was excluded from shape and size analysis. In total, the analysis of 23 800 images yielded 11 000 where useful information could be deducted. These images were on average taken about one meter away from the ice underside and yielded a spatial resolution of 4-5 mm.

The detection algorithm works well in most situations, but due to its simple nature detection is problematic in some cases and 54% of the images had to be excluded from the analysis. This is mostly related to inhomogeneous backlighting within the image at the transition between different ice features, where dark features of the ice get misinterpreted as aggregates. In addition, the separation of aggregates from small scale ice structures and air bubbles can be ambiguous even to a trained observer verifying the detection. Finally, aggregates which are not dense enough or too small to leave a significant signature in the pixels green value remain undetected.

To account for multiple sampling of some areas (e.g. in vicinity to the ROV-launch hole) all obtained parameters were gridded on a regular grid with 3x3m cell size, corresponding to the maximal uncertainty in the ROV position. All available images within a grid cell were selected and the average of all measurements from these pictures assigned to the grid cell. This method is a further improvement of the one used in Boetius et al. (2013) and Assmy et al. (2013) which were both based on subsets of the same dataset. While Assmy et al. (2013) analyzed only data from ice stations ICE-1 and ICE-2, Boetius et al. (2013) analyzed only one representative dive per ice station. As the image registration required manual post-processing it was not available onboard the ship and thus Boetius et al. (2013) reported only percent cover instead of aggregate abundance or biomass.

Biomass estimation

To estimate aggregate biomass, the two-dimensional distribution deducted from the images was converted into a three dimensional volumetric information, including assumptions about the

aggregate shape. While the assumption of a uniform algal layer thickness is more applicable to typical ice algal bottom layers in spring, we chose to represent the typically very much rounded aggregates by compact spheres. The diameter *d* of the aggregate was determined as the equivalent circular diameter of the connected pixel region from the regions area *A* ($d = \sqrt{4A/\pi}$).

We used different methods to obtain an estimate of the aggregate volume per area. Comparison between the different approaches enables us to evaluate the accuracy of our biomass estimates and the disadvantages of single approaches. Names given in parentheses identify the different approaches later in the text:

For a first approach, aggregate volume was calculated for every detected aggregate. The single aggregate volumes were then added up and divided by the survey area ("aggregate list"). This approach does not take into account multiple sampling of some aggregates and should thus result in an overestimate of total biovolume.

In a second approach, the aggregate volume *V* was calculated using abundance *a* and diameter *d* values averaged over all images ("global mean"):

$$V = a \cdot \frac{4}{3}\pi \left(\frac{d}{2}\right)^3 \quad \text{(Equation 1)}$$

As sphere volume is dependent on the third power of diameter (Equation 1), this method was repeated with a median diameter instead of average diameter, to avoid overestimation of biovolume for large likely not spherical aggregates ("global median").

To avoid influences from multiple sampling, the same calculation was repeated with average and median values obtained after gridding of the results ("gridded mean" and "gridded median"). The "gridded median" method was also used in Assmy et al. (2013).

As larger round aggregates can occur in some areas, they can contribute significantly to biomass which gets lost when averaging over many grid cells. Thus in a last approach, biovolume was calculated from abundance and diameter in each grid cell separately and averaged afterwards ("raster cells"). In the case where aggregates deviate much from a spherical shape, the last approach, however can significantly overestimate biovolume.

To convert the estimated biovolume to carbon content, we used the measured carbon content of 389.69 mg C L^{-1} of two sampled aggregates with known volume (Assmy et al. 2013).

Patchiness and size distribution

To analyze the spatial patchiness of the aggregate distribution, we used the index of mean crowding and Lloyds Index of Patchiness (Lloyd 1967; George 1981; Gutt et al. 1991) on the gridded data.

The frequency distribution of the size of aggregating particles is often described using a power law

$f\ d\ = cd^b$ (Equation 2)

with d the diameter, b the characteristic slope and a normalization constant c. The characteristic slope varies for different types of phytoplankton usually around a value of -3 (Alldredge and Gotschalk 1989; Guidi et al. 2009). Equation 2 was used to fit a power law to the aggregate size distributions obtained from the list of all detected aggregates and to determine the value of the characteristic slope. The characteristic slope and size distributions were interpreted in comparison with the marine particle aggregation model from Jackson (1990).

Results

ROV observations

ROV surveys underneath sea ice using upward looking video imagery provide a useful tool to quantify the abundance and spatial distribution of ice algal aggregates. The upward-looking imagery resulted in a continuous observation along the dive tracks, covering the entire variability of summer sea ice conditions in this region. The large spatial coverage during rather short station time is of great advantage to map the patchy under-ice ecosystem without bias towards sites with more abundant biomass. The upward looking video imagery enabled us to quantify the amount and distribution of ice algal aggregates. Subsequent analysis of several subsets of the entire dataset reveals that due to the high spatial patchiness, the result is to some extent dependent on the area covered by the survey. Reasonably good estimates of percent cover could be achieved with the analysis of just one ROV transect if it was selected as representative from all available dives by the ROV pilot. Nevertheless some transects differ significantly from the rest of the station. A comparison of the results retrieved from three different approaches shown in Table 1.

Percent cover *p* and abundance *a* are correlated to some extent ($a = 2.6 + 60.9 \cdot p$, R^2=0.2), but show some differences as expected from different aggregate sizes.

We observed mainly two types of aggregates: The spherical aggregates floating free underneath the sea ice were typically composed of pennate diatoms (Figure 2a), while more elongated filamentous strings attached to or floating underneath the sea ice where mainly composed of *Melosira arctica* (Figure 2b). Details on the composition, development and fate of these aggregates have been described elsewhere (Assmy et al. 2013; Boetius et al. 2013; Fernandez-Méndez et al. submitted 2014). Aggregates were observed both under first-year as well as under multiyear sea ice.

During the cruise we observed different conditions of the sea-ice cover. While dense first-year ice with a thickness of 1.0 to 1.5 m dominated the first two stations located in the transpolar drift, the area of stations ICE-3 to ICE-6 was dominated by extremely rotten sea ice with a thickness of less than 1.0 m in an advanced melting stage. Later in the cruise, we observed freezing conditions, with ice covers of several cm forming on the melt ponds. Stations ICE-7 and ICE-8 in the central pack ice were formed of multiyear ice with a thickness of 1.8 m. In contrast to the previous stations along the ice edge, the ice was less deteriorated by melt and we observed the first snowfall at the end of summer. The repeated visit to the first floe during ICE-9 was strongly affected by the fall freeze-up with a snow cover of about 10 cm and refrozen ponds. In contrast, the topography of the ice underside had not changed dramatically. All observations were made at the end of the productive season, so that algal biomass was in general low as compared to the spring season and in particular no ice algal layer could be observed at the ice bottom.

Spatial distribution

The aggregate distribution is exhibits high variation, which is also indicated by high values of Lloyd's index of patchiness, especially for stations with low aggregate abundance (Table 2). Maps of aggregate distributions were constructed from the data and an example can be found in Figure 3 and all other stations in the electronic supplement (Figure S1-S7).The average aggregate properties are given in Table 2.

According to the visual impression from upward and forward looking ROV cameras, most of the aggregates are floating freely up against the underside of the sea ice. Due to this buoyancy, most of them are situated in dome like structures with a depth of just a few centimeters (Figure 2d).

The buoyancy state of the aggregates could be assessed after detachment from their original position by thruster disturbance. After disturbance they slowly rose up against the ice-water interface again, indicating slightly positive buoyancy. The aggregates are also frequently found in rougher parts of the ice and particularly at the edges of transitions to thicker or ridged ice.

No direct correlation of the spatial distribution of light transmittance and the aggregate distribution was found. As already indicated by the visual observations, the only relation of aggregate abundance was found when comparing it to maps of ice thickness and roughness (Figure 3 and Figures S1-S7). High aggregate abundances often occurred at the boundaries of ridge keels in level ice with moderate roughness (Figure 4).

Biomass estimation

Results of the biomass estimates obtained by the different calculation approaches are shown in Table 3. While the different methods yield a consistent picture of relative aggregate biomass at the different stations, they exhibit large quantitative differences. Biomass estimates are spanning up to three orders of magnitude from <0.01 to 20.45 mg C m^{-2} even though they are derived with only slightly varying algorithms from the same dataset. When considering only the two most reliable algorithms average aggregate biomass accounts for 0.1 to 6 mg C m^{-2}.

Aggregate Properties

Mean properties of the detected aggregates are given in Table 2. Mean aggregate diameters ranged from 2.1 to 4.1 cm and mean abundances range from 1 to 5 aggregates per m^2 with extreme values from 0.3 up to 16.0 aggregates per m^2. Mean aggregate eccentricities ranged from 0.76 to 0.88. The minima and maxima of observed eccentricities coincide with the visual observation of sole occurrence of round and filamentous aggregates. Thus we deduced aggregate type fractions from a linear mapping to the eccentricity value (Figure 1). While elongated filaments dominated the stations close to the Laptev Sea and in the central pack ice, the stations further down the transpolar drift towards Fram Strait were dominated by round aggregates. These contributions of different aggregate types estimated from ROV image analysis match the observations of investigated aggregate sampled during the ice stations.

The size distribution of algal aggregates obtained from the image analysis for all stations generally follows the expected power law (Figure 5). The characteristic slope obtained from power law fitting ranges from -1.3 to -3.1 which is smaller than for typical phytoplankton (McCave 1984). It showed a correlation to the latitude of the ice station (R^2=0.67). However, some important deviations between the different ice stations can be recognized. A distinct and unexpected feature is that the size distribution on ice stations 3, 5, 6 and 9 is flattening out towards larger aggregates. This flattening of the size distribution towards larger sizes could be reproduced, by deactivating the sinking term in the aggregate formation model from Jackson (1990).

Discussion

Patchiness and biomass estimates

The patchy spatial distribution of algal aggregates makes accurate large scale estimates of the aggregate biomass and thus their importance in the ecosystem very challenging. As our results show, not only the choice and range of sampling sites, but also the method of estimating biomass from the data may heavily impact the estimates. In consequence, small scale surveys of the under-ice ecosystem such as diver observations are heavily influenced by the choice of sampling site. When comparing between different surveys from ROVs and diver studies, differences of several orders of magnitude might simply arise due to differences in sampling strategy and data processing. These differences can be even more dramatic when comparing to results obtained by classical ice coring. Larger scale surveys will likely give a more realistic estimate (Assmy et al. 2013) including large areas empty of aggregates, which are certainly under-represented in any kind of spot measurements. Estimates obtained on smaller spatial scales can significantly overestimate the areal average biomass (Gutt 1995; Glud et al. 2014), because observations are conducted where something interesting can be observed without accounting for the empty stretches in between. Hence, those should be considered as upper limits and if at all used carefully for upscaling calculations. As estimates of aggregate biomass are highly dependent on diameter, approaches that resolve spatial differences in aggregate properties ("raster cells") and account for multiple sampling ("gridded median") should give the most reliable results. Due to their patchy distribution, algal aggregates will be difficult to include in ecosystem models, as low areal average biomass cannot describe their role as hotspots of biological activity (Assmy et al. 2013).

In comparison to our results, the study of (Ambrose et al. 2005) shows a much higher percent coverage of 40-90% of algae. This is due to the fact, that the study was conducted much earlier in the year on the shelf and apart from aggregations also included the thin algal layer at the ice bottom into the analysis. Percent cover is a challenging proxy of total biomass. While in our dataset percent cover was only weakly correlated to aggregate abundance (R^2=0.29), it was a better indicator of total aggregate volume (R^2=0.79-0.97 for the different algorithms). Aggregate abundance measured off Greenland in June/July varied between <1 and 50 aggregates m^{-2} (Gutt 1995) and compare well to our study with an average abundance of <1 up to 16 aggregates m-2 with peak detections in few images of maximal 200 aggregates per m^2. Recent investigations from an ice floe in the FRAM Strait also revealed abundances of 6.3 ± 3.1 aggregates m^{-2} (Glud et al. 2014). While abundance values compare well, Glud et al. (2014) derived biomass estimates of up to 2.94 mg Chl *a* m^{-2} which equals 319-616 mg C m^{-2} assuming carbon to chlorophyll ratios from Assmy et al. (2013). This is significantly exceeding our estimates of <0.01 to 20.45 mg C m^{-2}. The large difference can very likely be explained, by the different approaches of sampling and biomass calculation as well as the seasonal variability in carbon to chlorophyll ratios.

Spatial distribution

Our results show that the spatial distribution of under-ice algal-aggregate biomass is mostly dependent on the topography of the ice underside and the hydrodynamic regime. Ridge edges, dome-like structures, pockholes and small scale roughness trap the loosely floating aggregates leading to accumulations of aggregates in such topographic features. In contrast, pressure ridges itself, did not host aggregate accumulations due to their large drafts, but rather act as barrier hindering further aggregate movement. The aggregate distribution is likely very dynamic and can easily be changed by changing ice relative currents, such as strong winds or tides (Assmy et al. 2013; Glud et al. 2014). In such events, algal-aggregates can get suspended in the mixed layer and drift along the ice until they get trapped again in the next ice feature. These main mechanisms of physical aggregate redistribution are summarized in Figure 6. This is different from the spatial distribution patterns of actively swimming zooplankton, which can use pressure ridges as a shelter (Gradinger et al. 2010). Typical habitat properties determining organism distribution such as light availability could not explain the aggregate distribution, as the individual aggregate cannot position itself actively. Its position is determined passively by a complex hydrodynamic interaction between buoyancy, under-ice currents and turbulence as well as the topography of the

ice underside. Nevertheless, a wide range of habitat properties like the availability of light and nutrients as well as grazing of course influence the growth of sea-ice algae, the formation of aggregates, and their fate related to sinking or suspension. While these factors impact the overall aggregate biomass and might be responsible for the large biomass variation observed in this and other studies, the spatial distribution of aggregates is determined by the topography of the ice-underside.

Aggregate biomass as quantified by abundance or percent-cover showed some positive correlation to geographical latitude (R^2=0.6-0.7) indicating, that aggregate biomass is greater within the Central Arctic basin than at the ice edge at the end of the summer. According to the shape analysis (Figure 1), the fraction of filamentous aggregates of *Melosira arctica* seems to be decreasing with increasing distance from the Laptev Sea. This is consistent with previous observations. Ambrose et al. (2005) and Melnikov (1997) described *Melosira arctica* to occur on the shelves of the Arctic, where its spores can get incorporated during ice formation in polynias and transported into the central basin (Smetacek 1985). The fraction of round aggregates composed of pennate diatoms is increasing towards the ice edge. Syvertsen (1991) described a similar succession of pelagic and ice-algal flocs in the Barents Sea, followed by filaments of *Melosira arctica* towards the central pack-ice.

Implications for the aggregation process and carbon export

The ice-algal aggregates described in this study are of extraordinary size, when compared to size-ranges observed in flocculation studies in other seas (Riebesell et al. 1991; Alldredge and Gotschalk 1989). When applying relationships between diameter and sinking speed from the literature (Jackson 1990) aggregates with a diameter of 3 cm will reach the deep-sea floor surprisingly fast within a single day once they lose buoyancy at the surface. This is consistent with observations of fresh ice-algal aggregates in water depths around 4000m from Boetius et al. (2013).

The ice floe of ice station ICE-1 (10 August) could be resampled almost two months later on 29 September at the end of the productive season, when light availability was strongly reduced. Assuming that the ice floe was in both cases representative for the area and that thus deplacement of aggregates by advection can be neglected, we can deduce some information about the changes of the aggregate distribution during that time period. Along with the decrease of aggregate abundance from 2.8 to 0.4 aggregates per m^2 and the decrease in median diameter

from 2.1 to 1.5cm we estimate, that 67-94% of the biomass present during the first sampling sank to the deep sea until end of September. The aggregate size distributions of both samplings reveal significant differences in the buoyancy status of the aggregate population. While the size distribution in August resembles a more typical distribution of aggregates prone to sinking, the size distribution end of September levels out towards larger aggregates. This indicates, that aggregates that are still present in September are buoyant and have so far avoided sinking, while the non-buoyant portion of the aggregate population sank down between the first and second sampling.

Analyzing the size distributions, we found a signature of buoyant aggregates mainly in the stations closest to the Laptev Sea shelf edge. In this area we observed extremely rotten and melting sea-ice with favorable conditions for aggregate floatation due to sufficient light available for oxygen production (Glud et al. 2014; Chapter III).

The theory of particle aggregation also yields critical POC concentrations above which phytoplankton exhibits a high aggregation potential (Jackson 1990). Water column concentrations of 70-100 μg L^{-1} POC from our field sites (Chapter III) thus imply, that with typical under ice shear rates between 0.001 and 1s^{-1} (McPhee and Morison 2001), the sticking efficiency must be very high. Accordingly the Kolmogorov length scale of turbulence, describing the length scale at which aggregates are prone to breakup processes, is only 0.2 to 3 cm. The aggregates must thus be bond together strongly, avoiding aggregate breakup. This matches previous stickiness estimates (Riebesell 1991; Hansen and Kiorboe 1997) and our observations that the aggregates even withstand thruster wash of the ROV.

Limitations of aggregate detection

Even though the analysis of upward looking ROV images yields good results, one needs to keep in mind some limitations of the method. First, the method is only able to detect macroscopic aggregates bigger than a few mm floating directly underneath the sea ice. This relatively high detection limit leads to an underestimation of the total algal biomass but is irrelevant in the light of the huge range of biomass estimates caused by the different estimation algorithms. Second, close lying aggregates that are detected as a single one, as well as aggregates with a strong deviation from the spherical shape can lead to an overestimation of total aggregate volume. To reduce this effect, we excluded clumped aggregates from the analysis. Third, aggregates are often located in transition zones between different ice types, which at the same time are often

discarded during image processing, as the darker background of the thicker ice type gets classified as aggregates by the threshold algorithm. Overall, our method as used in this study might be rather underestimating ice algal aggregates. Future studies could thus benefit from a more sophisticated image classification technique and machine learning for automation of the detection.

We conclude that the spatial distribution of under-ice algal aggregates is mainly governed by the topography of the ice underside. Aggregates float up against any dome shape structures and ridge edges inhibit further movement. Thus sea ice ridges play an important role in structuring the spatial distribution of ice algal aggregates. On the large scale, filamentous aggregates of *Melosira arctica* dominate the inner part of the Central Arctic pack-ice, while closer to the ice edge under melting sea ice, round aggregates mainly formed by sea-ice algae dominate. The size distribution of aggregates indicate, that at least some portion of them does stay afloat and can get incorporated into the ice during freeze-up. Even though our ROV based method has proved to be suitable to provide the first large scale quantitative estimate of aggregate biomass, it remains difficult to compare biomass estimates to other studies due to uncertainties in both sampling and in particular in different ways to derive areal average estimates from the observations.

Acknowledgements

We acknowledge the support of the captain, the crew, and the scientific cruise leader Antje Boetius of the RV Polarstern cruise ARK-XXVII/3, facilitating the ROV measurements. Martin Schiller, Larysa Istomina and Scott Sörensen contributed significantly to the success of the field measurements as part of the group. We thank Clara Stolle for help with the image processing. This study was funded through the Alfred-Wegener-Institut Helmholtz-Zentrum für Polar- und Meeresforschung. Additional funds supporting this work were provided to Antje Boetius by the European Research Council Advanced Investigator grant 294757.

References

Alldredge AL, Gotschalk CC (1989) Direct observations of the mass flocculation of diatom blooms: characteristics, settling velocities and formation of diatom aggregates. Deep Sea Research 36 (2):159-171. doi:10.1016/0198-0149(89)90131-3

Ambrose WG, von Quillfeldt C, Clough LM, Tilney PVR, Tucker T (2005) The sub-ice algal community in the Chukchi sea: large- and small-scale patterns of abundance based on images from a remotely operated vehicle. Polar Biol 28 (10):784-795. doi:10.1007/s00300-005-0002-8

Arrigo KR (2014) Sea Ice Ecosystems. Annual Review of Marine Science 6 (1):439-467. doi:10.1146/annurev-marine-010213-135103

Arrigo KR, van Dijken G, Pabi S (2008) Impact of a shrinking Arctic ice cover on marine primary production. Geophys Res Lett 35 (19):L19603. doi:10.1029/2008gl035028

Assmy P, Ehn JK, Fernández-Méndez M, Hop H, Katlein C, Sundfjord A, Bluhm K, Daase M, Engel A, Fransson A, Granskog MA, Hudson SR, Kristiansen S, Nicolaus M, Peeken I, Renner AHH, Spreen G, Tatarek A, Wiktor J (2013) Floating Ice-Algal Aggregates below Melting Arctic Sea Ice. PLoS ONE 8 (10):e76599. doi:10.1371/journal.pone.0076599

Boetius A, Albrecht S, Bakker K, Bienhold C, Felden J, Fernandez-Mendez M, Hendricks S, Katlein C, Lalande C, Krumpen T, Nicolaus M, Peeken I, Rabe B, Rogacheva A, Rybakova E, Somavilla R, Wenzhoefer F, Party RPA--SS (2013) Export of Algal Biomass from the Melting Arctic Sea Ice. Science 339 (6126):1430-1432. doi:10.1126/science.1231346

Fernandez-Méndez M, Wenzhöfer F, Peeken I, Sorensen HL, Glud R, Boetius A (submitted 2014) Composition, buoyancy regulation and fate of ice algal aggregates in the Central Arctic Ocean. PLoS ONE

George D (1981) Zooplankton patchiness. Reports of the Freshwater Biology Association 49:32-44

Glud R, Rysgaard S, Turner G, McGinnis D, Leaky R (2014) Biological and physical induced oxygen dynamics in melting sea ice of the Fram Strait. Limnol Oceanogr 59 (4):1097-1111. doi:doi:10.4319/lo.2014.59.4.1097

Gosselin M, Levasseur M, Wheeler PA, Horner RA, Booth BC (1997) New measurements of phytoplankton and ice algal production in the Arctic Ocean. Deep Sea Research Part II: Topical Studies in Oceanography 44 (8):1623-1644. doi: 10.1016/S0967-0645(97)00054-4

Gradinger R, Bluhm B (2010) Assessment of the Abundance and Diversity of Sea Ice Biota. In: Eicken H, Salganek M (eds) Field Techniques for Sea-Ice Research. University of Alaska Press, Fairbanks, AK, p 294

Gradinger R, Bluhm B, Iken K (2010) Arctic sea-ice ridges-Safe heavens for sea-ice fauna during periods of extreme ice melt? Deep-Sea Research Part Ii-Topical Studies in Oceanography 57 (1-2):86-95. doi:10.1016/j.dsr2.2009.08.008

Guidi L, Stemmann L, Jackson GA, Ibanez F, Claustre H, Legendre L, Picheral M, Gorsky G (2009) Effects of phytoplankton community on production, size and export of large aggregates: A world-ocean analysis. Limnol Oceanogr 54 (6):1951-1963. doi:DOI 10.4319/lo.2009.54.6.1951

Gutt J (1995) The Occurrence of Sub-Ice Algal Aggregations Off Northeast Greenland. Polar Biol 15 (4):247-252

Gutt J, Gorny M, Arntz W (1991) Spatial distribution of Antarctic Shirmps (Crustacea, Decapoda) by underwater photography. Antarctic Science 3 (4):363-369

Haas C, Pfaffling A, Hendricks S, Rabenstein L, Etienne J-L, Rigor I (2008) Reduced ice thickness in Arctic Transpolar Drift favors rapid ice retreat. Geophys Res Lett 35 (17):L17501. doi:10.1029/2008gl034457

Hansen JLS, Kiorboe T (1997) Quantifying interspecific coagulation efficiency of phytoplankton. Marine Ecology Progress Series 159:75-79

Horner R, Ackley SF, Dieckmann GS, Gulliksen B, Hoshiai T, Legendre L, Melnikov IA, Reeburgh WS, Spindler M, Sullivan CW (1992) Ecology of Sea Ice Biota .1. Habitat, Terminology, and Methodology. Polar Biol 12 (3-4):417-427

Horner RA, Syvertsen EE, Thomas DP, Lange C (1988) Proposed Terminology and Reporting Units for Sea Ice-Algal Assemblages. Polar Biol 8 (4):249-253. doi:Doi 10.1007/Bf00263173

Jackson GA (1990) A model of the formation of marine algal flocs by physical coagulation processes. Deep-Sea Research Part a-Oceanographic Research Papers 37 (8):1197-1211. doi:10.1016/0198-0149(90)90038-w

Katlein C, Nicolaus M, Petrich C (2014) The anisotropic scattering coefficient of sea ice. Journal of Geophysical Research: Oceans:n/a-n/a. doi:10.1002/2013JC009502

Krembs C, Eicken H, Deming JW (2011) Exopolymer alteration of physical properties of sea ice and implications for ice habitability and biogeochemistry in a warmer Arctic. Proc Natl Acad Sci U S A 108 (9):3653-3658. doi:10.1073/pnas.1100701108

Kwok R, Rothrock DA (2009) Decline in Arctic sea ice thickness from submarine and ICESat records: 1958-2008. Geophys Res Lett 36. doi:10.1029/2009gl039035

Lee SH, McRoy CP, Joo HM, Gradinger R, Cui XH, Yun MS, Chung KH, Kang SH, Kang CK, Choy EJ, Son SH, Carmack E, Whitledge TE (2011) Holes in Progressively Thinning Arctic Sea Ice Lead to New Ice Algae Habitat. Oceanography 24 (3):302-308

Legendre L, Ackley SF, Dieckmann GS, Gulliksen B, Horner R, Hoshiai T, Melnikov IA, Reeburgh WS, Spindler M, Sullivan CW (1992) Ecology of Sea Ice Biota .2. Global Significance. Polar Biol 12 (3-4):429-444

Leu E, Soreide JE, Hessen DO, Falk-Petersen S, Berge J (2011) Consequences of changing sea-ice cover for primary and secondary producers in the European Arctic shelf seas: Timing, quantity, and quality. Prog Oceanogr 90 (1-4):18-32. doi:10.1016/j.pocean.2011.02.004

Leu E, Wiktor J, Soreide JE, Berge J, Falk-Petersen S (2010) Increased irradiance reduces food quality of sea ice algae. Mar Ecol-Prog Ser 411:49-60. doi:10.3354/meps08647

Lloyd M (1967) `Mean Crowding'. Journal of Animal Ecology 36 (1):1-30. doi:10.2307/3012

Markus T, Stroeve JC, Miller J (2009) Recent changes in Arctic sea ice melt onset, freezeup, and melt season length. J Geophys Res-Oceans 114. doi:10.1029/2009jc005436

Maslanik JA, Fowler C, Stroeve J, Drobot S, Zwally J, Yi D, Emery W (2007) A younger, thinner Arctic ice cover: Increased potential for rapid, extensive sea-ice loss. Geophys Res Lett 34 (24):L24501. doi:10.1029/2007gl032043

McCave IN (1984) Size spectra and aggregation of suspended particles in the deep ocean. Deep Sea Research Part A Oceanographic Research Papers 31 (4):329-352. doi:http://dx.doi.org/10.1016/0198-0149(84)90088-8

McPhee M, Morison J (2001) Under-ice boundary layer. Encyclopedia of Ocean Sciences:3069-3076

Melnikov I (1997) The Arctic sea ice ecosystem. Cambridge Univ Press,

Melnikov IA, Bondarchuk LL (1987) To the ecology of the mass aggregations of colonial diatom algae under the Arctic drifting sea ice. Okeanologiya 27 (2):317-321

Nansen F (1906) Protozoa on the ice-floes of the North Polar sea. The Norw. North Polar Exp. 1893-96. Scientific results ed by F Nansen Kristiania (Jacob Dybwad) Vol. 5 ((No. XVI)):22

Nicolaus M, Hudson SR, Gerland S, Munderloh K (2010) A modern concept for autonomous and continuous measurements of spectral albedo and transmittance of sea ice. Cold Reg Sci Tech 62 (1):14-28. doi:10.1016/j.coldregions.2010.03.001

Nicolaus M, Katlein C (2013) Mapping radiation transfer through sea ice using a remotely operated vehicle (ROV). The Cryosphere 7 (3):763-777. doi:10.5194/tc-7-763-2013

Nicolaus M, Katlein C, Maslanik J, Hendricks S (2012) Changes in Arctic sea ice result in increasing light transmittance and absorption. Geophys Res Lett 39: L24501. doi:10.1029/2012gl053738

Perovich DK, Roesler CS, Pegau WS (1998) Variability in Arctic sea ice optical properties. J Geophys Res-Oceans 103 (C1):1193-1208. doi:10.1029/97jc01614

Poulin M, Underwood GJC, Michel C (2014) Sub-ice colonial Melosira arctica in Arctic first-year ice. Diatom Research 29 (2):213-221. doi:10.1080/0269249X.2013.877085

Riebesell U (1991) Particle aggregation during a diatom bloom: 1. Physical aspects. Marine Ecology Progress Series 69 (3):273-280. doi:10.3354/meps069273

Riebesell U, Schloss I, Smetacek V (1991) Aggregation of Algae Released from Melting Sea Ice - Implications for Seeding and Sedimentation. Polar Biol 11 (4):239-248

Roesel A, Kaleschke L (2012) Exceptional melt pond occurrence in the years 2007 and 2011 on the Arctic sea ice revealed from MODIS satellite data. J Geophys Res 117 (C5):C05018. doi:10.1029/2011jc007869

Serreze MC, Holland MM, Stroeve J (2007) Perspectives on the Arctic's Shrinking Sea-Ice Cover. Science 315 (5818):1533-1536. doi:10.1126/science.1139426

Smetacek VS (1985) Role of sinking in diatom life-history cycles: ecological, evolutionary and geological significance. Mar Biol 84 (3):239-251. doi:10.1007/BF00392493

Syvertsen EE (1991) Ice algae in the Barents Sea: types of assemblages, origin, fate and role in the ice-edge phytoplankton bloom. Polar Res 10 (1):277-288. doi:10.1111/j.1751-8369.1991.tb00653.x

Wassmann P, Reigstad M (2011) Future Arctic Ocean Seasonal Ice Zones and Implications for Pelagic-Benthic Coupling. Oceanography 24 (3):220-231

Werner I, Lindemann F (1997) Video observations of the underside of Arctic sea ice-features and morphology on medium and small scales. Polar Res 16 (1)

Figure 1. Map of the cruise track of the IceArc expedition and positions of ice stations where under-ice algal aggregates were observed with the ROV. The size of the circles represents aggregate abundance, while the fraction of the two aggregate types as determined from mean aggregate eccentricity is depicted by the pie charts. Green color stands for the fraction of elongated aggregates, while yellow depicts the fraction of round aggregates. Mean sea ice concentration during the cruise period is shown in the background.

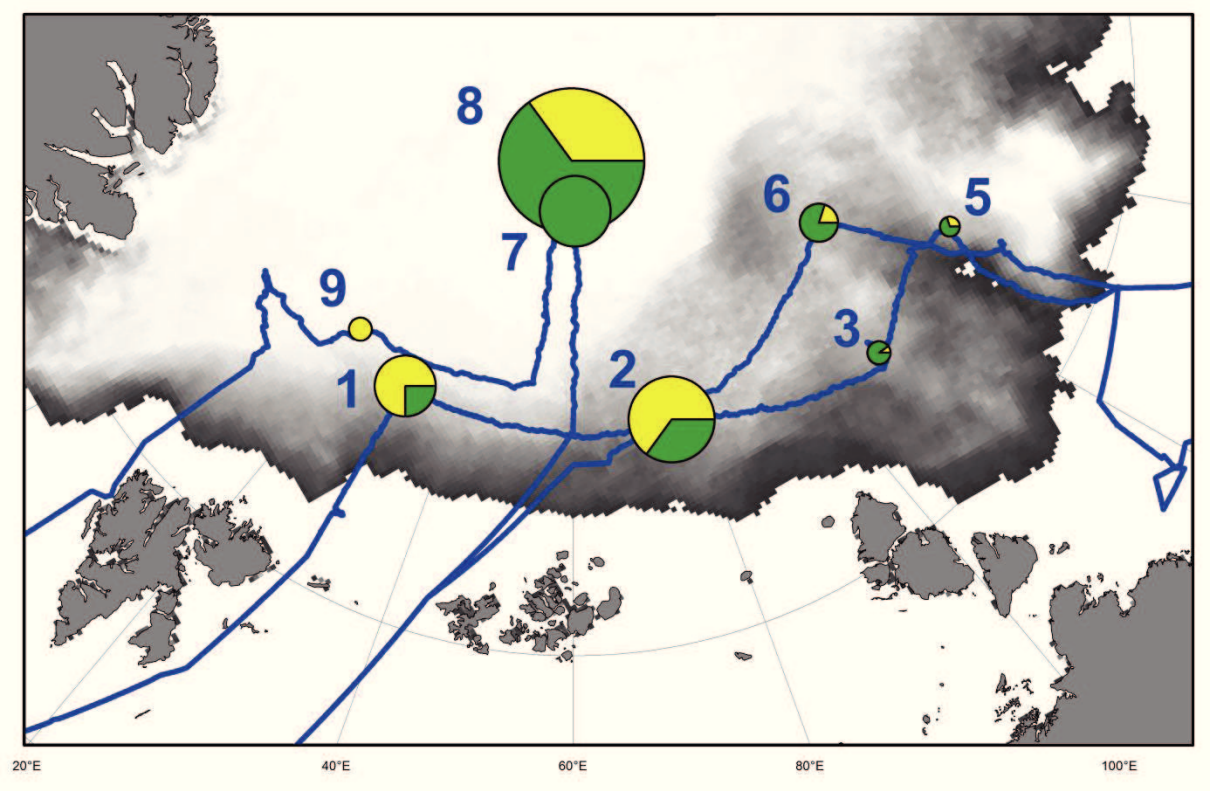

Figure 2. Example images from the upward looking ROV camera: a) round aggregates dominated by pennate diatoms b) filamentous aggregates of *Melosira arctica* c) a regular cover of small aggregates close to the detection limit of the method d) a tilted view from greater depth shows, that aggregates are often trapped within dome-like or rough ice structures.

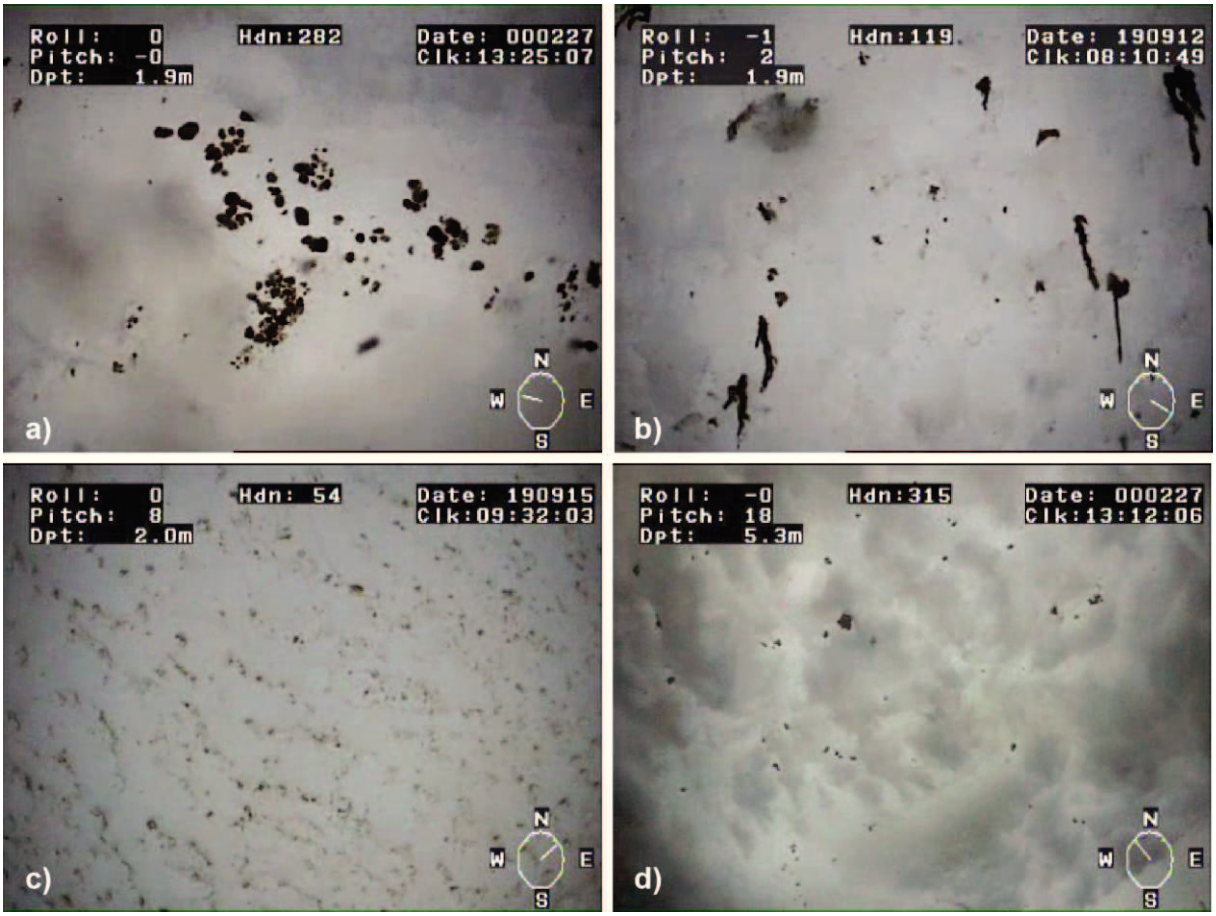

Figure 3. Spatial distribution of aggregates (a), ice draft (b), ice roughness (c) and light transmittance (d) on station ICE-8. Distribution maps of the other stations can be found in the electronic supplement (Fig. S1-S7). Positions are given in a floe fixed coordinate system relative to the ship's GPS receiver.

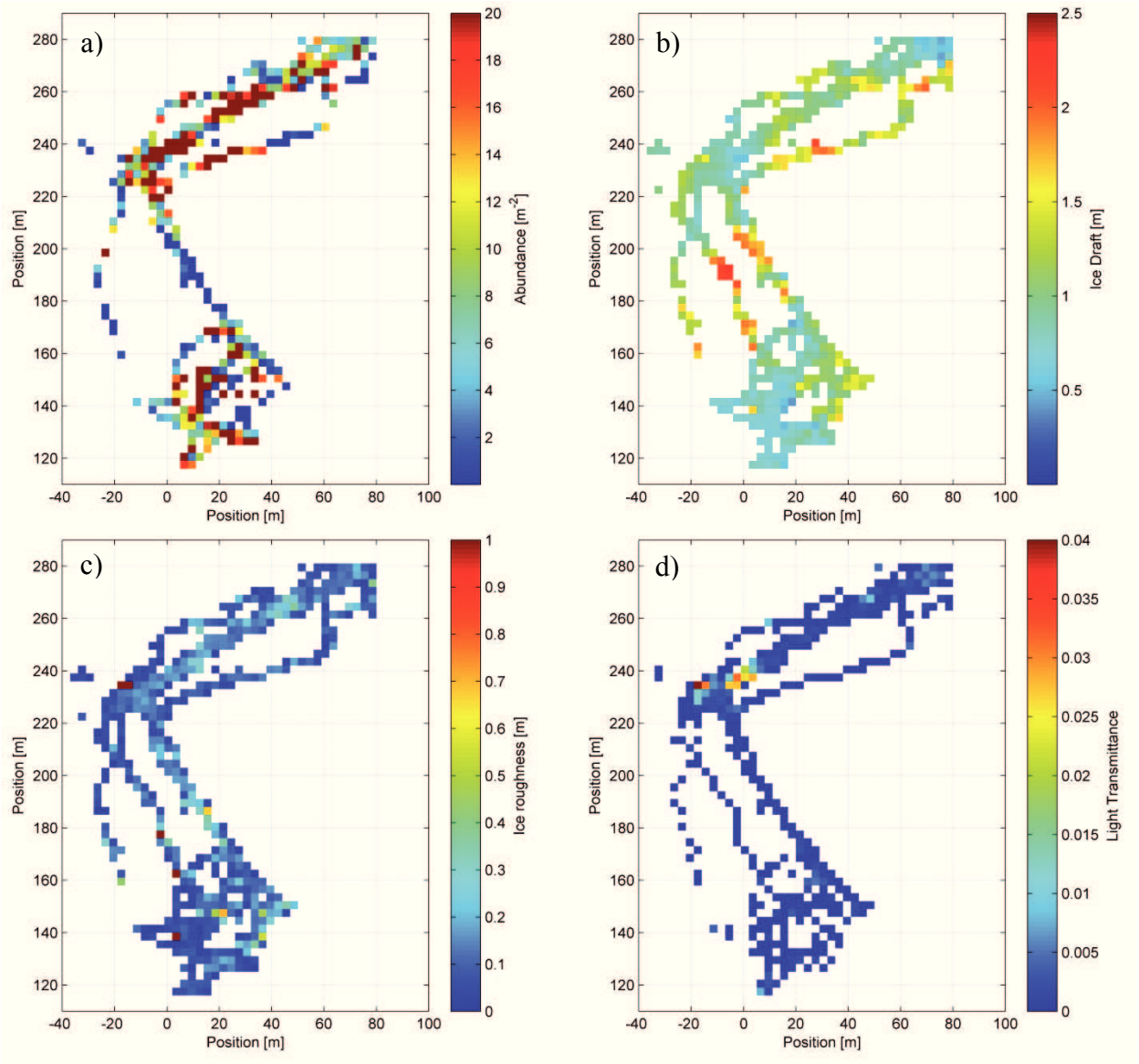

Figure 4. Dependence of aggregate abundance on a) sea-ice draft and b) sea-ice roughness

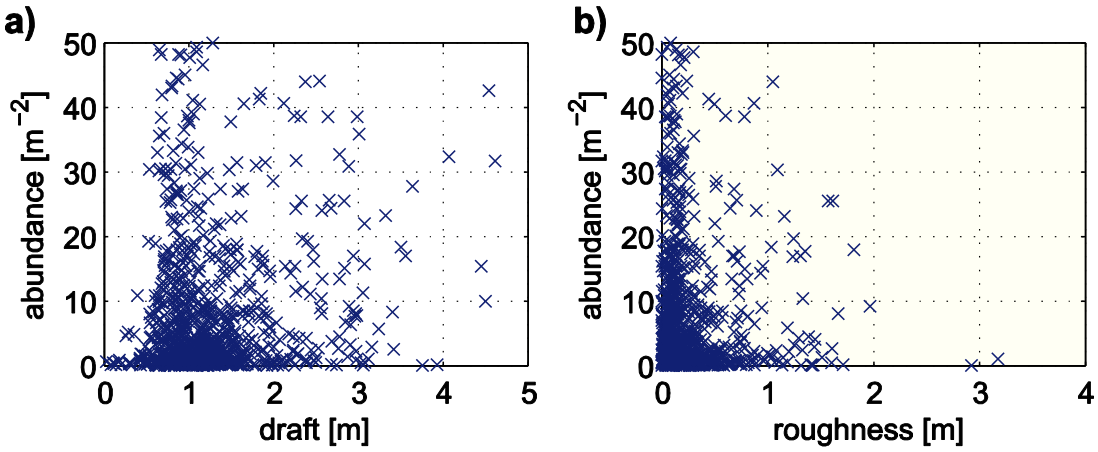

Figure 5. Aggregate size distribution on the different ice stations. Size distributions that flatten out towards big aggregates are shown by dashed lines.

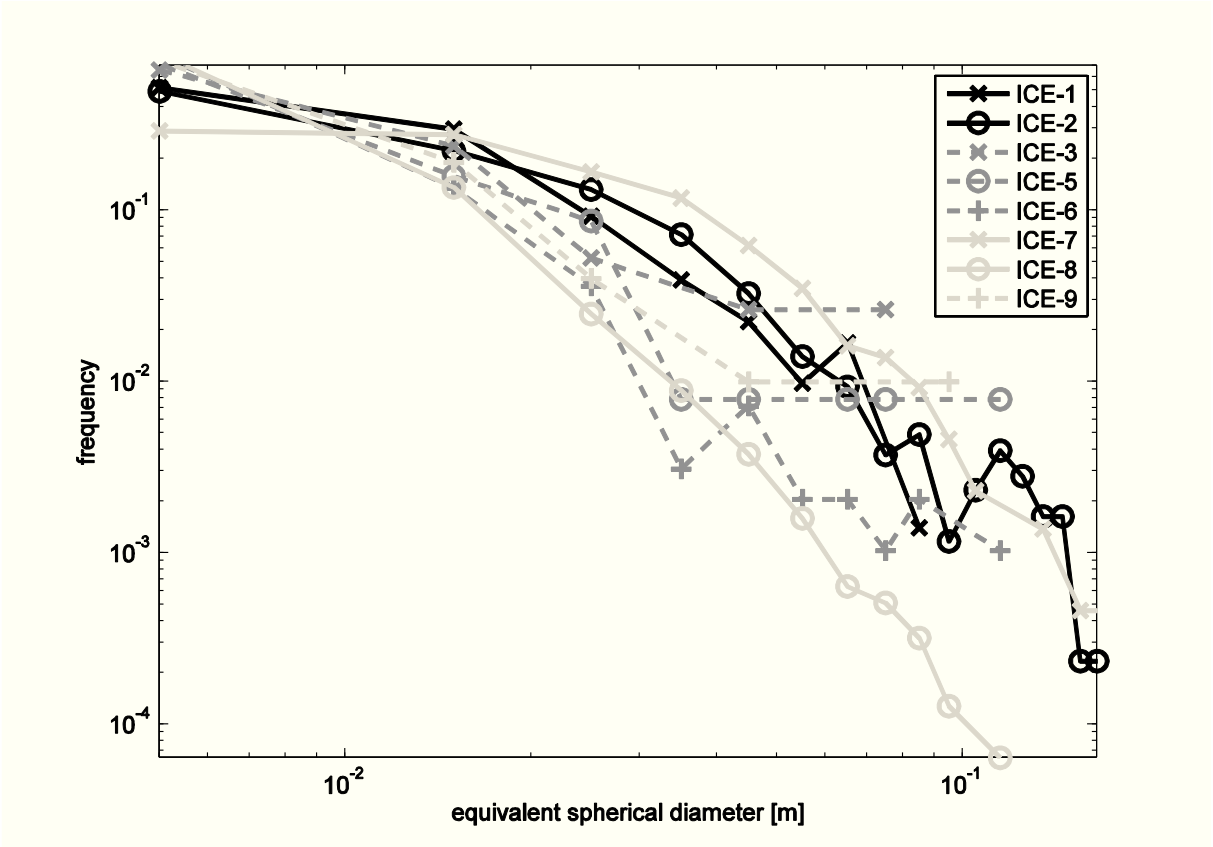

Figure 6. Summary of the four main physical processes governing the spatial distribution of aggregates: a) Buoyant aggregates are floating up against the ice and accumulate in level ice and dome shaped structures; b) During Ice drift, pressure ridges skim through the water and can press the aggregates towards ridge edges; c) Location of the aggregates in the level ice and dome shaped structures provides shelter from under-ice currents; b) When these get stronger, aggregates get transported further by turbulent water motion.

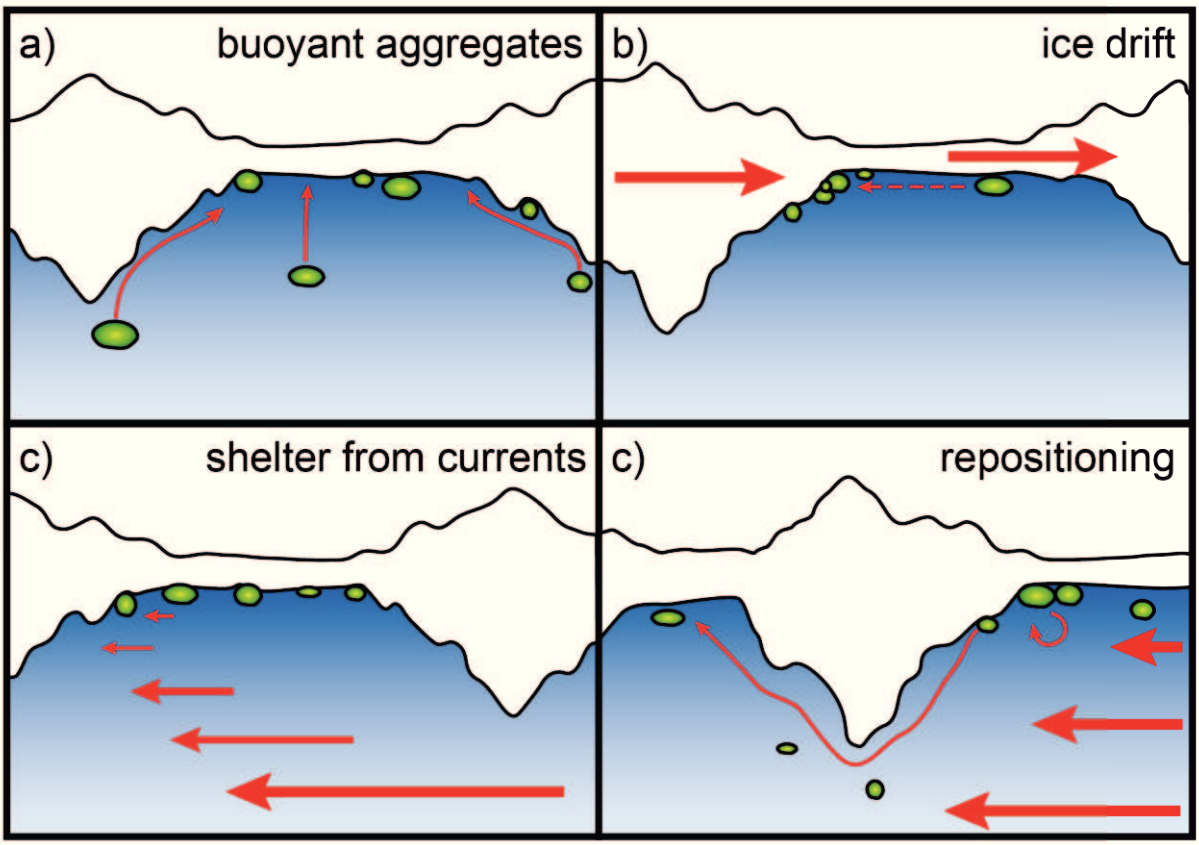

Table 1. Comparison of aggregate percent coverage and abundance retrieved from different image treatment approaches using varying subsets of the dataset

Icestation	**ICE-1**	**ICE-2**	**ICE-3**	**ICE-5**	**ICE-6**	**ICE-7**	**ICE-8**	**ICE-9**
%-coverage								
Boetius et al. (2013)	0.04	0.19	<0.001	0.04	0.03	0.55	0.13	-
Assmy et al. (2013)	0.01	0.03	-	-	-	-	-	-
full dataset	0.026	0.062	0.005	0.003	0.008	0.163	0.093	0.0035
Abundance [agg m^{-2}]								
Boetius et al. (2013)	-	-	-	-	-	-	-	-
Assmy et al. (2013)	0.79	5.06	-	-	-	-	-	-
full dataset	2.85	5.69	0.48	0.32	1.13	3.85	16.07	0.41

Table 2. Environmental parameters at the ice stations and average aggregate properties

Ice station	Units	ICE-1	ICE-2	ICE-3	ICE-5	ICE-6	ICE-7	ICE-8	ICE-9
Station number		224	237	255	323	335	349	360	384
Latitude	°	84.00	83.95	82.86	82.88	85.06	87.93	88.83	84.35
Longitude	°	30.00	76.85	109.86	130.76	122.52	60.95	58.53	17.73
Date in 2012		10 Aug	15Aug	20 Aug	5 Sep	8 Sep	19 Sep	22 Sep	29 Sep
Water depth	m	4300	4300	4290	4020	4000	3250	4090	3700
Ice-concentration	%	80	80	70	60	50	100	100	100
Abundance	Agg m^{-2}	2.8	5.6	0.4	0.3	1.1	3.8	16.0	0.4
Diameter (median)	cm	2.1	2.0	3.4	2.1	1.6	3.5	2.0	1.5
Diameter (mean)	cm	2.5	2.9	4.1	2.9	2.2	4.0	2.4	2.1
Circularity	-	0.79	0.77	0.66	0.70	0.68	0.64	0.71	0.84
Eccentricity	-	0.79	0.81	0.89	0.87	0.85	0.88	0.87	0.76
Indexof Patchiness	-	11.5	9.2	67.4	17.9	74.0	3.1	3.3	5.2
Distance to ice edge	km	180	190	380	300	510	600	700	320
Distance to Laptev sea	km	1450	910	580	490	740	1210	1210	1560
Melt water[a]	m	0.5	0.7	0.7	2.3	2.2	0.8	0.9	-
Deep-sea algae cover[a]	%	0	0.003	1.3	0.5	0.8	2.2	10.4	-
slope of size distribution	-	-1.9	-2.2	-1.3	-1.7	-2.3	-2.2	-3.1	-1.6
slope (Ø>2cm)	-	-3.0	-3.0	-0.6 [b]	-1.2 [b]	-2.0 [b]	-3.2	-3.9	-1.0 [b]

[a] Data from Boetius et al. (2013), [b] $R^2<0.8$

Table 3. Biomass estimates obtained by different approaches. "Global" refers to averages over all images with valid information, while "gridded" refers to averages determined after spatial gridding of the results. "Mean" and "median" refer to whether mean or median diameters where used in the calculation. "Raster cells" refers to biomass calculation within the spatial grid cells before averaging over the survey area, while "aggregate list" refers to a calculation based on the list of all aggregate detections. The approaches "gridded median" and "raster cells" should provide the most reasonable estimates.

Ice station	**ICE-1**	**ICE-2**	**ICE-3**	**ICE-5**	**ICE-6**	**ICE-7**	**ICE-8**	**ICE-9**	**mean**
Aggregate volume [ml m^{-2}]									
global mean	0.4	2.1	0.02	0.03	0.04	10.4	1.1	0.03	1.8
global median	0.2	0.5	<0.01	0.01	0.01	4.8	0.5	0.01	0.7
gridded mean	2.5	6.0	0.7	0.3	0.4	16.8	6.5	0.3	4.2
gridded median	**0.9**	**1.4**	**0.5**	**0.1**	**0.2**	**21.9**	**4.1**	**0.3**	**3.7**
raster cells	**5.2**	**16.3**	**4.7**	**1.6**	**3.0**	**38.6**	**6.9**	**1.7**	**9.7**
aggregate list	2.2	20.4	0.2	0.5	0.7	52.5	6.9	0.4	10.5
Carbon content [mg C m^{-2}]									
global mean	0.2	0.8	0.01	0.01	0.02	4.0	0.4	0.01	0.7
global median	0.1	0.2	<0.01	<0.01	<0.01	1.9	0.2	<0.01	0.3
gridded mean	1.0	2.3	0.3	0.1	0.1	6.5	2.5	0.1	1.6
gridded median	**0.4**	**0.5**	**0.2**	**0.03**	**0.07**	**8.5**	**1.6**	**0.1**	**1.4**
raster cells	**2.0**	**6.4**	**1.8**	**0.6**	**1.2**	**15.0**	**2.7**	**0.7**	**3.8**
aggregate list	0.8	8.0	0.1	0.2	0.3	20.4	2.7	0.1	4.1

Chapter V

Photosynthetic production in the Central Arctic during the record sea ice minimum in 2012

M. Fernández-Méndez[1,2], C. Katlein[1], B. Rabe[1], M. Nicolaus[1], I. Peeken[1,3], K. Bakker[4], H. Flores[1,5], and A. Boetius[1,2]

[1]Alfred-Wegener Institute Helmholtz-Zentrum für Polar und Meeresforschung, Bremerhaven, Germany.

[2] Max Planck Institute for Marine Microbiology, Bremen, Germany.

[3] MARUM, Centre for Marine Environmental Sciences, University of Bremen, Germany.

[4] Royal Netherlands Institute for Sea Research, Texel, The Netherlands.

[5] University of Hamburg, Zoological Institute and Zoological Museum, Biocenter Grindel, Hamburg, Germany.

For submission to Biogeosciences

Abstract

The ice-covered Central Arctic Ocean is characterized by low primary productivity due to light and nutrient limitations. The recent reduction in ice cover has the potential to substantially increase phytoplankton primary production, but little is yet known about the fate of the ice-associated primary production and of nutrient supply with increasing warming. This study presents results from the Central Arctic Ocean collected during summer 2012, when sea-ice reached a minimum extent since the onset of satellite observations. Net primary productivity (NPP) was measured in the water column, sea ice and melt ponds by $^{14}CO_2$ uptake at different irradiances. Photosynthesis vs. irradiance (PI) curves were established in laboratory experiments and used to upscale measured NPP to the deep Eurasian Basin (north of 78°N) using the irradiance-based Central Arctic Ocean Primary Productivity (CAOPP) model. In addition, new annual production was calculated from the seasonal nutrient drawdown in the mixed layer since last winter. Results show that ice algae can contribute up to 60% to primary production in the Central Arctic at the end of the season. The ice-covered water column had lower NPP rates than open water due to light limitation. According to the nutrient ratios in the euphotic zone, nitrate limitation was detected in the Siberian Seas (Laptev Sea area), while silicate was the main limiting nutrient at the ice margin near the Atlantic inflow. Although sea-ice cover was substantially reduced in 2012, total annual new production in the Eurasian Basin was 17 ± 7 Tg C yr^{-1}, which is similar to estimates of previous years. However, when including the contribution by sub-ice algal filaments, the annual production for the deep Eurasian Basin (north of 78°N) could double previous estimates with a plus of 16 Tg C yr^{-1}. Our data suggest that sub-ice algae are an important component of the ice-covered central Arctic productivity, and it remains an important question if their contribution to productivity could be fully replaced by phytoplankton with increasing sea-ice retreat.

Keywords: Primary Production, Arctic, phytoplankton, sea-ice algae, melt ponds, nutrient limitation, photosynthesis-irradiance curves, carbon cycle.

Introduction

Estimates of annual primary production (PP) in the ice-covered Central Arctic Basins are among the lowest of all oceans worldwide (Sakshaug et al., 2004). On an annual base, the total incoming irradiance and the depth of the winter mixing are the two main factors that constrain Arctic primary production (Ardyna et al., 2011; Popova et al., 2010). Available irradiance is generally sparse due to the low angle of the sun around the North Pole, and the attenuation effect of sea-ice (Sakshaug and Slagstad, 1991). However, during the summer months the total incoming irradiance increases since daylight is available during 24h. Nutrient supply is low due to strong vertical stratification and reduced wind driven mixing affected by sea ice (Carmack et al., 2006). The Central Arctic is divided into two deep basins separated by the Lomonosov Ridge: the Eurasian and the Amerasian Basins. These central basins cover 40% of the Arctic Ocean, but due to their inaccessibility, data for this region is scarce (Matrai et al., 2013). The different methodologies to estimate PP in and under the ice, as well as in ice-free regions together with the high spatial and temporal variability result in poorly constrained PP values for the Central Arctic Basins. These range from 1 Tg C yr^{-1}, when assuming no production in ice covered areas (Hill et al., 2013), to 119 Tg C yr^{-1} when taking into account the total amount of nutrients used for PP from water column budgets (Codispoti et al., 2013). The annual areal NPP estimates for the Eurasian Basin including sea ice algae range between 10-15 g C m^{-2} yr^{-1}, twice as much as in the Amerasian Basin (Codispoti et al., 2013; Gosselin et al., 1997; Sakshaug et al., 2004; Wheeler et al., 1996). In the Central Arctic sea-ice algae can contribute up to 57% of the NPP in summer (Gosselin et al., 1997), but their patchy distribution, and technological challenges in sampling them and in producing *in situ* estimates of their PP cause a high uncertainty in the overall estimates (Assmy et al., 2013; Fernández-Méndez et al., 2014; Glud et al., 2014).

When enough light becomes available for PP between May and September (Arndt and Nicolaus, 2014; Leu et al., 2011), Arctic phototrophs grow in the water column (phytoplankton), in and below sea ice (sea-ice algae), and in melt ponds (melt pond algae). Light is the main limiting factor for the phytoplankton below thick ice at the beginning of the productive season (Sherr et al., 2003). North of 78 °N latitude, the productive season is shorter (June to September) than in southern Arctic regions since it is restricted by the amount of light penetrating through the formerly permanent sea ice cover (Leu et al., 2011). Nutrients become limiting as the season

advances (Tremblay and Gagnon, 2009). The two Central Basins differ in the inflow of waters: low salinity, phosphate rich and nitrate depleted Pacific waters enter the Amerasian Basin through the Bering Strait. Warm, high salinity Atlantic waters with a higher N:P ratio enter the Eurasian Basin through the Fram Strait (Jones et al., 1998), but remain submerged under a layer of fresher Arctic surface water until upwelling events bring them to the surface. Since most of the studies regarding nutrient limitation in Arctic waters come from the Amerasian Basin, nitrate is considered the main limiting nutrient for primary production in the Central Arctic (Tremblay and Gagnon, 2009). However, nutrient ratios in the Eurasian Basin are very different to the Amerasian pointing towards silicate limitation rather than nitrate in some regions (Wheeler et al., 1997). In late summer, mostly regenerated production based on ammonium takes place (Martin et al., 2012). Grazing pressure and the microbial loop also play an important role controlling recycling of nutrients vs export (Boetius et al., 2013; Olli et al., 2007; Yager et al., 2011), but remain understudied in the Central Arctic.

Recent evidence suggests that the rapid Arctic warming and sea-ice retreat are changing key factors governing primary productivity, including the Central Arctic Basins. The percentage of thick multi-year ice (MYI) is decreasing rapidly (Laxon et al., 2013; Maslanik et al., 2007; Stroeve et al., 2012). The lowest sea-ice extent since the beginning of recorded observations was reached in September 2012 (National Snow and Ice Data Center (NSIDC), 2012) leaving 45% of the Eurasian Basin north of 78ºN ice-free (<15% ice cover). Furthermore, an increase in melt pond covered sea ice has been observed (Rösel and Kaleschke, 2012), enlarging the habitat of planktonic and sea-ice algae (Kramer and Kiko, 2011; Lee et al., 2011). All these changes combined lead to an increase in the amount of irradiance reaching the water column in the Central Arctic (Nicolaus et al., 2012). On the other hand, nutrient availability in the euphotic zone is probably decreasing due to the stronger stratification caused by increased freshwater storage. An increase in nutrients from river origin has been hypothesized, but a recent study by Le Fouest et al., (2012) indicates that the contribution of these nutrients will not be enough to increase primary production substantially, and any effect may be constrained to the shelf seas. Furthermore, changes in light conditions and nutrient availability might affect the timing of sea ice and water column blooms and the composition of the autotrophic biomass, this will have implications for timing and food quality available for grazers (Leu et al., 2010; Slagstad et al., 2011) and for total export to the deep sea (Lalande et al., 2013).

This study examines primary productivity in the Eurasian Basin of the Central Arctic at the time of the sea ice minimum in summer 2012, in comparison to the few previous estimates available. It aims to quantify the relative contribution of sea ice, melt ponds and water column to total NPP, both *in situ* and for the entire Eurasian Basin, with a focus on the bottom up limiting factors of NPP (light and nutrients) at different time scales. We test the hypothesis that primary productivity could increase significantly with decreasing ice-cover in the Central Arctic.

Methods

Study site and sampling

Sea ice, melt ponds and water column were sampled during the RV Polarstern expedition ARK-XXVII/3 to the Eurasian Basin of the Central Arctic Ocean during summer 2012 (Boetius, 2013) (Fig. 1). The expedition started in early August visiting the ice margin and heading towards the Laptev Sea. At the beginning of September the ice-free shelf edge of the Laptev Sea (77-80°N, 118-133°E) was sampled and at the end of the month the Central Arctic was reached (85-88°N. 52-123°E). The expedition covered a large portion of the Eurasian Basin and included 33 water stations in waters near the Atlantic inflow, and 8 ice stations expanding through different nutrient regimes, ice coverage (from ice free waters to 100% ice cover) and ice types according to age, thickness, pond and snow cover and topography: first year ice (FYI) is rather flat with a high coverage of melt ponds and multiyear ice (MYI) is thicker and has more snow on top (Table 1).

Sea ice concentration and melt pond coverage were assessed during the entire cruise by observations from the bridge (Hendricks et al., 2012) (Table S1). Sea-ice thickness was additionally measured with an air-borne electromagnetic (EM) Bird as described in Haas et al. (2009). Sea ice was sampled using an ice corer (Kovacs Enterprise, Roseburg, USA). Ice cores were cut into two equal sections (top and bottom) for primary productivity measurements and in 10 cm sections for biomass and nutrient measurements. Ice cores were melted in the dark at 4°C for 24 h on a shaker (Mikkelsen et al., 2008). Filtered seawater (200 ml per cm of ice) was only added to the ice sections used for pigment analysis (Thomas and Dieckmann, 2010).

Melt pond water samples were obtained with a hand pump (Model 6132-0010, Nalgene, Penfield, NY, USA) and melt pond depth, temperature and salinity were measured *in situ* using a hand-held conductivity meter (315i with TetraCon electrode cell, WTW GmbH, Weilheim in Oberbayern, Germany). Water column profiles of temperature and salinity were obtained using the Conductivity Temperature Depth (CTD) system with a Carousel Water Sampler (Sea-Bird Electronics Inc., Washington, USA).Water below the ice was sampled using a peristaltic pump (Masterflex® E/S™ portable sampler, 115 VAC, Oldham, UK), while water samples in ice free areas were collected during the upcast of the CTD Rosette sampler. To exclude the effect of propeller mixing in the upper 20 m of CTD profiles, additional vertical profiles of under ice salinity, temperature and fluorescence were obtained by manually lowering a CTD probe through holes in the ice floes sampled ('ice-CTD'; Sea and Sun Technology CTD75M, Trappenkamp, Germany). Fluorescence in the water column was measured with two fluorometers (Turner Cyclops, California, USA) attached to the ship CTD and the ice-CTD, respectively. Fluorescence values were calibrated *a posteriori* with chlorophyll *a* (Chl *a*) concentrations from water samples using high-performance liquid chromatography (HPLC) as described in Tran et al., (2013) and David et al., (2014). Chl *a* in the ice and melt ponds was measured using the same HPLC method.

For the nutrient addition experiments, 20 L of seawater were collected at station 3 at the depth of the maximum Chl *a* concentration (25 m) using the ships CTD sampler, and a piece of brown ice of 40 cm x 40 cm was cut with an ice saw at station 8 and melted in the dark in 0.2 μm filtered seawater from the same location (Rozanska et al., 2009; Thomas and Dieckmann, 2010).

In situ Net Primary Production

Net Primary Production (NPP) was measured using the ^{14}C uptake method (Steemann Nielsen, 1952) with minor modifications. Melted sea ice, seawater, and melt pond samples were spiked with 0.1 μCi ml^{-1} of ^{14}C labelled sodium bicarbonate (Moravek Biochemicals, Brea, USA) and distributed in 10 clear bottles (20 ml each). Subsequently they were incubated for 12 h at -1.3°C under different scalar irradiances (0–420 μmol photons m^{-2} s^{-1}) measured with a spherical sensor (Spherical Micro Quantum Sensor US-SQS/L, Heinz Walz, Effeltrich, Germany). At the end of the incubation, samples were filtered onto 0.2 μm nitrocellulose filters and the particulate

radioactive carbon uptake was determined by liquid scintillation counting using Filter count scintillation cocktail (Perkin Elmer, Waltham, USA). The carbon uptake values in the dark were subtracted from the carbon uptake values measured in the light incubations.

Dissolved inorganic carbon (DIC) was measured for each sample using the flow injection system (Hall and Aller, 1992). The DIC concentration was taken into account to calculate the amount of labeled bicarbonate incorporated into the cell. Carbon fixation rates were normalized volumetrically and by chlorophyll *a* (doi:10.1594/PANGAEA.834221). Photosynthesis-irradiance curves (PI curves) were fitted using MATLAB® according to the equation proposed by Platt et al. (1980) including a photoinhibition parameter (β) and providing the main photosynthetic parameters: maximum Chl *a* normalized carbon fixation rate if there were no photoinhibition (P^b) and the initial slope of the saturation curve (α). The derived parameters: light intensity at which photosynthesis is maximal (I_m), the carbon fixation rate at that maximal irradiance (P^b_m) and the adaptation parameter or photoacclimation index (I_k) were calculated according to Platt et al. (1982).

Depth-integrated *in situ* rates were calculated for each environment as a function of the available photosynthetically active radiation (PAR). Irradiance profiles were calculated for each environment (sea ice, melt pond, water under the ice and open water) from the daily average incoming solar shortwave irradiance measured by a pyranometer (Kipp & Zonen, Delft, Netherland) mounted on the ship. We used light attenuation coefficients of 10 m^{-1} for snow, 1.5 m^{-1} for sea ice (Perovich, 1996) and 0.1 m^{-1} for Atlantic-influenced Arctic seawater, based on literature values and observations during the cruise. Planar irradiance was transformed to scalar irradiance according to Ehn and Mundy (2013) and Katlein et al., (2014). Water column production was integrated over the euphotic zone (1% of incoming irradiance) and sea ice production over the ice core thickness. Melt pond coverage and sea ice concentration were taken into account when calculating the total primary production per area.

Central Arctic Ocean Primary Productivity model

Integrated Chl *a* concentrations obtained from sea-ice Chl *a* measurements and water column ship-based and ice-CTD casts (Table 1) and average PI curves were estimated for each

environment (Fig. S1): melt ponds (MP), multi-year ice (MYI), first-year ice (FYI), water under the ice (WUI) and open water (OW). Key parameters for photosynthetic activity were calculated from the available PI curves, excluding those were the coefficient of determination of the fit was smaller than 0.5 (Table 2). Open water samples correspond to the Laptev Sea shelf edge. Net Primary Production (NPP) was calculated analogous to section 2.2 for each point in a 10 km polar stereographic grid as a vertical integration with a resolution of 10 cm in the ice and 1 m in the water column. Downwelling solar irradiances at the surface (PAR) were calculated from the European Centre for Medium-Range Weather Forecast (ECMWF) Era Interim re-analyses (Dee et al., 2011). Downwelling transmitted irradiances underneath the sea-ice were calculated using the parameterization of Arndt and Nicolaus (2014) and light extinction in all media was assumed to follow an exponential decay. For water and sea ice we used the same light extinction coefficients as presented above. NPP was calculated as a function of PAR for every depth multiplied with the according Chl *a* concentration and integrated over the euphotic zone (1% incoming PAR). For pixels with a sea ice concentration >15%, the WUI average PI curve was used, while for pixels with < 15% sea ice concentration the OW average PI curve was used. For melt ponds, an average depth of 0.4 m was used based on observations during the expedition (Hendricks et al., 2012). Since satellite-based melt pond cover data were not available for summer 2012, a constant melt pond concentration was used for FYI: 26% and for MYI: 29% following Arndt and Nicolaus (2014) and Rösel and Kaleschke (2012). These values are similar to the average melt pond coverage observed during our cruise (30±15 %) (Hendricks et al., 2012). Total INPP was calculated as an average of the three compartments "open water", "water covered by sea ice" and "water covered by sea ice with melt ponds" weighted with the respective areal fraction. To estimate the total range of INPP we ran the CAOPP model three times using the average, the minimum and the maximum photosynthetic parameters.

Nutrient addition experiments

Two nutrient addition experiments were performed during the cruise at ice stations 3 and 8 (Fig. 1). For the first one, seawater from the depth of the Chl *a* maximum (25m) was collected, and for the second one, multiyear ice with a brown coloration due to the high content of sea-ice algae, was melted in filtered seawater taken at the same spot. Both samples were pre-filtered through a

100 μm mesh to remove grazers and kept at 0ºC and 65 μmol photons m^{-2} s^{-1} in 25 L transparent bottles until the start of the experiment. Chl *a* was monitored every day with a Turner Trilogy Fluorometer (model 7200-000) (Turner, California, USA) to identify the end of possible lag effect. Once Chl *a* reached a stable concentration (6 days for sea water and 4 days for sea ice) the sample was mixed and distributed in 10 transparent 5L-Nalgene bottles (2L in each). The initial biomass concentration in the samples was estimated by measuring Chl *a* and particulate organic matter. A sub-sample (0.5 L) was filtered through a pre-combusted glass fiber filter (GF/F) (0.7 μm poresize, Whatman, Kent, United Kingdom) and analyzed with an elemental analyser (EA3024-IRMS, EuroVetorSpA, Milan, Italy) to quantify particulate organic carbon (POC) and nitrogen (PON). For Chl *a* quantification a sub-sample (0.5 L) was filtered through a GF/F filter and the pigments were extracted with 90% acetone during 24 h (Parsons et al., 1984) and the fluorescence was then measured with a Turner Fluorometer (Turner, California, USA).

Nutrient concentrations (nitrate, phosphate and silicate) were measured with a standard photometric method using a Technicon TRAACS 800 continuous flow auto analyzer (Technicon Corporation) according to established methods (Boetius et al., 2013). Five different treatments in duplicate were incubated at 75 μmol photons m^{-2} s^{-1}. This irradiance corresponds to 33 W m^{-2}, which is slightly higher than the average irradiance below the ice at the end of the productive season to avoid light limitation and prevent photoinhibition. The five treatments consisted on a negative control with no nutrient addition (C-), a positive control with the three nutrients added (C+) and three treatments with one nutrient added in each (N+, P+ and Si+). In each treatment, the added nutrient concentration resembled the concentration of that nutrient in deep waters (>100 m) at the same ice station. Biomass (Chl *a*, POC and PON) and nutrients were measured in each treatment after 2 days and compared to the initial value. In parallel a sub-set of four samples (20 ml each) from each treatment were spiked with ^{14}C bicarbonate to estimate NPP as described above. Three samples were incubated under light conditions (75 μmol photons m^{-2} s^{-1}) and one in the dark for 24 h. At the end of the experiments the qualitative algal composition from each treatment was studied with a plankton chamber (Hydro-Bios, Altenholz, Germany) and an inverted light microscope with phase contrast optics (Axiovert 40C, Carl Zeiss, Jena, Germany) with integrated camera (AxioCamMRc, Carl Zeiss, Jena, Germany).

Annual New Production

All oceanographic data used in this study are available from the Earth system data base PANGAEA (Rabe et al., 2012) (Table S1). We determined the mixed layer depth during the previous winter from temperature in our summer CTD profiles of the upper Arctic Ocean, following Rudels (1995) and Korhonen et al.(2013). In the temperature profiles during the Arctic Ocean melting season, the winter mixed layer depth is indicated by a temperature minimum above the lower halocline. Any conservative property, such as salinity, observed at the depth of this temperature minimum, represents the conditions of the mixed layer during the previous winter. An estimate of the change from the previous winter is given by the difference between a conservative property in summer and its reference value at the depth of the temperature minimum. The vertical integral of these differences represents the addition or removal of a quantity or substance, for example nitrate, since the previous winter.

Nutrients (phosphate, silicate, and nitrate) in the water column were measured at discrete depths (2, 10, 20, 30, 50, 75 and 100 m) as described above (Bakker, 2014) (Table S1). Subsequently we interpolated total inorganic nitrogen (TIN = NO^-_3+NO^-_2), phosphate and silicate to the vertical resolution of the continuous temperature profiles (Reiniger et al., 1968), to calculate the nutrient inventory in the layer above the temperature minimum. We then derived the uptake since last winter by calculating the difference between the surface and the nutrient value at the temperature minimum depth. This approach is similar to the one used by Codispoti et al., (2013) with the main difference that they used the available winter nutrient concentrations. The annual TIN, phosphate and silicate uptake was then transformed to carbon units using the Redfield ratio 106C:16N:15Si:1P (Brzezinski, 1985; Codispoti et al., 2013; Cota et al., 1996; Harrison et al., 1977; Smith et al., 1997) giving annual new production estimates for sea ice and water column during the Arctic productive season. Since the description of new production refers to production based on nitrate, most of the annual new production estimates are based on nitrogen draw-down. Higher than Redfield C:N ratios (7.3-8.3) seem to be common in Arctic phytoplankton and sinking material (Frigstad et al., 2013; Tamelander et al., 2013; Tremblay et al., 2008). Using these ratios would result in a ~10% increase in the estimates, but to be able to compare our results with previous estimates we chose the commonly used Redfield ratio. Silicate can also be used to estimate diatom-based new production (Yool et al., 2007). Both, higher and

lower N:Si ratios have been reported for Arctic diatoms (Simpson et al., 2013; Spilling et al., 2010) depending on the time of the year and the amount of detritus material present. To be consistent with the nitrogen-based estimates, we used Redfield ratios for silicate as well. To calculate an average daily rate, we assumed a productive season of 120 days (Gradinger et al., 1999). This method assumes that lateral input of nutrients from rivers or shelves is negligible which should be the case in the Central Arctic (Le Fouest et al., 2012).

Results

Environmental conditions

Sea ice, melt ponds, and water column environments were sampled in the Eurasian Basin in August and September 2012 at the end of the productive season, including completely and partially ice covered areas above the abyssal basins as well as open waters on the Eurasian shelf. From the eight ice stations sampled, stations 1, 2 and 3 represent the ice margin (Nansen Basin) in early August (Fig.1A); 4, 5 and 6 represent the degraded ice cover (average 1 m thickness) above the continental slope of the Eurasian margin (Fig.1B), and 7 and 8 represent multiyear ice (average 1.8 m thickness) in the Central Arctic (Amundsen Basin) in late September (Fig.1C). In September, a thin snow cover of 0.02 and 0.06 m depth was observed. Melt pond cover varied between 10 and 50%, and from mid-September most of the melt ponds were frozen over (<0.1 m ice thickness). Salinity in the ice (0-4) and the water column (30-34) were in typical ranges for these environments, while steep gradients were found in melt ponds (vertical gradients of 0.4 at the surface to 32 at the bottom), depending if they were open to the seawater below. The daily mean incoming irradiance showed a strong temporal decrease from a 24 h average of 250 μmol photons m^{-2} s^{-1} in early August to 13 μmol photons m^{-2} s^{-1} in late September. In the water column directly below the ice, photosynthetically active radiation (PAR) decreased from 20 μmol photons m^{-2} s^{-1} in early August to 0.2 μmol photons m^{-2} s^{-1} in late September.

Integrated nutrient inventories were very low in all environments in accordance with the time of the year (Table 3). Nutrient distributions in the euphotic zone of the water column were reflected in the N:P and N:Si ratios (Fig.S3) leading to the characterization of three distinct nutrient regimes during the cruise: (1) silicate-depleted ice margin in early August, (2) nitrate-depleted Laptev Sea margin, and (3) all nutrients depleted high Central Arctic (north of 85 ºN) in late September (Fig. 2).

Photosynthesis and irradiance

Despite the high spatial and temporal variability present in our data set, certain patterns emerged when comparing the photosynthetic parameters of sea-ice algae, melt pond phototrophs and water column phytoplankton (Table 2). Sea-ice algae showed the best adaptation to low light (initial slope of the PI curve α) and maximum photosynthetic rates (P^b_m). Photoinhibition (β) was lower in sea-ice algae than in melt pond phototrophs and under-ice phytoplankton, but higher than for phytoplankton in ice-free waters (Table 2). Sea-ice algae were adapted to light intensities between 17 and 100 μmol photons m^{-2} s^{-1}, similar to the under-ice phytoplankton (14-80 μmol photons m^{-2} s^{-1}). These irradiances were generally higher than the average irradiance available under the ice (0.2-20 μmol photons m^{-2} s^{-1}, Table 2). Phytoplankton showed higher photoinhibition below the ice than in ice-free waters. Furthermore, under-ice phytoplankton showed a higher range of light intensities at which photosynthesis is maximal (I_m) than phytoplankton in open waters or at the Chl *a* max. Melt pond phototrophs reached the highest carbon fixation rates (P^b_m), but they also showed the highest photoinhibition rates at high irradiances (Table 2), despite being adapted to higher irradiances (I_k: 30-290 μmol photons m^{-2} s^{-1}) than sea-ice algae and phytoplankton. In general, the light intensity to which the surface communities were adapted (I_k) and the light intensity at which photosynthesis is maximal (I_m) were similar to what they received (I) at the time of sampling.

Net primary production in sea ice, melt ponds and water column

Phytoplankton constituted most of the integrated phototrophic biomass, expressed in Chl *a* units, in all FYI stations (70-98%), while sea-ice algae accounted for 68-86% of the biomass in the two MYI stations (Table 1). MYI contained almost one order of magnitude more Chl *a* than FYI. Melt pond water, excluding algal aggregates located at the bottom (Fernández-Méndez et al. 2014), contributed the least to integrated biomass (0.1-6%). The two melt ponds with the highest Chl *a* values (~0.3 mg m^{-2}) had the highest salinity (18 and 30 respectively).

NPP of the water column was integrated over the depth of the euphotic zone, which varied spatially. In open waters north of Svalbard and the Laptev Sea margin, the euphotic zone depth was 45 m. In the partially ice covered areas of the ice margin it ranged between 24 and 33 m, and below thicker ice, north of 85ºN in late September, it was between 7 and 15 m deep (Fig.S2). Water column integrated NPP (INPP) measured from samples collected with the ship´s CTD varied from 18 to 308 mg C m^{-2} d^{-1} (Average 95±78, n=11) in ice-free waters of the Central Arctic in summer 2012 and from 0.1 to 232 mg C m^{-2} d^{-1} (Average 33±50, n=22) in ice-covered waters (Fig.2). The highest INPP rates occurred at stations close to the shelves at the beginning of August in a water mass that was not yet nutrient depleted (Fig. 2). The area adjacent to the Laptev Sea, which showed nitrate depletion, had INPP rates ~100 mg C m^{-2} d^{-1}. The lowest INPP rates of <1 mg C m^{-2} d^{-1} were measured in nutrient-depleted ice-covered waters north of 85 ºN in late September where PAR below the ice was 0.2-12 μmol photons m^{-2} s^{-1} (Fig. 2).

Total INPP rates including water below the ice, sea ice and melt ponds (0.8-60 mg C m^{-2} d^{-1}, n=8), also showed highest values along the ice edge and lowest in the northernmost stations, decreasing from late summer to early fall (Table S2). INPP in the water under the ice (0.1-60 mg C m^{-2} d^{-1}), sampled with the peristaltic pump from the ice floe, contributed 63-99.5% to total INPP at ice margin stations (Ice stations 1 to 6), while sea ice, in an advanced melting stage, contributed 0.1-33% (0.2-13 mg C m^{-2} d^{-1}; Table S2 and Fig. 3). Melt ponds INPP ranged between 0.01 and 4 mg C m^{-2} d^{-1}, and their contribution to total INPP was highly variable (0.05-34%). They contributed significantly to INPP at stations 3, 7 and 8 (24-34%). Sea-ice algae contributed significantly (50-62%) to total INPP at stations 7 and 8, despite their low total INPP

rates (1.5 and 0.5 mg C m^{-2} d^{-1} respectively), because the water column production was very low (Fig. 3).

Arctic primary production model: CAOPP estimates

Average PI curves were calculated for each environment and were used to calculate NPP as a function of available PAR for the Eurasian Basin of the Arctic Ocean (78–90 ºN, 135º E–45 ºW) using the CAOPP model. We will present here the results calculated with average parameters, but the minimum and maximum values are available in Table 4. The average total INPP for the Eurasian Basin was 54 mg C m^{-2} d^{-1} in August and 34 mg C m^{-2} d^{-1} in September 2012. From the results derived using the CAOPP model, we observed a decreasing temporal trend from August to September, in parallel with a decrease in incoming irradiance (Fig.4). On average, in late summer/early autumn, sea-ice algae contributed 6% to total INPP in the Eurasian Basin, while melt ponds were almost negligible at a basin scale (1%, Fig.S5). Algal aggregates trapped in melt ponds were not taken into account due to their patchiness and difficulty to upscale their contribution to NPP (Fernández-Méndez et al., 2014; Katlein et al., 2014a)(Chapters III and IV). Ice covered waters contributed significantly less (36%) to total NPP per month than open water (57%) north of 78 ºN.

We detected few regional differences between different sectors in the Eurasian Basin north of 78 ºN. In general, in the Laptev, Kara and Barents Sea sectors similar amounts of carbon were fixed per month during the summer season (average of 1.5, 1.7, and 1.2 Tg C during August and September respectively), while in the Greenland Sea sector there was a lower net carbon fixation (0.5 Tg C in August and September), mostly related to the small open water area in this sector (Table 4).

Nutrient addition experiments

For the first nutrient addition experiment, seawater was collected from 25 m depth at ice station 3. It had low nitrate (1.3 μmol L^{-1}), phosphate (0.1 μmol L^{-1}) and silicate (1.2 μmol L^{-1}) concentrations, and a Chl *a* concentration of 1.6 μg L^{-1}. Four days after the addition of 13 μmol L^{-1} NO_3^-, 0.8 μmol L^{-1} PO_4^{3-}, and 10 μmol L^{-1} SiO_4^{3-}, to reach concentrations below the mixed layer, NPP increased in the silica (Si+) treatment and in the positive control with all nutrients (C+) (Fig.5A). POC, PON and Chl *a* only increased significantly when all nutrients were added (Fig.S6A). The increase in NPP corresponded to a carbon yield of 1.3 mg C L^{-1} d^{-1}, matching the POC increase of 1.6 mg C L^{-1} d^{-1} and the increase in PON (0.15 mg N L^{-1} d^{-1}). The C:N ratio in the Si+ and C+ treatments increased from 10 to 14 compared to the other treatments. Silicate uptake increased significantly in the Si+ and C+ treatments (1.7 and 1.9 μmol L^{-1} d^{-1}) compared to the control with no nutrient addition (0.2 μmol L^{-1} d^{-1}, Fig. 5B). This would correspond to a silicate yield of 0.07 mg Si L^{-1} d^{-1}. The organism responsible for the response was the chain forming diatom *Chaetoceros socialis* (Fig.S7A).

The sea ice sampled at station 8 was depleted in nutrients with very low nitrate (0.2 μmol L^{-1}), phosphate (0.1 μmol L^{-1}) and silicate (1 μmol L^{-1}) concentrations. In this case, the addition of nutrients resulted in measurable nutrient uptake, but neither in an increase in biomass nor in NPP (Fig.5C, D and S7B). Nitrate yield in the N+ treatment was 0.019 mg N L^{-1} d^{-1}, twice as much as the PON increase (0.008 mg N L^{-1} d^{-1}), indicating nitrate storage in the cells. The community composition of this sample was formed by typical sea-ice diatoms in a healthy state (with visible green chloroplasts): *Nitzschia sp.*, *Pseudonitzschia sp.*, *Fragilariopsis sp.* and *Entomoneis sp.* (Fig. S6B).

Annual new primary production

The depth of the temperature minimum associated with haline convection during last winter had a mean of 55 m but ranged from 15 to 93 m depth. Stations north of 85 °N showed the deepest convection values. According to the nutrient profiles at the end of the productive season, the

total inorganic nitrogen (NO^-_3+NO^-_2) consumption was 119 ± 46 mmol m^{-2}. Using the Redfield ratio (106C:16N), we estimated the carbon used up for annual new production from nitrogen consumption to be between 0.6 and 17 g C m^{-2} yr^{-1} (Average: 9.4 ± 3.6 g C m^{-2} yr^{-1}, Fig. S8). Assuming a productive season of 120 days, the average NPP rate for the Eurasian Basin was 78 ± 30 mg C m^{-2} d^{-1}, which is in the upper range of our *in situ* measurements in late summer including sea-ice NPP. This value decreases if we increase the length of the productive period. We chose a productive season length of 120 days according to (Gradinger, 2009; Subba Rao et al., 1984). However, due to earlier sea-ice retreat it might be that the productive season in the Central Arctic was longer in 2012. Annual new production is homogenously distributed through the Eurasian basin. Only the most northern stations show higher annual NPP (13-17 g C m^{-2} yr^{-1}), corresponding to a deeper winter haline convection depth (70-80 m) and therefore, a higher integrated depth for nutrient draw-down.

New production based on phosphate drawdown using Redfield gives a similar range (1-16 g C m^{-2} yr^{-1}). Using silicate draw-down in the ratio typical for diatoms (106C:15Si) gives an annual carbon uptake range of 0.01-7 g C m^{-2} yr^{-1} , meaning that around 10-50% of the annual carbon uptake based on nitrate was performed by this group of phytoplankton (Fig. S8). Sea-ice algae sampled in August-September showed an C:Si ratio average of 9. This value is higher than the Redfield C:Si ratio we used to calculate new production based on silicate (7). Using the measured sea ice C:Si ratio, assuming that sea-ice algae are the main consumer of silicate during the growth season, would yield annual carbon uptake values 20-30% higher. However, sea-ice algae probably have a C:Si ratio closer to Redfield during the growing season when new production occurs. Therefore, we assume that both phytoplankton and sea-ice diatoms consume silicate during the growth season, when nutrients are available, at a ratio closer to Redfield. Unfortunately, no particulate biogenic silicate measurements are available for the sub-ice algal aggregates described in Chapters I and III. Since, they seem to play an important role in annual production, future studies should determine their silicate to carbon uptake rates so that they can be taken into account for new production estimates using silicate drawdown.

Discussion

Limitations and uncertainties of Arctic NPP estimates

The Central Arctic remains one of the most challenging environments to sample due to the restricted access to ice-covered waters. The majority of Arctic NPP estimates are from seasonally ice-free waters, mainly shelves, sampled during the spring or summer months (Matrai et al., 2013). Ice-associated NPP has been widely neglected in previous Arctic primary productivity estimates probably due to methodological and logistical problems (Tremblay et al., 2012). Two orders of magnitude uncertainties in NPP estimates for the Central Arctic reflect the high spatial and temporal variability characteristic for this environment (Ferland et al., 2011; Tremblay et al., 2012). Thus it remains difficult to establish regionally representative baselines in Arctic NPP, to be able to detect significant changes in productivity related to the ongoing sea-ice retreat.

This study provides summer *in situ* NPP data from the under-sampled Eurasian Basin north of 70 ºN including water column, sea-ice and melt pond estimates that can be used to validate ocean general circulation models that try to predict changes in Arctic primary production (Popova et al., 2012; Vancoppenolle et al., 2013). Photosynthetic parameters derived from PI curves are a powerful tool to model primary productivity (Behrenfeld and Falkowski, 1997). Most of the Central Arctic is covered by ice during the entire year, making it inaccessible for satellite based primary productivity estimates. Therefore, a combination of *in situ* obtained photosynthetic parameters and a light parameterization for light transmittance of sea-ice (CAOPP model) enabled us to estimate INPP for the entire Eurasian Basin, including ice-covered areas. Although the CAOPP model does not include nutrient information, the PI curves were measured at the end of the season in nutrient limited waters. Therefore, estimates of NPP using the CAOPP model for summer do consider nutrient limitation. However, when using the model for estimations earlier in the season, when more nutrients are available, it might underestimate productivity. In addition, since photosynthetic parameters can be very variable (Manes and Gradinger, 2009; Palmer et al., 2011; Sakshaug and Slagstad, 1991), our calculations are only representative for the phytoplankton and sea-ice algae adapted to late summer light and nutrient conditions in the Eurasian Basin. Another limitation of our upscaling using the CAOPP model is

that the light parameterization assumes a constant extinction coefficient in the water column and is not spectrally resolved (Alver et al., 2014). This could lead to NPP overestimation in open water coastal areas (Arrigo et al., 2011; Bélanger et al., 2012). A recent INPP estimate for the Arctic Ocean Basin including the Amerasian Basin where they measured NPP only in ice-free waters (0.4 Tg C $month^{-1}$ Hill et al., (2013)) is at the lower end of our estimated range for the water under the ice in the Eurasian Basin in August (0.2-6.8 Tg C $month^{-1}$). This indicates that by using an appropriate parameterization of light transfer in and under sea-ice, our summer INPP estimates for the time period when the photosynthetic parameters where obtained, give realistic estimates. Seasonality remains a critical issue in the Central Arctic since there are still no measurements of early spring photosynthetic parameters from communities thriving in and under the ice. Assessing the algal biomass below the ice using Ice Tethered Profiles (ITPs) that drift with the ice during an entire year might be a great step forward to improve our understanding of the annual cycle of primary production in the central basins (Laney et al., 2014).

Light and nutrients as limiting factors

Seasonal light availability in the Central Arctic Ocean drives photosynthesis (Leu et al., 2011; Wassmann and Reigstad, 2011). Our *in situ* measurements and modelling results clearly show the strong effect of sea-ice cover and season on NPP (Fig. 2 and 4). The comparison between ice-free and ice-covered waters of the Eurasian Basin reveals the indirect effect of sea ice through light attenuation, limiting phytoplankton productivity in ice-covered waters. This is noticeable at the end of the productive season (mid-September), north of 87 ºN, below MYI, where the euphotic zone is reduced to the upper 7-15 m (Fig.S2).

Sea-ice algae are adapted to low light but can profit from increased light availability in thin ice in late summer (I_k range from sea-ice and melt ponds 17-290 μmol photons m^{-2} s^{-1}; Table 2). However, lack of snow covering the ice at the beginning of the growth season can also be detrimental for the sea-ice community due to photoinhibition and ice bottom ablation (Juhl and Krembs, 2010; Lund-Hansen et al., 2014; Mundy et al., 2011). In our study, evidence for photoinhibition was only recorded in August on sea-ice algae trapped at the ice surface of melt ponds where the irradiance was maximal (up to 340 μmol photons m^{-2} s^{-1}, Fig. S1). However, the highest irradiance fluxes in 2012 occurred in June (Arndt and Nicolaus, 2014) so the potential for

photoinhibition was higher in the earlier summer months, especially if no snow was covering the ice. Phytoplankton on the contrary showed almost no photoinhibition under irradiances up to 420 μmol photons m^{-2} s^{-1}, allowing them to potentially benefit even more from an increase in irradiance reaching the water column.

Besides constraining the total amount of carbon that can be converted into biomass during the productive season (Codispoti et al., 2013), nutrients also play an important role since they determine algal photoadaptation (Sakshaug and Slagstad, 1991). During our cruise we identified three different nutrient regimes from integrated molar ratios over the euphotic zone at the end of the productive season (Fig. 2). Along the ice margin in the Nansen Basin in August, silicate was the most depleted nutrient with N:Si ratios as high as 3 (Fig.S3), which were also reported in summer 1994 by (Gosselin et al., 1997). This may be due to nitrate input from Atlantic waters (Rudels, 2012), but little is known about upward nutrient mixing rates. In the area adjacent to the Laptev Sea, silicate concentrations were higher, probably due to riverine input (Le Fouest et al., 2012), with N:Si ratios below 1 and N:P ratios (6-8) below Redfield, indicating nitrate depletion. In late September at the northernmost stations, all depth integrated nutrient concentrations were low. This indicates a general nutrient and light depletion typical of the end of the season (Wheeler et al., 1997), partly due to the reduced euphotic zone (7-15 m).

When calculating the annual new production from nutrient drawdown for the Eurasian Basin in 2012, estimates derived from nitrogen and phosphate yield similar results (1-17 g C m^{-2} yr^{-1}), which are in accordance with the latest net community production estimates for this region based on very scarce data (14 g C m^{-2} yr^{-1}, Codispoti et al., 2013). Estimates derived from silicate, using a C:Si ratio of 7 (Brzezinski, 1985; Harrison et al., 1977), yield annual NPP rates half of the estimates derived from nitrogen or phosphate, suggesting that diatom production makes up for about 50% of annual new production, as biogenic silica is the main component of diatom frustules (Martin-Jézéquel et al., 2000). Assuming that sea-ice algae would contribute the most to silicate uptake during the growth season and that they have a higher C:Si ratio (9) as measured at the end of the season, the contribution of diatoms to annual production would increase up to 70%. However, both sea-ice algae and planktonic diatoms typically have Redfield carbon to nutrient ratios during the growing season when nutrients are available, and ratios above Redfield when nutrients are scarce (Harrison et al., 1977). This means that our assumption of a Redfield

ratio for nutrient uptake to estimate new production is probably more realistic than using measured carbon to nutrient ratios measured in the cells at the end of the productive season. The observed N:Si ratios (Fig.S3) suggest that nitrate was limiting NPP in the Amundsen Basin (from the Laptev Sea slope to the North Pole), but silicate was limiting NPP in the Nansen Basin (close to the ice margin in the Kara and Barents sectors) of the Eurasian Basin, that is influenced by Atlantic waters. Thus, diatoms are probably limited in the Eurasian Basin as soon as the first spring bloom has consumed all the silicate in the mixed layer. Indeed, the increase in NPP and biomass of the diatom *Chaetoceros socialis* in a sample from the water below the ice at the ice margin, after silicate addition, supports this idea (Fig. 5A and B). Taking into account the export of sub-ice algae earlier in the season 2012 (Average 9 g C m^{-2}, Boetius et al., 2013) and the average C:Si mass ratio measured in ice algae during the cruise (1.9 w:w), an average of 160 mmol Si m^{-2} had already been removed from surface waters before August. Since sea-ice algal production starts earlier than phytoplankton productivity, sea-ice algae might contribute to nutrient removal in surface waters at the beginning of the season leaving only some nutrients left for the phytoplankton bloom. However, since most of the sea ice in the Central Arctic originates in the shelf areas of the Eurasian Basin and is then transported by the transpolar drift (Pfirman et al., 1997), the sub-ice algae growing attached to the bottom of the ice might have had access to the nutrients mixed up on the shelves, upwelled at the shelf-edge or ice-edge earlier in the season and to the surface nutrients of a wider area while they drift with the ice (Carmack et al., 2006; Syvertsen, 1991).

Besides the bottom-up control of primary production, there are other factors limiting the amount of biomass present in the ice or the water column, such as grazing. Arctic zooplankton and under-ice fauna is known to feed on sea-ice algae and phytoplankton (Ji et al., 2013; Slagstad et al., 2011), transferring the fixed carbon to higher trophic levels. In the Central Arctic grazing has been reported to consume 15% of NPP (Olli et al 2007). At the time of sampling, the theoretical carbon demand of the dominant zooplankton and under-ice grazers (*Calanus spp*. and the ice amphipod *Apherusa glacialis*) was on average 19 mg C m^{-2} d^{-1} in the Eurasian Basin calculated from all stations investigated in this study (David et al., 2014). This would correspond to more than 80 % of the mean daily NPP measured in ice covered areas, indicating that algal biomass could periodically be significantly controlled by grazers in the Central Arctic Ocean, especially at the end of the productive season. However, the POC export fluxes measured in August/September with short-time sediment traps was 31 mg C m^{-2} d^{-1} on average (Lalande et al., 2014), which is

higher than the average NPP measured *in situ* (24 mg C m^{-2} d^{-1}). However, the amount of algal carbon exported in August/September was very low. The carbon flux was mainly composed of debris and the few algae found in the sediment traps were flagellates. According to seafloor observations in 2012 in the same area, the largest amount of algal carbon export had occurred already in June/July in 2012 during the main melting event, and was due to the productivity of sub-ice algal communities (Boetius et al. 2013). These results indicate that at the time of sampling the system was predominantly heterotrophic and that most of the productivity is consumed before sinking in late summer.

Using the CAOPP model and according to the light fluxes calculated by Arndt & Nicolaus (2014), we estimate that 88% of the annual PP occurs between May-July, and only 12% in August and September, using late summer NPP rates and biomass measurements to extrapolate to the earlier part of the season. This model estimate matches very well with our estimates based on *in situ* NPP in August and September and the annual new production estimate based on nitrate drawdown, where we estimate that 15% of the annual PP occurs in late summer and the rest earlier in the season. A more elaborate model taking into consideration seasonal shifts in standing stock and nutrient availability, such as Palmer et al., (2014) would be necessary to improve this estimate and to accurately predict primary productivity under different scenarios, but biological ground truth data for the entire season in the Central Arctic are still needed.

Importance of sea-ice productivity in the Central Arctic

The role of sea-ice algae varies regionally and seasonally in the Arctic Ocean (Dupont, 2012; Legendre et al., 1992). In agreement with previous data by Gosselin et al., (1997) for August 1994, sea-ice algae contributed up to 60% to total NPP in those parts of the Central Arctic covered by MYI at the end of the productive season in 2012. However, our contribution estimate is conservative, since the sub-ice algal aggregates formed by *Melosira arctica* that we observed at all stations can contribute up to 90% of total NPP at a local scale (Fernández-Méndez et al., 2014). Due to their patchy distribution and the difficulties in upscaling their contribution to NPP (Katlein et al., 2014a), they were not included in the sea ice NPP estimates presented in this study.

In areas covered by FYI, sea-ice productivity contributed only 1-30% to total INPP (Fig.S4). MYI has different physical properties than FYI (Lange et al., 2014; Spindler, 1994) and generally hosts higher algal biomass concentration (Werner et al., 2007). In total, MYI and FYI together fixed 0.31 Tg C during August and September 2012, without taking the patchily distributed under-ice and melt-pond algal aggregates into account (Fernández-Méndez et al., 2014). This corresponds to 6 % of the total carbon fixed in the Eurasian Basin north of 78ºN in summer. This estimate is in agreement with annual estimates from a biophysical model where sea-ice primary production contributes 7.5% to total annual PP for the whole Arctic (Dupont, 2012).

However, our sea-ice INPP measurements (0.1-13 mg C m^{-2} d^{-1}) in August and September fell in the lower end of the range of previously reported values (0.5-310 mg C m^{-2} d^{-1}, Gosselin et al., 1997). The higher end of the range in that study (AOS expedition, 1994) refers to sub-ice algal communities formed by sea-ice diatoms like *Melosira arctica*. This sub-ice diatom was also found to comprise much of the total algal biomass during our expedition at station 7, showing an INPP of 13-40 mg C m^{-2} d^{-1}, similar to the AOS expedition estimates (Fernández-Méndez et al., 2014). The rapid sea-ice melt in July/August 2012 lead to a major export of fresh algal biomass to the seafloor of the Arctic basins (Boetius et al. 2013). An estimated PP of 9 g C m^{-2} by filamentous sub-ice algae sedimented during July and August would result in an additional INPP of 16 Tg C if upscaled to the Eurasian Basin north of 78 °N (1.8 x 10^{12} m^2). From our NO^-_2+NO^-_3 annual draw-down, we calculated a total carbon uptake of 17 ± 7 Tg C in the Eurasian Basin north of 78 ºN. Considering that sub-ice algae drift together with the sea ice and have access to constant nutrient replenishment during their drift, the total new production could be 17 + 16= 33 ± 7 Tg C yr^{-1} in the deep basins of the Eurasian Basin. The overall contribution of sea-ice productivity would be 50%. When including sub-ice algal aggregations such as *Melosira arctica* filaments, the average total production of 33 Tg C yr^{-1} in the Central Arctic is higher than previously estimated (22 Tg C yr^{-1}, Codispoti et al., (2013)). Therefore, studies that do not include sea-ice productivity and sub-ice algal aggregations may substantially underestimate annual NPP in the Central Basins.

Melt ponds contributed up to 4% to total INPP, which is in the range of previously reported estimates (<1 to 10%, Arrigo, 2014; Lee et al., 2012). Some melt ponds also contain significant accumulations of algal biomass (Fernández-Méndez et al. 2014), and hence might also become

more important for total Arctic primary production as their coverage continues to increase (Lee et al., 2011; Rösel and Kaleschke, 2012). Some of the sea-ice algae trapped in melt ponds can rapidly adapt to the changing conditions as we observed in their high Chl *a* normalized maximum photosynthetic rates compared to all other environments. Sea-ice algae are low light adapted (Table 2; Cota, 1985) and show lower photoinhibition in late summer (Michel et al., 1988; Mundy et al., 2011). However, in June-July when they receive 90% of the annual light flux (Arndt and Nicolaus, 2014) they are probably able to adapt to higher light conditions and have their peak in production. This would have already been exported to the deep sea when we did our sampling in August-September.

An important question concerns the ability of sea-ice algae to deal with nutrient limitations. Inside the sea-ice and in melt ponds, nutrient concentrations integrated over the ice thickness, were significantly lower than in the water column. N:P molar ratios in sea-ice were in general below Redfield (16:1) indicating prior production by ice algae limited by nitrate (Maestrini et al., 1986; Smith et al., 1997). Very high N:Si ratios (> 3) at some stations point towards silicate limitation as well. Sea-ice diatoms can store nutrients in their cytoplasma (Kamp et al., 2011; Needoba and Harrison, 2004). Our nutrient addition experiment (Fig. 5D) suggests that sea-ice algal communities can take up nutrients without increasing their biomass. This may be another useful physiological advantage for sea-ice algae in the oligotrophic conditions of the Central Arctic.

Effects of sea-ice reduction on primary production in the Central Arctic

An increase in open water NPP due to sea-ice retreat has already been observed by satellite in the Eurasian Arctic (Arrigo and van Dijken, 2011; Vetrov and Romankevich, 2014), especially in the Kara and Barents Seas (Pabi et al., 2008). However, changes in productivity in sea-ice and in the water under the ice cannot be detected by satellites. In September 2012, during our cruise, sea-ice extent reached its minimum ever recorded (Parkinson and Comiso, 2013) and a model study predicted enhanced productivity in the East Siberian and Laptev Seas due to the great summer cyclone (Zhang et al., 2013). By comparing our results with previous estimates from the Eurasian Basin and recent syntheses of all PP data available (Codispoti et al., 2013; Hill et al., 2013; Matrai

et al., 2013), we have tried to assess the impact of sea-ice retreat on NPP. The sea-ice retreat in 2012 in the Eurasian Basin increased the open water area in August-September by 45% compared to earlier years. The NPP rates measured in the open waters of the Laptev region (84 ± 38 mg C m^{-2} d^{-1}) are higher than NPP measurements from the same area in August 1995 when most of the Laptev Sea area was ice covered (21 ± 8 mg C m^{-2} d^{-1}, Grossmann and Gleitz, unpublished measurements from Polarstern expedition ARK XI/1). The average from satellite data from 2003 to 2012 for open waters of this region is also slightly lower than our measurements during the sea-ice record minimum (71 mg C m^{-2} d^{-1} (Vetrov and Romankevich, 2014).

As retreating sea-ice leaves behind more open water areas in summer, different Arctic regions are expected to react differently to the increase in irradiance received (Arrigo et al., 2008). To test this, we removed the ice cover in our forcing input data from our CAOPP model and compared the results from August and September with our 2012 results. Total INPP for the two summer months would increase by 230% in the Greenland sector, 78% in the Barents, 74% in the Laptev and 40% in the Kara sector. However, the loss of ice-attached biomass as sea-ice disappears might counteract the increase in water column primary production. The regional variability of changes is due to different sea-ice coverage of the different areas. However, sea-ice retreat will not only affect light transmission, but also water column stratification that might hinder nutrient upwelling (Carmack et al., 2006; Codispoti et al., 2013). Depending on the future role of winds and sea ice drift vs stratification by freshening and warming, nutrient availability in the euphotic zone could change. Most likely, sea-ice algal productivity might increase (Tedesco et al., 2012) and shift to earlier periods of the year, and their rapid export from the melting of their habitat in July and August will decrease nutrient availability (Boetius et al., 2013; Lalande et al., 2009). The phytoplankton community will probably shift from diatoms towards small picoplankton, especially in the silicate limited area of the Eurasian Basin (Ardyna et al., 2011; Li et al., 2009), with potentially detrimental consequences for the Arctic food web.

Conclusions

The Central Arctic basins have been generally regarded as low productivity areas. Due to their inaccessibility they have remained largely under-sampled leading to a lack of baseline data to assess current changes. This study provides measurements of primary productivity during the record sea-ice minimum in the Eurasian Basin in 2012, and new estimates for all environments where phototrophs thrive: sea-ice, melt ponds and water column. Sea-ice algae can contribute up to 60% to the total INPP in the Central Arctic at the end of the productive season. Comparing our results from 2012 with previous estimates of NPP in the Central Arctic, we conclude that an overall change in NPP magnitude would be foremost related to a change in the role of the ice algal production and export of sub-ice algal aggregates. Melt ponds can contribute up to 34% locally, but at a larger scale their contribution to INPP is <4 %, excluding local aggregations of sea-ice algae. Ice-covered waters sustain lower NPP than open waters in the late summer season, but over the annual productive period, the role of sub-ice algae may be increasing with the overall thinning of sea-ice. Light is still an important limiting factor for NPP in the Central Arctic. Therefore, an increase in irradiance transmitted through the ice will probably lead to an increase in water column NPP in the Central Basins and a shift towards earlier sea-ice based NPP. These shifts in the timing and location of ice algal blooms are likely to impact life cycle strategies and community composition of zooplankton and under-ice fauna, with unknown consequences for the under ice food-web and export fluxes. However, nutrients will still constrain the annual budget of new production both for sea-ice algae and phytoplankton. In the Eurasian Basin, nitrate limits NPP in the Amundsen Basin and silicate limits diatom-based NPP at the ice margin near the Atlantic water inflow (Nansen Basin). Better understanding of the overall development of Arctic productivity will need year-round long-term observations of nutrient supplies and light availability, as well as of mixing processes and grazer populations.

Acknowledgements

We would like to thank the captain and the crew of RV POLARSTERN for their support during the expedition. We thank Gerhard Dieckmann, Victor Smetacek, Philipp Assmy and Catherine Lalande for fruitful discussions. The technical assistance of Christiane Lorenzen, Rafael Stiens and Jölund Asseng is greatly appreciated. Finally, we thank Mathieu Ardyna and Michel Gosselin for sharing all the AOS data. This study was supported by the Alfred-Wegener-Institut Helmholtz-Zentrum für Polar- und Meeresforschung and the Max Planck Society, as well as the ERC Advanced Grant Abyss (no.294757) to AB, and the "Transpolardrift Project" of the BMBF.

References

Alver, M. O., Hancke, K., Sakshaug, E. and Slagstad, D.: A spectrally-resolved light propagation model for aquatic systems: Steps toward parameterizing primary production, J. Mar. Syst., 130, 134–146, doi:10.1016/j.jmarsys.2012.03.007, 2014.

Ardyna, M., Gosselin, M., Michel, C., Poulin, M. and Tremblay, J.-É.: Environmental forcing of phytoplankton community structure and function in the Canadian High Arctic: contrasting oligotrophic and eutrophic regions, Mar. Ecol. Prog. Ser., 442, 37–57, doi:10.3354/meps09378, 2011.

Arndt, S. and Nicolaus, M.: Seasonal cycle of solar energy fluxes through Arctic sea ice, Cryosph. Discuss., 8, 2923–2956, doi:doi:10.5194/tcd-8-2923-2014, 2014.

Arrigo, K. R.: Sea ice ecosystems, Ann. Rev. Mar. Sci., 6, 439–67, doi:10.1146/annurev-marine-010213-135103, 2014.

Arrigo, K. R. and van Dijken, G. L.: Secular trends in Arctic Ocean net primary production, J. Geophys. Res., 116(C09011), 1–15, doi:10.1029/2011JC007151, 2011.

Arrigo, K. R., van Dijken, G. and Pabi, S.: Impact of a shrinking Arctic ice cover on marine primary production, Geophys. Res. Lett., 35(19), L19603, doi:10.1029/2008GL035028, 2008.

Arrigo, K. R., Matrai, P. A. and van Dijken, G. L.: Primary productivity in the Arctic Ocean: Impacts of complex optical properties and subsurface chlorophyll maxima on large-scale estimates, J. Geophys. Res., 116(C11), doi:10.1029/2011JC007273., 2011.

Assmy, P., Ehn, J. K., Fernández-Méndez, M., Hop, H., Katlein, C., Sundfjord, A., Bluhm, K., Daase, M., Engel, A., Fransson, A., Granskog, M. a., Hudson, S. R., Kristiansen, S., Nicolaus, M., Peeken, I., Renner, A. H. H., Spreen, G., Tatarek, A. and Wiktor, J.: Floating ice-algal aggregates below melting arctic sea ice, edited by S. Ban, PLoS One, 8(10), e76599, doi:10.1371/journal.pone.0076599, 2013.

Bakker, K.: Nutrients measured on water bottle samples during POLARSTERN cruise ARK-XXVII/3 (IceArc) in 2012. Unpublished dataset #834081, Texel., 2014.

Behrenfeld, M. J. and Falkowski, P. G.: A consumers guide to phytoplankton primary productivity models, Limnol. Oceanogr., 42(7), 1479–1491, 1997.

Bélanger, S., Babin, M. and Tremblay, J.-É.: Increasing cloudiness in Arctic damps the increase in phytoplankton primary production due to sea ice receding, Biogeosciences Discuss., 9, 13987–14012, doi:10.5194/bgd-9-13987-2012, 2012.

Boetius, A.: The expedition of the research vessel "Polarstern" to the Arctic in 2012 (ARK-XXVII/3) , Berichte zur Polar- und Meeresforschung 663, Bremerhaven. 2013.

Boetius, A., Albrecht, S., Bakker, K., Bienhold, C., Felden, J., Fernández-Méndez, M., Hendricks, S., Katlein, C., Lalande, C., Krumpen, T., Nicolaus, M., Peeken, I., Rabe, B., Rogacheva, A., Rybakova, E., Somavilla, R., Wenzhöfer, F. and Party, R. P. A.-3-S. S.: Export of algal biomass from the melting Arctic sea ice, Science, 339, 1430–1432, doi:10.1126/science.1231346, 2013.

Brzezinski, M. A.: The Si:C:N ratio of marine diatoms: internespecific variability and the effect of some environmental variables, J. Phycol., 21, 347–357, 1985.

Carmack, E., Barber, D., Christensen, J., Macdonald, R., Rudels, B. and Sakshaug, E.: Climate variability and physical forcing of the food webs and the carbon budget on panarctic shelves., Prog. Oceanogr., 71, 145–181, doi:10.1016/j.pocean.2006.10.005, 2006.

Codispoti, L. A., Kelly, V., Thessen, A., Matrai, P., Suttles, S., Hill, V., Steele, M. and Light, B.: Synthesis of primary production in the Arctic Ocean: III. Nitrate and phosphate based estimates of net community production., Prog. Oceanogr., 110, 126–150, doi:10.1016/j.pocean.2012.11.006, 2013.

Cota, G. F.: Photoadaptation of high Arctic ice algae., Nature, 315, 219–222, 1985.

Cota, G. F., Pomeroy, L. R., Harrison, W. G., Jones, E. P., Peters, F., Sheldon, W. M. and Weingartner, T. R.: Nutrients, primary production and microbial heterotrophy in the southeastern Chukchi Sea: Arctic summer nutrient depletion and heterotrophy., Mar. Ecol. Prog. Ser., 135, 247–258, 1996.

David, C., Flores, H., Lange, B. and Rabe, B.: Community structure of under-ice fauna in the Eurasian central Arctic Ocean in relation to environmental properties of sea ice habitats., Mar. Ecol. Prog. Ser., submitt., 2014.

Dee, D., Uppala, S., Simmons, A., Berrisford, P., Poli, P., Kobayashi, S., Andrae, U., Balmaseda, M., Balsamo, G. and Bauer, P.: The ERA - Interim reanalysis: Configuration and performance of the data assimilation system., Quaterly J. R. Meteorol. Soc., 137(656), 553–597, 2011.

Dupont, F.: Impact of sea-ice biology on overall primary production in a biophysical model of the pan-Arctic Ocean, J. Geophys. Res., 117, C00D17, doi:10.1029/2011JC006983, 2012.

Ehn, J. K. and Mundy, C. J.: Assessment of light absorption within highly scattering bottom sea ice from under-ice light measurements: Implications for Arctic ice algae primary production, Limnol. Oceanogr., 58(3), 893–902, doi:10.4319/lo.2013.58.3.0893, 2013.

Ferland, J., Gosselin, M. and Starr, M.: Environmental control of summer primary production in the Hudson Bay system: The role of stratification, J. Mar. Syst., 88(3), 385–400, doi:10.1016/j.jmarsys.2011.03.015, 2011.

Fernández-Méndez, M., Wenzhöfer, F., Peeken, I., Sørensen, H. L., Glud, R. N. and Boetius, A.: Composition, buoyancy regulation and fate of ice algal aggregates in the Central Arctic Ocean, PLoS One, accepted, 2014.

Le Fouest, V., Babin, M. and Tremblay, J.-É.: The fate of riverine nutrients on Arctic shelves, Biogeosciences Discuss., 9(10), 13397–13437, doi:10.5194/bgd-9-13397-2012, 2012.

Frigstad, H., Andersen, T., Bellerby, R. G. J., Silyakova, A. and Hessen, D. O.: Variation in the seston C:N ratio of the Arctic Ocean and pan-Arctic shelves., J. Mar. Syst., doi:10.1016/j.jmarsys.2013.06.004, 2013.

Glud, R. N., Rysgaard, S., Turner, G., McGinnis, D. F. and Leakey, R. J.: Biological and physical induced oxygen dynamics in melting sea-ice of the Fram Strait, Limnol. Oceanogr., 59(4), 1097–1111, doi:10.4319/lo.2014.59.4.1097, 2014.

Gosselin, M., Levasseur, M., Wheeler, P. A., Horner, R. A. and Boothg, B. C.: New measurements of phytoplankton and ice algal production in the Arctic Ocean, Deep Sea Res. Part II, 44(8), 1623–1644, doi:10.1016/S0967-0645(97)00054-4, 1997.

Gradinger, R.: Sea-ice algae: Major contributors to primary production and algal biomass in the Chukchi and Beaufort Seas during May/June 2002, Deep Sea Res. Part II, 56, 1201–1212, doi:10.1016/j.dsr2.2008.10.016, 2009.

Gradinger, R., Friedrich, C. and Spindler, M.: Abundance, biomass and composition of the sea ice biota of the Greenland Sea pack ice., Deep Sea Res. Part IITopical Stud. Oceanogr., 46(6-7), 1457–1472, doi:10.1016/S0967-0645(99)00030-2, 1999.

Haas, C., Lobach, J., Hendricks, S., Rabenstein, L. and Pfaffling, A.: Helicopter-borne measurements of sea ice thickness, using a small and lightweight, digital EM bird, J. Appl. Geophys., 67, 234 – 241, doi:10.1016/j.jappgeo.2008.05.005, 2009.

Hall, P. O. J. and Aller, R. C.: Rapid, small-volume, flow injection analysis for CO_2 and NH_4^+ in marine and freshwaters, Limnol. Oceanogr., 37(5), 1113–1119, 1992.

Harrison, P. J., Conway, H. L., Holmes, R. W. and Davis, C. O.: Marine diatoms grown in chemostats under silicate or ammonium limitation. III. Cellular chemical composition and morphology of *Chaetoceros debilis*, *Skeletonema costatum*, and *Thalassiosira gravida*, Mar. Biol., 43(1), 19–31, doi:10.1007/BF00392568, 1977.

Hendricks, S., Nicolaus, M. and Schwegmann, S.: Sea ice conditions during POLARSTERN cruise ARK-XXVII/3 (IceArc) in 2012., 2012.

Hill, V. J., Matrai, P. A., Olson, E., Suttles, S., Steele, M., Codispoti, L. A. and Zimmerman, R. C.: Synthesis of integrated primary production in the Arctic Ocean: II. *In situ* and remotely sensed estimates, Prog. Oceanogr., 110, 107–125, doi:10.1016/j.pocean.2012.11.005, 2013.

Ji, R., Jin, M., Varpe, Ø., Jil, R. and Varpe, O.: Sea ice phenology and timing of primary production pulses in the Arctic Ocean, Glob. Chang. Biol., 19(3), 734–41, doi:10.1111/gcb.12074, 2013.

Jones, E. P., Anderson, L. G. and Swift, J. H.: Distribution of Atlantic and Pacific waters in the upper Arctic Ocean: Implications for circulation distinguish between oceanic waters of Pacific, Geophys. Res. Lett., 25(6), 765–768, 1998.

Juhl, A. R. and Krembs, C.: Effects of snow removal and algal photoacclimation on growth and export of ice algae., Polar Biol., 33, 1057–1065, 2010.

Kamp, A., de Beer, D., Nitsch, J. L., Lavik, G. and Stief, P.: Diatoms respire nitrate to survive dark and anoxic conditions., Proc. Natl. Acad. Sci. U. S. A., 108(14), 5649–54, doi:10.1073/pnas.1015744108, 2011.

Katlein, C., Fernández-Méndez, M., Wenzhöfer, F. and Nicolaus, M.: Distribution of algal aggregates under summer sea ice in the Central Arctic, Polar Biol., submitted, 2014a.

Katlein, C., Nicolaus, M. and Petrich, C.: The anisotropic scattering coefficient of sea ice, J. Geophys. Res., 119(2), 842–855, doi:10.1002/2013JC009502, 2014b.

Korhonen, M., Rudels, B., Marnela, M., Wisotzki, A. and Zhao, J.: Time and space variability of freshwater content, heat content and seasonal ice melt in the Arctic Ocean from 1991 to 2011, Ocean Sci., 9(6), 1015–1055, doi:10.5194/os-9-1015-2013, 2013.

Kramer, M. and Kiko, R.: Brackish meltponds on Arctic sea ice — a new habitat for marine metazoans, Polar Biol., 34, 603–608, doi:10.1007/s00300-010-0911-z, 2011.

Lalande, C., Bauerfeind, E., Nöthig, E.-M. and Beszczynska-Möller, A.: Impact of a warm anomaly on export fluxes of biogenic matter in the eastern Fram Strait, Prog. Oceanogr., 109, 70–77, doi:10.1016/j.pocean.2012.09.006, 2013.

Lalande, C., Bélanger, S. and Fortier, L.: Impact of a decreasing sea ice cover on the vertical export of particulate organic carbon in the northern Laptev Sea, Siberian Arctic Ocean, Geophys. Res. Lett., 36(21), L21604, doi:10.1029/2009GL040570, 2009.

Lalande, C., Nöthig, E.-M., Somavilla, R., Bauerfeind, E., Schevschenko, V., Okolodkov, Y. and Shevshenko, V.: Variability in under-ice export fluxes of biogenic matter in the Arctic Ocean, Global Biogeochem. Cycles, 28, doi:10.1002/2013GB004735, 2014.

Laney, S. R., Krishfield, R. a., Toole, J. M., Hammar, T. R., Ashjian, C. J. and Timmermans, M.-L.: Assessing algal biomass and bio-optical distributions in perennially ice-covered polar ocean ecosystems, Polar Sci., 8(2), 73–85, doi:10.1016/j.polar.2013.12.003, 2014.

Lange, B., Beckers, J., Alec, C., Flores, H., Meisterhans, G., Niemi, A., Haas, C. and Michel, C.: Comparison of biogeochemical and physical properties of multi-year and first-year sea ice in the Lincoln Sea., J. Geophys. Res., in press., 2014.

Laxon, S. W., Giles, K. A., Ridout, A. L., Wingham, D. J., Willatt, R., Cullen, R., Kwok, R., Schweiger, A., Zhang, J., Haas, C., Hendricks, S., Krish, R., Kurtz, N., Farrell, S. and Davidson, M.: CryoSat-2 estimates of Arctic sea ice thickness and volume, Geophys. Res. Lett., 40, 1–6, doi:10.1002/GRL.50193, 2013.

Lee, S. H., McRoy, C. P. P., Joo, H. M., Gradinger, R., Cui, X., Yun, M. S., Chung, K. H., Choy, E. J., Son, S., Carmack, E. and Whitledge, T. E. TE: Holes in progressively thinning Arctic sea ice lead to new ice algae habitat, Oceanography, 24(3), 302–308, doi:10.5670/oceanog.2011.81, 2011.

Lee, S. H., Stockwell, D. A., Joo, H., Son, Y. B., Kang, C. and Whitledge, T. E.: Phytoplankton production from melting ponds on Arctic sea ice, J. Geophys. Res., 117(C04030), 1–11, doi:10.1029/2011JC007717, 2012.

Legendre, L., Horner, R., Ackley, S. F., Dieckmann, G. S., Gulliksen, B., Hoshiai, T., Melnikov, I. A., Reeburgh, W. S., Spindler, M. and Sullivan, C. W.: Ecology of sea ice biota: 2. Global significance, Polar Biol., 12, 429 – 444, doi:10.1007/BF00243113, 1992.

Leu, E., Søreide, J. E. E., Hessen, D. O. O., Falk-Petersen, S. and Berge, J.: Consequences of changing sea-ice cover for primary and secondary producers in the European Arctic shelf seas: Timing, quantity, and quality., Prog. Oceanogr., 90(1-4), 18–32, doi:10.1016/j.pocean.2011.02.004, 2011.

Leu, E., Wiktor, J., Søreide, J., Berge, J. and Falk-Petersen, S.: Increased irradiance reduces food quality of sea ice algae, Mar. Ecol. Prog. Ser., 411, 49–60, doi:10.3354/meps08647, 2010.

Li, W. K. W., McLaughlin, F. A., Lovejoy, C. and Carmack, E. C.: Smallest algae thrive as the Arctic Ocean freshens., Science, 326, 539, doi:10.1126/science.1179798, 2009.

Lund-Hansen, L. C., Hawes, I., Sorrell, B. K. and Nielsen, M. H.: Removal of snow cover inhibits spring growth of Arctic ice algae through physiological and behavioral effects., Polar Biol., 37, 471–481, 2014.

Maestrini, S. Y., Rochet, M., Legendre, L. and Demers, S.: Nutrient limitation of the bottom-ice microalgal biomass (Southeastern Hudson Bay, Canadian Arctic), Limnol. Oceanogr., 31(5), 969–982, 1986.

Manes, S. S. and Gradinger, R.: Small scale vertical gradients of Arctic ice algal photophysiological properties., Photosynth. Res., 102, 53–66, doi:10.1007/s11120-009-9489-0, 2009.

Martin, J., Tremblay, J.-É. and Price, N. M.: Nutritive and photosynthetic ecology of subsurface chlorophyll maxima in the Canadian Arctic waters, Biogeosciences Discuss., 9, 6445–6488, doi:10.5194/bgd-9-6445-2012, 2012.

Martin-Jézéquel, V., Copernic, P. N., Plouzane, F.-, Brzezinski, M. A. and Hildebrant, M.: Silicon metabolism in diatoms implications for growth, J. Phycol., 36, 821–840, 2000.

Maslanik, J. A., Fowler, C., Stroeve, J., Drobot, S., Zwally, J., Yi, D. and Emery, W.: A younger, thinner Arctic ice cover: increased potential for rapid, extensive sea-ice loss, Geophys. Res. Lett., 34, L24501, doi:10.1029/2007GL032043, 2007.

Matrai, P., Olson, E., Suttles, S., Hill, V. J., Codispoti, L. A., Light, B., Steele, M., Boothbay, E., Hole, W. and Sciences, A.: Synthesis of primary production in the Arctic Ocean: I . Surface waters, Prog. Oceanogr., 110, 93–106, doi:10.1016/j.pocean.2012.11.004, 2013.

Michel, C., Legendre, L., Demers, S. and Therriault, J.-C.: Photoadaptation of sea-ice microalgae in springtime: photosynthesis and carboxylating enzymes, Mar. Ecol. Prog. Ser., 50, 177–185, 1988.

Mikkelsen, D. M., Rysgaard, S. and Glud, R. N.: Microalgal composition and primary production in Arctic sea ice: a seasonal study from Kobbefjord (Kangerluarsunnguaq), West Greenland, Mar. Ecol. Prog. Ser., 368, 65–74, doi:10.3354/meps07627, 2008.

Mundy, C., Michel, G., Jens, K. E., Claude, B., Poulin, M., Alou, E., Roy, S., Hop, H., Lessard, S., Papakyriakou, T. N., Barber, D. G. and Stewart, J.: Characteristics of two distinct high-light acclimated algal communities during advanced stages of sea ice melt, Polar Biol., 34, 1869–1886, doi:10.1007/s00300-011-0998-x, 2011.

National Snow and Ice Data Center (NSIDC): Report 2012. http://nsidc.org/arcticseaicenews/, 2012.

Needoba, J. a. and Harrison, P. J.: Influence of Low Light and a Light: Dark Cycle on NO3 Uptake, Intracellular NO3 , and Nitrogen Isotope Fractionation By Marine Phytoplankton, J. Phycol., 40(3), 505–516, doi:10.1111/j.1529-8817.2004.03171.x, 2004.

Nicolaus, M., Katlein, C., Maslanik, J. and Hendricks, S.: Changes in Arctic sea ice result in increasing light transmittance and absorption, Geophys. Res. Lett., 39(L24501), 1–6, doi:10.1029/2012GL053738, 2012.

Olli, K., Wassmann, P., Reigstad, M., Ratkova, T. N., Arashkevich, E., Pasternak, A., Matrai, P. a., Knulst, J., Tranvik, L., Klais, R. and Jacobsen, A.: The fate of production in the central Arctic Ocean – top–down regulation by zooplankton expatriates?, Prog. Oceanogr., 72, 84–113, doi:10.1016/j.pocean.2006.08.002, 2007.

Pabi, S., van Dijken, G. L. and Arrigo, K. R.: Primary production in the Arctic Ocean, 1998–2006, J. Geophys. Res., 113(C8), C08005, doi:10.1029/2007JC004578, 2008.

Palmer, M. A., Arrigo, K. R., Ehn, J. K., Mundy, C. J., Gosselin, M., Barber, D. G., Martin, J., Alou, E., Roy, S. and Tremblay, J.-É.: Spatial and temporal variation of photosynthetic parameters in natural phytoplankton assemblages in the Beaufort Sea , Canadian Arctic, Polar Biol., 34, 1915–1928, doi:10.1007/s00300-011-1050-x, 2011.

Palmer, M. A., Saenz, B. T. and Arrigo, K. R.: Impacts of sea ice retreat, thinning, and melt-pond proliferation on the summer phytoplankton bloom in the Chukchi Sea, Arctic Ocean, Deep Sea Res. Part II Top. Stud. Oceanogr., 1–20, doi:10.1016/j.dsr2.2014.03.016, 2014.

Parkinson, C. L. and Comiso, J. C.: On the 2012 record low Arctic sea ice cover: Combined impact of preconditioning and an August storm, Geophys. Res. Lett., 40, 1356–1361, doi:10.1002/grl.50349, 2013.

Parsons, T. R., Maita, Y. and Lalli, C. .: A Manual of chemical and biological methods for seawater analysis, Pergamon Press, Toronto., 1984.

Perovich, D. K.: The optical properties of sea ice, Cold Reg. Res. Eng. Lab., Monograph , 1–31, 1996.

Pfirman, S. L., Colony, R., Niirnberg, D., Eicken, H. and Rigor, I.: Reconstructing the origin and trajectory of drifting Arctic sea ice., J. Geophys. Res., 102(c6), 575–586, 1997.

Platt, T., Gallegos, C. L. and Harrison, W. G.: Photoinhibition of photosynthesis in natural assemblages of marine phytoplankton., J. Mar. Res., 38, 687–701, 1980.

Platt, T., Harrison, W. G., Irwin, B., Horne, E. P. and Gallegos, C. L.: Photosynthesis and photoadaptation of marine phytoplankton in the Arctic, Deep Sea Res., 29(10), 1159–1170, doi:10.1016/0198-0149(82)90087-5, 1982.

Popova, E. E., Yool, A., Coward, A. C., Aksenov, Y. K., Alderson, S. G., de Cuevas, B. a. and Anderson, T. R.: Control of primary production in the Arctic by nutrients and light: insights from a high resolution ocean general circulation model, Biogeosciences Discuss., 7(4), 5557–5620, doi:10.5194/bgd-7-5557-2010, 2010.

Popova, E. E., Yool, A., Coward, A. C., Dupont, F., Deal, C., Elliott, S., Hunke, E., Jin, M., Steele, M. and Zhang, J.: What controls primary production in the Arctic Ocean? Results from an intercomparison of five general circulation models with biogeochemistry, J. Geophys. Res., 117(C00D12), 1–16, doi:10.1029/2011JC007112, 2012.

Rabe, B., Wisotzki, A., Rettig, S., Somavilla Cabrillo, R. and Sander, H.: Physical oceanography measured on water bottle samples during POLARSTERN cruise ARK-XXVII/3., Bremerhaven., 2012.

Reiniger, R. F., Ross, C. K. and Rosst, C. K.: A method of interpolation with application to oceanographic data, Deep Sea Res., 15, 185–193, 1968.

Rösel, A. and Kaleschke, L.: Exceptional melt pond occurrence in the years 2007 and 2011 on the Arctic sea ice revealed from MODIS satellite data, J. Geophys. Res., 117(C05018), 1–8, doi:10.1029/2011JC007869, 2012.

Rozanska, M., Gosselin, M., Poulin, M., Wiktor, J. and Michel, C.: Influence of environmental factors on the development of bottom ice protist communities during the winter–spring transition., Mar. Ecol. Prog. Ser., 386, 43–59, doi:10.3354/meps08092, 2009.

Rudels, B.: The thermohaline circulation of the Arctic Ocean and the Greenland Sea, Philos. Trans. Phys. Sci. Eng., 352(1699), 287–299, 1995.

Rudels, B.: Arctic Ocean circulation and variability – advection and external forcing encounter constraints and local processes, Ocean Sci., 8, 261–286, doi:10.5194/os-8-261-2012, 2012.

Sakshaug, E. and Slagstad, D.: Light and productivity of phytoplankton in polar marine ecosystems: a physiological view, in Proceedings of the Pro Mare Symposium on Polar Marine Ecology, vol. 1906, edited by E. Sakshaug, C. Hopkins, and N. Oritsland, pp. 69–85, PolarResearch, Trondheim., 1991.

Sakshaug, E., Stein, R. and Macdonald, R. W.: Primary and secondary production in the Arctic Seas., in The Organic Carbon Cycle in the Arctic Ocean, edited by R. Stein and R. W. Macdonald, pp. 57–82, Springer., 2004.

Sherr, E. B., Sherr, B. F., Wheeler, P. A. and Thompson, K.: Temporal and spatial variation in stocks of autotrophic and heterotrophic microbes in the upper water column of the central Arctic Ocean, Deep Sea Res. Part I Oceanogr. Res. Pap., 50, 557–571, doi:10.1016/S0967-0637(03)00031-1, 2003.

Simpson, K. G., Tremblay, J.-É. and Price, N. M.: Nutrient dynamics in the western Canadian Arctic. I. New production in spring inferred from nutrient draw-down in the Cape Bathurst Polynya, Mar. Ecol. Prog. Ser., 484, 33–45, doi:10.3354/meps10275, 2013.

Slagstad, D., Ellingsen, I. H. H. and Wassmann, P.: Evaluating primary and secondary production in an Arctic Ocean void of summer sea ice: an experimental simulation approach, Prog. Oceanogr., 90(1-4), 117–131, doi:10.1016/j.pocean.2011.02.009, 2011.

Smith, R. E. H., Gosselin, M. and Taguchi, S.: The influence of major inorganic nutrients on the growth and physiology of high arctic ice algae, J. Mar. Syst., 11, 63–70, 1997.

Spilling, K., Tamminen, T., Andersen, T. and Kremp, A.: Nutrient kinetics modeled from time series of substrate depletion and growth: dissolved silicate uptake of Baltic Sea spring diatoms, Mar. Biol., 157(2), 427–436, doi:10.1007/s00227-009-1329-4, 2010.

Spindler, M.: Notes on the biology of sea ice in the Arctic and Antarctic, Polar Biol., 14(5), 319–324, doi:10.1007/BF00238447, 1994.

Steemann Nielsen, E.: The use of radio-active carbon (C^{14}) for measuring organic production in the sea ., J. Cons. Int. Explor. Mer., 18, 117–140, 1952.

Stroeve, J. C., Serreze, M. C., Holland, M. M., Kay, J. E., Malanik, J. and Barrett, A. P.: The Arctic's rapidly shrinking sea ice cover: a research synthesis, Clim. Change, 110, 1005–1027, doi:10.1007/s10584-011-0101-1, 2012.

Subba Rao, D. V., Platt, T., Rao, D. V. S. and Bay, B.: Primary production of Arctic waters, Polar Biol., 3, 191–201, 1984.

Syvertsen, E. E.: Ice algae in the Barents Sea: types of assemblages, origin, fate and role in the ice-edge phytoplankton bloom, Proc. Pro Mare Symp. Polar Mar. Ecol., (1961), 277–287, 1991.

Tamelander, T., Reigstad, M., Olli, K., Slagstad, D. and Wassmann, P.: New production regulates export stoichiometry in the ocean., PLoS One, 8(1), e54027, doi:10.1371/journal.pone.0054027, 2013.

Tedesco, L., Vichi, M. and Thomas, D. N.: Process studies on the ecological coupling between sea ice algae and phytoplankton, Ecol. Modell., 226, 120–138, doi:10.1016/j.ecolmodel.2011.11.011, 2012.

Thomas, D. N. and Dieckmann, G. S.: Sea Ice, Second., edited by D. N. Thomas and G. S. Dieckmann, Wiley-Blackwell, West Sussex., 2010.

Tran, S., Bonsang, B., Gros, V., Peeken, I., Sarda-Esteve, R., Berhardt, A. and Belvisio, S.: A survey of carbon monoxide and non-methane hydrocarbons in the Arctic Ocean during summer 2010, Biogeosciences, 10, 1909–1935, doi:10.5194/bg-10-1909-2013, 2013.

Tremblay, J.-É. and Gagnon, J.: The effects of irradiance and nutrient supply on the productivity of Arctic waters: a perspective on climate change, in Influence of Climate Change on the

Changing Arctic and Sub-Arctic Conditions, edited by J. Nihoul and A. Kostianoy, pp. 73–93, Springer Science + Business Media B.V., 2009.

Tremblay, J.-É., Robert, D., Varela, D. E., Lovejoy, C., Darnis, G., Nelson, R. J. and Sastri, A. R.: Current state and changing trends in Canadian arctic marine ecosystems : I . Primary production, Clim. Change, 115, 161–178, 2012.

Tremblay, J.-É., Simpson, K., Martin, J., Miller, L., Gratton, Y., Barber, D. and Price, N. M.: Vertical stability and the annual dynamics of nutrients and chlorophyll fluorescence in the coastal, southeast Beaufort Sea, J. Geophys. Res., 113(C7), C07S90, doi:10.1029/2007JC004547, 2008.

Vancoppenolle, M., Bopp, L., Madec, G., Dunne, J., Ilyina, T., Halloran, P. R. and Steiner, N.: Future Arctic Ocean primary productivity from CMIP5 simulations: Uncertain outcome, but consistent mechanisms, Global Biogeochem. Cycles, 27, 1–15, doi:10.1002/gbc.20055, 2013.

Vetrov, A. A. and Romankevich, E. A.: Primary production and fluxes of organic carbon to the seabed in the Eurasian Arctic seas, 2003–2012, Dokl. Earth Sci., 454(1), 44–46, doi:10.1134/S1028334X14010073, 2014.

Wassmann, P. and Reigstad, M.: Future Arctic Ocean seasonal ice zones and implications for pelagic-benthic coupling., Oceanography, 24(3), 220–231, 2011.

Werner, I., Ikävalko, J. and Schünemann, H.: Sea-ice algae in Arctic pack ice during late winter, Polar Biol., 30(11), 1493–1504, doi:10.1007/s00300-007-0310-2, 2007.

Wheeler, P. A., Gosselin, M., Sherr, E., Thibault, D., Kirchman, D. L., Benner, R. and Whitledge, T. E.: Active cycling or organic carbon in the central Arctic Ocean, Nature, 380, 697–699, doi:10.1038/380697a0, 1996.

Wheeler, P. A., Watkins, J. M. and Hansing, R. L.: Nutrients , organic carbon and organic nitrogen in the upper water column of the Arctic Ocean : implications for the sources of dissolved organic carbon, Deep Sea Res. Part II, 44(8), 1571–1592, 1997.

Yager, P. L., Connelly, T. L., Mortazavi, B., Wommack, K. E., Bauer, J. E., Opsahl, S. and Hollibaugh, J. T.: Dynamic bacterial and viral response to an algal bloom at subzero temperatures., Limnol. Oceanogr., 46(4), 790–801, 2011.

Yool, A., Martin, A. P., Fernández, C. and Clark, D. R.: The significance of nitrification for oceanic new production., Nature, 447(7147), 999–1002, doi:10.1038/nature05885, 2007.

Zhang, J., Ashjian, C., Campbell, R., Hill, V., Spitz, Y. H. and Steele, M.: The great 2012 Arctic Ocean summer cyclone enhanced biological productivity on the shelves, J. Geophys. Res. Ocean., doi:10.1002/2013JC009301, 2013.

Table 1. Physical parameters and autotrophic biomass of the eight ice stations sampled during the expedition ARKXXVII/3 to the Eurasian basin of the Central Arctic during August-September 2012.

Station Number	1	2	3	4	5	6	7	8
Station ID	PS80/3_224	PS80/3_237	PS80/3_255	PS80/3_277	PS80/3_323	PS80/3_335	PS80/3_349	PS80/3_360
Date (dd/mm/yyyy)	09/08/2012	14/08/2012	20/08/2012	25/08/2012	04/09/2012	07/09/2012	18/09/2012	22/09/2012
Latitude	84° 3.03' N	83° 59.19' N	82° 40.24' N	82° 52.95' N	81° 55.53' N	85° 6.11' N	87° 56.01' N	88° 49.66' N
Longitude	31° 6.83' E	78° 6.20' E	109° 35.37' E	130° 7.77' E	131° 7.72' E	122° 14.72' E	61° 13.04' E	58° 51.81' E
Incoming PAR (µmol photons m^{-2} s^{-1})	249 ± 90	174 ± 90	104 ± 71	101 ± 57	81 ± 63	49 ± 43	25 ± 15	13 ± 7
Ice cover	80%	80%	70%	80%	60%	50%	100%	100%
Ice thickness (m)	1.2	1.2	0.9	0.9	0.8	1.4	1.9	1.8
Ice type (FYI/MYI)	FYI	FYI	FYI	FYI	FYI	FYI	MYI	MYI
Melt Pond coverage (%)	40%	20%	40%	50%	10%	30%	20%	20%
Melt Pond depth (m)	0.6	0.2	0.3	0.4	0.3	0.2	0.3	0.3
Melt Pond Salinity	18	1	0.5	2	14	0.4	30	12
Euphotic zone depth (m)	24	29	30	29	33	29	15	7
Euphotic zone Chl *a* (mg m^{-2})	3.2	17	8	8	11	17	3	1.2
Sea ice Chl *a* (mg m^{-2})	1.2	1.7	0.6	0.4	0.3	0.4	8	8
Melt ponds Chl *a* (mg m^{-2})	0.3	0.02	0.1	0.02	0.1	0.02	0.3	0.04

Ice was classified in two types: first year (FYI) and multiyear (MYI) according to its structure and physical properties.

The euphotic zone depth is a weighted average of the euphotic zone depth below bare ice, ponded ice and open water at each station.

Chlorophyll a (Chl *a*) was integrated for the melt pond depth, the sea ice thickness and the euphotic zone depth. A C:Chl *a* conversion factor of ~600could be applied to obtain carbon units.

Table 2. Photosynthetic parameters and incoming irradiance of the different environments in the Central Arctic.

	Photosynthetic parameters						
	P^b	P^b_m	α	β	I_m	I_k	I
Environment (n PI curves)	(mg C (mg Chl *a*)$^{-1}$ h^{-1})		(mg C (mg Chl *a*)$^{-1}$ (µmol photons m^{-2} s^{-1})$^{-1}$ h^{-1})		(µmol photons m^{-2} s^{-1})		(µmol photons m^{-2} s^{-1})
	Median (Min-Max)						
Melt Pond (n=8)	34 (1.4-6670)	1.4 (0.4-8)	0.02 (0.002-0.15)	0.04 (0.001-50)	210 (135-785)	73 (30-290)	87 (12-340)
Sea Ice (n=20)	0.1 (0.04-380)	0.1 (0.04-0.7)	0.003 (0.001-0.01)	0 (0-2.3)	170 (96-876)	52 (17-98)	25 (1-220)
Water under the ice (n=8)	0.6 (0.2-1160)	0.4 (0.2-1.4)	0.015 (0.003-0.02)	0 (0-7.3)	200 (102-787)	35 (14-80)	2 (0.2-20)
Open water (n=7)	0.5 (0.4-0.9)	0.5 (0.3-0.9)	0.03 (0.02-0.05)	0 (0-0.001)	85 (59-734)	15 (9-26)	16 (1.3-240)

P_b is the maximum Chl *a* normalized carbon fixation rate if there was no photoinhibition; α is the initial slope of the saturation curve; β is the photoinhibition parameter; P^b_m is the carbon fixation rate at maximal irradiance; I_m is the light intensity at which photosynthesis is maximal; I_k is the adaptation parameter or photoacclimation index. I is the average daily irradiance received in each environment from the surface to the bottom of the pond, the ice or the euphotic zone in the water column.

* Open waters correspond to the Laptev Sea region.

Table 3. Nutrient inventories and molar ratios in each environment during summer 2012.

	Nutrients				
	Nitrate	Phosphate	Silicate	N:P	N:Si
		(mmol m^{-2})			mol:mol
Melt Pond	0.06-0.81	0-0.15	0.1-0.54	1-114	0.2-8
Sea Ice	0.16-1.67	0.01-1.3	0.01-1.66	0.6-16	0.6-16
Water under the ice	4-155	1.5-14	12-144	1.4-11	0.1-2.8
Open water	37-157	9.6-19	43-219	3.7-10	0.2-2

Nutrient concentrations in mol L^{-1} are available in PANGAEA (doi in Table S1). Nutrient concentrations were integrated for melt pond depth, sea-ice thickness and water column euphotic zone (1% incoming PAR).

Table 4. Integrated Net Primary Production in the Central Arctic at different times and spatial scales. The number of daily measurements is given in Table 2. The values per sector include water, sea-ice and melt-pond productivity. Algal aggregates are not included.

	Integrated Net Primary Production (INPP)					
	Daily			Monthly		Annual
	In situ		August	September		2012
	Mean ± STDEV		Mean (Min-Max)			Mean ± STDEV
INPP in the Eurasian Basin	mg C m^{-2} d^{-1}		mg C m^{-2} d^{-1}			g C m^{-2} yr^{-1}
Total	24± 19	54	(21-180)	34	(21-65)	9.4 ± 3.6
Sea Ice	2.2 ± 4.1	5.8	(0.06-42)	2.6	(0.02-20)	
Melt Ponds	0.9 ± 1.3	0.5	(0.2-1.7)	0.7	(0.06-3)	
Water under the ice	20 ± 20	31	(4.5-116)	12	(3-50)	
Open water	84± 38	97	(62-115)	56	(43-50)	
	Mean*Area		Sum			Sum
INPP in the Central Arctic (78° N)	Tg C d^{-1}		Tg C $month^{-1}$			Tg C yr^{-1}
Total	0.09 ± 0.07	5.7	(1.7-24)	3.4	(1.78-8.45)	36
INPP in the Eurasian Basin	Tg C d^{-1}		Tg C $month^{-1}$			Tg C yr^{-1}
Total	0.04 ± 0.03	3.1	(1.2-10)	1.9	(1.1-3.6)	17.4±6.7
Sea Ice	0.004 ± 0.007	0.2	(0.002-1.7)	0.08	(0.0008-0.6)	
FYI	0.004 ± 0.009	0.05	(0.002-0.4)	0.008	(0.0004-0.06)	
MYI	0.002 ± 0.001	0.2	(0.0003-1.2)	0.07	(0.0002-0.5)	
Melt Ponds	0.002 ± 0.002	0.02	(0.007-0.07)	0.02	(0.002-0.09)	
Water under the ice	0.04 ± 0.04	1.3	(0.2-6.8)	0.4	(0.1-1.6)	
Open water	0.16 ± 0.071	1.5	(1-1.8)	1.4	(1-1.3)	
INPP per sector	Tg C d^{-1}		Tg C $month^{-1}$			Tg C yr^{-1}
Laptev (78-90N, 90-135 E)	0.015 ± 0.011	0.9	(0.3-3.5)	0.6	(0.4-1.2)	4.7±1.7
Kara (78-90 N, 45-90 E)	0.006 ± 0.007	1.1	(0.6-2.4)	0.7	(0.5-0.8)	5.5±2.0
Barents (78-90N, 0-45 E)	0.019	0.77	(0.3-2.4)	0.5	(0.3-0.8)	4.7±1.9
Greenland (78-90 N, 45W-0E)	n.d.	0.34	(0.02-2.1)	0.1	(0.01-0.8)	n.d.

Figure 1. Cruise track and stations sampled in the Eurasian Basin during summer 2012. The different panels show the sea ice concentration at the time of sampling the first ice station in early August (A), the fifth station at the beginning of September (B), and the last ice station in early autumn (C). The sea ice extent minimum record was reached in early September 2012 and refreezing started two weeks later.

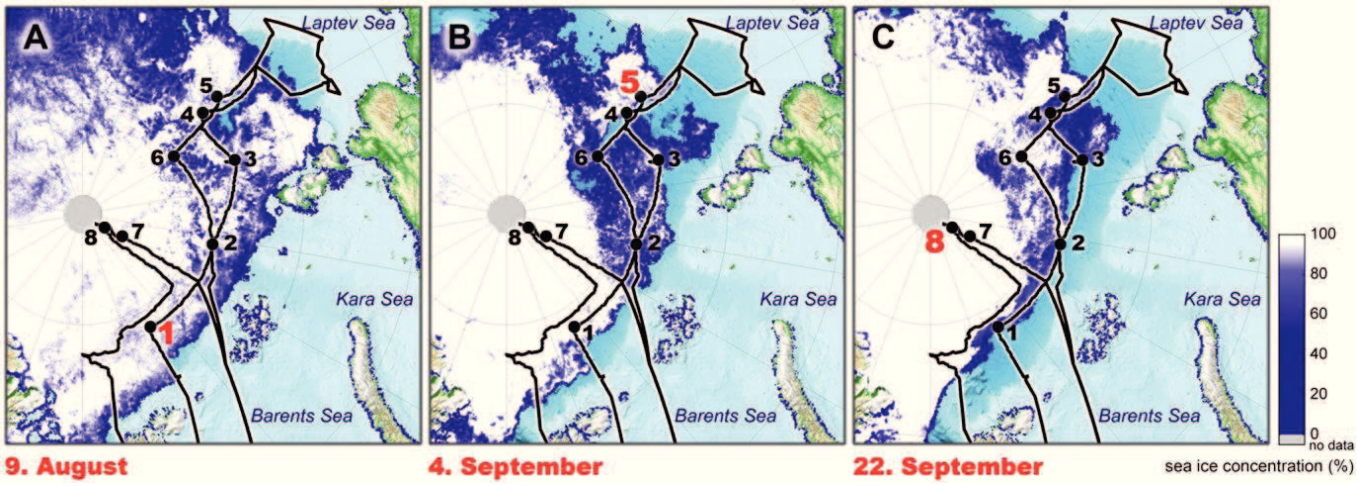

Figure 2. Integrated Net Primary Productivity (INPP) in the water column of the Central Arctic Eurasian Basin in August-September 2012. The three boxes indicate different nutrient regimes characterized by the concentrations of nitrate (N), phosphate (P), and silicate (Si) in the water column. The superscripts on each nutrient indicate if there was high (+), medium (~) or low (-) amounts of that nutrient in the euphotic zone. High is defined as concentrations of nitrate >3 μmol L^{-1} nitrate, phosphate >0.3 μmol L^{-1}, and silicate >3 μM. Low or depleted is defined as concentrations of nitrate < 1 μmol L^{-1}, phosphate < 0.2 μmol L^{-1}, and silicate < 1.5 μmol L^{-1}.

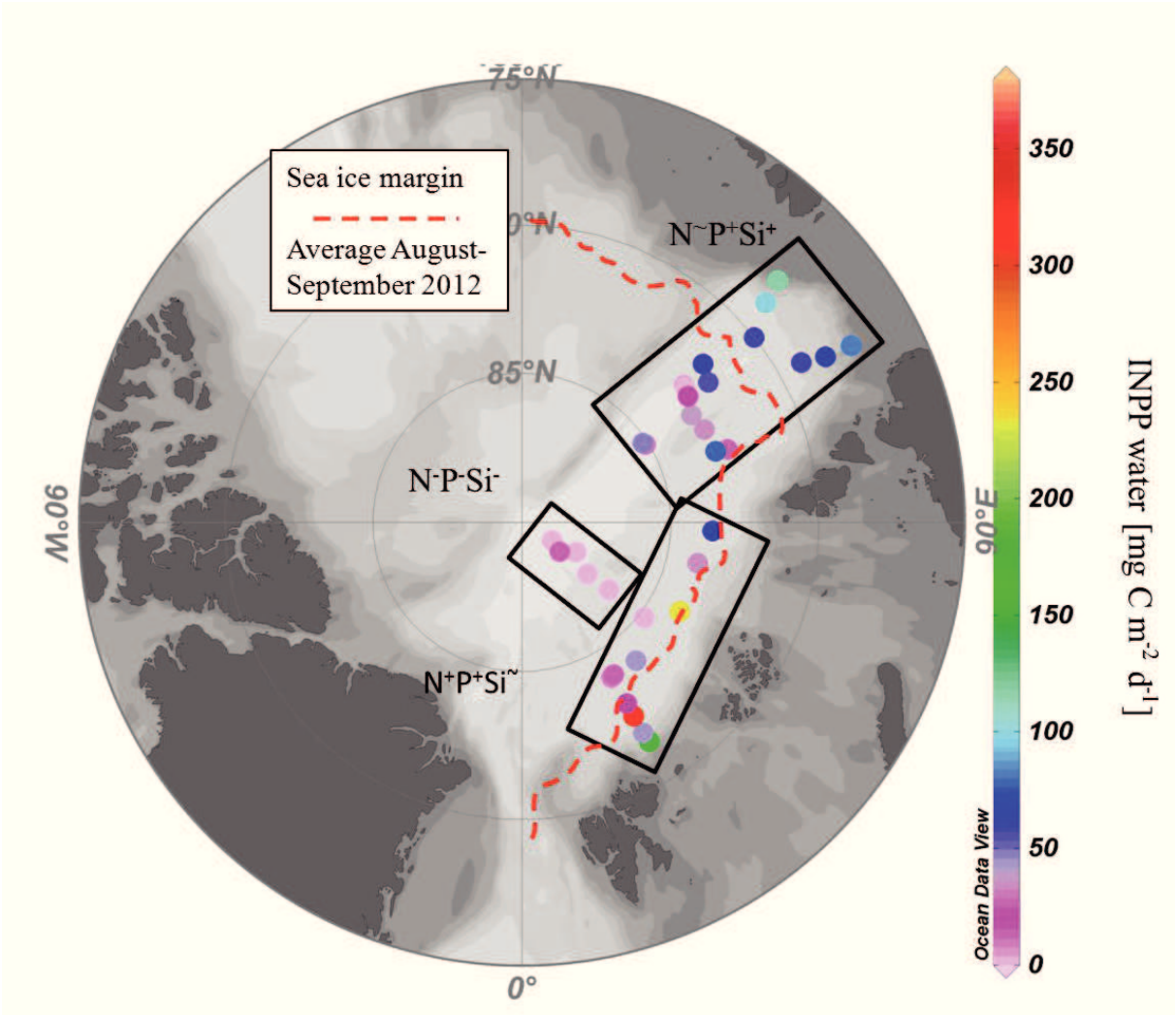

Figure 3. Depth Integrated Net Primary Productivity (INPP) and the contribution of sea ice, melt ponds and water at eight ice stations in the Eurasian Basin during summer 2012. The size of the pie chart represents the magnitude being the smallest (Ice8) 0.8 mg C m^{-2} d^{-1} and the biggest (Ice5) 60 mg C m^{-2} d^{-1}.

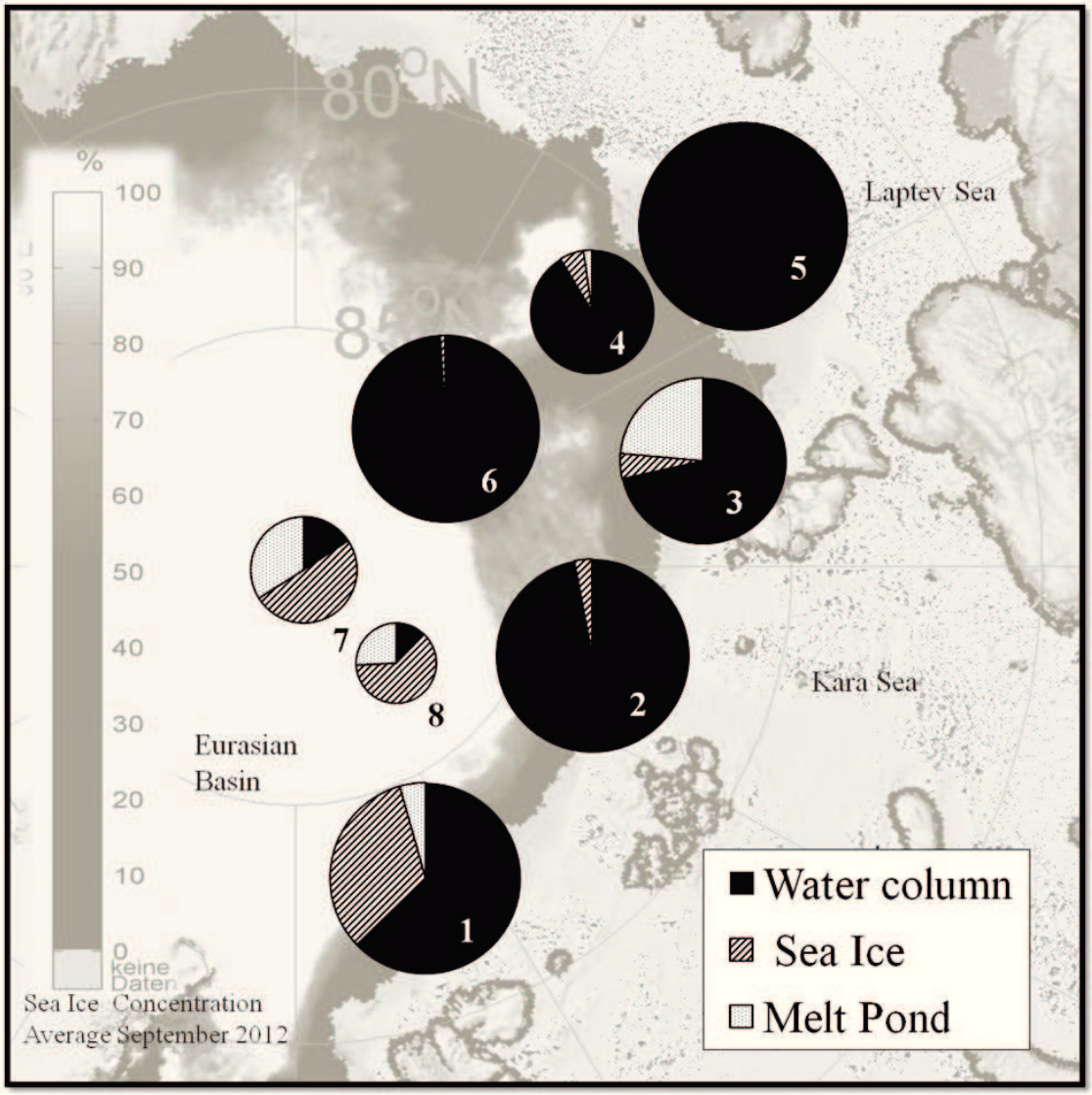

Figure 4. Total mean NPP and in each environment: melt ponds, sea ice and water in the Central Arctic during August and September 2012 as modeled with the CAOPP model.

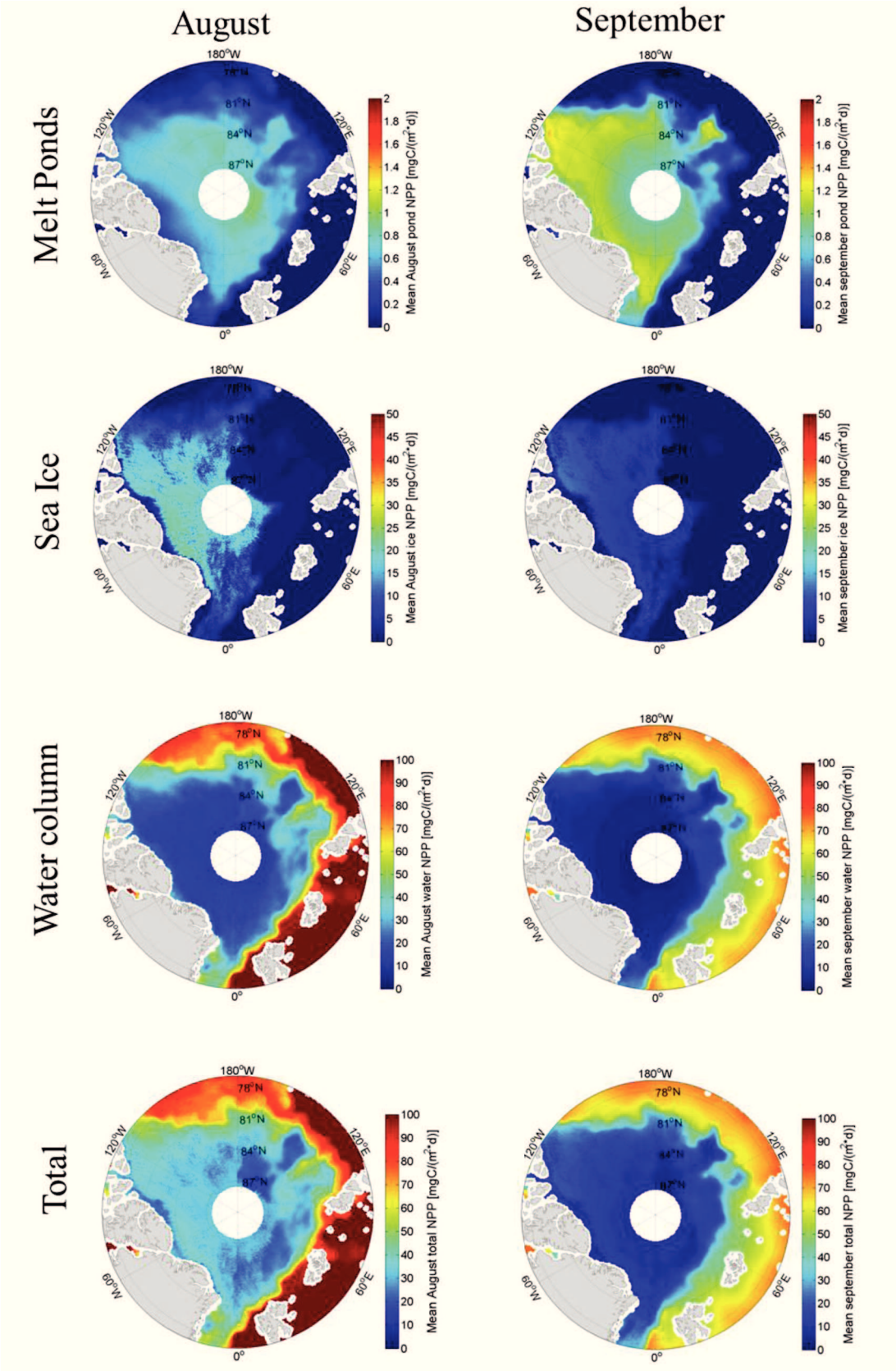

Figure 5. Nutrient addition experiments on sea water from Ice station 3 (A and B) and sea ice from Ice station 8 (C and D). Panels A and C show the NPP rate of each treatment after 24 h of nutrient addition. Panels B and D show the nutrient uptake in each treatment after nutrient addition. C^- negative control, N^+ nitrate, P^+ phosphate, Si^+ silicate, C^+ all nutrients added.

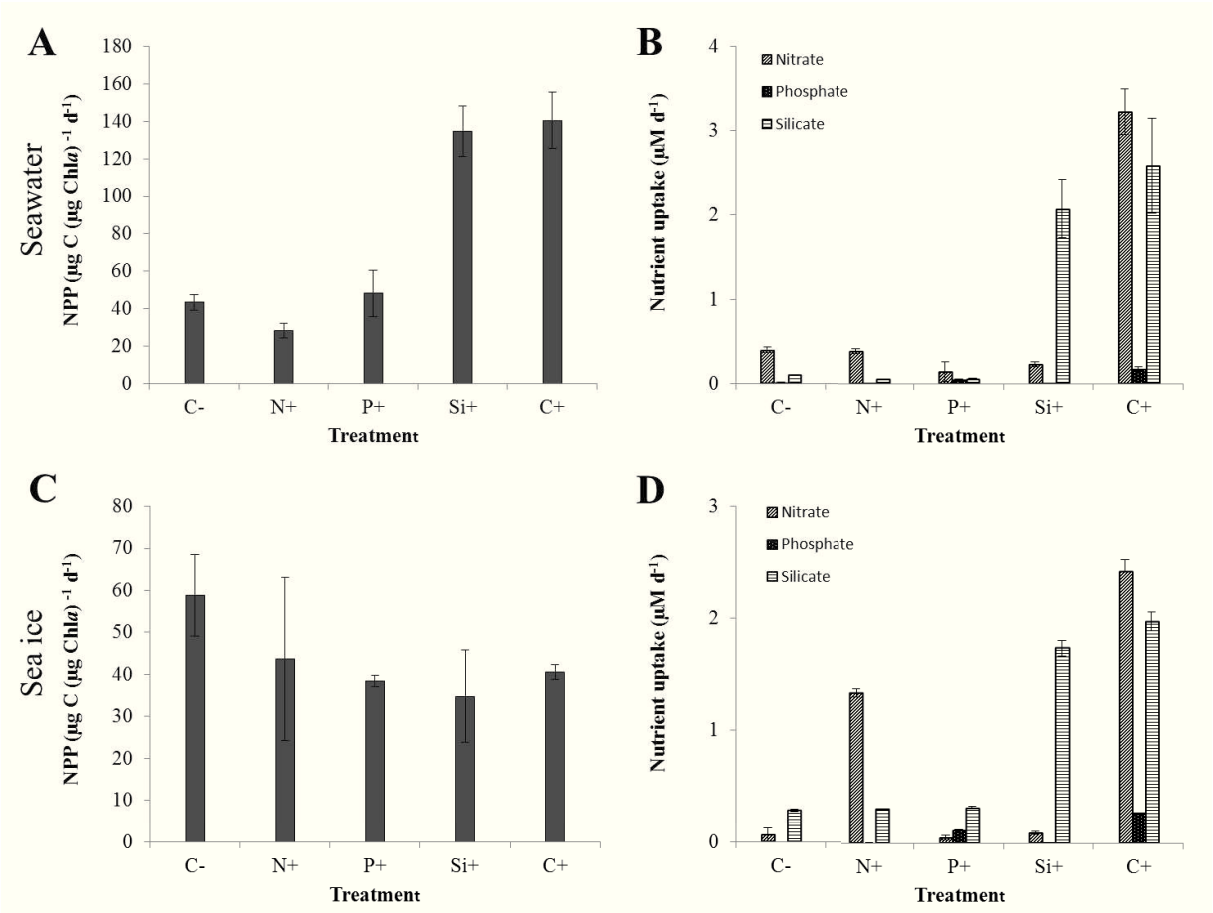

Figure S1. Average photosynthesis versus irradiance curves (PI curve) for each environment. The average fitted curve and the photosynthetic parameters derived from the PI curve equation, were used to calculate the *in situ* primary production in each environment during August and September for the Eurasian Basin. The dots represent the experimental measurements, the black solid line is the fitted curve, the dashed lines are the minimum and the maximum, and the grey shaded area is the standard deviation. Average PI parameters are represented on the top left corner.

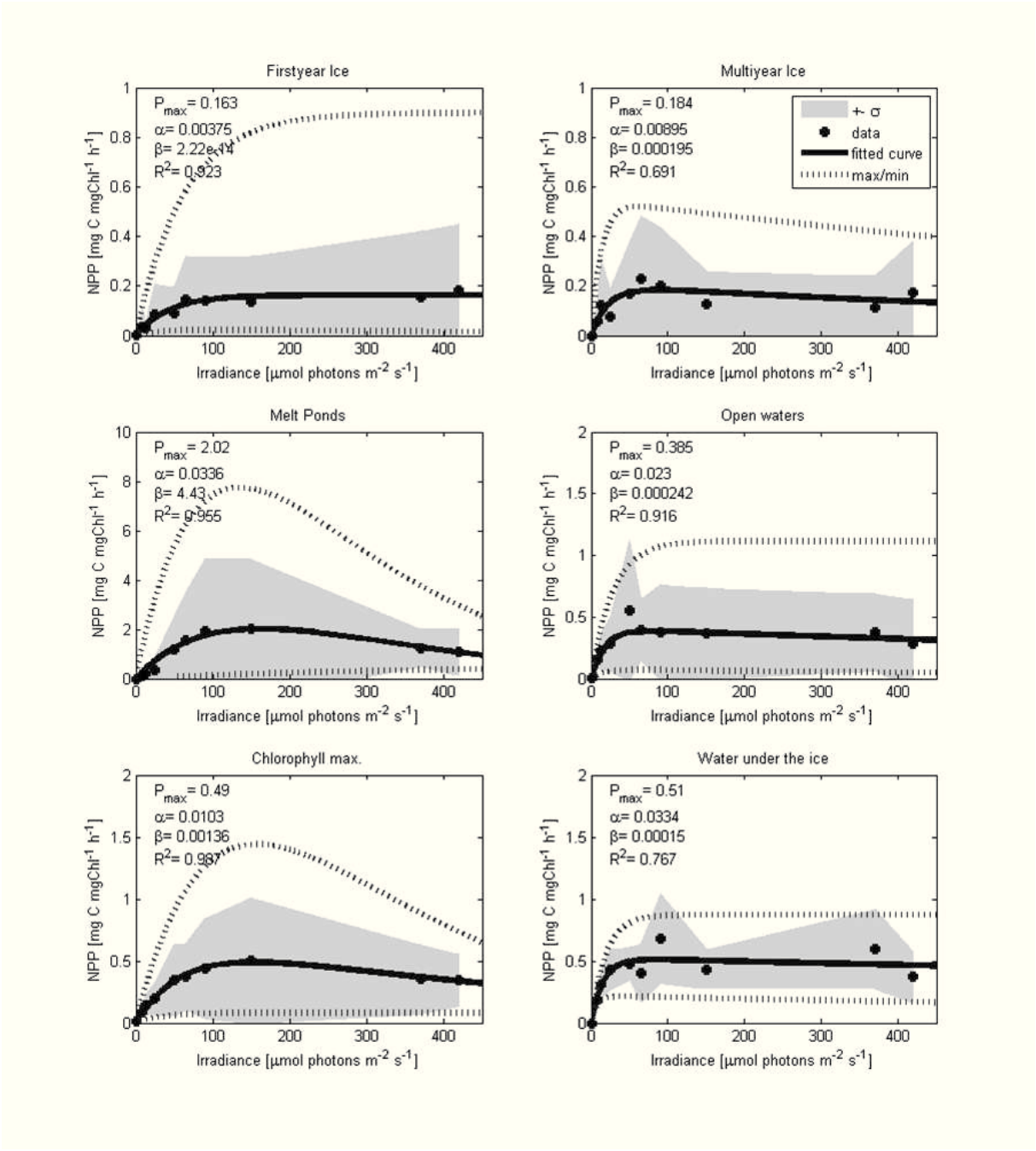

Figure S2. Euphotic zone depth (1% PAR) weighted average (A), and winter mixed layer depth (B) estimated from summer temperature profiles. Average and standard deviations: Euphotic zone depth 34 ± 6 m; Winter mixed layer depth 54 ± 15 m.

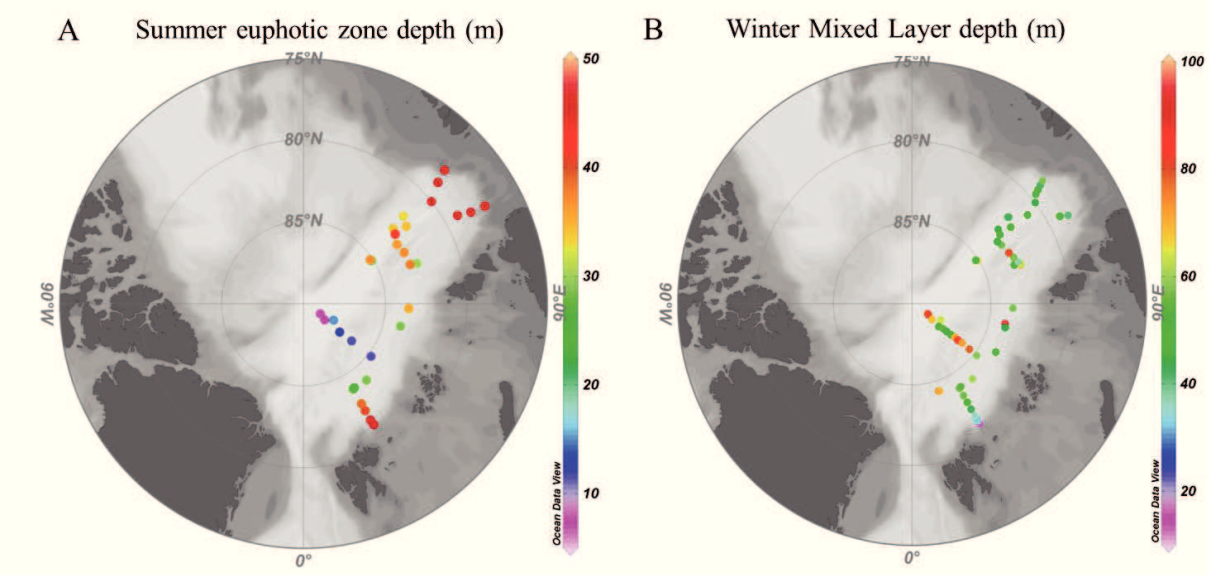

Figure S3. N:Si and N:P molar ratios in the euphotic zone of the water column during summer 2012. The green range represents ratios according to Redfield, red marks an excess of N, blue-purple represents depletion.

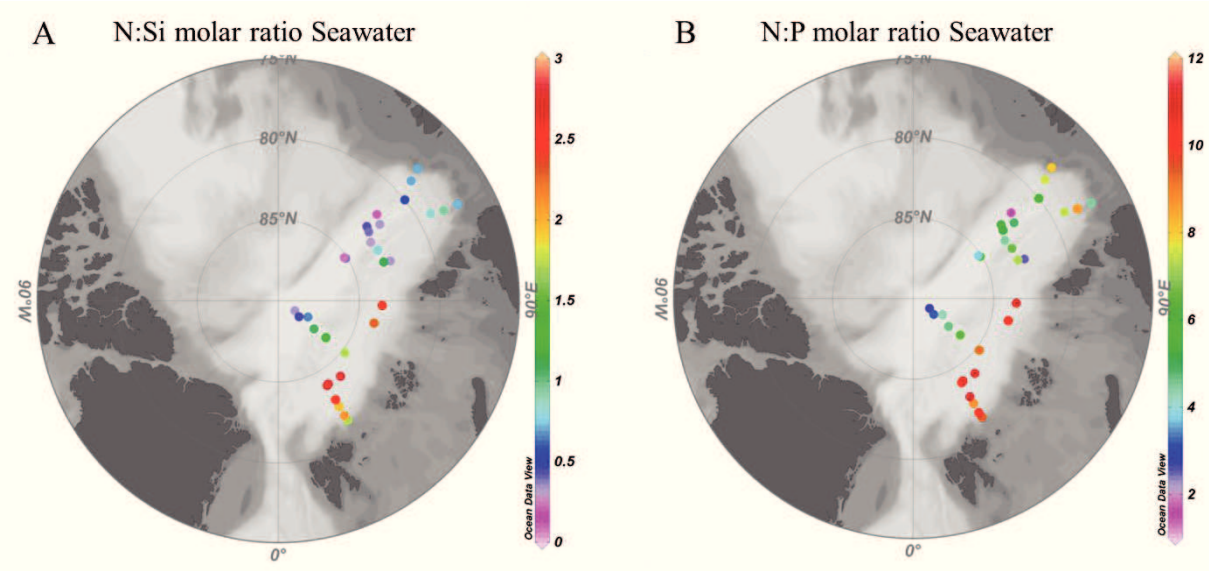

Figure S4. Fraction contribution of NPP in each environment (melt ponds, sea ice and water column) to total NPP in the Central Arctic during August and September 2012 according to CAOPP model. The assumptions for key factors governing NPP are explained in the materials and method section.

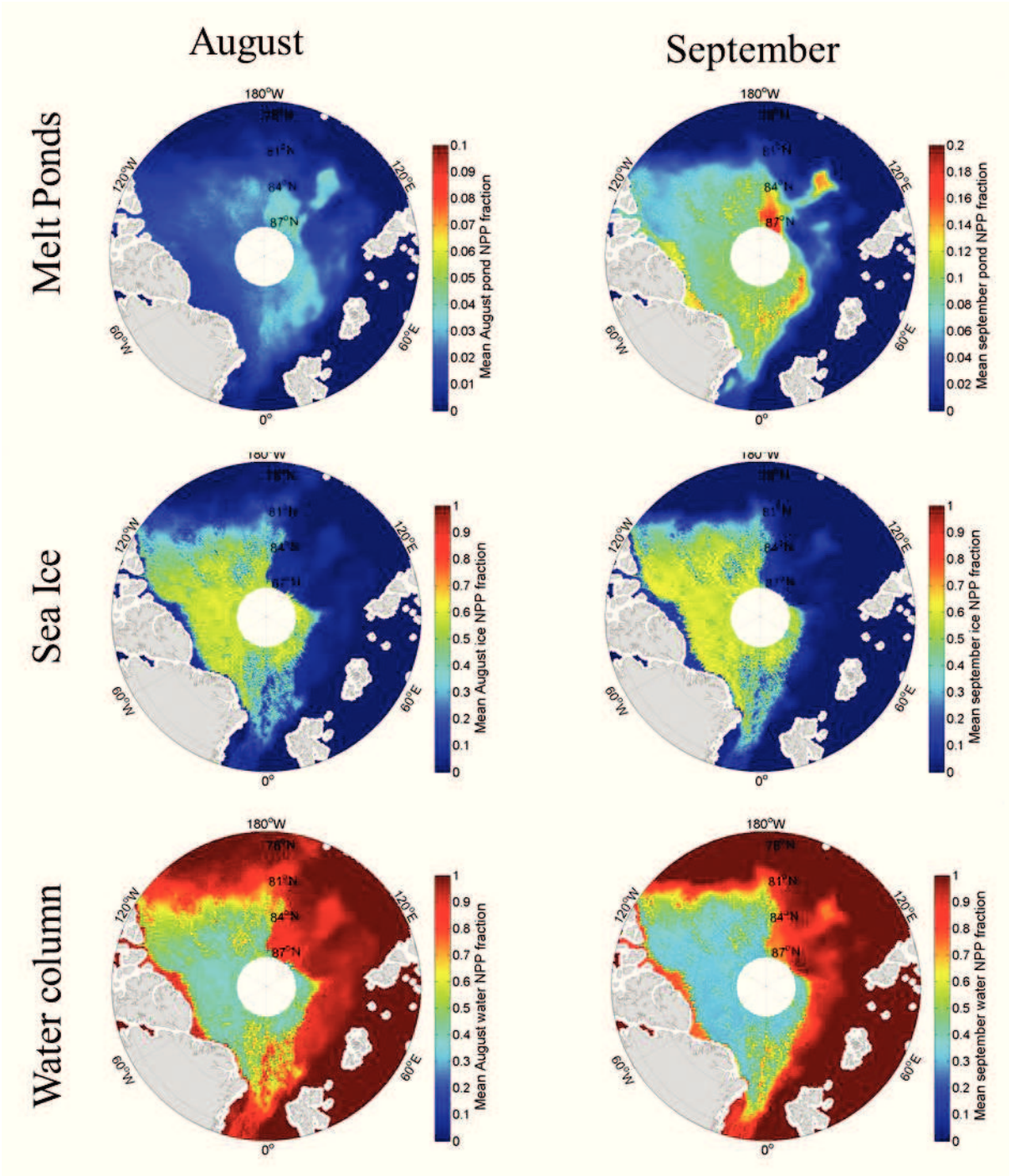

Figure S5. Mean of NPP with ice concentrations as in summer 2012 (A) and for an ice-free Arctic (B) calculated with CAOPP model assuming that only sea-ice cover changed. All other parameters remain as in 2012 as described in the materials and methods.

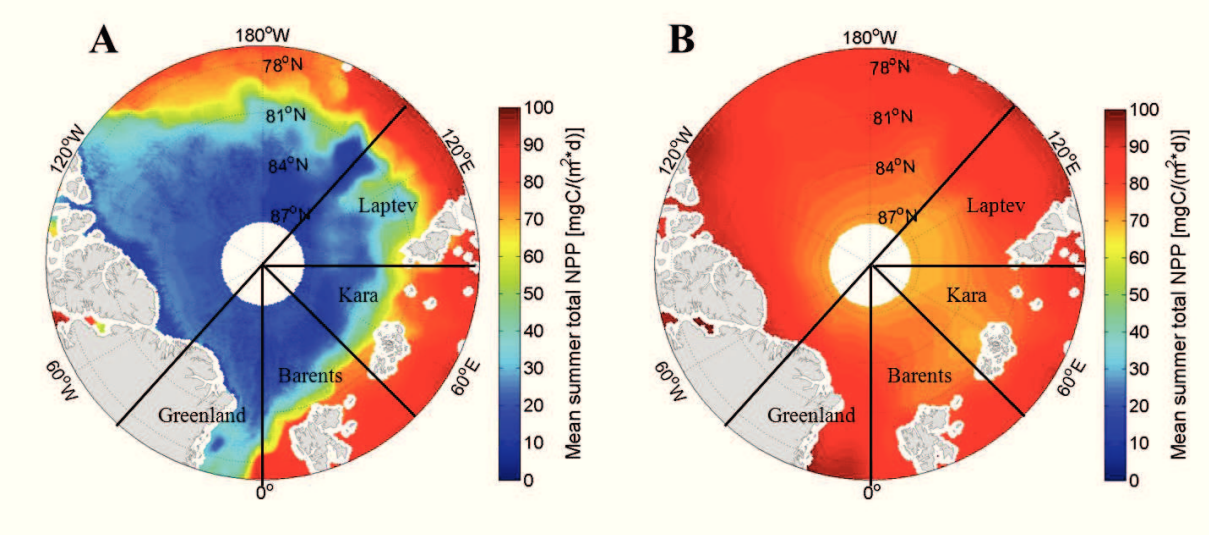

Figure S6. Biomass changes in nutrient addition experiments. (A) Nutrient addition experiment with seawater from the Chl *a* max depth at station 3. (B) Nutrient addition experiment with sea ice from station 8. Duplicates of each treatment were incubated for 2 days after nutrient addition.

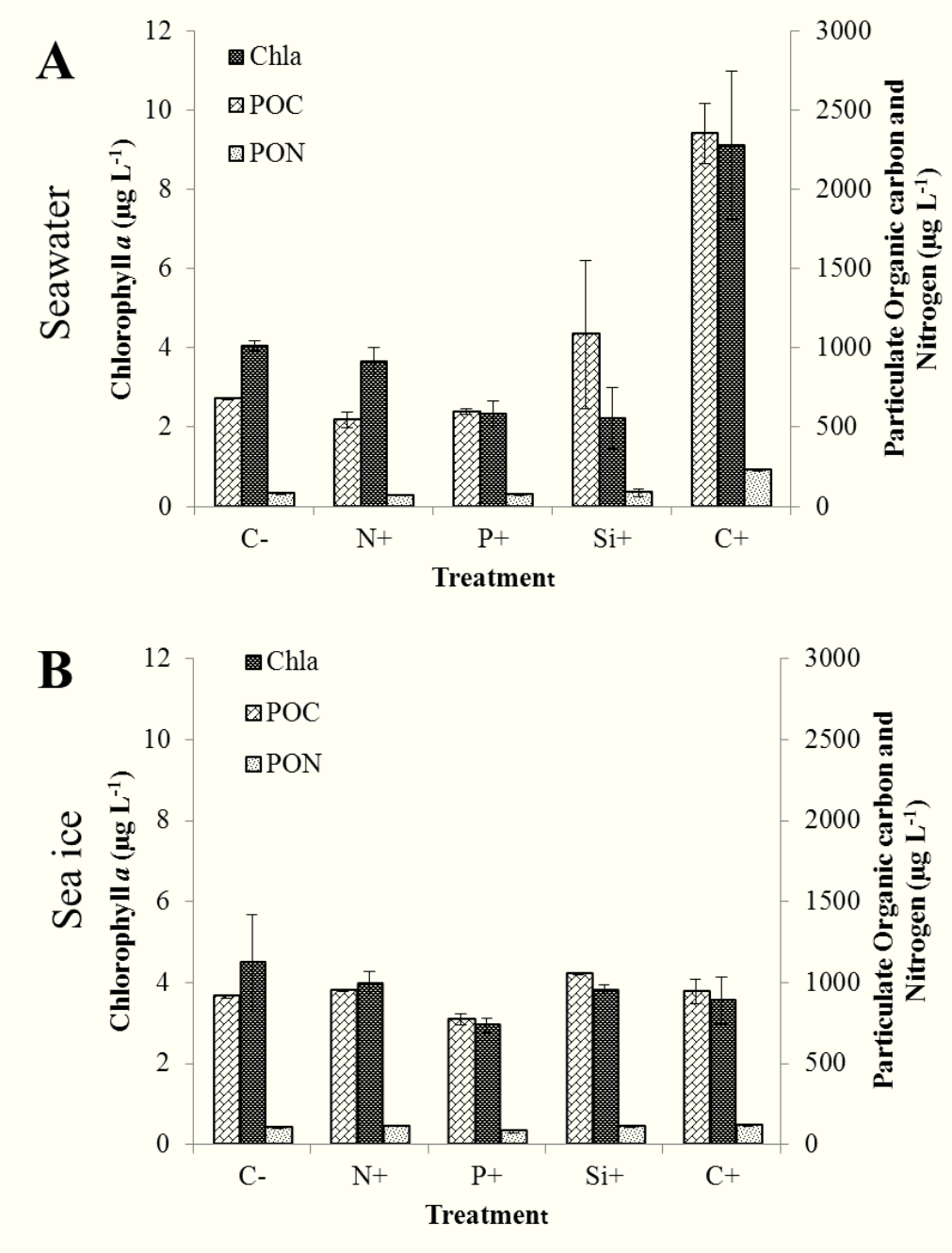

Figure S7. Microscopy images of the community composition of the two nutrient experiments: (A) sea water phytoplankton and (B) sea-ice algae.

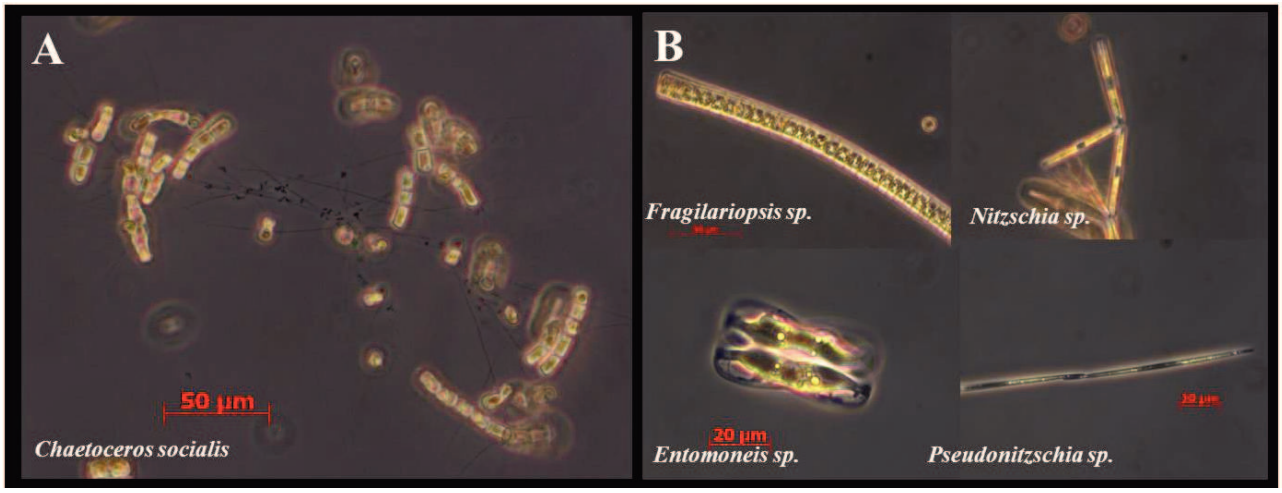

Figure S8. New production in the Eurasian Basin during 2012. Carbon uptake since last winter estimated from nitrogen (A), phosphate (B) and silicate (C) drawdown in the mixed layer. Redfield ratio C:N:Si:P of 106:16:15:1 was used to convert nutrient uptake into annual new production.

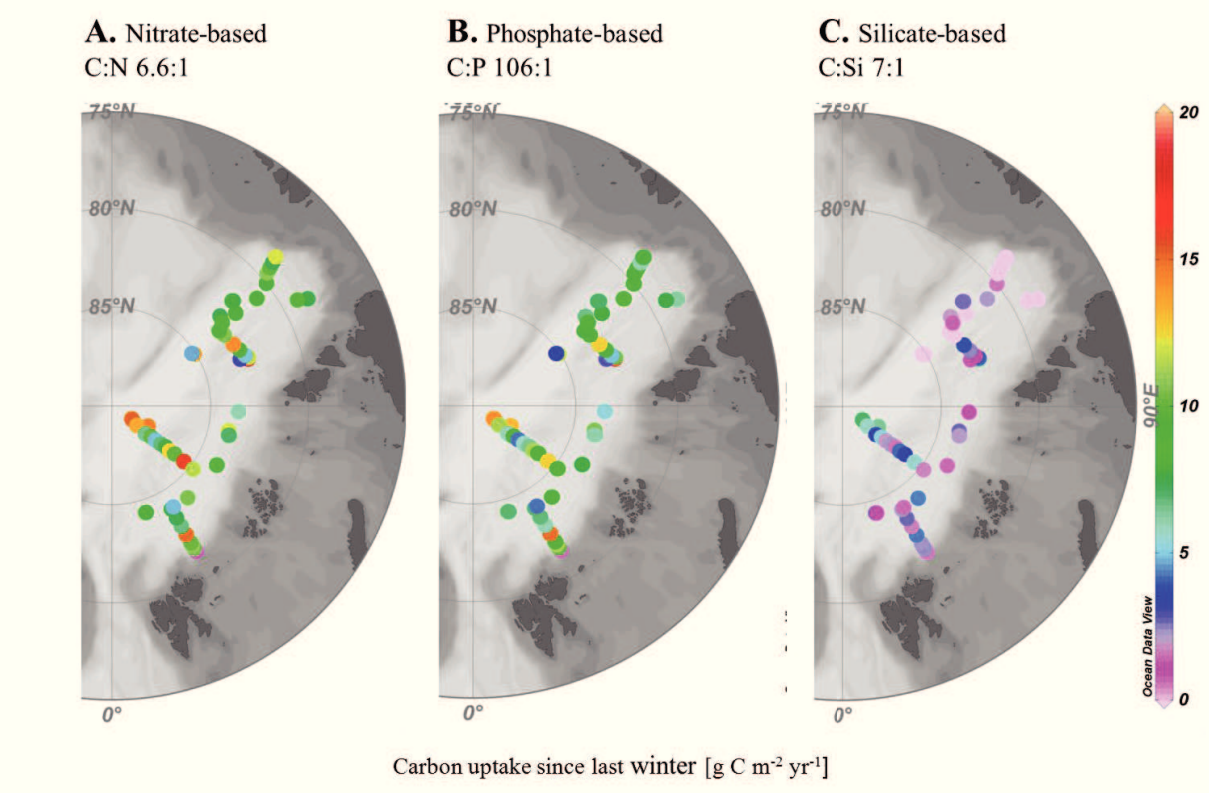

Table S1. Datasets related to this publication stored in the Earth system science database PANGAEA.

Dataset	PANGAEA doi	Reference
Sea-ice conditions	doi:10.1594/PANGAEA.803221	(Hendricks et al., 2012)
Physical oceanography	doi:10.1594/PANGAEA.802904	(Rabe et al., 2012)
Physical oceanography	doi:10.1594/PANGAEA.819452	(Rabe et al., 2012)
Net primary productivity	doi:10.1594/PANGAEA.834221	(Fernández-Méndez et al., 2014)
Nutrients water column	doi:10.1594/PANGAEA.834081	(Bakker, 2014)
Nutrients sea ice	doi:10.1594/PANGAEA.834084	(Bakker., 2014)

Table S2. *In situ* rates of depth integrated net primary productivity in melt ponds, sea ice and water column at eight ice stations sampled during summer 2012. Sea-ice and melt pond productivity were integrated through their thickness and depth respectively, and water column was integrated for the euphotic zone (1% PAR). Ice thickness, melt pond depth and euphotic zone depth are described for each station in Table 1. Only PI curves with an R^2>0.5 were used for the NPP calculations. The average error of the carbon uptake measurements was 15%.

	Integrated Net Primary Productivity *in situ* mg C m^{-2} d^{-1} (% Contribution to total)							
Station Number	1	2	3	4	5	6	7	8
Melt Pond	2 (4)	0.01 (0)	4 (24)	0.2 (2)	0.2 (0)	0.02 (0)	1 (34)	0.2 (26)
Sea Ice	13 (33)	1 (3)	0.8 (5)	0.4 (7)	0.1 (0)	0.2 (1)	1.5 (50)	0.5 (62)
Water under the ice	25 (63)	31 (97)	11 (71)	6 (91)	60 (100)	28 (99)	0.5 (16)	0.1 (12)
Total	40	32	16	7	60	29	3	0.8

Chapter VI

Diazotroph diversity in sea-ice, melt ponds and water column of the Central Arctic Ocean

Mar Fernández-Méndez[1], Kendra Turk-Kubo[2], Josephine Z. Rapp[1], Thomas Krumpen[1], Jonathan Zehr[2] and Antje Boetius[1].

[1] Alfred-Wegener-Institut Helmholtz-Zentrum für Polar- und Meeresforschung, Germany.

[2] Department of Ocean Sciences, University of California Santa Cruz, Santa Cruz, CA, USA.

In preparation for Frontiers in Aquatic Microbiology

Abstract

Recent studies indicate the presence of nitrogen fixing microorganisms, diazotrophs, in Arctic coastal waters, and speculate about their potentially terrestrial origin with air or river outflow. Here we investigated the presence of diazotrophs in the Central Arctic basins during the rapid ice melt in summer 2012. We could identify diverse potential diazotrophic communities north of 78ºN by amplifying the *nifH* gene that encodes the iron protein of the nitrogenase enzyme. We amplified 528 *nifH* sequences that resolved into 106 clusters (97% amino acid sequence identity) from 28 samples from different Arctic environments: melt ponds, sea ice and water column. Most of the sequences recovered belonged to Cluster I, including putative *Alpha- Beta-, Gamma-* and *Deltaproteobacteria*, and to Cluster III, including anaerobic microorganisms. One cyanobacterial phylotype related to *Nodularia sp.* was retrieved from Arctic sea-ice and 105 non-cyanobacterial phylotypes were retrieved from different Arctic marine environments. This implies that heterotrophic diazotrophs were more diverse than autotrophic diazotrophs during our sampling in the Central Arctic. Few phylotypes found in the ice could originate from the river-influenced Laptev Sea where the ice floes were formed. However, in general both *nifH* and 16SrRNA tag sequencing analysis revealed that surface waters close to the Laptev Sea had a distinct community compared to the ice-related environments. These results reveal a potential for marine microbial N_2 fixation north of 78ºN and is the first record of diazotrophs in the Central Arctic. Further studies should determine if the proteins encoded by these genes are metabolically active to assess the importance of nitrogen fixation in the nitrate limited Arctic Ocean.

Introduction

The biological fixation of N_2 by diazotrophs is an important source of nitrogen to nutrient-limited pelagic ecosystems (LaRoche and Breitbarth, 2005), influencing primary productivity and carbon export to the seafloor (Codispoti et al., 2001, Arrigo, 2005). Diazotrophic cyanobacteria contribute the most to nitrogen fixation rates in surface waters of tropical, subtropical and some temperate oceans (Langlois et al., 2008; Moisander et al., 2010; Turk-Kubo et al., 2012). Heterotrophic diazotrophs have also been characterized from numerous pelagic marine environments (Falcón et al., 2004; Farnelid et al., 2011; Moisander et al., 2014; Riemann et al., 2010), although the importance of non-cyanobacterial diazotrophs in oceanic nitrogen fixation remains poorly understood (Turk-Kubo et al., 2014).

According to current estimates, denitrification in seafloor sediments and water column is greater than nitrogen fixation rates in the world´s oceans, indicating an imbalance in the marine nitrogen cycle (Codispoti, 2007; Gruber and Galloway, 2008), although this remains controversial (Deutsch et al., 2007; Ward et al., 2007). Several factors are thought to constrain oceanic nitrogen fixation: low temperatures, high dissolved oxygen, high N:P ratios, and iron or phosphate limitation (Mills and Arrigo, 2010; Monteiro et al., 2011; Paerl and Zehr, 2000; Riemann et al., 2010). These limitations are mainly due to the oxygen sensitivity of the iron-rich enzyme responsible for nitrogen fixation (nitrogenase) and the competitive exclusion of diazotrophs if nitrate is in excess, and phosphate and iron are not available (Ward et al., 2013; Zehr et al., 2003).

Nitrogen cycling is understudied in the polar oceans (Luo et al., 2012). In the highly stratified Arctic Ocean, primary production is generally limited by nitrate most of which is delivered via inflow of Pacific and Atlantic waters (Codispoti et al., 2013). The Arctic Ocean is surrounded by broad shelves that contribute to denitrification (Devol et al., 1997; Rysgaard et al., 2004), but little is known about the role of nitrogen fixation. Riverine input of nitrogen especially from the Lena river that discharges into the Laptev Sea may be another important source of nitrate, as well as atmospheric deposition with snow (Beine et al., 2003), recycling of organic matter, and nitrogen fixation in the ice. Current nutrient budgets suggest an imbalance of the Arctic nitrogen supply, demand and export, and a potential role for nitrogen fixation in closing the budget (Torres-Valdés et al., 2013).

Diazotrophy has been hypothesized to be favored by the low N:P molar ratio (<9) in the western Arctic (Tremblay et al., 2008). The high iron concentrations in Arctic waters (Klunder et al., 2012) would also favor nitrogen fixation. However, cyanobacteria, which are the most common

diazotrophs in the ocean, are present in very low abundances in polar marine waters (Lovejoy and Potvin, 2010; Vincent, 2000). This, together with the low temperatures and the high dissolved oxygen in Arctic waters, supports the long-held assumption that nitrogen fixation is unlikely in the Arctic Ocean. Nevertheless, nitrogen fixation rates and potential diazotrophs have been recently identified close to the Mackenzie River in the Canadian Arctic shelves (Blais et al., 2012), and high cyanobacterial *nifH* gene diversity has been described in sea ice and waters of the Fram Strait (Díez et al., 2012). Despite recent efforts, data on nitrogen fixation from the Arctic is scarce, especially from the Central Basins, and to date there is no record of diazotroph presence north of 76 ºN. Sea-ice retreat in northerly latitudes has caused an increase in light transmitted through the ice, and potentially elevated primary productivity (Arrigo et al., 2008; Nicolaus et al., 2012), enhancing the overall nitrogen demand. Nitrogen fixation in the Central Arctic Ocean could potentially influence new production, alleviating the current nitrate limitation.

The *nifH* gene, coding for the iron protein subunit of the highly conserved nitrogenase enzyme, is commonly used to assess diazotroph diversity (Zehr and Mcreynolds, 1989; Zehr and Turner, 2001), especially to tackle low abundant diazotrophs that are usually missed by 16S rRNA pyrosequencing (Díez et al., 2012; Taton et al., 2003). The database for *nifH* genes has become one of the largest non-ribosomal gene datasets on uncultivated microorganisms (Luo et al., 2012; Zehr et al., 2003). Since nitrogen fixing capacity can rarely be inferred from 16S rRNA phylogenetic affiliation, and diazotrophs are usually outnumbered by other prokaryotes, *nifH* gene studies are the best way to assess diazotroph diversity in the environment (Zehr and Turner, 2001; Zehr et al., 2003). *NifH* gene sequences and their cluster affiliation correspond approximately with 16S rRNA phylogeny for some subclusters of Cluster I and II, but not of Clusters III and IV (Zehr et al., 2003). In addition, many uncultivated diazotrophs have been identified by using the *nifH* gene but their 16S rRNA is unknown.

Hence, we assessed the distribution of the *nifH* gene in melt pond, sea-ice and seawater samples, to characterize the diazotroph diversity in different Arctic environments and to evaluate the N_2-fixing potential of their microbial communities. Specifically we wanted to test the hypothesis that potential diazotrophs in the Central Arctic may occur in nitrate limited waters of the Eurasian Basin, and that potential diazotrophs in the pack-ice originate from coastal areas where the ice is formed.

Materials and Methods

Sampling

A total of 52 samples were taken for molecular analysis onboard the German icebreaker R/V POLARSTERN during the ARKXXVII/3 cruise to the Central Arctic (77-88° N and 30-133° E) from 7 August to 30 September 2012 (Fig.1). Sea ice, melt ponds and seawater were sampled at 9 ice stations and 13 water stations covering a wide range of ice conditions and nutrient regimes. Sea-ice samples (n=21) were taken using an ice corer (Kovacs Entreprise, Roseburg, USA) and were melted in the dark at 4°C in clean plastic containers that had been rinsed with ultrapure water and ethanol. Melt pond water (n=8) and algal aggregates (n=5) found in melt ponds were collected using a hand pump (Model 6132-0010, Nalgene, Penfield, NY, USA). Water under the ice (n=5) was collected using a peristaltic pump (Masterflex® E/S™ portable sampler, 115 VAC, Oldham, UK). Surface water at all other stations (n=13) was sampled with a rosette sampler equipped with Niskin bottles and a Conductivity Temperature Depth (CTD) profiler (Sea-Bird Electronics Inc., Washington, USA). Surface waters sampled with the Niskin bottles were separated into two categories: surface waters below the ice and open waters from the Laptev Sea region. In addition, ultrapure water was sampled to check for possible contaminations from the onboard water purification system (Milli-Q Gradient A10, Millipore) when using this water to rinse the sampling equipment.

Environmental parameters

Temperature and salinity were determined in sea ice and melt ponds with a hand-held conductivity meter (315i with TetraCon electrode cell, WTW GmbH, Weilheim in Oberbayern, Germany), and in the water column with the CTD profiler. Inorganic nutrient concentrations (nitrate, phosphate and silicate) in the different environments were measured with a standard photometric method using a Technicon TRAACS 800 continuous flow auto analyzer (Technicon Corporation) as described in Chapter V.

Ice thickness and melt pond coverage are stored in the public database PANGAEA (Hendricks et al., 2012). To determine the origin of the ice floes that we sampled in late summer, an ice tracking algorithm was used (Pfirman et al., 1997). The algorithms backtracks ice particles based on different remote sensing ice drift products obtained from passive microwave satellites. The tracking procedure is stopped, once the particles reach land or surrounding ice concentration drops below 15 % (open water).

Molecular analysis

On board the ship, 0.3 to 2 L of melted sea ice, melt pond water, melt pond aggregate slurries, water under the ice or surface seawater samples were filtered through Sterivex filters (0.2 μm pore size) (Durapore, Milipore, Darmstadt, Germany) using a multichannel peristaltic pump (Model PD 51; Heidolph, Schwabach, Germany). Filters were stored at -80°C until further processing.

Total community DNA was extracted using the DNeasy Plant Mini Kit (QIAGEN, Valencia, CA, USA) and partially automated using a QIAcube following the manufacturer's instructions (Bombar et al., 2013). To amplify the *nifH* gene, a nested polymerase chain reaction (PCR) with two sets of degenerate primers was used (Zehr and Turner, 2001). PCR amplifications were performed in a MyCycler Thermal Cycler (BioRad, Berkeley, CA, USA). The first PCR amplification of *nifH* was performed for each sample with 2 μl of DNA template in 24 μl of PCR reaction containing 4 mM $MgCl_2$, 0.4 mM dNTPs, 1X GoTaq Buffer, 1.25 U (0.2 μl) Platinum TaqDNA Polymerase (Invitrogen) and 0.5 μM of the forward *nifH*3 (5'-ATR TTR TTN GCN GCR TA-3') and reverse *nifH*4 primers (5'-TTY TAY GGN AAR GGN GG-3') (Zehr and Turner, 2001). The amplification protocol consisted of 25 cycles of 3 min at 95°C, 30 seconds of denaturalization at 95°C, 30 seconds of annealing at 55°C and 45 seconds of elongation at 72°C. The second amplification step was as described above except that we used 1μl of the PCR product from the first amplification step as the template and the forward *nifH*1 (5'-TGY GAY CCN AAR GCN GA-3') and reverse *nifH* primers (5'-ADN GCC ATC ATY TCN CC-3') (Zehr and Turner, 2001). In addition, the annealing temperature was increased to 57°C. In both steps negative controls without addition of DNA template were performed.

PCR products from the second amplification were gel purified with a QIAquick Gel Extraction Kit (Qiagen) and cloned with the TOPO® TA Cloning® Kit for Sequencing with One Shot® TOP10 Chemically Competent *E. coli* (Invitrogen) following the manufacturer´s guidelines. Depending on the number of positive clones retrieved, 12 to 48 clones were selected for each sample, the plasmids were extracted using the Millipore Montage Plasmid $Miniprep_{96}$KitsMiniprep kit (Millipore, Darmstadt, Germany) and the inserts were sequenced using the Sanger sequencing method at the University of California, Berkeley. The 528 sequences retrieved from 28 different samples will be submitted to GenBank prior to publication.

Nucleic acid sequences were trimmed and quality checked using Sequencher® sequence analysis software (Gene Codes Corporation, Ann Arbor, MI, USA). Subsequently, they were imported into the software program ARB (Ludwig et al., 2004), translated to amino acid sequences and

imported into the *nifH* database of the Zehr Lab (Heller et al., 2014; updated in July 2012). Amino acid sequences were aligned using a Hidden Markov Model from PFAM (Finn et al., 2010). Subsequently, the nucleotide sequences were re-aligned to the amino acid sequences in ARB. A total of 106 clusters with ≥97% amino acid sequence identity were identified using the web server CD-HIT suite (Huang et al., 2010). A neighbor-joining tree of partial *nifH* sequences was constructed in ARB including our confirmed *nifH* Arctic sequences, the closest relatives *nifH* sequences coming from complete genomes included in the Zehr database (Heller et al., 2014) and representative sequences of two previous Arctic studies (Blais et al., 2012; Díez et al., 2012). Our confirmed *nifH* sequences included 1 PCR blank and 28 ultrapure water sequences that clustered together with 16 of our environmental sequences. This cluster (>94% amino acid sequence identity) was considered as contaminants. Branch lengths were computed using the Kimura correction in the ARB software. Bootstrapping was also performed in ARB (1000 replicates). Clusters were collapsed manually in ARB checking that they had an amino acid sequence identity ≥92%, and named according to the cluster classification of the closest genome relative following the four cluster taxonomy of Zehr et al. (2003).

A combination of molecular fingerprinting using Automated Ribosomal Intergenic Spacer Analysis (ARISA) (Fisher and Triplett, 1999) and 454 massively parallel tag sequencing (454 MPTS) of the V4-V6 region of the 16S rRNA gene were performed for a detailed description of the total bacterial communities in which diazotrophs had been identified. Amplicon pyrosequencing was performed by the company MR DNA in Texas, Arizona, USA using the method described in Dowd and Sun (2008). The primers used were 16S rRNA universal eubacterial primers 530F and 1100R. A single-step PCR was performed using the HotStarTaq Plus Master Mix Kit (Qiagen, Valencia, CA). A total of 30 cycles were done under the following conditions: 94ºC for 3 minutes, 94ºC for 30 seconds; 53ºC for 40 seconds and 72ºC for 1 minute; after which a final elongation step at 72ºC for 5 minutes was performed. Subsequently, all amplicon products from different samples were mixed in equal concentrations and purified using Agencourt Ampure beads (Agencourt Bioscience Corporation, MA, USA). Samples were sequenced utilizing Roche 454 FLX titanium instruments and reagents and following manufacturer's guidelines. Nucleotide sequences were denoised using *mothur* (Schloss et al., 2009) and classified using SILVAngs pipeline (Quast et al., 2013) as described in (Rapp, 2014).

Statistics

Differences in diazotroph community structure were visualized by non-metric multidimensional scaling (NMDS) based on Jaccard dissimilarity measure using statistics package "vegan" in R version 3.1.1 (Oksanen et al., 2013). Differences in total bacterial community structure were also

visualized by NMDS, but based on Bray Curtis dissimilarity measure. With NMDS, we mapped the dissimilarities non-linearly onto a two-dimensional ordination space. Similarity of samples based on the presence or absence of the different *nifH* clusters or 16S rRNA operational taxonomic units (OTUs) is approximated by their distance to each other in the plot. Stress values reflect the degree of correspondence between points in the NMDS plot and in the original dissimilarity matrix. Analysis of similarity (ANOSIM) and a post hoc test were also performed in R to test for significant differences between *a priori* defined groups based on Jaccard dissimilarity.

Results and Discussion

Presence of nifH genes in the Central Arctic

During our study in summer 2012, *nifH* genes could be amplified from 28 of the 52 samples collected in all Arctic environments: sea ice, melt ponds and water column (Fig.1). A total of 528 sequences were retrieved, 40% of them from the upper part of the sea ice (Table 1). The degenerated primers used, *nifH*1 and *nifH*4, cover >94% of available *nifH* sequences allowing us to cover the entire currently known diazotroph diversity (Gaby and Buckley, 2012). The nested PCR approach, with a high number of amplification cycles applied (n=50), is a high sensitivity method. After the nested PCR approach, 5.6 x 10^{14} copies of each *nifH* gene template are obtained, corresponding to 2 x 10^{6} ng of DNA. Consequently, enough amplicon product can be obtained from a single template gene copy for cloning. However, the potentially extremely low abundance of some diazotrophs (<1 cell L^{-1}), might have avoided their amplification in some samples. Furthermore, in several water samples collected below the ice (stations 255, 263,277 and 323) unspecific amplification occurred and only a few *nifH* gene amplicons were obtained.

Low temperatures have been suggested as a potential limiting factor for nitrogen fixation (Karl et al., 2002). During our cruise in August-September 2012, seawater temperatures ranged between -1.7°C below the ice and up to 4°C close to the Laptev Sea shelf (Fig.2). Nitrogen fixation genes from putative heterotrophs were amplified from samples along the entire temperature range sampled, indicating *a priori* no temperature limitation for the presence of heterotrophic diazotrophs. However, potential nitrogen fixing cyanobacteria were only amplified in one sample

(Ice top of station 224, -0.2°C), supporting previous hypotheses that this group of nitrogen fixers might be temperature limited in the Arctic (Murphy and Haugen, 1985). However, cyanobacteria are known to grow in glaciers (Telling et al., 2011; Yallop et al., 2012), and other cold environments such as Antarctic lakes (Olson et al., 1998), hence it remains an interesting question if they have also realized a niche in the nitrogen limited Arctic waters.

Marine nitrogen fixation rates are in general correlated with sea surface temperatures (Karl et al., 2002). With current trends of warming in Arctic waters (Polyakov et al., 2010) this potential temperature limitation might decrease. Nevertheless, the most important oceanic nitrogen fixing cyanobacteria species such as *Trichodesmium sp.* and *Nodularia spumigena* are known to thrive in a temperature range of 20-34ºC (Breitbarth et al., 2006; Lehtimaki et al., 1997), that will not be reached in the Central Arctic Ocean. The predicted increase in surface water temperatures in the Arctic by the end of the century is between 1 and 6ºC depending on the carbon dioxide emission scenario (IPCC, 2013). The average fixation rates measured in the Canadian Arctic are at the lower end of temperate and tropical oceans rates (average 0.14 nmol N L^{-1} d^{-1}, Blais et al., 2012). However, the method used based on acetylene reduction might underestimate the real nitrogen fixation rates (Mohr et al., 2010). According to Blais et al., (2012), the effect of temperature on nitrogen fixation rates was only significant for estuarine samples and not for marine samples, suggesting that an increase in Arctic water temperature will have a small effect on potential nitrogen fixation rates.

Nitrogen fixation is favored in waters with low N:P ratios (Tyrrell, 1999). Diazotrophs are most competitive in nitrogen limited marine regions where iron and phosphate are not limiting (Ward et al., 2013). Iron is present in relatively high concentrations in the Eurasian Basin of the Arctic Ocean due to riverine input (Klunder et al., 2012), although it can also have a co-limiting role in some Arctic regions like the Beaufort Sea (Taylor et al., 2013). During summer in the Central Arctic, two nutrient regimes could be identified in the euphotic zone of the water column according to the nitrate and phosphate concentrations (Fig.3A). Although all N:P molar ratios were below Redfield (>16:1) indicating general nitrate limitation, the Atlantic water influenced ice margin in the Nansen Basin and the Laptev Sea have higher N:P ratios around 10, while the more Central Arctic waters in the Amundsen Basin have N:P ratios below 5. In the sea ice, nutrient concentration were in general lower than in the water column and the N:P ratios more variable. N:P ratios at ice stations 335 and 349 were close to Redfield, while the rest ranged between 5 and 11 (Fig.3B). Presence of *nifH* genes in the different environments was not related to the N:P ratio in sea ice and seawater at the time of sampling. This result suggests that diazotrophs in the Arctic could be present independently of the nutrient regime.

Nitrogen fixation is an energetically expensive process and the set of genes encoding the enzymes needed for it are only retained on evolutionary time scales if they are functional (Dos Santos et al., 2012). However, the presence and diversity of diazotrophs does not imply high nitrogen fixation rates (Moisander et al., 2007). Assuming that the upper limit of N_2 fixation estimated by Blais et al., (2012) in the Canadian Arctic (up to 0.14 nmol N L^{-1} d^{-1} transformed to carbon using a C:N ratio of 7.3: 0.6 mg C m^{-2} d^{-1}) would also take place in the Central Arctic, the nitrogen fixed by the diazotrophs could sustain ~7% of the new primary production (9.4 ± 3.6 g C m^{-2} yr^{-1}, Chapter V).

Composition of diazotrophic taxa and microbial communities

Diazotrophs have long been assumed to be absent from Arctic marine habitats, despite their presence in Arctic terrestrial and freshwater environments (Yergeau et al., 2010). To the best of our knowledge there are only three studies in which potential diazotrophs have been identified in the Arctic Ocean: one in the Fram Strait (Díez et al., 2012) and two in the Canadian shelf close to the Mackenzie river and Baffin bay (Blais et al., 2012; Farnelid et al., 2011). These studies include water, snow and sea-ice samples. Our study adds melt ponds and algal aggregates to the range of investigated habitats, and provides the first description of potential diazotrophs in the Central Arctic, north of 78 ºN. The *nifH* sequences detected in this study are distributed across all four main *nifH* clusters I-IV defined by Zehr et al., (2003) (Fig.4). Cluster I contained mainly *Proteobacteria*, *Cyanobacteria*, *Firmicutes* and uncultivated microorganisms. Cluster II contained *Proteobacteria*, *Firmicutes*, and members of the Archaea. Cluster III contained putative anaerobes including sulfate reducing genera of the *Deltaproteobacteria*, and genera such as *Clostridium*. Cluster IV contained non-functional nitrogenases. Comparing these results with a global surface waters *nifH* study, showed that all prominent members of other oceans are also present in the Arctic, although in this study only Cluster III and IV were amplified in Baffin Bay (Farnelid et al., 2011). However, *nifH* sequences from the other two marine Arctic studies were mainly distributed between Cluster I and III (Blais et al., 2012; Díez et al., 2012).

Cyanobacteria are rare in polar marine waters as indicated by microscopy and 16SrRNA analysis (Lovejoy et al., 2011; Vincent, 2000). In this study, we could amplify only 5 cyanobacterial *nifH* sequences; limited to the upper part of the sea ice (top 50 cm of a snow-free core) of station 224

(Cluster 1B in Fig.5). These sequences were all closely related (≥92% amino acid sequence identity) to *Nodularia*, a cyanobacterial genus that contributes to nitrogen fixation in the Baltic Sea (Bostrom et al., 2007). In previous Arctic *nifH* diversity studies, sequences from the same order, *Nostocales*, were found in the Beaufort Sea (Blais et al., 2012). Also other cyanobacterial phylotypes, such as *Cyanothece* and *Trichodesmium*, were retrieved in Fram Strait (Díez et al., 2012), but not at the sites investigated here in the Central Arctic, neither by *nifH* clone libraries (Fig.5), nor by 16SrRNA tag sequencing (Fig.S1).

The vast majority of sequences, which were retrieved in the different environments of the Central Arctic belonged to heterotrophic diazotrophs, dominated by Cluster I (Fig.4). In this cluster, 53% of the sequences belonged to the subcluster 1G that contains genera such as *Azotobacter*, *Brenneria*, *Teredinibacter* and *Pseudomonas*. Subcluster 1K comprised 29% of the sequences, containing both *Alpha-* and *Betaproteobacteria* such as *Bradyrhizobium* and *Azospirillum sp*. Most of these genera include nitrogen fixing species typical for soils. Cluster III sequences accounted for up to 20% of the sequences retrieved by clone libraries (Fig.4). Cluster III sequences were thought to be rare in brackish or marine surface waters (Moisander et al., 2007), but they are often recovered from ocean waters (Langlois et al., 2008; Turk-Kubo et al., 2014) and they seem to be abundant in the Canadian Arctic shelf (Farnelid et al., 2011). Only 12 sequences corresponding to non-functional nitrogenases (Cluster IV) were retrieved from sea-ice and melt pond samples, but they were not closely related to any cultivated organism. Heterotrophic marine bacteria are known to thrive at low water temperatures (Riemann et al., 2010) and reported to be relevant for nitrogen fixation in other oligotrophic oceans (Bombar et al., 2013; Moisander et al., 2014) and in the Baltic Sea (Farnelid et al., 2013). In the 16S rRNA sequence tag data base obtained from the same study sites, only *Gamma* and *Alphaproteobacteria* were prominently represented of all *nifH* gene clusters detected. Our data suggest that nitrogen fixation in the Central Arctic could be dominated by heterotrophic diazotrophs, although further quantitative studies together with rate measurements are needed to confirm this.

Diazotroph and microbial community diversity patterns in different environments of the Central Arctic

Comparing the distribution of the *nifH* subclusters across the studied Arctic environments, differences could be observed between the Laptev Sea open waters and the sea-ice related environments. NMDS of *nifH* subclusters showed a clustering of the Laptev Sea samples together, separated from all the sea-ice related environments, including melt ponds, ice top, ice

bottom, water under the ice and algal aggregates (Fig.6). ANOSIM confirmed significant differences between the sea ice environment and the Laptev Sea diazotrophic communities (ANOSIM R=0.46; Post-hoc test p=0.003), indicating that the majority of sea-ice related diazotrophs were probably not originated from the Lena Delta river that influences the Laptev Sea. In comparison, NMDS of the 16S rRNA showed that Laptev Sea and other surface waters had similar bacterial communities and they both differ from the sea-ice related environments (Fig.7).

Sea ice and Laptev Sea open waters showed the highest diversity of *nifH* genes. These two environments had four subclusters in common (1A, 1K, 1P and 2C) (Table S1). Most of the recovered *nifH* sequences in the ice top belonged to subclusters 1G and 1K containing *Gamma-* and *Alphaproteobacteria* respectively, while at the ice bottom diversity was higher because of the presence of sequences of subcluster 1A (*Deltaproteobacteria*) and Cluster III (Fig.4). Melt ponds, formed on top of the ice, only shared 1G subcluster sequences with the ice top, and additionally contained sequences from Cluster III and IV (Fig.4). These subclusters are also typically found in fresh water lakes (Zehr et al., 2003), in accordance with the low salinity of the melt ponds sampled (salinity 2-12). Algal aggregates composed by sea-ice algal species contained mainly sequences from subcluster 1G and from Cluster III, similarly to melt ponds. However, at a higher phylogenetic resolution, Cluster III sequences differed between both habitats (Fig.5). It is difficult to infer phylogeny from Cluster III sequences, yet, according to their similarity to *nifH* genes sequenced from cultured microorganisms in the phylogenetic tree, some of our sequences are closely related to *Deltaproteobacteria*. For example four sequences retrieved from the floating algal aggregate (AGG) were related to the genus *Desulfobacter* that is common in marine sediments, brackish waters and anoxic zones (Herbert, 1999). Algal aggregates can have an anoxic interior and therefore have the potential to host anaerobic processes such as denitrification (Fernández-Méndez et al., 2014; Lehto et al., 2014) (Chapter III).

Overall, the similarity of the microbial community structure according to the 16S rRNA tag sequencing of ice vs water samples was low, with a significant difference between the water and the ice samples (ANOSIM post hoc test R=0.29, p=0.008) (Fig.7). More than half of the *nifH* sequences retrieved from the water collected below the ice clustered together with ice bottom sequences, an anticipated result because these two environments are in constant connection. However, the rest of the sequences found in the water belonged to subclusters not represented in ice or melt ponds: 1F (*Epsilonproteobacteria*), 1O (*Gammaproteobacteria*) and 2B (*Archaea*). The 1F subcluster also appeared in the open water samples from the Laptev Sea region (latitudes 77-79N°) but in lower relative sequence abundance. This subcluster contains diazotrophs from the

genus *Arcobacter* that occur in roots of salt marsh plants but also sulfidic environments like cold seeps and hydrothermal vents (Mehta et al., 2003). This genus was also detected with the tag sequencing of the 16S rRNA, but only in the floating algal aggregates.

The major subclusters present in our Laptev Sea open water samples were 1A and 2A. Subcluster 1A contains non-sulfate reducing *Deltaproteobacteria* such as *Geobacter sp.* and subcluster 2A contains fermenting bacteria from the genus *Pelosinus* and *Paludibacter*. *Deltaproteobacteria* from Cluster III formed around 20% of the sequences from open waters (Fig.4). In Cluster III only a few sequences retrieved from surface waters of stations 263 and 308 clustered close to previous Arctic sequences (Fig.5) (Blais et al., 2012). *Alpha-* and *Gammaproteobacteria* dominate heterotrophic diazotrophic assemblages in the Atlantic and Pacific Oceans (Falcón et al., 2004) and were present in lower abundances in the Canadian Arctic shelves (Blais et al., 2012).

Origin and potential role of Arctic diazotrophs

Our initial hypothesis was that potential diazotrophs in the Central Arctic´s pack ice, would come from the coastal areas influenced by rivers such as the Lena River. The Lena River is a source of organic matter and iron that could provide favorable conditions for nitrogen fixation in the Laptev Sea (Lara et al., 1998). Our results, however, show a distinct diazotroph community in the Laptev Sea region, close to the Lena Delta, when compared to the sea-ice communities (Fig.6 and 7).

The ice floes sampled at the end of the productive season originated in polynyas (area of open water surrounded by ice) or from land fast ice in the Laptev and Kara seas (Fig.S2). This, together with winds that might transport dust and microorganisms offshore (Harding et al., 2011) might explain the high relative abundance of *nifH* sequences related to *Bradyrhizobium sp.* (*Alphaproteobacteria* 1K subcluster), a symbiotic soil bacterium present in the nodules of leguminose plants (Hennecke, 1990). In addition, some sea-ice sequences clustered with the endospore forming *Paenibacillus* (subcluster 1E) that has also been found in high Arctic soils (Jordan et al., 1978). However, some of these freshwater or soil diazotrophic bacteria might not thrive in the marine environment due to its high salinity (Fernandes et al., 1993).

In general, neither the 16SrRNA gene-based, nor the *nifH* gene-based microbial community composition of Laptev Sea water was similar to sea-ice or water under the ice, giving little evidence for riverine origin of the diazotrophs present in the Central Arctic. Sequences retrieved from the brown ice (with a high a concentration of phaeopigments from diatoms) collected at station 335 are an exception, since they clustered with sequences from the Laptev Sea waters and other riverine influenced environments from the Kugmallit Bay and the Mackenzie River in the Canadian Basin (subcluster 1A in Fig.7). Hence, a coastal (land or riverine) origin of the potential diazotrophs in the Central Arctic is possible, but our data indicates that it is not likely the main process for diazotroph dispersal in the Eurasian Basin. In the extensive Arctic shelves, denitrification is high (1 mmol N m^{-2} d^{-1}, Devol et al 1997) and the overall mismatch in the nitrogen budget may call for a more significant contribution of nitrogen fixation (Torres-Valdés et al., 2013).

Conclusions

The potential for nitrogen fixation was found in all Central Arctic environments, including sea ice, melt ponds and water column. Nitrogen fixation genes were retrieved from environments with a wide range of physical and chemical conditions. Potential diazotrophs were found in sea ice with high N:P molar ratio (>16) and in waters with low temperatures (-1.7ºC). Most of the sequences retrieved belonged to heterotrophic diazotrophs from Clusters I and III. Only one cyanobacterial phylotype was found in sea ice close to the Fram Strait. Sea ice appeared to host a great diversity of diazotrophs, but only a few phylotypes were related with Laptev Sea phylotypes, which is the area where the ice floes were formed.

This study reveals potential for nitrogen fixation in the Central Arctic, far away from the coastal shelves, where diazotrophs had been identified before. The real contribution of these potential diazotrophs to nitrogen fixation still needs to be assessed before any further conclusions can be drawn regarding their role in the ecosystem. If their activity can be confirmed in future studies, Arctic diazotrophs might alleviate nitrate limitation, fostering the expected increase in water column primary production due to ice retreat.

Acknowledgments

We thank the captain and crew of the RV Polarstern for their support during the ARK XXVII/3 expedition. We are particularly thankful to Anique Stecher, Christiane Uhlig, Ben Lange, Heidi

L.Sørensen, Ilka Peeken and Hauke Flores for their help during the sampling. The technical help of Mary Hogan and Brandon Carter at UCSC is greatly appreciated. This study was supported by the Alfred-Wegener-Institut Helmholtz-Zentrum für Polar- und Meeresforschung and the Max Planck Society, as well as the ERC Advanced Grant Abyss (no.294757) to AB.

References

Arrigo, K. R.: Marine microorganisms and global nutrient cycles, Nature, 437, 349–356, doi:10.1038/nature04158, 2005.

Arrigo, K. R., van Dijken, G. and Pabi, S.: Impact of a shrinking Arctic ice cover on marine primary production, Geophys. Res. Lett., 35(19), L19603, doi:10.1029/2008GL035028, 2008.

Beine, H. J., Domine, F., Ianniello, A., Nardino, M., Allegrini, I., Teinilä, K. and Hillamo, R.: Fluxes of nitrates between snow surfaces and the atmosphere in the European high Arctic, Atmos. Chem. Phys., 3, 335–346, 2003.

Blais, M., Tremblay, J.-É., Jungblut, A. D., Gagnon, J., Martin, J., Thaler, M. and Lovejoy, C.: Nitrogen fixation and identification of potential diazotrophs in the Canadian Arctic, Global Biogeochem. Cycles, 26, GB3022, doi:10.1029/2011GB004096, 2012.

Bombar, D., Turk-Kubo, K. a, Robidart, J., Carter, B. J. and Zehr, J. P.: Non-cyanobacterial *nifH* phylotypes in the North Pacific Subtropical Gyre detected by flow-cytometry cell sorting., Environ. Microbiol. Rep., 5(5), 705–15, doi:10.1111/1758-2229.12070, 2013.

Bostrom, K. H., Riemann, L., Zweifel, U. L. and Hagstrom, a.: Nodularia sp. *nifH* gene transcripts in the Baltic Sea proper, J. Plankton Res., 29(4), 391–399, doi:10.1093/plankt/fbm019, 2007.

Breitbarth, E., Oschlies, A. and LaRoche, J.: Physiological constraints on the global distribution of Trichodesmium-effect of temperature on diazotrophy., Biogeosciences Discuss., 3, 779–801, 2006.

Codispoti, L. A.: An oceanic fixed nitrogen sink exceeding 400 Tg N a^{-1} vs the concept of homeostasis in the fixed-nitrogen inventory, Biogeosciences, 4, 233–253, doi:10.5194/bg-4-233-2007, 2007.

Codispoti, L. A., Kelly, V., Thessen, A., Matrai, P., Suttles, S., Hill, V., Steele, M. and Light, B.: Synthesis of primary production in the Arctic Ocean: III. Nitrate and phosphate based estimates of net community production., Prog. Oceanogr., 110, 126–150, doi:10.1016/j.pocean.2012.11.006, 2013.

Deutsch, C., Sarmiento, J. L., Sigman, D. M., Gruber, N. and Dunne, J. P.: Spatial coupling of nitrogen inputs and losses in the ocean., Nature, 445, 163–167, doi:10.1038/nature05392, 2007.

Devol, A., Codispoti, L. A. and Christensen, J.: Summer and winter denitrification rates in western Arctic Shelf sediments., Cont. Shelf Res., 17, 1029−1050, 1997.

Díez, B., Bergman, B., Pedrós-Alió, C., Antó, M. and Snoeijs, P.: High cyanobacterial *nifH* gene diversity in Arctic seawater and sea ice brine., Environ. Microbiol. Rep., 4(3), 360–6, doi:10.1111/j.1758-2229.2012.00343.x, 2012.

Dowd, S. E. and Sun, Y.: Bacterial tag-encoded FLX amplicon pyrosequencing (bTEFAP) for microbiome studies: bacterial diversity in the ileum of newly weaned Salmonella-infected pigs., Foodborne Pathog Dis, 5(4), 459–472, 2008.

Falcón, L. I., Carpenter, E. J., Cipriano, F., Bergman, B. and Capone, D. G.: N_2 Fixation by unicellular bacterioplankton from the Atlantic and Pacific Oceans: Phylogeny and *in situ* rates., Appl. Environ. Microbiol., 70(2), 765–770, doi:10.1128/AEM.70.2.765, 2004.

Farnelid, H., Andersson, A. F., Bertilsson, S., Al-Soud, W. A., Hansen, L. H., Sørensen, S., Steward, G. F., Hagström, Å. and Riemann, L.: Nitrogenase gene amplicons from global marine surface waters are dominated by genes of non-cyanobacteria., PLoS One, 6(4), e19223, doi:10.1371/journal.pone.0019223, 2011.

Farnelid, H., Bentzon-Tilia, M., Andersson, A. F., Bertilsson, S., Jost, G., Labrenz, M., Jürgens, K. and Riemann, L.: Active nitrogen-fixing heterotrophic bacteria at and below the chemocline of the central Baltic Sea., ISME J., 7, 1413–23, doi:10.1038/ismej.2013.26, 2013.

Fernandes, T. A., Iyer, V. and Apte, S. K.: Differential responses of nitrogen-fixing cyanobacteria to salinity and osmotic stresses, Appl. Environ. Microbiol., 59(3), 899–904, 1993.

Fernández-Méndez, M., Wenzhöfer, F., Peeken, I., Sørensen, H. L., Glud, R. N. and Boetius, A.: Composition, buoyancy regulation and fate of ice algal aggregates in the Central Arctic Ocean, PLoS One, accepted, 2014.

Finn, R., Mistry, J., Tate, J., Coggill, P., Heger, A. and JE, P.: The Pfam protein families database., Nucleic Acids Res., 38, D211–D222, 2010.

Fisher, M. M. and Triplett, E. W.: Automated approach for ribosomal intergenic spacer analysis of microbial diversity and its application to freshwater bacterial communities., Appl. Environ. Microbiol., 65, 4630–4636, 1999.

Gaby, J. C. and Buckley, D. H.: A comprehensive evaluation of PCR primers to amplify the *nifH* gene of nitrogenase., PLoS One, 7(7), e42149, doi:10.1371/journal.pone.0042149, 2012.

Gruber, N. and Galloway, J. N.: An Earth-system perspective of the global nitrogen cycle., Nature, 451(7176), 293–6, doi:10.1038/nature06592, 2008.

Harding, T., Jungblut, A. D., Lovejoy, C. and Vincent, W. F.: Microbes in high arctic snow and implications for the cold biosphere., Appl. Environ. Microbiol., 77(10), 3234–43, doi:10.1128/AEM.02611-10, 2011.

Heller, P., Tripp, H. J., Turk-Kubo, K. and Zehr, J. P.: ARBitrator: A software pipeline for on-demand retrieval of auto-curated *nifH* sequences from GenBank., Bioinformatics, doi:doi: 10.1093/bioinformatics/btu417, 2014.

Hendricks, S., Nicolaus, M. and Schwegmann, S.: Sea ice conditions during POLARSTERN cruise ARK-XXVII/3 (IceArc) in 2012., 2012.

Hennecke, H.: Nitrogen fixation genes involved in the Bradyrhizobium japonicum-soybean symbiosis., FEBS Lett., 268(2), 422–6, 1990.

Herbert, R. A.: Nitrogen cycling in coastal marine ecosystems., FEMS Microbiol. Rev., 23, 563–90, 1999.

Huang, Y., Niu, B., Gao, Y., Fu, L. and Li, W.: CD-HIT Suite: a web server for clustering and comparing biological sequences., Bioinformatics, 26(680), 2010.

IPCC: Climate Change 2013: The Physical Science Basis. Contribution of working group I to the Fifth Assessment Report of the IPCC., 2013.

Jordan, D. C., McNicol, P. J. and Marshall, M. R.: Biological nitrogen fixation in the terrestrial environment of a high Arctic ecosystem (Truelove Lowland, Devon Island, N.W.T.), Can. J. Microbiol., 24(6), 643–649, 1978.

Karl, D., Michaels, A., Bergman, B., Capone, D., Carpenter, E., Letelier, R., Lipschultz, F., Paerl, H., Sigman, D. and Stal, L.: Dinitrogen fixation in the world ' s oceans, Biogeochemistry, 57/58, 47–98, 2002.

Klunder, M. B., Bauch, D., Laan, P., de Baar, H. J. W., van Heuven, S. and Ober, S.: Dissolved iron in the Arctic shelf seas and surface waters of the central Arctic Ocean: Impact of Arctic river water and ice-melt, J. Geophys. Res., 117(C1), C01027, doi:10.1029/2011JC007133, 2012.

Langlois, R. J., Hümmer, D. and LaRoche, J.: Abundances and distributions of the dominant *nifH* phylotypes in the Northern Atlantic Ocean., Appl. Environ. Microbiol., 74(6), 1922–31, doi:10.1128/AEM.01720-07, 2008.

Lara, R. J. R. J., Rachold, V., Kattner, G., Hubberten, H. W., Guggenberger, G., Skoog, A. and Thomas, D. N.: Dissolved organic matter and nutrients in the Lena River, Siberian Arctic: Characteristics and distribution, Mar. Chem., 59(3-4), 301–309, doi:10.1016/S0304-4203(97)00076-5, 1998.

LaRoche, J. and Breitbarth, E.: Importance of the diazotrophs as a source of new nitrogen in the ocean, J. Sea Res., 53(1-2), 67–91, doi:10.1016/j.seares.2004.05.005, 2005.

Lehtimaki, J., Moisander, P., Sivonen, K., Kononen, K., Moisander, P. I. A. and Sivonen, K.: Growth, nitrogen fixation and nodularin production by two baltic sea cyanobacteria., Appl. Environ. Microbiol., 63(5), 1647, 1997.

Lehto, N., Glud, R., Nordi, G., Zang, H. and Davison, W.: Anoxic microniches in marine sediments induced by aggregate settlement: Biogeochemical dynamics and implications., Biogeochemistry, doi:10.1007/s10533-014-9967-0, 2014.

Lovejoy, C., Galand, P. E. and Kirchman, D. L.: Picoplankton diversity in the Arctic Ocean and surrounding seas, Mar. Biodivers., 41, 5–12, doi:10.1007/s12526-010-0062-z, 2011.

Lovejoy, C. and Potvin, M.: Microbial eukaryotic distribution in a dynamic Beaufort Sea and the Arctic Ocean, J. Plankton Res., 33(3), 431–444, doi:10.1093/plankt/fbq124, 2010.

Ludwig, W., Strunk, O., Westram, R., Richter, L., Meier, H., Yadhukumar, Buchner, A., Lai, T., Steppi, S., Jobb, G., Förster, W., Brettske, I., Gerber, S., Ginhart, A. W., Gross, O., Grumann, S., Hermann, S., Jost, R., König, A., Liss, T., Lüßmann, R., May, M., Nonhoff, B., Reichel, B., Strehlow, Robert Stamatakis, Alexandros Stuckmann, N., Vilbig, A., Lenke, M., Ludwig, T., Bode,

A. and Schleifer, K.-H.: ARB: a software environment for sequence data., Nucleic Acids Res., 32(4), 1363–1371, 2004.

Luo, Y.-W., Doney, S. C., Anderson, L. A., Benavides, M., Berman-Frank, I., Bode, A., Bonnet, S., Boström, K. H., Böttjer, D., Capone, D. G., Carpenter, E. J., Chen, Y. L., Church, M. J., Dore, J. E., Falcón, L. I., Fernández, A., Foster, R. A., Furuya, K., Gómez, F., Gundersen, K., Hynes, A. M., Karl, D. M., Kitajima, S., Langlois, R. J., LaRoche, J., Letelier, R. M., Maranon, E., D, M. J., Moisander, P. H., Moore, C. M., Mourino-Carballido, B., Mulholland, M. R., Needoba, J. A., Orcutt, K. M., Poulton, A. J., Rahav, E., Raimbault, P., Rees, A. P., Riemann, L., Shiozaki, T., Subramaniam, A., Tyrrell, T., Turk-Kubo, K., Varela, M., Villareal, T. A., Webb, E. A., White, A. E., Wu, J. and Zehr, J. P.: Database of diazotrophs in global ocean: abundance, biomass and nitrogen fixation rates, Earth Syst. Sci. data, 4, 47–73, doi:10.5194/essd-4-47-2012, 2012.

Mehta, M. P., Butterfield, D. A. and Baross, J. A.: Phylogenetic diversity of nitrogenase (*nifH*) genes in deep-sea and hydrothermal vent environments of the Juan de Fuca Ridge, Appl. Environ. Microbiol., 69(2), 960–970, doi:10.1128/AEM.69.2.960, 2003.

Mills, M. M. and Arrigo, K. R.: Magnitude of oceanic nitrogen fixation influenced by the nutrient uptake ratio of phytoplankton, Nat. Geosci., 3(6), 412–416, doi:10.1038/ngeo856, 2010.

Mohr, W., Grosskopf, T., Wallace, D. W. R. and LaRoche, J.: Methodological underestimation of oceanic nitrogen fixation rates., PLoS One, 5(9), e12583, doi:10.1371/journal.pone.0012583, 2010.

Moisander, P. H., Beinart, R. A., Hewson, I., White, A. E., Johnson, K. S., Carlson, C. A., Montoya, J. P. and Zehr, J. P.: Unicellular cyanobacterial distributions broaden the oceanic N_2 fixation domain., Science, 327, 1512–4, doi:10.1126/science.1185468, 2010.

Moisander, P. H., Morrison, A. E., Ward, B. B., Jenkins, B. D. and Zehr, J. P.: Spatial-temporal variability in diazotroph assemblages in Chesapeake Bay using an oligonucleotide *nifH* microarray., Environ. Microbiol., 9(7), 1823–35, doi:10.1111/j.1462-2920.2007.01304.x, 2007.

Moisander, P. H., Serros, T., Paerl, R. W., Beinart, R. a and Zehr, J. P.: Gammaproteobacterial diazotrophs and *nifH* gene expression in surface waters of the South Pacific Ocean., ISME J., 1–12, doi:10.1038/ismej.2014.49, 2014.

Monteiro, F. M., Dutkiewicz, S. and Follows, M. J.: Biogeographical controls on the marine nitrogen fixers, Global Biogeochem. Cycles, 25(GB2003), doi:10.1029/2010GB003902, 2011.

Murphy, L. and Haugen, E.: The distribution and abundance of phototrophic ultraplankton in the North Atlantic., Limnol. Oceanogr., 30, 47–58, 1985.

Nicolaus, M., Katlein, C., Maslanik, J. and Hendricks, S.: Changes in Arctic sea ice result in increasing light transmittance and absorption, Geophys. Res. Lett., 39(L24501), 1–6, doi:10.1029/2012GL053738, 2012.

Oksanen, J., Blanchet, F. Guillaume Kindt, R., Legendre, P., Minchin, P. R., O'Hara, R. B., Simpson, G. L., Solymos, P., Stevens, M. H. H. and Wagner, H.: vegan: Community Ecology Package. R package version 2.0-10.

Olson, J., Steppe, T., Litaker, R. and Paerl, H.: N_2-fixing microbial consortia associated with the ice cover of Lake Bonney, Antarctica., Microb. Ecol., 36(3), 231–238, 1998.

Paerl, H. W. and Zehr, J. P.: Marine nitrogen fixation, in Microbial ecology of the Oceans, edited by D. L. Kirchman, pp. 387– 426, Wiley-Liss, New York., 2000.

Pfirman, S. L., Colony, R., Niirnberg, D., Eicken, H. and Rigor, I.: Reconstructing the origin and trajectory of drifting Arctic sea ice., J. Geophys. Res., 102(c6), 575–586, 1997.

Polyakov, I. V., Timokhov, L. a., Alexeev, V. a., Bacon, S., Dmitrenko, I. a., Fortier, L., Frolov, I. E., Gascard, J.-C., Hansen, E., Ivanov, V. V., Laxon, S., Mauritzen, C., Perovich, D., Shimada, K., Simmons, H. L., Sokolov, V. T., Steele, M. and Toole, J.: Arctic Ocean warming contributes to reduced polar ice cap, J. Phys. Oceanogr., 40(12), 2743–2756, doi:10.1175/2010JPO4339.1, 2010.

Quast, C., Pruesse, E., Yilmaz, P., Gerken, J., Schweer, T., Yarza, P., Peplies, J. and Glöckner, F. O.: The SILVA ribosomal RNA gene database project: improved data processing and web-based tools., Nucleic Acids Res., 41(Database issue), D590–6, doi:10.1093/nar/gks1219, 2013.

Rapp, J. Z.: Bacterial diversity in sea ice, melt ponds, water column, ice algal aggregates and deep-sea sediments of the Central Arctic Ocean., 99 pp., Universität Bremen., 2014.

Riemann, L., Farnelid, H. and Steward, G.: Nitrogenase genes in non-cyanobacterial plankton: prevalence, diversity and regulation in marine waters, Aquat. Microb. Ecol., 61(3), 235–247, doi:10.3354/ame01431, 2010.

Rysgaard, S., Glud, R. N., Risgaard-Petersen, N. and Dalsgaard, T.: Denitrification and anammox activity in Arctic marine sediments, Limnol. Oceanogr., 49(5), 1493–1502, doi:10.4319/lo.2004.49.5.1493, 2004.

Dos Santos, P. C., Fang, Z., Mason, S. W., Setubal, J. C. and Dixon, R.: Distribution of nitrogen fixation and nitrogenase-like sequences amongst microbial genomes., BMC Genomics, 13, 162, doi:10.1186/1471-2164-13-162, 2012.

Schloss, P. D., Westcott, S. L., Ryabin, T., Hall, J. R., Hartmann, M., Hollister, E. B., Lesniewski, R. a, Oakley, B. B., Parks, D. H., Robinson, C. J., Sahl, J. W., Stres, B., Thallinger, G. G., Van Horn, D. J. and Weber, C. F.: Introducing mothur: open-source, platform-independent, community-supported software for describing and comparing microbial communities., Appl. Environ. Microbiol., 75(23), 7537–41, doi:10.1128/AEM.01541-09, 2009.

Taton, A., Grubisic, S., Brambilla, E., Wit, D., Wilmotte, A. and Wit, R. De: Cyanobacterial diversity in natural and artificial microbial mats of Lake Fryxell (McMurdo Dry Valleys , Antarctica): a morphological and molecular approach, Appl. Environ. Microbiol., 69(9), 5157–5169, doi:10.1128/AEM.69.9.5157, 2003.

Taylor, R. L., Semeniuk, D. M., Payne, C. D., Zhou, J., Tremblay, J.-É., Cullen, J. T. and Maldonado, M. T.: Colimitation by light, nitrate, and iron in the Beaufort Sea in late summer, J. Geophys. Res. Ocean., 118, 3260–3277, doi:10.1002/jgrc.20244, 2013.

Telling, J., Anesio, A. M., Tranter, M., Irvine-Fynn, T., Hodson, A., Butler, C. and Wadham, J.: Nitrogen fixation on Arctic glaciers, Svalbard, J. Geophys. Res., 116, G03039, doi:10.1029/2010JG001632, 2011.

Torres-Valdés, S., Tsubouchi, T., Bacon, S., Naveira-Garabato, A. C., Sanders, R., McLaughlin, F. a., Petrie, B., Kattner, G., Azetsu-Scott, K. and Whitledge, T. E.: Export of nutrients from the Arctic Ocean, J. Geophys. Res. Ocean., 118(4), 1625–1644, doi:10.1002/jgrc.20063, 2013.

Tremblay, J.-É., Simpson, K., Martin, J., Miller, L., Gratton, Y., Barber, D. and Price, N. M.: Vertical stability and the annual dynamics of nutrients and chlorophyll fluorescence in the coastal, southeast Beaufort Sea, J. Geophys. Res., 113(C7), C07S90, doi:10.1029/2007JC004547, 2008.

Turk-Kubo, K., Achilles, K. M., Serros, T. R. C., Ochiai, M., Montoya, J. P. and Zehr, J. P.: Nitrogenase (*nifH*) gene expression in diazotrophic cyanobacteria in the Tropical North Atlantic

in response to nutrient amendments., Front. Microbiol., 3(386), 1–17, doi:10.3389/fmicb.2012.00386, 2012.

Turk-Kubo, K., Karamchandani, M., Capone, D. G. and Zehr, J. P.: The paradox of marine heterotrophic nitrogen fixation: abundances of heterotrophic diazotrophs do not account for nitrogen fixation rates in the Eastern Tropical South Pacific., Environ. Microbiol., doi:10.1111/1462-2920.12346, 2014.

Tyrrell, T.: The relative influences of nitrogen and phosphorus on oceanic primary production, Nature, 400, 525–531, 1999.

Vincent, W. F.: Cyanobacterial dominance in the polar regions., in The ecology of cyanobacteria:their diversity in space and time, edited by B. A. Whitton and M. Potts, pp. 321–340, Kluwer Acad., Dordrecht, Netherlands., 2000.

Ward, B. A., Dutkiewicz, S., Moore, C. M. and Follows, M. J.: Iron, phosphorus, and nitrogen supply ratios define the biogeography of nitrogen fixation, Limnol. Oceanogr., 58(6), 2059–2075, doi:10.4319/lo.2013.58.6.2059, 2013.

Ward, B. B., Capone, D. G. and Zehr, J. P.: What 's new in the nitrogen cycle?, Oceanography, (June), 101–109, 2007.

Yallop, M. L., Anesio, A. M., Perkins, R. G., Cook, J., Telling, J., Fagan, D., MacFarlane, J., Stibal, M., Barker, G., Bellas, C., Hodson, A., Tranter, M., Wadham, J. and Roberts, N. W.: Photophysiology and albedo-changing potential of the ice algal community on the surface of the Greenland ice sheet., ISME J., 6, 2302–2013, doi:10.1038/ismej.2012.107, 2012.

Yergeau, E., Hogues, H., Whyte, L. G. and Greer, C. W.: The functional potential of high Arctic permafrost revealed by metagenomic sequencing, qPCR and microarray analyses., ISME J., 4, 1206–14, doi:10.1038/ismej.2010.41, 2010.

Zehr, J. P., Jenkins, B. D., Short, S. M. and Steward, G. F.: Nitrogenase gene diversity and microbial community structure : a cross-system comparison, Environ. Microbiol., 5(7), 539–554, 2003.

Zehr, J. P. and Mcreynolds, L. A.: Use of degenerate oligonucleotides for amplification of the *nifH* gene from the marine cyanobacterium *Trichodesmium thiebautii*, Appl. Environ. Microbiol., 55(10), 2522, 1989.

Zehr, J. P. and Turner, P. J.: Nitrogen fixation: Nitrogenase genes and gene expression, in Methods in Marine Microbiology, edited by J. H. Paul, pp. 271–286, Academic, San Diego, California., 2001.

Table 1. Number of samples screened for *nifH* gene amplification and confirmed *nifH* gene sequences retrieved.

Environment	**Total Samples**	**Samples with *nifH***	**Sequences retrieved**
Melt Ponds	8	3	26
Ice Top	8	8	211
Ice Bottom	13	4	91
Water under the ice	12	7	112
Open water	6	5	42
Algal aggregates	5	1	43

Figure 1. Stations sampled for *nifH* analysis in the Eurasian Basin of the Central Arctic during summer 2012. Average sea-ice concentration data source: www.meereisportal.de.

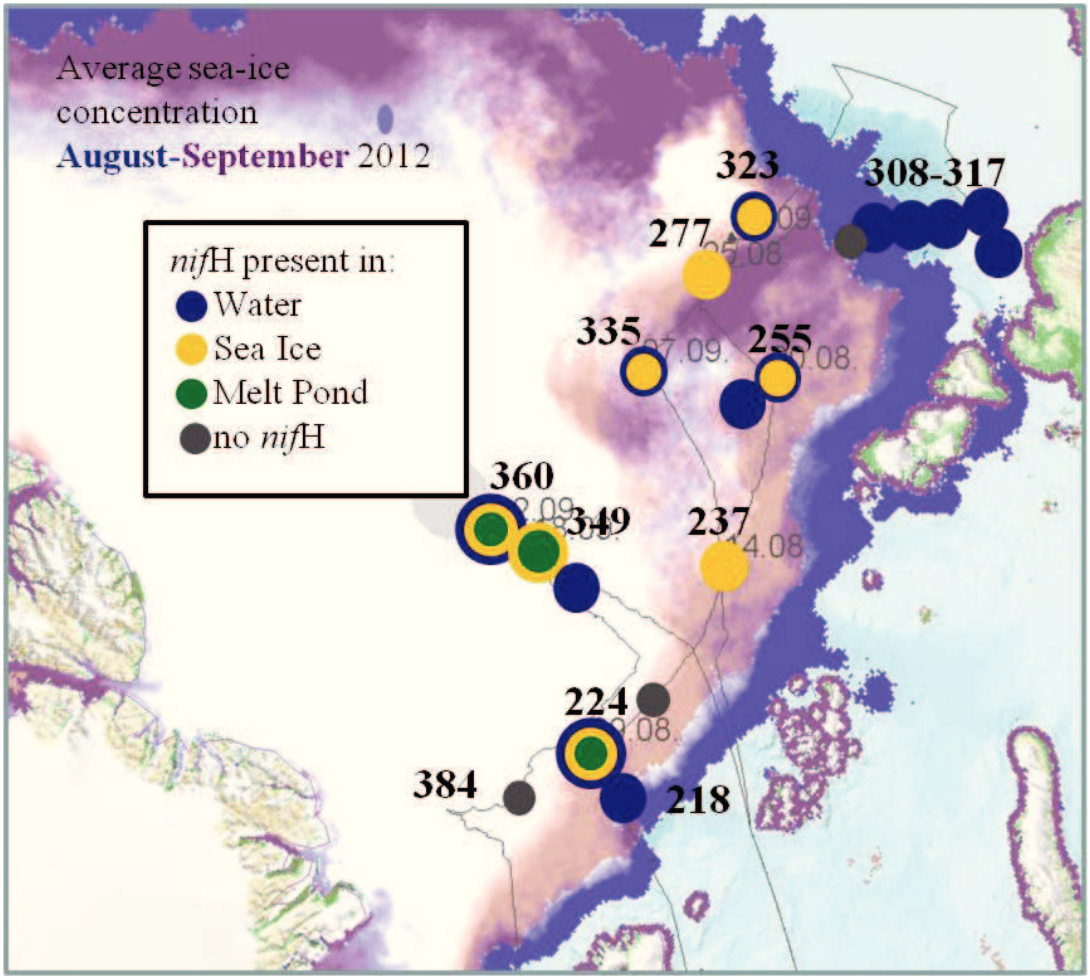

Figure 2. Surface water temperature during ARKXXVII/3 cruise in August-September 2012.

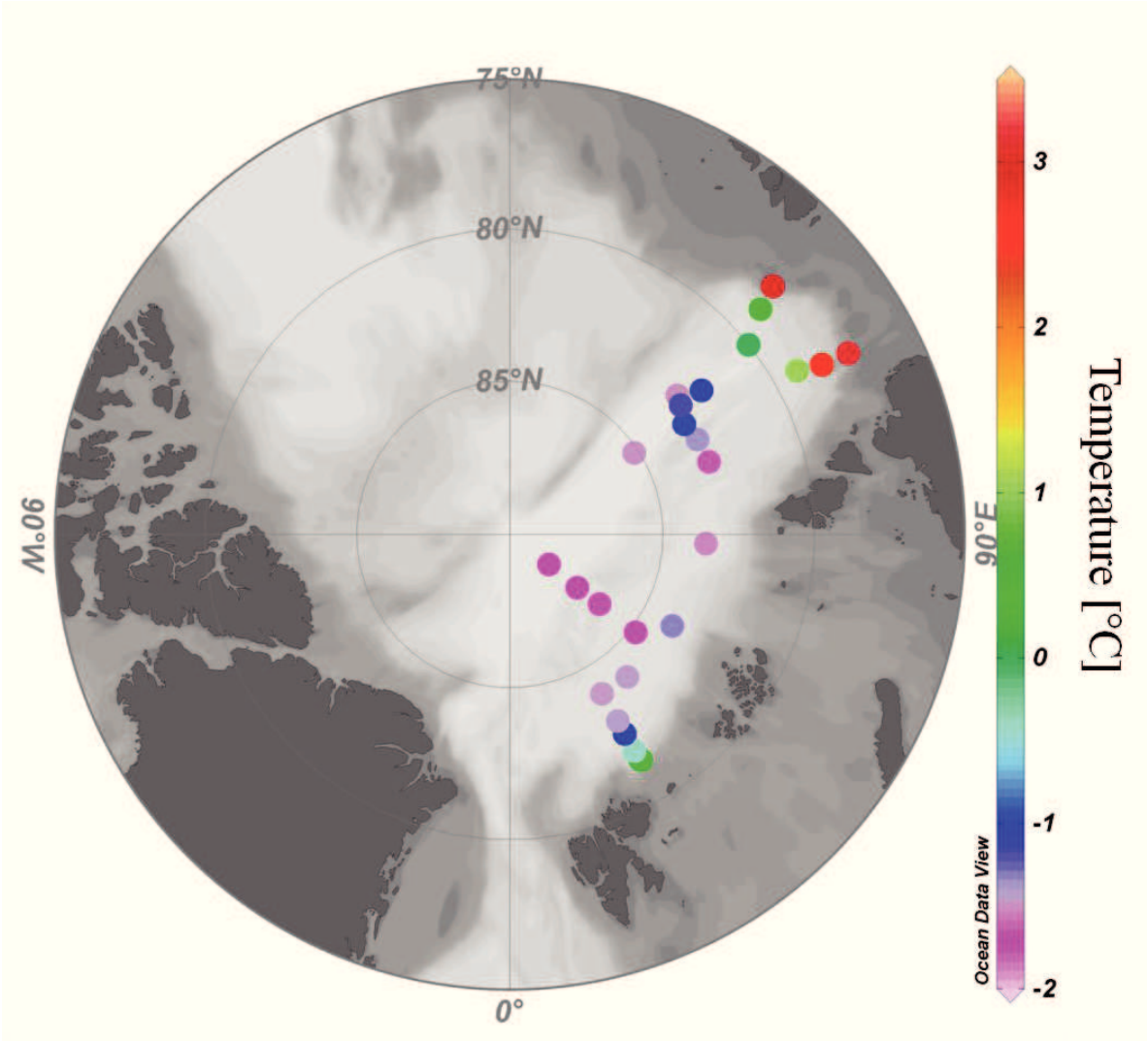

Figure 3. Nitrogen to phosphorous molar ratios in the water column and sea ice.

Values were calculated for the integrated euphotic zone (1% incoming irradiance) in the water column and for the average sea-ice thickness at each ice station. Bathymetry of the Arctic from Ocean Data View.

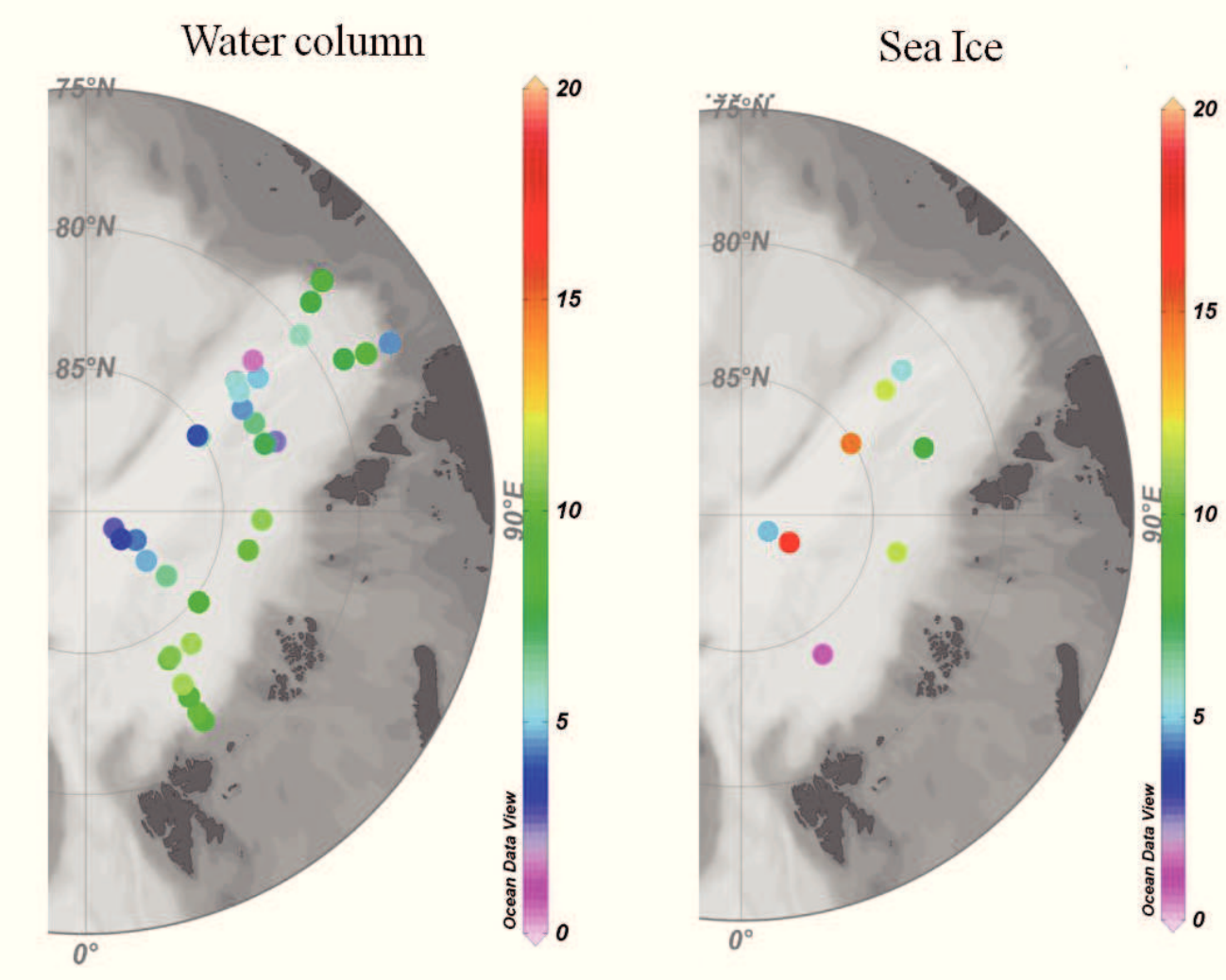

Figure 4. Relative sequence abundance of different subclusters of *nifH* genes. The number of sequences retrieved from each environment, are shown in brackets. Open waters correspond to the region close to the Laptev Sea.

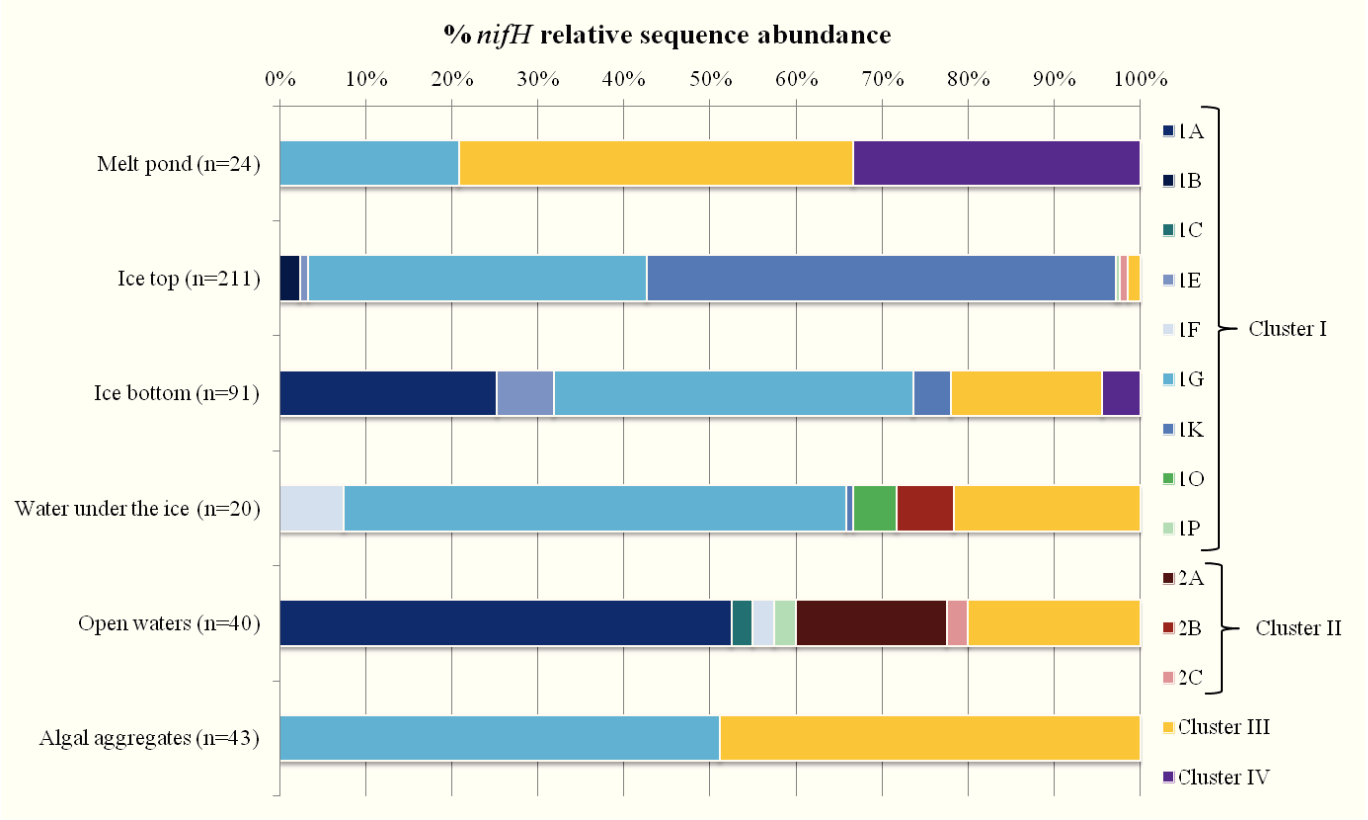

Figure 5. Neighbor-joining phylogenetic tree of *nifH* partial amino acid sequences.

Clones recovered in this study are in bold, *nifH* sequences from genome analysis are in italics and clones recovered in other Arctic marine studies are in grey (Blais et al. 2012 and Diez et al. 2012). The numbers in the clusters indicate the number of sequence in that cluster. Relationships were calculated with 1000 bootstraps and values >50% are shown. The origin of our sequences is indicated in the name. The station number is followed by the environment from which it originates: Ice Top (IT), Ice Bottom (IB), Brown Ice (BI), Melt Pond (MP), Algal aggregate (AGG), Water under the ice (WUI) and Surface water (SW). The number of the subcluster is indicated after the name.

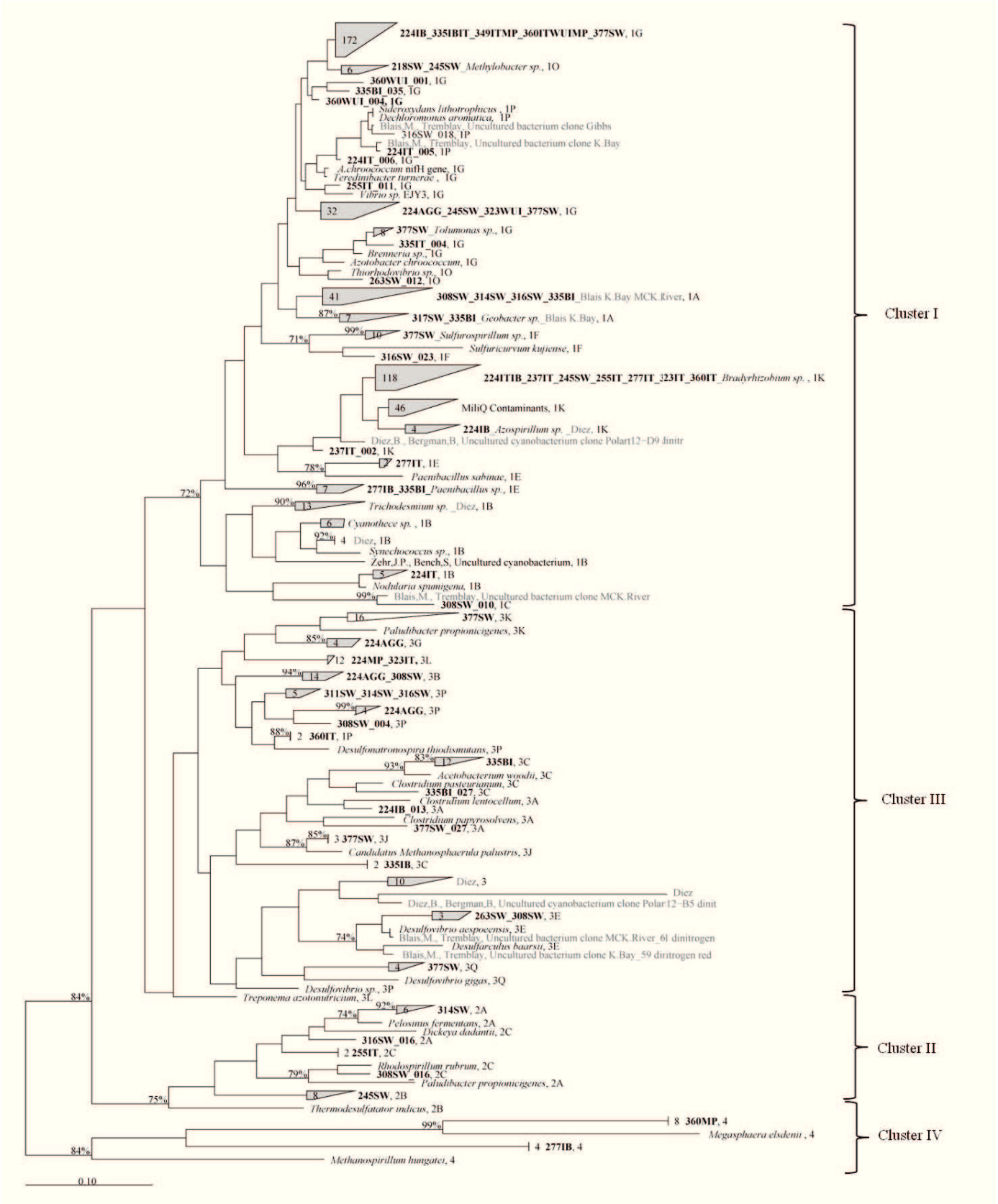
224IB_335IBIT_349ITMP_360ITWUIMP_377SW, 1G
218SW_245SW_Methylobacter sp., 1O
360WUI_001, 1G
335BI_035, 1G
360WUI_004, 1G
Sideroxydans lithotrophicus , 1P
Dechloromonas aromatica, 1P
Blais,M., Tremblay, Uncultured bacterium clone Gibbs
316SW_018, 1P
Blais,M., Tremblay, Uncultured bacterium clone K.Bay
224IT_005, 1P
224IT_006, 1G
A.chroococcum nifH gene, 1G
Terednibacter turnerae , 1G
255IT_011, 1G
Vibrio sp. EJY3, 1G
224AGG_245SW_323WUI_377SW, 1G
377SW_Tolumonas sp., 1G
335IT_004, 1G
Brenneria sp., 1G
Azotobacter chroococcum, 1G
Thiorhodovibrio sp., 1O
263SW_012, 1O
308SW_314SW_316SW_335BI_Blais K.Bay MCK.River, 1A
317SW_335BI_Geobacter sp._Blais K.Bay, 1A
377SW_Sulfurospirillum sp., 1F
Sulfuricurvum kujiense, 1F
316SW_023, 1F
224ITIB_237IT_245SW_255IT_277IT_323IT_360IT_Bradyrhizobium sp. , 1K
MiliQ Contaminants, 1K
224IB_Azospirillum sp._Diez, 1K
Diez,B., Bergman,B, Uncultured cyanobacterium clone Polart12−D9 dinitr
237IT_002, 1K
277IT, 1E
Paenibacillus sabinae, 1E
277IB_335BI_Paenibacillus sp., 1E
Trichodesmium sp._Diez, 1B
Cyanothece sp. , 1B
Diez, 1B
Synechococcus sp., 1B
Zehr,J.P., Bench,S, Uncultured cyanobacterium, 1B
224IT, 1B
Nodularia spumigena, 1B
Blais,M., Tremblay, Uncultured bacterium clone MCK.River
308SW_010, 1C
377SW, 3K
Paludibacter propionicigenes, 3K
224AGG, 3G
224MP_323IT, 3L
224AGG_308SW, 3B
311SW_314SW_316SW, 3P
224AGG, 3P
308SW_004, 3P
360IT, 1P
Desulfonatronospira thiodismutans, 3P
335BI, 3C
Acetobacterium woodii, 3C
Clostridium pasteurianum, 3C
335BI_027, 3C
Clostridium lentocellum, 3A
224IB_013, 3A
Clostridium papyrosolvens, 3A
377SW_027, 3A
377SW, 3J
Candidatus Methanosphaerula palustris, 3J
335IB, 3C
Diez, 3
Diez
Diez,B., Bergman,B, Uncultured cyanobacterium clone Polar12−B5 dinit
263SW_308SW, 3E
Desulfovibrio aespoeensis, 3E
Blais,M., Tremblay, Uncultured bacterium clone MCK.River_61 dinitrogen
Desulfarculus baarsii, 3E
Blais,M., Tremblay, Uncultured bacterium clone K.Bay_59 diritrogen red
377SW, 3Q
Desulfovibrio gigas, 3Q
Desulfovibrio sp., 3P
Treponema azotonutricium, 3L
314SW, 2A
Pelosinus fermentans, 2A
Dickeya dadantii, 2C
316SW_016, 2A
255IT, 2C
Rhodospirillum rubrum, 2C
308SW_016, 2C
Paludibacter propionicigenes, 2A
245SW, 2B
Thermodesulfatator indicus, 2B
360MP, 4
Megasphaera elsdenii , 4
277IB, 4
Methanospirillum hungatei, 4
0.10
Cluster I
Cluster III
Cluster II
Cluster IV

Figure 6. Two dimensional NMDS ordination plot of *nifH* subclusters in each sample (Jaccard dissimilarity index).

Laptev Sea (LS) samples are in dark blue, Ice Top (IT) in brown, Ice bottom (IB) in yellow, Surface waters (SW) in blue, Melt Ponds (MP) in light blue, and Aggregates (AGG) in green. Points within each group are connected to their group centroid with a spider diagram. The light pink ellipses show 95% dispersion of each group. The stress of the plot is 0.08. An ANOSIM post hoc test showed that the Laptev Sea samples are significantly different from the sea-ice environment samples (R=0.46, p=0.003).

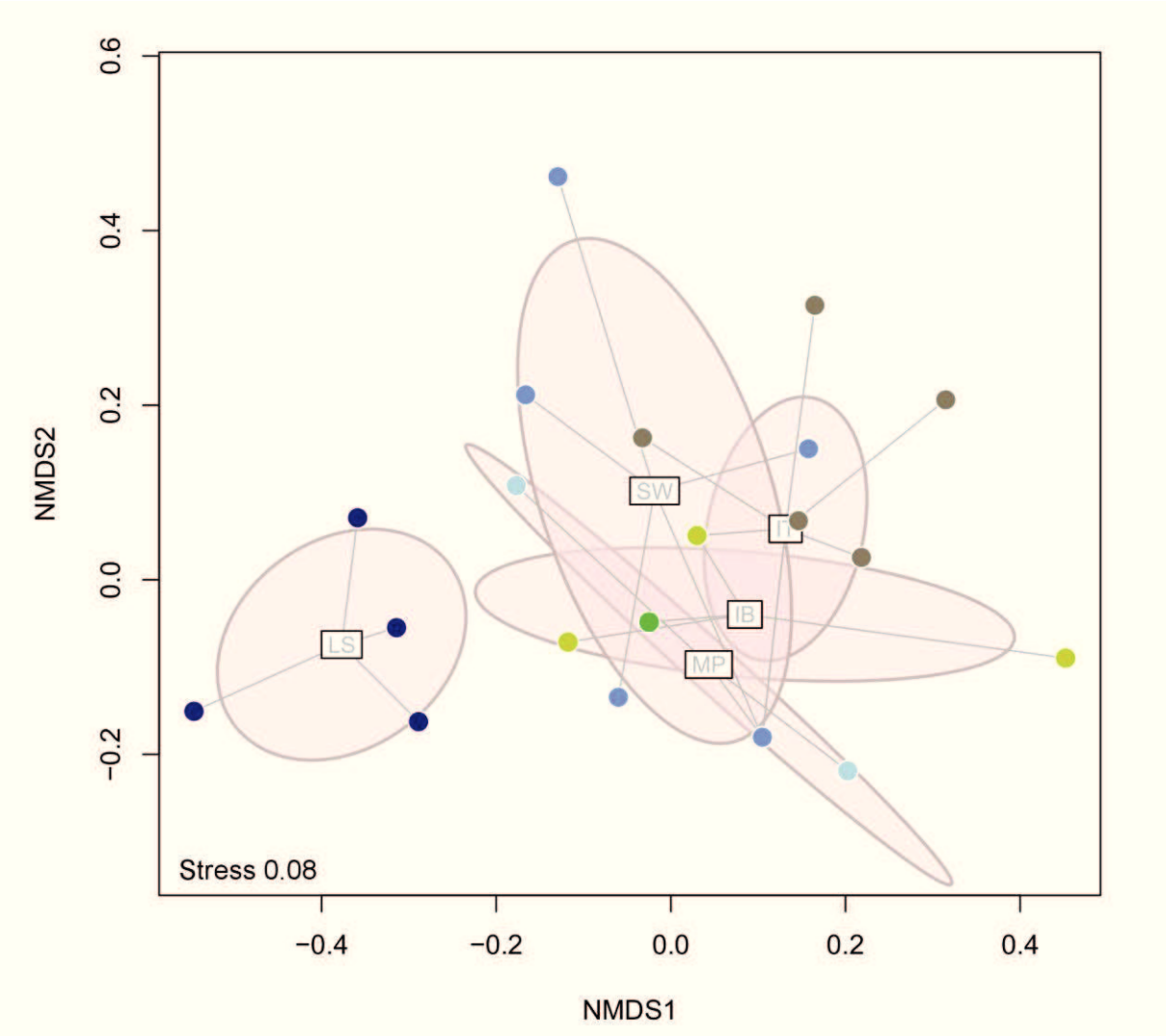

Figure 7. Two dimensional NMDS ordination plot of 16S rRNA OTUs in each sample (Bray Curtis dissimilarity index).

Laptev Sea (LS) samples are in dark blue, Ice Top (IT) in brown, Ice bottom (IB) in yellow, Surface waters (SW) in blue, Melt Ponds (MP) in light blue, and Aggregates (AGG) in green. Points within each group are connected to their group centroid with a spider diagram. The light pink ellipses show 95% dispersion of each group. The stress of the plot is 0.13. An ANOSIM post hoc test showed that the Surface water (R=0.29, p=0.008), Ice Top (R=0.22, p=0.01) and Aggregate (R=0.8, p=0.02) samples are significantly different from the rest.

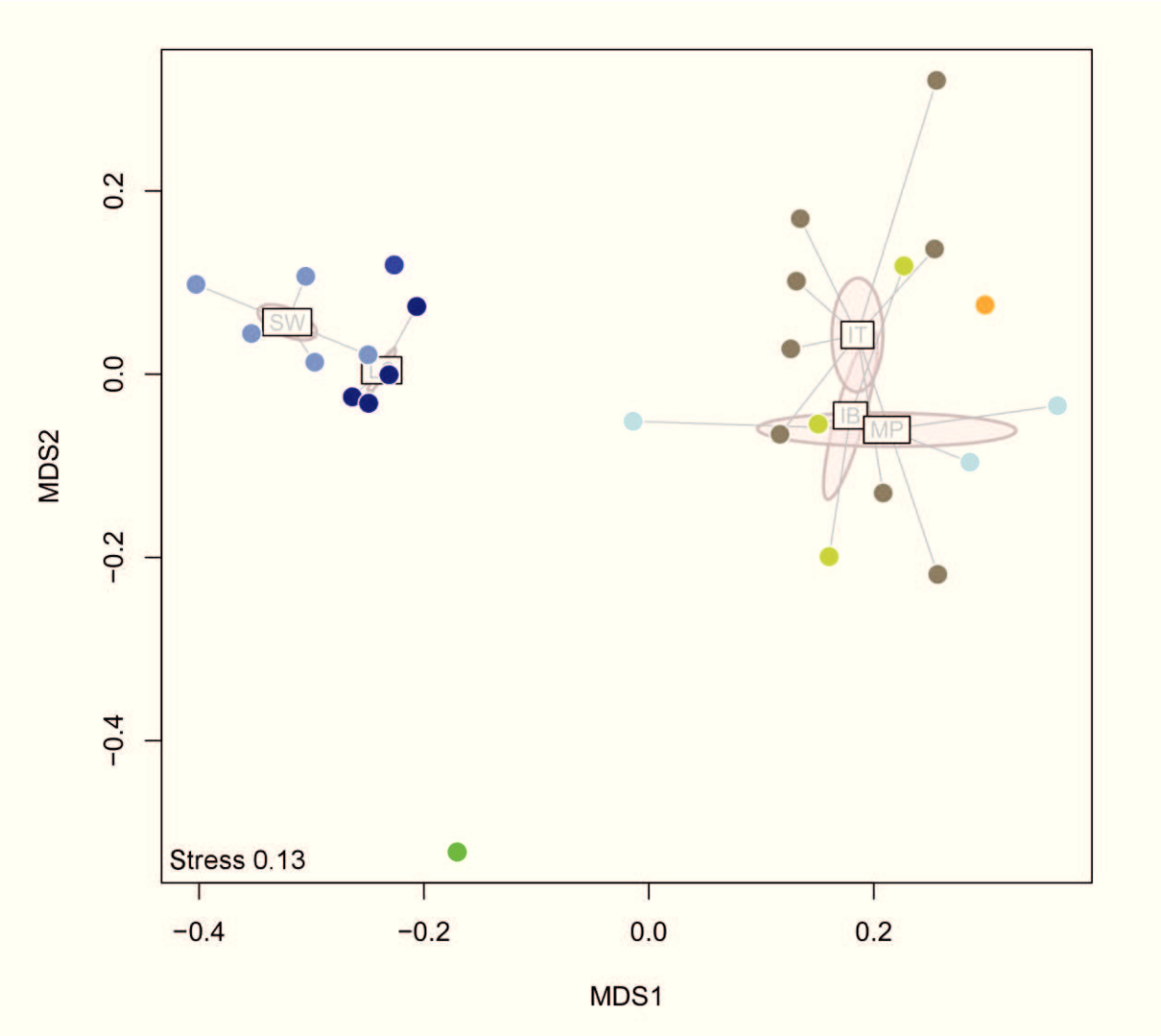

Table S1. Main subclusters and number of sequences retrieved in each Arctic environment.

Subcluster (#sequences)	**Sea Ice (310)**	**Algal aggregate (43)**	**Melt Ponds (26)**	**Water under the ice (123)**	**Open waters (42)**	**Major phylogenetic group based on 16SrRNA Class (Genus)**
Sample #	12	1	3	7	5	Total=28
1A (44)	■				■	*Deltaproteobacteria (Geobacter)*
1B (5)	■					*Cyanobacteria*
1C (1)					■	No cultivated isolates
1E (8)	■					*Firmicutes (Paenibacillus)*
1F (10)				■	■	*Epsilonproteobacteria (Arcobacter)*
1G (218)	■	■	■	■		*Gammaproteobacteria (Azotobacter)*
1K (120)	■		■	■	■	*Alpha- and Betaproteobacteria*
1O (6)				■		*Gammaproteobacteria (Methylobacter)*
1P (2)	■				■	*Betaproteobacteria*
2A (7)					■	*Firmicutes (Pelosinus) and Bacteroidetes (Paludibacter)*
2B (8)				■		*Archaea*
2C (3)	■				■	*Alphaproteobacteria (Rhodobacter)*
Cluster III (85)	■	■	■	■	■	*Deltaproteobacteria, Firmicutes and Spirochaetes.*
Cluster IV (12)	■		■			Non-functional nitrogenases. *Archaea*

Figure S1. Comparison between *nifH* and 16SrRNA relative sequence abundance of samples with potential diazotrophs at stations 224 and 349.

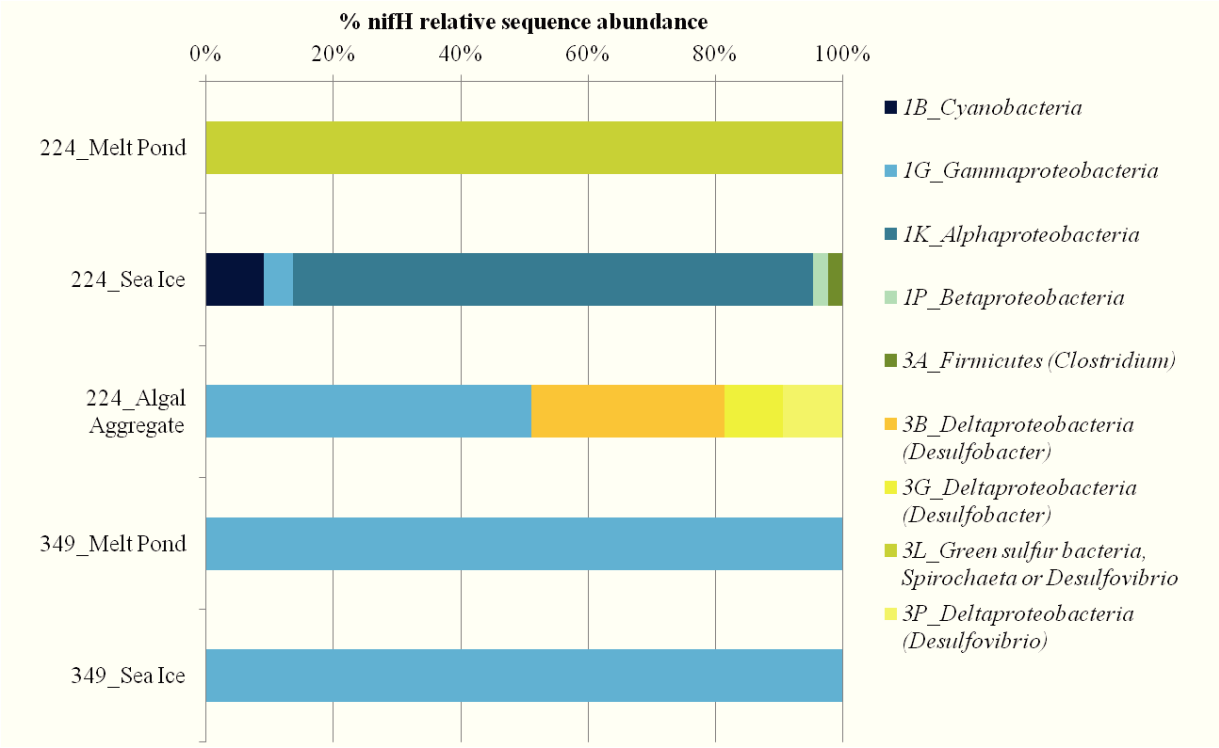

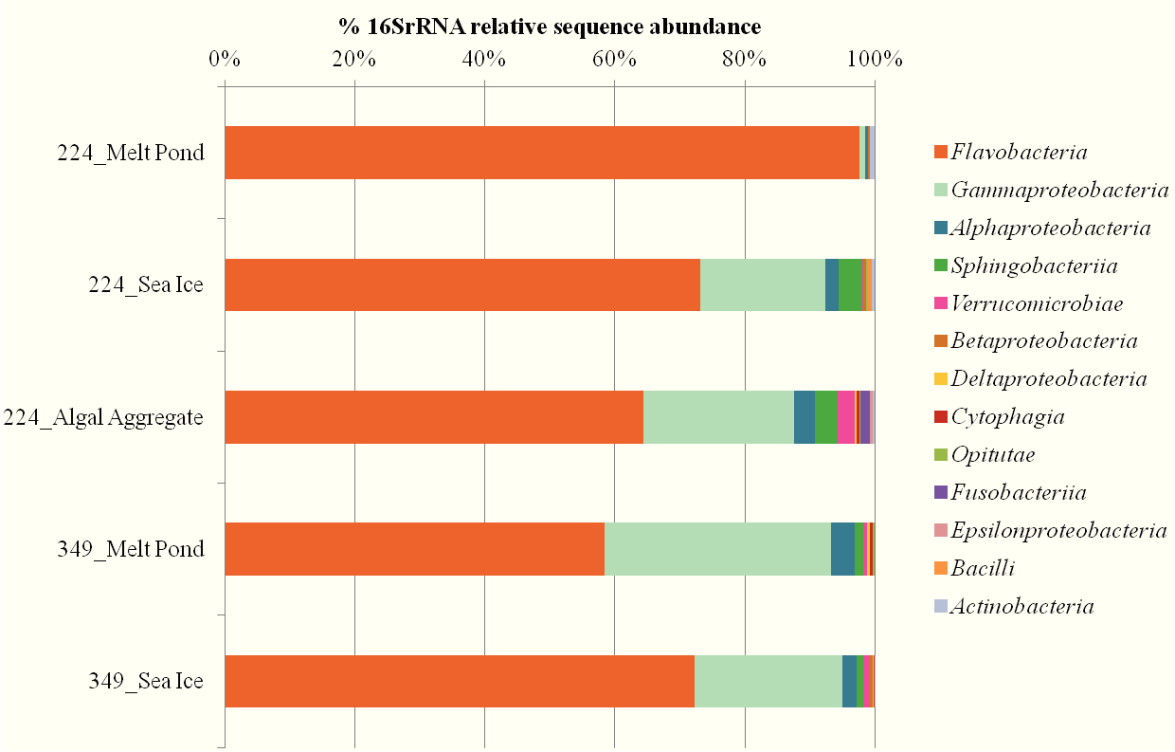

Figure S2. Ice flow tracking of ice floes sampled in summer 2012.

Grey lines represent the track of the ice floes sampled in summer 2012 from their formation close to the coast to the moment of sampling.

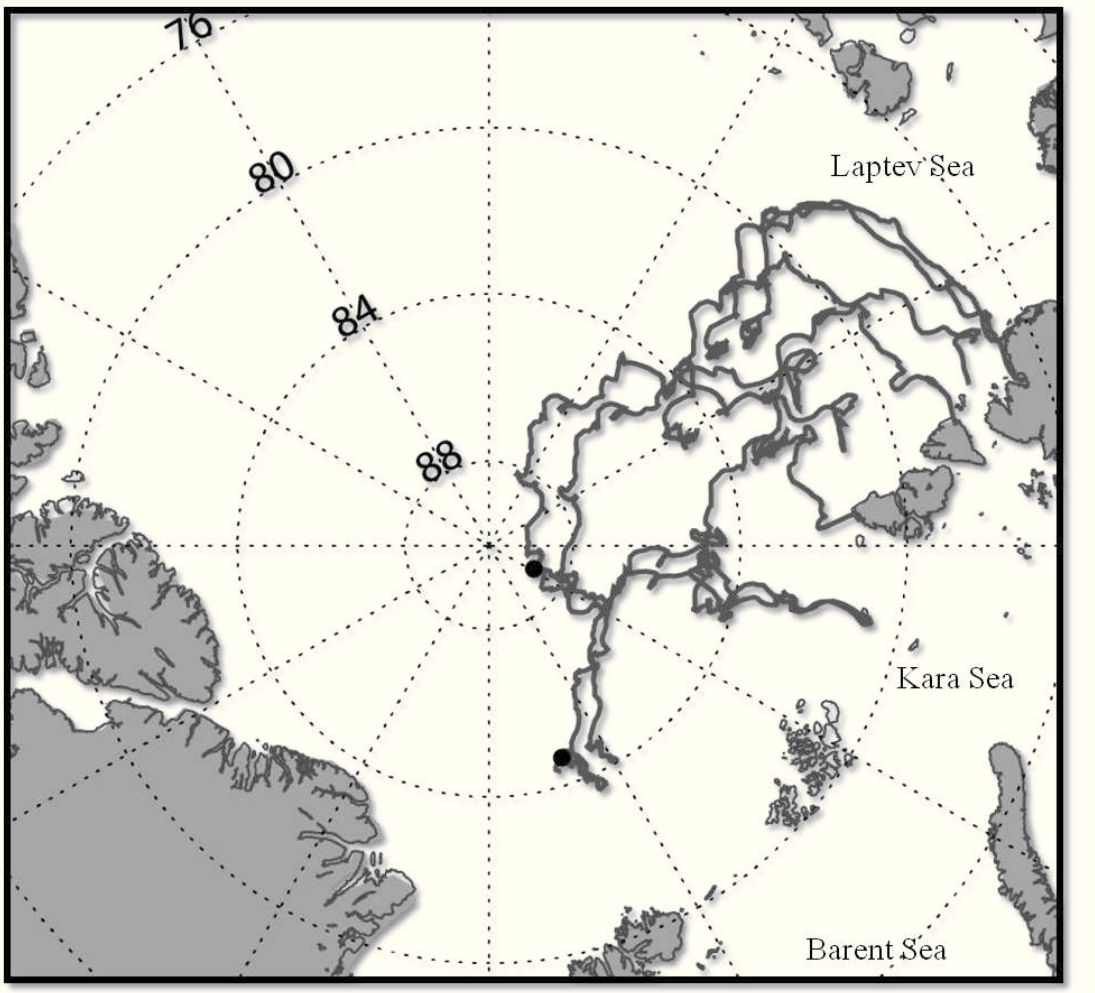

3. Discussion

The Central Arctic basins cover half of the Arctic Ocean, yet, due to their difficult access little is known about the ecological processes occurring in and below the mostly perennial (MYI) sea-ice cover. When I started this thesis there were only two studies that included measurements of primary productivity in water and sea ice of the Central Arctic basins (Gosselin et al., 1997; Olli et al., 2007). Many questions were unanswered, such as, how much productivity does the Central Arctic host, and how does sea ice affect the limiting factors of photosynthetic carbon fixation. Moreover, the Arctic´s ice cover has been receding rapidly due to global warming in the last decades (Polyakov et al., 2012; Stroeve et al., 2012), emphasizing the urgency to understand the processes regulating the amount of energy entering the ecosystem, as well as to define the boundary conditions in which change will most likely occur. This is crucial to predict how further sea-ice retreat will affect primary productivity in the Central Arctic Ocean.

In the following sections, first, the contribution of this thesis to improve our understanding of the Central Arctic ecosystem at different scales will be discussed from a broader perspective. Secondly, the role of sea-ice algal aggregates on carbon and nutrient fluxes, the impacts of sea-ice retreat on primary production, and the role of diazotrophs in constraining new production in the Central Arctic Ocean will be discussed. Finally, two potential future scenarios for Central Arctic primary production based on the acquired knowledge will be proposed.

3.1. Improvements in our understanding of the Central Arctic ecosystem.

The variety of methods used during this thesis allowed us to characterize and quantify primary productivity in the Central Arctic, as well as enabling us to determine the factors limiting primary production at different temporal and spatial scales. Yet, the main limitations to assessing the impact of sea-ice retreat on Central Arctic primary production were the lack of a comprehensive baseline, and high spatial variability. However, this thesis contributes both to creating a baseline for future studies and to increasing the number of observations of the highly variable and under-sampled Central Arctic.

We have shown that the ice-covered Central Arctic hosted substantial new annual production in 2012 (9 ± 3 g C m^{-2} yr^{-1}, Chapter V). This value is low compared to some of the Arctic shelves and adjacent seas (100-160 g C m^{-2} yr^{-1} in the Barents and Chukchi Sea, Sakshaug et al., 2004), but is one order of magnitude higher than previous estimates for the Central Arctic Basins (~1 g C m^{-2} yr^{-1}, Sakshaug et al., 2004). Although sea-ice cover was substantially reduced in 2012, we could not detect significant changes in annual new production compared to other new production estimates calculated with the few pre-bloom nutrient profiles available from all years for the Central Basins (Codispoti et al., 2013). To assess the impact of sea-ice retreat on annual primary production in the Central Arctic, long term measurements are required.

In agreement with one previous study from the Central Arctic in summer 1994 (Gosselin et al., 1997), we have confirmed that sea-ice algae strongly contribute (up to 60%) to total net primary productivity (NPP), in particular at the end of the productive season, north of 80 ºN (Chapter V). Furthermore, our results showed that sub-ice algal aggregates, which were not considered before in estimates of primary productivity, can contribute between 20 and 90% to total primary productivity at a local scale (Chapter III). Constraining this range and scaling up their contribution to the entire basin still remains a challenge due to their patchiness. Nevertheless, our results suggested that these sub-ice algal aggregates were relevant for carbon export to the benthos early in the season (July), and relevant as a food source for under-ice fauna at the end of the productive season (August-September) in 2012.

Previous to this study, the Amerasian and Eurasian Basins were both considered similarly oligotrophic areas of the Central Arctic. However, according to our nutrient measurements in the Eurasian Basin in August 2012, the areas influenced by Atlantic water inflow still contained nitrate in the mixed layer (2-4 μmol L^{-1}). Indeed, recent nutrient synthesis studies suggest that the Amerasian Basin has lower nutrient concentrations than the Eurasian Basin; the first being more nutrient limited and the latter more light limited (Codispoti et al., 2013; Popova et al., 2010). However, these synthesis studies point out that their conclusions are based on very scarce data from the Central Basins. Our N:Si ratios in the euphotic zone in 2012, revealed two different nutrient regimes in the Eurasian Basin in late summer: a nitrate limited region close to the Laptev Sea region in the Amundsen Basin and a silicate limited region close to the ice margin in the Nansen Basin (Chapter V). This dataset refines and increases our knowledge of the Eurasian Basin. However, further oceanographic data is needed to understand inter-annual variability and seasonal nutrient supply mechanisms. In

particular, the role of advection needs to be quantified since in the strongly stratified Central Arctic Ocean lateral transport is more likely to provide nutrients than vertical mixing (Popova et al., 2013).

From a modeling perspective, strong efforts have been made in the last 5 years to determine the temporal and spatial scales on which nutrients and light modulate primary productivity to predict future changes in productivity due to sea-ice retreat (Popova et al., 2012). However, there is still a lack of ground truth data from the Central Arctic to validate remote sensing data and model simulation results. To calculate NPP from available light, the photosynthetic parameters derived from PI curves measured *in situ* are needed (Behrenfeld and Falkowski, 1997). This thesis provides the first comprehensive set of photosynthetic parameters for sea ice, melt ponds and water column of the Central Arctic (Chapter V). However, due to the high spatial and temporal variability of the dataset, the ranges for each environment are not as well constrained as in other studies in which samples were taken within a smaller area in a shorter period of time (e.g. Palmer et al., 2014). Moreover, measurements presented in this thesis, as well as in other studies, are only representative of algae in late summer (Huot et al., 2013; Mundy et al., 2011). Therefore, further seasonal studies are needed to improve predictions of annual primary production.

State of the art physical ice-ocean models capture seasonal and interannual variations of Arctic sea-ice area and water circulation correctly (Jin et al., 2012). The light parameterization developed during this thesis in collaboration with the sea-ice physics group has improved our ability to quantify the amount of light that is transmitted through the ice and fuels under-ice productivity (Arndt and Nicolaus, 2014; Katlein et al., 2014; Nicolaus et al., 2012). This light parameterization can be applied to existing Arctic primary productivity models that include sea-ice cover. However, despite improvements in sea-ice dynamics and light parameterization, even state of the art predictive models disagree on the direction of change for primary production in an ice-free Arctic (Vancoppenolle et al., 2013). The main reason for this uncertainty is the lack of nutrient data from the Central Basins especially for pre-bloom situations (Codispoti et al., 2013). Therefore, in order to improve the capability of models to predict primary productivity in the Arctic Ocean, a better nutrient climatology needs to be developed. Moreover, biological parameters such as zooplankton annual life cycles and carbon demand need to be further investigated in the central basins to improve our primary

production predictions. Despite all the remaining unanswered questions, this thesis provides insight into key processes that were previously uncharacterized in the Central Arctic.

3.2. The role of sea-ice algal aggregates on carbon and nutrient fluxes

Sea-ice algal aggregates have been observed trapped in melt ponds, floating or hanging below the sea-ice and in the deep sea (Gutt, 1995; Melnikov, 1977; Syvertsen, 1991). However, their role in the Arctic ecosystem has never been studied in depth mainly due to their patchiness and difficulties in sampling them. There are two main types of sub-ice algal aggregates: spherical aggregates formed by pennate diatoms and filamentous aggregates formed by *Melosira arctica* (Chapter III). In this thesis, the characterization and quantification of the role of Arctic sub-ice algal aggregates in carbon and nutrient cycling was carried out for the first time.

Our observations of freshly-sedimented algal aggregates on the deep seafloor of the Eurasian Basin during the sea-ice minimum record in summer 2012 showed that sea-ice algal aggregate sedimentation is relevant (85%) for carbon export in years of extensive ice melt (Chapter I). Increases in the carbon export flux to the seafloor due to sea-ice retreat had been previously observed in the Lapteve Sea in summer 2007 when sea-ice extent reached its first minimum record (6.5 g C m^{-2} yr^{-1}, Lalande et al., 2009). However, this carbon flux was mainly composed by detritus and not fresh ice algae. The high amounts of ice algal carbon observed at the sea floor in summer 2012 (median 9 g C m^{-2}), was 10 times higher than total carbon export fluxes measured in the Central Arctic using the thorium disequilibrium method in summer 2007 (~0.1 g C m^{-2}, Cai et al., 2010) and two orders of magnitude higher than total carbon export fluxes measured with short-term sediment traps in August-September 2012 during the same expedition (Average 0.03 g C m^{-2} d^{-1}, Lalande et al., 2014). This indicates that the main ice algal export event in 2012, occurred earlier in the season, probably in July, stressing the importance of the time of sampling for carbon export estimates.

The contribution of these algal aggregates to total new annual production was estimated to be 45% in the Eurasian Basin (Chapter I). Thus, primary production studies or models that neglect sea-ice algae are missing a potentially important part of the productivity. Furthermore, the aggregates that remained below the ice at the end of the season contributed 20-90% to depth integrated NPP at a local scale (Chapter III). Due to their patchiness it still remains a

challenge to extrapolate their contribution to larger scale. As discussed in Chapter IV, their contribution can vary several orders of magnitude depending on the carbon conversion and the upscaling method used. In general, improvements have been made in quantifying this very patchy and rarely studied phenomenon (Ambrose et al., 2005), but further large scale surveys are needed to be able to include sub-ice algal aggregates in primary productivity models. Once they are properly quantified and the mechanisms responsible for their distribution understood, their contribution to carbon fixation and export in a potentially ice-free future Arctic can be predicted.

Besides their significant contribution to biomass and productivity, our studies indicate that sub-ice algal aggregates have an important role in the ecosystem. At the end of the productive season, sub-ice algal aggregates that did not sink, were either floating below the ice or trapped in melt ponds. Aggregates trapped in melt ponds were mainly degraded (yellow-whitish color) probably due to high irradiances and low nutrient concentrations (Kiorboe and Hansen, 1993), while aggregates floating below the ice were dark green-brownish and contained a healthy algal community (Chapter III). Grazers such as ciliates, copepods and amphipods were observed feeding on the green-brownish aggregates formed by pennate diatoms. In addition, pigments indicative of grazing were detected in the aggregates (Chapter II). These observations suggest that sub-ice algal aggregates were an important food source for ice-associated fauna at the end of the productive season (September) when the sea-ice algae and phytoplankton blooms were already over. Preliminary experiments to understand the processes regulating buoyancy versus sinking showed that algal aggregate buoyancy might be regulated by photosynthetic oxygen production (Chapter III). Previous physiological studies with diatoms have shown a correlation between increased light input and reduced sinking rates (Waite et al., 1992). If the regulating effect of light on aggregate buoyancy is confirmed, we hypothesize that on the short term, as sea-ice is getting thinner in summer (Renner et al., 2014), small aggregates (1-30 cm) below the ice will receive more light (Nicolaus et al., 2012) and remain floating longer before sinking, depleting nutrients further in the mixed layer .

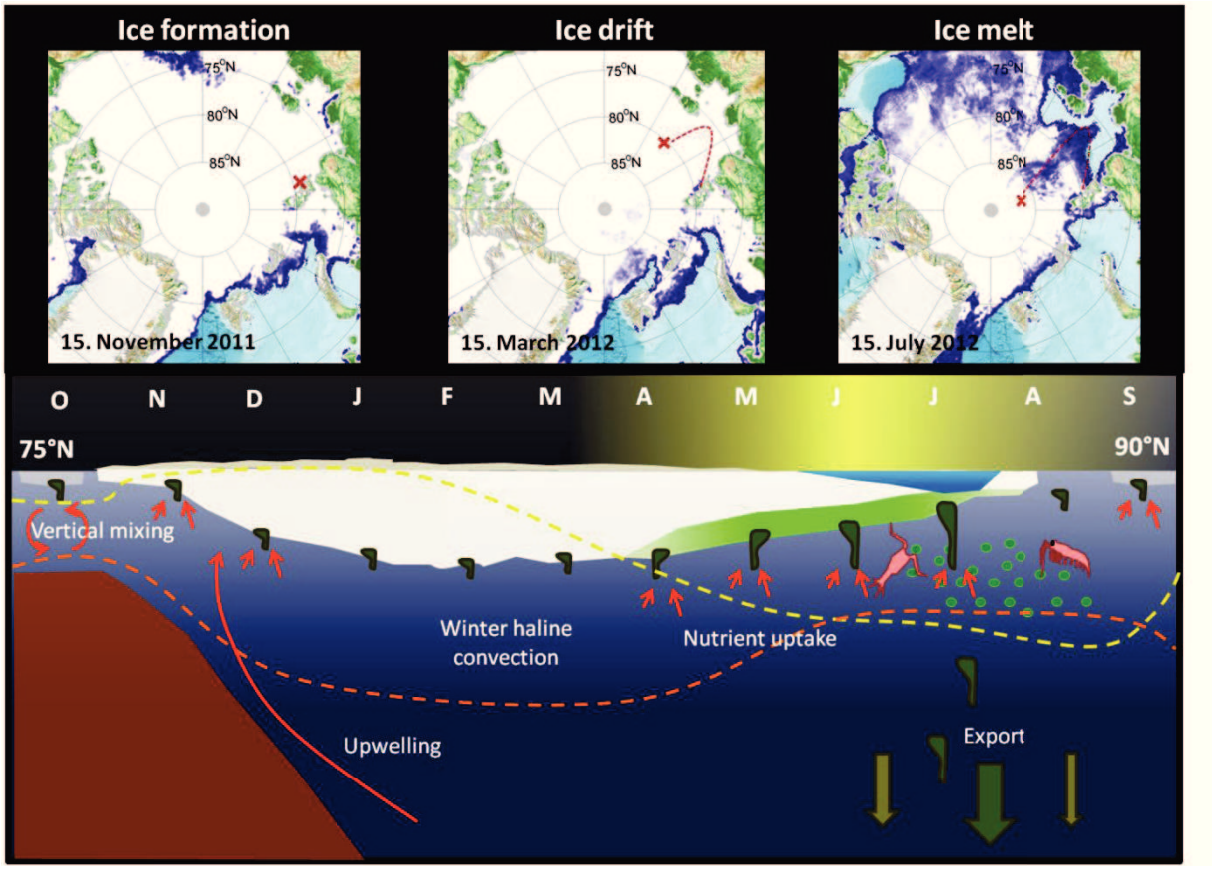

Figure 6. Conceptual scheme of the life cycle of sub-ice algal filaments of *Melosira arctica* in the Eurasian Basin.

The upper panels show the sea ice concentration evolution from winter to summer 2011-2012. The red cross symbolizes the location of the processes presented in the lower panel. The lower panel shows the evolution of sea ice from its formation in winter on the shelves to its melt in the Central Arctic after being transported by the Transpolar Drift. The orange dashed line symbolizes the mixed layer depth and the yellow dashed line the euphotic zone depth. Sub-ice algal filaments take up nutrients (small orange arrows) during winter from the shelves and the shelf edge upwelling and store them in their cytoplasm. When the ice gets thinner (1m) and they get enough light they start growing and in a short period of time they build up large biomass below the ice. In early July as the ice melts rapidly, the largest filaments (15-100 cm) sink to the deep sea and some smaller (2-15 cm) aggregates remain as food source for under ice fauna and zooplankton. Some filaments remain floating as the ice melts and gets refrozen into newly formed ice in autumn.

Our experiments indicate that sub-ice algal aggregates contribute both to nutrient remineralization (Lehto et al., 2014) and depletion below summer sea-ice while they remain

floating (Chapter III). An interesting question remains regarding the mechanism used by sub-ice algal aggregates to retrieve enough nutrients to sustain their elevated biomass in such an oligotrophic ocean. Apart from having high C:N ratios (10-28) and therefore, low nitrate requirements (at least at the end of the season), sea-ice algae might have the capacity to store nutrients in their cytoplasm (Kamp et al., 2011), as we observed in our nutrient addition experiments (Chapter V). We suggest that the filament-forming sub-ice algae *Melosira arctica* drifts together with the sea ice, accessing a wide area of surface water nutrients (Fig.6). With the shift from MYI to FYI, sub-ice algae now have less time to grow and form long filaments, but observations of up to 1m long strings hanging from FYI indicate that it is possible (Poulin et al., 2014). Observations from sediments traps (Lalande et al., 2014) and with a ROV under the ice (Chapter IV) indicate that *Melosira* filaments are mainly found in shelf areas, following the transpolar drift. Sea ice is formed at the shelves, where vertical mixing supplies the surface with nutrients (Rudels, 1995). In addition a large quantity of suspended particulate matter is incorporated into this newly formed ice that is then transported into the deep Arctic Ocean by strong southerly winds (Wegner et al., 2005). Sub-ice algae can store nutrients while the ice is formed and use them later while the ice drifts. During the growth season they can access nutrients from surface waters as they drift towards the Central Arctic. When the bottom of the ice starts melting in July, the biggest filaments detach and sink to the deep sea feeding the benthos (Chapter I), while some smaller filaments remain floating below the ice (Chapter II-IV). The aggregates that avoid grazing and sinking can get refrozen in newly formed ice and seed the sub-ice algal filaments next spring (Fig.6).

In the long term, however, when the Arctic crosses its tipping point and summer sea-ice disappears - around 2050 as suggested by model results (Wang and Overland, 2012) - their life cycle will not be sustainable anymore and they will disappear, resulting in a substantial decrease in sea-ice related productivity and ice-algal export to the benthos. Moreover, if it is confirmed that sub-ice algae´s initial growth takes place at the Arctic shelves, the effects of earlier sea-ice retreat at lower latitudes will affect their life cycle even before the Central Arctic is entirely ice-free.

3.3. Impacts of sea-ice retreat on primary production at different temporal and spatial scales.

Climate driven sea-ice retreat is already affecting the Central Arctic marine ecosystem (Wassmann et al., 2011). The reduction in MYI is causing a shift from perennial to seasonal ice zones in large areas of the Eurasian Basin. Yet how this shift will affect the carbon and nutrient cycles in the Central Arctic north of 78ºN is difficult to predict due to the complexity of the physical and biological feedback processes. Sea-ice retreat does not only imply loss of habitat for sea-ice algae, but also for under-ice fauna (Johannessen and Miles, 2011), as well as increased light reaching the water column (Nicolaus et al., 2012), increased freshening and stratification due to ice melt, and probably less upwelling events in the Central Basins (Carmack and McLaughlin, 2011).

A straight forward approach to study the effect of all these changes on primary production is to compare annual new production in years of low ice cover, such as the record minimum in 2012, with previous years of higher sea-ice cover. However, we encountered two problems when trying to do this for the Central Arctic Ocean. First, due to high spatial variability, the range of primary production estimates was quite large. Secondly, there was a lack of a proper baseline to compare our results to, with only one study using a similar method to estimate new production based on nutrient draw-down (Codispoti et al., 2013). Therefore, despite sampling during the sea-ice extent minimum record in summer 2012, when 45% of the Eurasian Basin was ice-free, we found no significant difference in the annual new production (9.4 ± 3.6 g C m^{-2} yr^{-1}, n=33) compared to previous estimates from years with more ice cover (13 ± 11 g C m^{-2} yr^{-1}, n=56, Codispoti et al., 2013) (Chapter V). Nevertheless, when adding the estimates of carbon exported to the deep sea early in the season to our calculations, the Eurasian Basin annual production estimate doubles (from 17 to 33 Tg C yr^{-1}). This calculation assumes that sub-ice algae access nutrients from broader areas and are therefore not taken into account when calculating nutrient draw-down from individual profiles. However, this does not necessarily mean that total annual production in the Central Arctic was higher due to sea-ice retreat. It could as well mean that previous estimates neglected sub-ice algal aggregate productivity due to the difficulty in sampling them and upscaling their contribution.

Primary productivity in the Arctic Ocean is bottom-up constrained by light and nutrient availability and top-down by grazers (Olli et al., 2007; Tremblay and Gagnon, 2009). Sea-ice

retreat will indirectly affect both physical and biological limiting factors with consequences for primary productivity. As sea ice gets thinner (Renner et al., 2014) and melt-pond coverage increases (Rösel and Kaleschke, 2012), more light is transmitted through sea ice (Frey et al., 2011; Nicolaus et al., 2012). Since sea-ice algae and under-ice phytoplankton in the ice-covered Central Arctic are light limited (Chapter V), this would enhance primary productivity in and below sea ice as observed in other Arctic regions (Palmer et al., 2014). This initial increase could be limited by photoinhibition as we observed for sea-ice algae trapped in melt ponds (Chapter V). NPP in the Central Arctic was lower below the ice than in open waters probably due to light limitation (Chapter V). Therefore, the increase in proportion of ice-free waters could favor phytoplankton productivity on a regional scale (Arrigo et al., 2008). However, increased cloudiness due to enhanced evaporation in open waters might lessen this increase (Bélanger et al., 2013; Bintanja and Selten, 2014). In addition, sea-ice retreats earlier in the season increasing the length of the productive season (Stroeve et al., 2012). As we hypothesized in Chapter V, this could promote an earlier sea-ice algal bloom that could consume most of the nutrients in surface waters and then sink to the seafloor, followed by a weak phytoplankton bloom below the ice.

The magnitude of the increase in primary productivity caused by higher light availability is also constrained by nutrients. Melting of sea ice can both enhance and reduce nutrient supply. Freshwater accumulation increases stratification limiting the nutrient supply from deep layers and shelves, while uplifted isohaline surfaces can supply nutrients from the deep layers in the Eurasian Basin (Nishino et al., 2011) as we observed at an ice station close to the ice margin (Chapter V). In addition, later freezing facilitates wind-driven mixing that can promote a second phytoplankton bloom in autumn as it was observed in the Amerasian Basin (Ardyna et al., 2014). On the shelves, nutrient input may increase due to enhanced river runoff (Peterson et al., 2002). However, nutrients of riverine origin will probably be consumed at the shelves and will not reach the Central Basins (Le Fouest et al., 2012).

Our nutrient addition experiments and the nutrient ratios in the euphotic zone at the end of the productive season in 2012 showed that nitrate and silicate were the main limiting nutrients in the Eurasian Basin (Chapter V). According to a recent model study that included horizontal nutrient transport, the Eurasian Basin is replenished with nutrients through the Atlantic inflow waters that reach the surface by upwelling events after 5 years (Popova et al., 2013). According to our observations in 2012, the Atlantic influenced waters are rich in nitrate (3-8 μmol L^{-1}) and influence the Nansen Basin, where silicate is the limiting nutrient

for diatom growth (N:Si ratios >2). Current nutrient budgets suggest that there is an imbalance in the nitrate supply and demand in the Arctic Ocean and that there is a net export of silicate to the North Atlantic (Torres-Valdés et al., 2013). This indicates that there is a potential role for nitrogen fixation to close the nitrogen budget, and that silicate limitation may become more severe in a few decades.

The quantity and quality of particles sinking to the deep-sea floor in the Central Arctic is constrained by the amount of new production, which is dependent on nutrients, and by the carbon demand of grazers (Lalande et al., 2014; Olli et al., 2007; Wassmann et al., 2004). Our observations of entire algal filaments that had sunk to the seafloor without being grazed (Chapter I) may reflect a mismatch between primary and secondary producers in spring due to earlier sea-ice retreat (Ji et al., 2013; Soreide et al., 2010). In late summer, however, potential carbon demand was 80% of the measured NPP below the ice and the carbon flux contained almost no diatoms (Lalande et al., 2014). In addition, copepods and amphipods were observed grazing on the pennate diatom aggregates floating below the ice (Chapters II and III) indicating that almost no ice algae were sinking to the deep sea at the end of the productive season when the system was dominated by heterotrophy (Chapter V). Hence, grazers control primary productivity at the end of the productive season, but the total amount of biomass available to graze on an annual time scale is determined by the amount of nutrients in surface waters.

All these changes point towards a more oligotrophic Arctic Ocean in the future. In general, changes in light availability due to sea-ice retreat will increase primary productivity locally but for reduced periods of time, while nutrient availability will probably decrease, constraining primary production at a regional and annual scale.

3.4. The role of diazotrophs in constraining new production

The total amount of carbon entering the ecosystem every year is determined by the amount of primary production derived from allochthonous nutrients. This new production is constrained mainly by available nitrate in the Central Arctic, although other nutrients such as silicate also play a role as discussed before (Chapter V). During our studies in the Eurasian Basin in summer 2012, nitrate concentrations in the water column were low in surface waters

far away from the Atlantic inflow (0.1-3 μmol L^{-1}) and the N:P ratio was below Redfield. Such low Redfield ratios were most noticeable in the Laptev Sea area and in the northern most part of the Central Arctic in late September (Chapter V).

A potential role for nitrogen fixation in the Arctic Ocean as a nitrate source to balance nitrogen loses by denitrification on the shelves has been hypothesized (Devol et al., 1997; Torres-Valdés et al., 2013). In addition, the potentially elevated primary productivity due to increased light has elevated the overall nitrogen demand. Available nitrate is depleted in surface waters through uptake by phytoplankton and sea-ice algae to form new biomass (Fig.7). This nitrate is incorporated into organic nitrogen in autotrophic biomass and can either be transferred to higher trophic levels, remineralized by bacteria, or sink to the seafloor. At the seafloor organic nitrogen is remineralized to inorganic nitrogen and it is then replenished to surface waters of the Central Basins via haline convection in winter. Other sources of inorganic nitrogen to surface waters are vertical mixing and lateral transport from the shelves, upwelling events from deeper water masses at the shelf and ice edges, riverine input, and fixation of atmospheric nitrogen by diazotrophic bacteria (Fig.7) (LaRoche and Breitbarth, 2005; Popova et al., 2012; Rudels et al., 2004). However, the magnitude and frequency of mixing and upwelling events as well as the contribution of nitrogen fixers to the nitrogen cycle in the Central Arctic are still unknown.

Our results from molecular analysis targeting the nitrogen fixation gene, *nifH*, revealed a high diversity of non-cyanobacterial diazotrophs in sea ice and water column of the Central Arctic in summer 2012 (Chapter VI). Furthermore, the statistical analyses rejected the hypothesis that the diazotrophic community originates from the river influenced Laptev Sea waters, indicating that a marine nitrogen fixing community is present in the Central Arctic (Chapter VI). This is the first indication for potential nitrogen fixation north of 78 ºN. Although nitrogen fixation genes are usually only retained in evolutionary scales if they are functional (Dos Santos et al., 2012), a high diversity of diazotrophs does not imply high nitrogen fixation rates (Moisander et al., 2007). Only one previous study included nitrogen fixation measurements using the acetylene reduction method in the Canadian Arctic shelf (Blais et al., 2012). Assuming that the same maximum nitrogen fixation rate would also occur in the Central Arctic, diazotrophs could sustain 7% of the total annual production estimated at the moment (Chapter V). However, this might be an underestimate since the acetylene reduction method has been shown to underestimate nitrogen fixation rates (Mohr et al., 2010). In addition, diazotrophs require phosphate in high proportions to maintain growth. According

to the N:P ratios measured in the water column at the end of the season (5-11), which were below Redfield (16), phosphate would not limit diazotroph growth. Considering the vast understudied area of the Central Arctic, if nitrogen fixation is proven to contribute to nitrate availability, nitrate limitation might diminish in some areas.

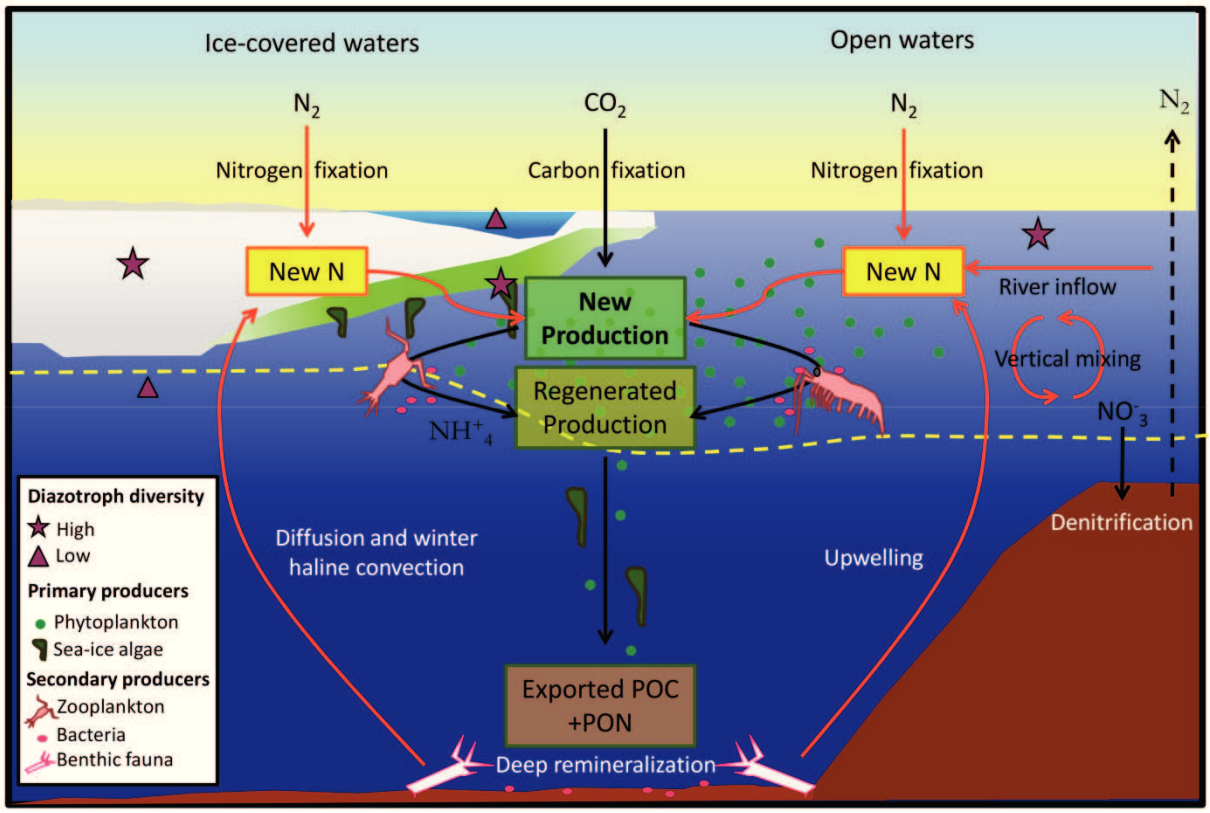

Figure 7. Conceptual model of the main processes affecting carbon and nitrogen cycles in the Arctic Ocean. The left part represents ice-covered waters and the right part open waters. Carbon dioxide (CO_2) is transformed into particulate organic carbon (POC) by primary producers (sea-ice algae and phytoplankton). If the nitrate (NO_3^-) used in this process comes from the winter haline convection or from nitrogen fixation it is considered to be new production. If primary producers use remineralized nitrate or ammonium produced by under-ice fauna, zooplankton or bacteria, it is considered to be regenerated production. The orange arrows symbolize nutrient supply mechanisms and the black arrows nutrient sinks. The yellow dashed line indicates the euphotic zone depth (1% PAR). High diazotroph diversity is symbolized by a star, while a triangle indicates low diversity.

According to previous studies of nitrogen fixing organisms in the coastal Arctic (Blais et al., 2012) and due to the fact that diazotrophs have been identified in several habitats related to land and rivers in the subpolar regions (DeLuca et al., 2013), a plausible origin of nitrogen fixing organisms in the Central Arctic is riverine input. However, our results showed a distinct diazotrophic community in the river-influenced Laptev Sea, compared to the Central Arctic pack-ice community (Chapter VI). Only a few groups of microorganisms, one of them closely related to *Geobacter sp.* (Subcluster 1A in Fig. 5 of Chapter VI), seem to be present in both environments. A more detailed study following the plume of the Lena River would be necessary to test if these organisms originate from riverine inputs. Furthermore, activity measurements to investigate if they are alive, in spore form, or dead, would be necessary to confirm this spreading theory from the shelves to the Central Arctic.

In the light of ongoing changes in the Arctic ecosystem, the diversity of potential diazotrophs observed in the Central Arctic could be amplified by a reduction in the temperature limitation for some nitrogen fixing groups such as *Cyanobacteria*. Although *Cyanobacteria* are not very abundant in the Arctic Ocean, they have been detected in several Arctic environments such as ice, snow and glaciers (Díez et al., 2012; Telling et al., 2011). The heavily studied representatives of this group, *Trichodesmium sp.* and *Nodularia sp.*, have optimal growth temperatures that range between 20 and 35 ºC (Breitbarth et al., 2006; Lehtimaki et al., 1997). Although these temperatures will not be reached in the Central Arctic Ocean with ongoing climate change, the predicted increase in sea surface temperatures of 1-6ºC over the next 100 years (IPCC, 2013) might allow some cyanobacterial species to thrive in Arctic waters.

In terms of activity, all metabolic rates, including nitrogen fixation, will increase with increased temperature (Holding et al., 2013; Vaquer-Sunyer et al., 2010). In the Eurasian Basin, the biological processes affecting the nitrogen cycle (Fig.7) include bacterial denitrification in sediments (Rysgaard et al., 2004) and new production that consumes nitrate, remineralization in the water column that produces nitrate and ammonium, and regenerated production that consumes ammonium. Apart from denitrification in sediments and new production in the water column, none of these processes of the Arctic nitrogen cycle has been adequately quantified in the Eurasian Basin. Therefore, in order to test the hypothesis that nitrogen fixation could enhance new production in the Central Arctic, further investigations are needed to quantify all sinks and sources of nitrogen.

3.5. Potential future scenarios for Arctic primary productivity.

The total amount of carbon fixed in the Arctic Ocean by primary producers is relevant in terms of total energy entering the ecosystem. Changes in primary production affect the entire food web, including the top predators such as polar bears and seals, as well as fish populations, which are of relevance for human populations. Due to global warming, it is very likely that many fish species will shift their distribution northwards (Reist et al., 2006). Hence, accurate predictions of the fate of Arctic primary productivity are of crucial importance, not only for the local Arctic communities living and fishing there, but also for the entire world population.

The timing of primary production and its composition is critical for the ecosystem. According to recent studies from other Arctic regions and the results presented in this thesis, we propose two possible scenarios for primary productivity in a summer ice-free Eurasian Basin, north of 78ºN, likely to happen by 2050 (Wang and Overland, 2012).

In the first scenario, phytoplankton will replace sea-ice algae when summer sea ice disappears from the Central Arctic. This will only occur if phytoplankton species are able to adapt to the higher light intensities reaching the euphotic zone (Frey et al., 2011; Nicolaus et al., 2012) and enough nutrients are available. Arctic phytoplankton are most efficient at low irradiances (Cota, 1985) but showed no photoinhibition in summer at irradiances up to 420 μmol photons m^{-2} s^{-1} (Chapter V). Arctic phytoplankton in open waters showed higher NPP rates than in ice-covered waters, indicating that adaptation is possible (Chapter V). Enhanced phytoplankton blooms have been observed below the ice due to increased light transmission through melting ice, supporting this scenario (Arrigo et al., 2014).Regarding nutrient availability in the Eurasian Basin in summer 2012, significant concentrations of nutrients were available below the euphotic zone (e.g. 10-15 μmol L^{-1} nitrate), meaning that if light penetrates further (up to 45-50 m as in open waters in summer 2012), these nutrients will be available for phytoplankton.

A possible variant of this first scenario could be that sea ice remains present in winter and early spring and part of the nutrients would be consumed by increased sea-ice algal productivity earlier in the season (Matrai and Apollonio, 2013; Tedesco et al., 2012). Our observations of high sub-ice algal biomasses that sunk to the deep sea earlier in the season (July) (Chapter I and V) resulting in nutrient reduction in surface waters might be a

transitional phase towards this kind of scenario. To sustain an increase in annual phytoplankton productivity, nutrients would need to be replenished in summer. This might occur in an ice-free Arctic due to increased wind-driven upwelling in summer (Carmack et al., 2006). An additional process for nutrient replenishment would be nitrogen fixation that might play a role in a warmer Arctic Ocean (Chapter VI). If enough nutrients are available, an early sea-ice algal bloom would be followed by an extensive phytoplankton bloom during the ice-free summer. If under-ice fauna and zooplankton are not able to adapt to the new phytoplankton dominated regime, this might lead to a mismatch between primary producers and grazers (Ji et al., 2013; Leu et al., 2011), leading to an increase in the carbon export favoring benthic communities. This would avoid carbon transfer to pelagic higher trophic levels inducing cascading effects through the entire ecosystem. Our observations of large algal aggregates in the deep sea indicate that these processes may already be happening in the Central Arctic (Chapter I).

In the second scenario sea-ice algae, which contribute significantly to total annual production (Chapter V) (Gosselin et al., 1997; Matrai and Apollonio, 2013), will not be able to maintain their life cycle in an Arctic free of ice in summer. . The disappearance of MYI, which sustains high biomasses of sea-ice algae (Chapter V), and the lack of ice formation on the shelves, which is a key process in the life cycle of sub-ice algae such as *Melosira arctica* (Fig.6), would contribute to the decrease in the contribution of sea-ice algae to total annual production and would lead to a general decrease in total productivity. This would be aggravated if phytoplankton would not be able to adapt to higher light intensities. In addition, in a summer ice-free Arctic Ocean, freshening due to complete melt of sea-ice cover in spring will increase stratification, hindering nutrient upwelling (Carmack and McLaughlin, 2011). Note that the stronger stratification due to ice melt would lead to a lower diffusion rate of nutrients across the mixed layer but this layer would not necessarily become shallower. In general all these changes would transform the Eurasian Basin to an even more oligotrophic region with low productivity. Freshening and nutrient depletion may lead to a shift in phytoplankton species composition towards smaller species with lower nutrient requirements (Ardyna et al., 2011; Li et al., 2009), which would reduce the amount of carbon exported to the benthos (Guidi et al., 2009).

There are limitations in our ability to predict how primary production will change in the Central Arctic Ocean. Whether phytoplankton blooms replace sea-ice algae in the ecosystem or not, changes in primary production will only occur within certain limits. The boundary

conditions for changes in primary production in an ice-free Arctic, assuming that nutrient upwelling does occur, are summarized in Table 2. It is worth noticing that even if all nutrients below the present-day mixed layer in the Eurasian Basin of the Central Arctic would be accessible for phytoplankton growth; annual new production would not increase more than 60 g C m^{-2} yr^{-1} (Assuming Redfield ratio of 6.6 and an euphotic zone depth of 50 m). This would be 6 times higher than present-day new production but still lower than current Chukchi and Bering Sea annual production (70-100 g C m^{-2} yr^{-1}, Codispoti et al., 2013). This compilation of existing data and possible future scenarios points out that the most important determining factor that is still unknown is the rate of nutrient supply. Indeed, state of the art predictive models for Arctic primary production disagree on nutrient dynamic predictions, especially in the vast Central Basins where a good nutrient climatology is missing (Vancoppenolle et al., 2013). The remaining challenge for the future is to be able to constrain those ranges and at the same time be able to account for the immense variability in the Arctic Ocean. Our focus needs to go towards interdisciplinarity and integration, since the Arctic ecosystem cannot be understood in regional isolation nor by studying only one of its components.

Table 2. Present and potential future ranges of environmental parameters related to primary production in the Eurasian Basin north of 78 ºN.

Parameter (Unit)	Present range	Future range	Potential cause of change
Irradiance at surface water (μmol photons m^{-2} s^{-1})	0.2-20	10-400	Thinning of sea ice and increased melt- pond cover.
Euphotic zone depth (m)	10-30	30-50	Greater light penetration in open waters.
Mixed layer depth (m)	10-20	5-20	Stronger stratification due to ice melt.
Nutrient concentrations in the mixed layer (μmol L^{-1})			Wind-driven vertical mixing. Enhanced upwelling events.
Nitrate	0-4	6-15	
Phosphate	0.05-0.2	0.4-1	
Silicate	0.5-6	7-12	
Net primary productivity (mg C m^{-2} d^{-1})			
Sea ice	0.1-15	0	Loss of habitat.
Water column	0.1-60*	100-300	Increased irradiance and nutrient supply to surface waters.
Annual new production (g C m^{-2} yr^{-1})	9-15	Up to 60	Increased nutrient availability in the euphotic zone.
Zooplankton carbon demand (mg C m^{-2} d^{-1})	10-20	Unknown	Mismatch between primary and secondary producers. Shift in species composition.
Carbon export to the deep sea (g C m^{-2} yr^{-1})	0.1-10	0-30	Depends on nutrient availability and grazing.

*Water column below the sea-ice. Net primary productivity and annual new production rates are from August-September 2012 (Chapter V).

4. Perspectives

Earth´s climate is changing due to anthropogenic greenhouse gas emissions (IPCC, 2013). Changes in the Arctic Ocean are more pronounced than elsewhere, making it an ideal laboratory for studying the manifestations of global change. Furthermore, changes in the Arctic Ocean will have repercussions beyond the Arctic by impacting oceanic circulation patterns, global transportation, fisheries and weather in lower latitudes (Coumou et al., 2014). Primary production provides energy to fuel the ecosystem and is strongly linked to sea-ice dynamics in the Arctic Ocean. Therefore, understanding the mechanisms influencing primary production in the Arctic Ocean to improve predictions of its fate as a response to increasing temperatures and sea-ice retreat is of crucial importance.

The two main limitations to assess changes driven by sea-ice loss in the Arctic ecosystem are the lack of a comprehensive baseline, especially in the Central Arctic, previous to the start of sea ice decline (around 1980), and the high spatial variability of Arctic biomass. This thesis has contributed to improving our knowledge of the under-sampled Central Arctic. Nevertheless, future studies focusing on solving seasonality and nutrient dynamics are needed to predict how sea-ice retreat will affect the deep Central Arctic basins. Additional challenges for future Arctic research are to identify and protect key areas of nutrient upwelling and sea-ice formation.

4.1. Remaining key scientific questions for Arctic primary productivity research.

Despite the global implications of changes in the Arctic, there are still significant deficiencies in our understanding of the Arctic marine ecosystem. Sea-ice decline is probably the most studied process in the Arctic Ocean, due to the available satellite record since 1978. However, model simulations to project changes in Arctic sea-ice cover still show large variations (Stroeve et al., 2012). Arctic ice-ocean models coupled to biogeochemical models are scarce and the large variability in their simulations points towards their low confidence in projecting future primary productivity (Vancoppenolle et al., 2013). This is partly due to the complexity of the Arctic system with numerous non-linear interactions between atmosphere, cryosphere, ocean and biosphere. The key questions that need to be answered in order to improve our

understanding of how each of those compartments might affect Arctic primary productivity in the future are:

- Atmosphere: What is the radiative effect of clouds? Will more open water enhance cloud formation dampening the increase in irradiance reaching the water column?
- Cryosphere: By which factor will the summer melt season increase? Which parts of the Central Arctic will shift first from perennial to seasonal sea-ice conditions?
- Ocean: At which temporal and spatial scales do vertical and lateral transport supply nutrients to surface waters? To which depth are winds expected to mix the water column in open waters? How strong and deep will stratification be due to freshening and warming?
- Biosphere: Can Arctic phytoplankton adapt to increased irradiances and lower salinities? Can sea-ice algae maintain their life cycles in the Central Arctic in a summerly ice-free Arctic? How much carbon fixed by primary producers is transferred to higher trophic levels, how much is exported to the deep sea and how much is recycled in the water column? What is the role of nitrogen fixers in the Arctic Ocean?

To answer these questions, interdisciplinary research in key Arctic locations is needed. Although keeping a pan-Arctic perspective is important to understand how different Arctic regions are linked, there are certain locations in the Arctic Ocean that are fundamental to include in future observations due to the processes occurring there. The Central Arctic, north of 78ºN, is relevant to monitor because of the dramatic changes that the ecosystem will suffer when it becomes a seasonal ice zone. In particular, areas becoming ice-free for the first time in millennia are important to identify, to study changes in ice-covered versus open waters. The Eurasian Basin will likely play an important role in the future of Arctic productivity as it contains more nutrients than the Amerasian Basin. Hence, waters entering the Arctic through Fram Strait from the North Atlantic, providing nutrients to the Arctic Ocean, should be closely monitored. In addition, prominent upwelling areas where deep waters reach the surface replenishing it with nutrients need to be identified and monitored.

4.2. Assessing the impact of sea-ice retreat on primary production in the Central Arctic.

Due to the complexity of the problem, the challenging logistics required to work in the Central Arctic Ocean and the increasing speed at which changes are happening, international and interdisciplinary scientific efforts are required to address the remaining key questions. The main focus on the field should be put on obtaining seasonal data and identifying the most relevant regions for nutrient supply to the surface waters of the Central Arctic. In the laboratory, key species for the Arctic food chain such as *Melosira arctica*, should be investigated from the genetic to the physiological level to understand how they will cope with changes in environmental conditions.

The Arctic Ocean has a strong seasonality, which controls productivity. Hence, it is crucial to reproduce this seasonal variability correctly in Arctic predictive models. Seasonal data from the atmosphere and ice surface can be obtained by satellite year round up to 88 ºN. However, oceanographic and biological seasonal data can only be obtained by autonomous buoys drifting with the ice, moorings or by scientists on drift ice camps. A combination of annual drift camps on representative FYI and MYI floes, together with several autonomous platforms spread through the Central Arctic for one or several years would be the ideal solution to obtain simultaneous and complementary datasets to understand the seasonality of biological and physical factors below the ice.

Drift camps could host a team of multidisciplinary scientists including atmospheric scientists, sea-ice physicists, oceanographers, biologists and deep sea ecologists. One drift camp should be deployed in autumn on the Siberian shelf on newly formed ice that is expected to drift through the Central Arctic following the Transpolar Drift. Another drift camp could be deployed on multiyear ice north of Greenland. The two drift camps could be supplied by icebreakers or airplanes. In parallel, in autumn, autonomous platforms should be deployed on the Laptev Sea shelf, the Siberian shelf and in the Central Arctic. These autonomous platforms should consist of a buoy array buried in the ice with an upper part on top of the ice and a hanging part below the ice. The upper part could provide various meteorological data including information about the radiation and water vapor budget, as well as snow cover, while a part in the ice could provide thermal information to assess ice mass balance and melt processes. Below the ice, an ice tethered profiler (ITP) with a fluorometers (Laney et al., 2014), nutrient sensors (Alkire et al., 2010; Glibert et al., 2008) and an oxygen sensor could

measure the upper 50 m of the water column below the ice once per day. Regular checks and calibrations of the autonomous platforms could be done by research vessels. All components should be water resistant and buoyant in case the ice melts.

Sea ice Chl *a* profiles are more complicated to obtain remotely. This is added to by the fact that sea-ice algae distribution is very patchy and the high spatial variability needs to be taken into account to upscale sea-ice biomass estimates. Recently developed methods to assess sea ice properties and biomass distribution from below the ice with a remotely operated vehicle (ROV), could cover large areas (1-2 km^2) around drift camps (Mundy et al., 2007; Nicolaus and Katlein, 2013) and describe the spatial variability.

To address the seasonal variability of sea-ice algae and phytoplankton productivity, besides Chl *a*, C:Chl *a* and C:N:P:Si uptake ratios and *in situ* carbon uptake rates at different light and nutrient conditions are needed. As shown in Chapter V, photosynthesis-irradiance curves are the key to upscaling and modeling primary productivity, and carbon to nutrient ratios are essential in estimating new production from nutrient draw-down. Therefore, constraining the range of photosynthetic parameters and carbon to nutrient ratios for sea-ice algae and phytoplankton for each season and ice type is a priority to improve primary productivity models. Currently there is no autonomous device available that could collect and analyze biological samples. Therefore, field work is still needed to perform biogeochemical analysis of the carbon and nutrient fluxes in Arctic water column and sea ice. In addition, grazing pressure must be accurately determined, since it can control the algal standing stock, especially at the end of the season (Chapter V). This work could be performed from drift camps or research vessels. Under-ice cameras mounted on the autonomous platform might also help determining under-ice fauna behavior and abundance.

Long-term sediment traps are also a good tool to study seasonality in the Arctic Ocean since they autonomously collect and store samples during an entire year. Available carbon export datasets from the marginal seas should be complemented with data from sediment traps in the Central Arctic (Lalande et al., 2014). These export fluxes could be complemented with deep sea surveys to quantify the amount of carbon and nutrients reaching the deep-sea floor and the remineralization rates taking place in the deep-sea sediments by bacteria.

Nevertheless, as discussed in this thesis, the missing key factor to predict the fate of primary production in an ice-free Arctic is nutrient dynamics. Oceanographic profiles of temperature

and salinity obtained with a CTD profiler enable us to track water masses and their properties, but are not enough to confirm nutrient supply events to surface waters, in particular when the profiles are measured from moorings that do not reach the upper 50 m of the water column. Comparing turbulence measurements at the base of the mixed layer from ice-covered waters (measured from drift camps or autonomous platforms) and from open waters, would help to predict how nutrient supply for phytoplankton growth might change in ice covered waters when they become open waters (Cota et al., 1987). The frequency and magnitude of upwelling events reaching the surface waters of the Central Arctic are likely to be observed close to the continental slope (Rudels et al., 2004). Therefore, including nutrient sensors on the drifting autonomous platform ITPs would help resolve vertical and lateral nutrient variability in the upper water column (Glibert et al., 2008). If specific areas are identified where upwelling events are more frequent, they should be monitored with mooring arrays.

In addition, for a decadal understanding of nutrient input to the Arctic Ocean, the nutrient content of the inflowing Atlantic waters at ~150 m depth through Fram Strait should be permanently monitored since it is one of the main sources of nutrients to the upper water layers (Popova et al., 2013; Rudels et al., 2004; Torres-Valdés et al., 2013). This could be achieved by adding nutrient sensors to the moorings at the HAUSGARTEN Long Term Observatory (Soltwedel et al., 2005). In general, the establishment of further long-term observatories in the Arctic Ocean would improve our ability to predict changes in Arctic primary productivity. In parallel, some efforts are needed to make the historic Russian literature and data from the North Pole ice camps available in English for the international scientific community (Wassmann et al., 2011). This would in some cases provide further baseline data to allow comparison of measurements.

Moreover, the role of nitrogen fixation in the Arctic nitrogen cycle needs to be verified. As described in Chapter VI, a high diversity of diazotrophs has been found in the Arctic but their activity remains unknown. Nitrogen fixation rate measurements with a more sensitive method (Mohr et al., 2010), should be performed not only *in situ* but also in the laboratory under different nutrient and light conditions to be able to predict the potential role of nitrogen fixation in the future Arctic Ocean.

Further laboratory investigations should be performed on key Arctic species, such as the sub-ice algae *Melosira arctica* and the abundant planktonic diatom *Chaetoceros socialis*. Their photosynthetic and sinking rates should be studied under different light and nutrient conditions to predict how changes in their natural environment might affect them. Physiological studies could be complemented with genomic and transcriptomic analysis to assess their genetic potential for adaptation.

Finally, as demonstrated in this thesis, interdisciplinary work is fundamental in Arctic research. Independently of the platform from which measurements are taken, improvements in our understanding of the Arctic ecosystem will only happen if sea-ice physicists, oceanographers, modelers and biologists work together and benefit from each other's knowledge.

Bibliography

Aagaard, K., Coachmann, L. K. and Carmack, E. C.: On the halocline of the Arctic Ocean, Deep Sea Res. Part A. Oceanogr. Res. Pap., 28(6), 529–545, doi:10.1016/0198-0149(81)90115-1, 1981.

Aagaard, K., Swift, J. H. and Carmack, E. C.: Thermohaline circulation in the Arctic Mediterranean Seas, J. Geophys. Res., 90(C3), 4833–4846, doi:10.1029/JC090iC03p04833, 1985.

Alkire, M. B., Falkner, K. K., Morison, J., Collier, R. W., Guay, C. K., Desiderio, R. a., Rigor, I. G. and McPhee, M.: Sensor-based profiles of the NO parameter in the central Arctic and southern Canada Basin: New insights regarding the cold halocline, Deep Sea Res. Part I, 57, 1432–1443, doi:10.1016/j.dsr.2010.07.011, 2010.

Ambrose, W. G., Quillfeldt, C. Von, Clough, L. M., Tilney, P. V. R. and Tucker, T.: The sub-ice algal community in the Chukchi sea: large- and small-scale patterns of abundance based on images from a remotely operated vehicle, Polar Biol., 28, 784–795, doi:10.1007/s00300-005-0002-8, 2005.

Anderson, L. G., Chierici, M. and Fransson, A.: Anthropogenic carbon dioxide in the Arctic Ocean: Inventory and sinks, J. Geophys. Res., 103(C12), 707–716, 1998.

Ardyna, M., Babin, M., Gosselin, M., Devred, E., Bélanger, S., Matsuoka, A. and Tremblay, J.-É.: Parameterization of vertical chlorophyll *a* in the Arctic Ocean: impact of the subsurface chlorophyll maximum on regional, seasonal and annual primary production estimates, Biogeosciences Discuss., 10, 1345–1399, doi:10.5194/bgd-10-1345-2013, 2013.

Ardyna, M., Babin, M., Gosselin, M., Devred, E., Rainville, L. and Tremblay, J.-É.: Recent Arctic Ocean sea-ice loss triggers novel fall phytoplankton blooms, Geophys. Res. Lett., doi:10.1002/2014GL061047, 2014.

Ardyna, M., Gosselin, M., Michel, C., Poulin, M. and Tremblay, J.-É.: Environmental forcing of phytoplankton community structure and function in the Canadian High Arctic: contrasting oligotrophic and eutrophic regions, Mar. Ecol. Prog. Ser., 442, 37–57, doi:10.3354/meps09378, 2011.

Arndt, S. and Nicolaus, M.: Seasonal cycle of solar energy fluxes through Arctic sea ice, Cryosph. Discuss., 8, 2923–2956, doi:doi:10.5194/tcd-8-2923-2014, 2014.

Arrigo, K. R.: Marine microorganisms and global nutrient cycles, Nature, 437, 349–356, doi:10.1038/nature04158, 2005.

Arrigo, K. R.: Sea ice ecosystems, Ann. Rev. Mar. Sci., 6, 439–67, doi:10.1146/annurev-marine-010213-135103, 2014.

Arrigo, K. R., van Dijken, G. and Pabi, S.: Impact of a shrinking Arctic ice cover on marine primary production, Geophys. Res. Lett., 35(19), L19603, doi:10.1029/2008GL035028, 2008.

Arrigo, K. R., Perovich, D. K., Pickart, R. S., Brown, Z. W., Dijken, G. L. Van, Lowry, K. E., Mills, M. M., Palmer, M. A., Balch, W. M., Bahr, F., Bates, N. R., Benitez-nelson, C., Bowler, B., Brownlee, E., Ehn, J. K., Frey, K. E., Garley, R., Laney, S. R., Lubelczyk, L., Mathis, J., Matsuoka, A., Mitchell, B. G., Moore, G. W. K., Ortega-retuerta, E., Pal, S., Polashenski, C. M., Reynolds, R. A., Schieber, B., Sosik, H. M., Stephens, M. and Swift, J. H.: Massive phytoplankton blooms under Arctic sea ice, Science, 336, 1408, 2012.

Arrigo, K. R., Perovich, D. K., Pickart, R. S., Brown, Z. W., van Dijken, G. L., Lowry, K. E., Mills, M. M., Palmer, M. a., Balch, W. M., Bates, N. R., Benitez-Nelson, C. R., Brownlee, E., Frey, K. E., Laney, S. R., Mathis, J., Matsuoka, A., Greg Mitchell, B., Moore, G. W. K., Reynolds, R. a., Sosik, H. M. and Swift, J. H.: Phytoplankton blooms beneath the sea ice in the Chukchi sea, Deep Sea Res. Part II Top. Stud. Oceanogr., 105, 1–16, doi:10.1016/j.dsr2.2014.03.018, 2014.

Bates, N. R., Garley, R., Frey, K. E., Shake, K. L. and Mathis, J. T.: Sea-ice melt CO_2-carbonate chemistry in the western Arctic Ocean: meltwater contributions to air-sea CO_2 gas exchange, mixed layer properties and rates of net community production under sea ice, Biogeosciences Discuss., 11(1), 1097–1145, doi:10.5194/bgd-11-1097-2014, 2014.

Bates, N. R. and Mathis, J. T.: The Arctic Ocean marine carbon cycle: evaluation of air-sea CO_2 exchanges, ocean acidification impacts and potential feedbacks, Biogeosciences, 6(11), 2433–2459, doi:10.5194/bg-6-2433-2009, 2009.

Behrenfeld, M. J. and Falkowski, P. G.: A consumers guide to phytoplankton primary productivity models, Limnol. Oceanogr., 42(7), 1479–1491, 1997.

Bélanger, S., Babin, M. and Tremblay, J.-É.: Increasing cloudiness in Arctic damps the increase in phytoplankton primary production due to sea ice receding, Biogeosciences Discuss., 9, 13987–14012, doi:10.5194/bgd-9-13987-2012, 2012.

Bélanger, S., Cizmeli, S. a., Ehn, J., Matsuoka, a., Doxaran, D., Hooker, S. and Babin, M.: Light absorption and partitioning in Arctic Ocean surface waters: impact of multi year ice melting, Biogeosciences Discuss., 10(3), 5619–5670, doi:10.5194/bgd-10-5619-2013, 2013.

Bintanja, R. and Selten, F. M.: Future increases in Arctic precipitation linked to local evaporation and sea-ice retreat., Nature, 509(7501), 479–82, doi:10.1038/nature13259, 2014.

Blais, M., Tremblay, J.-É., Jungblut, A. D., Gagnon, J., Martin, J., Thaler, M. and Lovejoy, C.: Nitrogen fixation and identification of potential diazotrophs in the Canadian Arctic, Global Biogeochem. Cycles, 26, GB3022, doi:10.1029/2011GB004096, 2012.

Bluhm, B. and Gradinger, R.: Regional variability in food availability for arctic marine mammals, Ecol. Appl., 18(2), 77–96, 2008.

Booth, B. C. and Horner, R. A.: Microalgae on the Arctic Ocean Section , 1994: species abundance and biomass, Deep Sea Res. Part II, 44(8), 1607–1622, 1997.

Bowman, J. P.: Sea-ice microbial communities, in The prokaryotes-prokaryotic communities and ecophysiology, edited by E. Rosenberg, E. F. DeLong, S. Lory, E. Stackebrandt, and F. Thompson, pp. 139–161, Springer Berlin Heidelberg, Berlin, Heidelberg., 2013.

Breitbarth, E., Oschlies, A. and LaRoche, J.: Physiological constraints on the global distribution of Trichodesmium-effect of temperature on diazotrophy., Biogeosciences Discuss., 3, 779–801, 2006.

Brown, Z. W. and Arrigo, K. R.: Contrasting trends in sea ice and primary production in the Bering Sea and Arctic Ocean, ICES J. Mar. Sci., 69(7), 1180–1193, doi:10.1093/icesjms/fss113, 2012.

Burek, K. A., Gulland, F. M. D. and O'Hara, T. M.: Effects of climate change on Arctic marine mammal health., Ecol. Appl., 18(2), S126–34, 2008.

Cai, P., Rutgers van der Loeff, M., Stimac, I., Nöthig, E.-M., Lepore, K. and Moran, S. B.: Low export flux of particulate organic carbon in the central Arctic Ocean as revealed by ^{234}Th: ^{238}U disequilibrium, J. Geophys. Res., 115(C10), C10037, doi:10.1029/2009JC005595, 2010a.

Cai, W., Chen, L., Chen, B., Gao, Z., Lee, S. H., Chen, J., Pierrot, D., Sullivan, K., Wang, Y., Hu,, X., Huang, W.-J., Zhang, Y., Xu, S., Murata, A., Grebmeier, J. M., Jones, E. P., Zhang, H., Hu, X. and Syllivan, K.: Decrease in the CO_2 uptake capacity in an ice free Arctic Ocean Basin., Science, 329(556), 556–559, doi:10.1126/science.1189338, 2010b.

Carmack, E., Barber, D., Christensen, J., Macdonald, R., Rudels, B. and Sakshaug, E.: Climate variability and physical forcing of the food webs and the carbon budget on panarctic shelves., Prog. Oceanogr., 71, 145–181, doi:10.1016/j.pocean.2006.10.005, 2006.

Carmack, E. and McLaughlin, F.: Towards recognition of physical and geochemical change in Subarctic and Arctic Seas, Prog. Oceanogr., 90(1-4), 90–104, doi:10.1016/j.pocean.2011.02.007, 2011.

Carmack, E. and Wassmann, P.: Food webs and physical–biological coupling on pan-Arctic shelves: Unifying concepts and comprehensive perspectives, Prog. Oceanogr., 71(2-4), 446–477, doi:10.1016/j.pocean.2006.10.004, 2006.

Carstens, M.: On the ecology of meltwater ponds on Arctic sea ice characteristics, seasonal dynamic and comparison with other aquatic habitats of polar regions, 1–352 pp., Universität Kiel., 2002.

Chapin, F. S., Berman, M., Callaghan, T. V., Convey, P., Crépin, A. S., Danell, K., Ducklow, H., Forbes, B., Kofinas, G., McGuire, A. D., Nuttall, M., Virginia, R., Young, O. and Zimov, S. A.: Ecosystems and human well-being. Volume 1: Current state and trends, in Polar systems., edited by R. Hassan, R. Scholes, and N. Ash, pp. 717–746, Island Press, Washington, District of Columbia., 2005.

Clark, G. F., Stark, J. S., Johnston, E. L., Runcie, J. W., Goldsworthy, P. M., Raymond, B. and Riddle, M. J.: Light-driven tipping points in polar ecosystems., Glob. Chang. Biol., 19(12), 3749–61, doi:10.1111/gcb.12337, 2013.

Codispoti, L. A., Kelly, V., Thessen, A., Matrai, P., Suttles, S., Hill, V., Steele, M. and Light, B.: Synthesis of primary production in the Arctic Ocean: III. Nitrate and phosphate based estimates of net community production., Prog. Oceanogr., 110, 126–150, doi:10.1016/j.pocean.2012.11.006, 2013.

Cota, G. F.: Photoadaptation of high Arctic ice algae., Nature, 315, 219–222, 1985.

Cota, G. F., Pomeroy, L. R., Harrison, W. G., Jones, E. P., Peters, F., Sheldon, W. M. and Weingartner, T. R.: Nutrients, primary production and microbial heterotrophy in the southeastern Chukchi Sea: Arctic summer nutrient depletion and heterotrophy., Mar. Ecol. Prog. Ser., 135, 247–258, 1996.

Cota, G. F., Prisenberg, S., Bennet, E. B., Loder, J. W., Lewis, M. R., Anning, J. L., Watson, N. and Harris, L. R.: Nutrient fluxes during extended blooms of Arctic ice algae, Arctic, 92(C2), 1951–1962, 1987.

Cota, G. F. and Smith, R. E. H.: Ecology of bottom ice algae: II . Dynamics, distributions and productivity., J. Mar. Syst., 2, 279–295, 1991.

Coumou, D., Petoukhov, V., Rahmstorf, S., Petri, S. and Schellnhuber, H. J.: Quasi-resonant circulation regimes and hemispheric synchronization of extreme weather in boreal summer, Proc. Natl. Acad. Sci., doi:10.1073/pnas.1412797111, 2014.

DeLuca, T. H., Zackrisson, O., Bergman, I., Díez, B. and Bergman, B.: Diazotrophy in alluvial meadows of subarctic river systems., PLoS One, 8(11), e77342, doi:10.1371/journal.pone.0077342, 2013.

Devol, A., Codispoti, L. A. and Christensen, J.: Summer and winter denitrification rates in western Arctic Shelf sediments., Cont. Shelf Res., 17, 1029−1050, 1997.

Díez, B., Bergman, B., Pedrós-Alió, C., Antó, M. and Snoeijs, P.: High cyanobacterial *nifH* gene diversity in Arctic seawater and sea ice brine., Environ. Microbiol. Rep., 4(3), 360–6, doi:10.1111/j.1758-2229.2012.00343.x, 2012.

Drinkwater, K.: Comparison of the response of Atlantic cod (*Gadus morhua*) in the high-latitude regions of the North Atlantic during the warm periods of the 1920s–1960s and the 1990s–2000s, Deep Sea Res. Part II Top. Stud. Oceanogr., 56, 2087–2096, doi:10.1016/j.dsr2.2008.12.001, 2009.

Duarte, C. M. and Wassmann, P.: Arctic tipping points, edited by C. M. Duarte and P. Wassmann, Fundación BBVA, Bilbao., 2011.

Dugdale, R. C. and Goering, J. J.: Uptake of new and regenerated forms of nitrogen in primary productivity., Limnol. Oceanogr., 12, 196–206, 1967.

Ehn, J. K. and Mundy, C. J.: Assessment of light absorption within highly scattering bottom sea ice from under-ice light measurements: Implications for Arctic ice algae primary production, Limnol. Oceanogr., 58(3), 893–902, doi:10.4319/lo.2013.58.3.0893, 2013.

Elser, J. J., Kyle, M., Steger, L., Nydick, K. R. and Baron, J. S.: Nutrient availability and phytoplankton nutrient limitation across a gradient of atmospheric nitrogen deposition., Ecology, 90(11), 3062–3073, 2009.

Fahl, K. and Nöthig, E.-M.: Lithogenic and biogenic particle fluxes on the Lomonosov Ridge (central Arctic Ocean) and their relevance for sediment accumulation: Vertical vs. lateral transport., Deep Sea Res. Part I, 54, 1256– 1272, doi:10.1016/j.dsr.2007.04.014, 2007.

Fahl, K. and Stein, R.: Modern seasonal variability and deglacial/Holocene change of central Arctic Ocean sea-ice cover: New insights from biomarker proxy records, Earth Planet. Sci. Lett., 351-352, 123–133, doi:10.1016/j.epsl.2012.07.009, 2012.

Falkowski, P. G. and Raven, J. A.: Aquatic Photosynthesis, 2nd ed., Princeton University Press, New Jersey., 2007.

Farnelid, H., Andersson, A. F., Bertilsson, S., Al-Soud, W. A., Hansen, L. H., Sørensen, S., Steward, G. F., Hagström, Å. and Riemann, L.: Nitrogenase gene amplicons from global marine surface waters are dominated by genes of non-cyanobacteria., PLoS One, 6(4), e19223, doi:10.1371/journal.pone.0019223, 2011.

Fernández-Méndez, M.: Primary Productivity of sea ice algae under different environmental conditions., 67 pp., University of Bremen., 2011.

Fetterer, F. and Untersteiner, N.: Observations of melt ponds on Arctic sea ice, J. Geophys. Res., 103(C11), 24821–24835, 1998.

Forest, A., Tremblay, J.-É., Gratton, Y., Martin, J., Gagnon, J., Darnis, G., Sampei, M., Fortier, L., Ardyna, M., Gosselin, M., Hattori, H., Nguyen, D., Maranger, R., Vaqué, D., Marrasé, C., Pedrós-Alió, C., Sallon, A., Michel, C., Kellogg, C., Deming, J., Shadwick, E., Thomas, H., Link, H., Archambault, P. and Piepenburg, D.: Biogenic carbon flows through the planktonic food web of the Amundsen Gulf (Arctic Ocean): A synthesis of field measurements and inverse modeling analyses, Prog. Oceanogr., 91, 410–436, doi:10.1016/j.pocean.2011.05.002, 2011.

Forget, M.-H., Sathyendranath, S., Platt, T., Pommier, J., Vis, C., Kyewalyanga, M. S. and Hudon, C.: Extraction of photosynthesis-irradiance parameters from phytoplankton production data: demonstration in various aquatic systems, J. Plankton Res., 29(3), 249–262, doi:10.1093/plankt/fbm012, 2007.

Le Fouest, V., Babin, M. and Tremblay, J.-É.: The fate of riverine nutrients on Arctic shelves, Biogeosciences Discuss., 9(10), 13397–13437, doi:10.5194/bgd-9-13397-2012, 2012.

Frey, K. E., Perovich, D. K. and Light, B.: The spatial distribution of solar radiation under a melting Arctic sea ice cover., Cryosph., 38(22), 1–20, doi:10.1029/2011GL049421, 2011.

Frigstad, H., Andersen, T., Bellerby, R. G. J., Silyakova, A. and Hessen, D. O.: Variation in the seston C:N ratio of the Arctic Ocean and pan-Arctic shelves., J. Mar. Syst., doi:10.1016/j.jmarsys.2013.06.004, 2013.

Galloway, R. A.: The use of isotopes in measuring primary productivity., Chesap. Sci., 10(3-4), 331–335, doi:10.2307/1350479, 1969.

Gautier, D. L., Bird, K. J., Charpentier, R. R., Grantz, A., Houseknecht, D. W., Klett, T. R., Moore, T. E., Pitman, J. K., Schenk, C. J., Schuenemeyer, J. H., Sørensen, K., Tennyson, M. E., Valin, Z. C. and Wandrey, C. J.: Assessment of undiscovered oil and gas in the Arctic., Science, 324, 1175–9, doi:10.1126/science.1169467, 2009.

Gerdes, B., Brinkmeyer, R., Dieckmann, G. and Helmke, E.: Influence of crude oil on changes of bacterial communities in Arctic sea-ice., FEMS Microbiol. Ecol., 53(1), 129–139, doi:10.1016/j.femsec.2004.11.010, 2005.

Gieskes, W. W. C., Kraay, G. W. and Baars, M. A.: Current ^{14}C methods for measuring primary production: Gross underestimates in oceanic waters., Netherlands J. Sea Res., 13(1), 58–78, 1979.

Glibert, P. M., Kelly, V., Alexander, J., Codispoti, L. A., Boicourt, W. C., Trice, T. M. and Michael, B.: *In situ* nutrient monitoring: A tool for capturing nutrient variability and the antecedent conditions that support algal blooms, Harmful Algae, 8(1), 175–181, doi:10.1016/j.hal.2008.08.013, 2008.

Glud, R. N., Rysgaard, S. and Kühl, M.: A laboratory study on O_2 dynamics and photosynthesis in ice algal communities: quantification by microsensors, O_2 exchange rates, ^{14}C incubations and a PAM fluorometer, Aquat. Microb. Ecol., 27, 301–311, doi:10.3354/ame027301, 2002.

Glud, R. N., Rysgaard, S., Turner, G., McGinnis, D. F. and Leakey, R. J.: Biological and physical induced oxygen dynamics in melting sea-ice of the Fram Strait, Limnol. Oceanogr., 59(4), 1097–1111, doi:10.4319/lo.2014.59.4.1097, 2014.

Gosselin, M., Legendre, L., Therriault, J., Demers, S. and Rochetl, M.: Physical control of the horizontal patchiness of sea-ice microalgae, Mar. Ecol. Prog. Ser., 29, 289–298, 1986.

Gosselin, M., Levasseur, M., Wheeler, P. A., Horner, R. A. and Boothg, B. C.: New measurements of phytoplankton and ice algal production in the Arctic Ocean, Deep Sea Res. Part II, 44(8), 1623–1644, doi:10.1016/S0967-0645(97)00054-4, 1997.

Gruber, N. and Galloway, J. N.: An Earth-system perspective of the global nitrogen cycle., Nature, 451(7176), 293–6, doi:10.1038/nature06592, 2008.

Guidi, L., Stemmann, L., Jackson, G. A., Ibanez, F., Claustre, H., Legendre, L., Picheral, M. and Gorsky, G.: Effects of phytoplankton community on production , size and export of large aggregates : A world-ocean analysis, Limnol. Oceanogr., 54(6), 1951–1963, 2009.

Gutt, J.: The occurrence of sub-ice algal aggregations off northeast Greenland, Polar Biol., 15, 247–252, doi:10.1007/BF00239844, 1995.

Harding, T., Jungblut, A. D., Lovejoy, C. and Vincent, W. F.: Microbes in high arctic snow and implications for the cold biosphere., Appl. Environ. Microbiol., 77(10), 3234–43, doi:10.1128/AEM.02611-10, 2011.

Harrison, P. J.: Book Review: Measurement of primary production from the molecular to the global scale, Limnol. Oceanogr., 40(6), 1183–1185, doi:10.1080/10543406.2013.834796, 1995.

Hill, V. J., Matrai, P. A., Olson, E., Suttles, S., Steele, M., Codispoti, L. A. and Zimmerman, R. C.: Synthesis of integrated primary production in the Arctic Ocean: II. *In situ* and remotely sensed estimates, Prog. Oceanogr., 110, 107–125, doi:10.1016/j.pocean.2012.11.005, 2013.

Ho, J.: The implications of Arctic sea ice decline on shipping, Mar. Policy, 34(3), 713–715, doi:10.1016/j.marpol.2009.10.009, 2010.

Holding, J. M., Duarte, C. M., Arrieta, J. M., Vaquer-Suyner, R., Coello-Camba, A., Wassmann, P. and Agustí, S.: Experimentally determined temperature thresholds for Arctic plankton community metabolism, Biogeosciences, 10, 357–370, doi:10.5194/bg-10-357-2013, 2013.

Horner, R. A., Syvertsen, E. E., Thomas, D. P. and Lange, C.: Proposed terminology and reporting units for sea ice algal assemblages, Polar Biol., 8, 249–253, doi:10.1007/BF00263173, 1988.

Huot, Y., Babin, M. and Bruyant, F.: Photosynthetic parameters in the Beaufort Sea in relation to the phytoplankton community structure, Biogeosciences, 10, 3445–3454, doi:10.5194/bg-10-3445-2013, 2013.

IPCC: Climate Change 2013: The Physical Science Basis. Contribution of working group I to the Fifth Assessment Report of the IPCC., 2013.

Jakob, T., Schreiber, U., Kirchesch, I. V, Langner, U. and Wilhelm, C.: Estimation of chlorophyll content and daily primary production of the major algal groups by means of multiwavelength

excitation PAM chlorophyll fluorometry: performance and methodological limits., Photosynth. Res., 83(3), 343–361, 2005.

Jakobsson, M., Grantz, A., Kristoffersen, Y. and Macnab, R.: Bathymetry and physiogeography of the Arctic Ocean and its constituent seas., in The Organic Carbon Cycle in the Arctic Ocean, edited by R. Stein and R. W. Macdonald, pp. 1–5, Springer, Berlin, Germany., 2004.

Ji, R., Jin, M., Varpe, Ø., Jil, R. and Varpe, O.: Sea ice phenology and timing of primary production pulses in the Arctic Ocean, Glob. Chang. Biol., 19(3), 734–41, doi:10.1111/gcb.12074, 2013.

Jin, M., Deal, C., Lee, S. H., Elliott, S., Hunke, E., Maltrud, M. and Jeffery, N.: Investigation of Arctic sea ice and ocean primary production for the period 1992–2007 using a 3-D global ice–ocean ecosystem model, Deep Sea Res. Part II, 81-84, 28–35, doi:10.1016/j.dsr2.2011.06.003, 2012.

Johannessen, O. M. and Miles, M. W.: Critical vulnerabilities of marine and sea ice – based ecosystems in the high Arctic, Reg. Environ. Chang., 11(Suppl 1), 239–248, doi:10.1007/s10113-010-0186-5, 2011.

Jones, E. P., Anderson, L. G. and Swift, J. H.: Distribution of Atlantic and Pacific waters in the upper Arctic Ocean: Implications for circulation distinguish between oceanic waters of Pacific, Geophys. Res. Lett., 25(6), 765–768, 1998.

Juhl, A. R. and Krembs, C.: Effects of snow removal and algal photoacclimation on growth and export of ice algae., Polar Biol., 33, 1057–1065, 2010.

Kamp, A., de Beer, D., Nitsch, J. L., Lavik, G. and Stief, P.: Diatoms respire nitrate to survive dark and anoxic conditions., Proc. Natl. Acad. Sci. U. S. A., 108(14), 5649–54, doi:10.1073/pnas.1015744108, 2011.

Katlein, C., Nicolaus, M. and Petrich, C.: The anisotropic scattering coefficient of sea ice, J. Geophys. Res., 119(2), 842–855, doi:10.1002/2013JC009502, 2014.

Kilias, E., Kattner, G., Wolf, C. and Metfies, K.: A molecular survey of protist diversity through the central Arctic Ocean, Polar Biol., 37(9), 1271–1287, doi:10.1007/s00300-014-1519-5, 2014.

Kinnard, C., Zdanowicz, C. M., Fisher, D. A., Isaksson, E., Vernal, A. De and Thompson, L. G.: Reconstructed changes in Arctic sea ice over the past 1,450 years, Nature, 479(7374), 509–512, doi:10.1038/nature10581, 2011.

Kiorboe, T. and Hansen, J. L. S.: Phytoplankton aggregate formation: observations of patterns and mechanisms of cell sticking and the significance of exopolymeric material, J. Plankton Res., 15(9), 993–1018, doi:10.1093/plankt/15.9.993, 1993.

Klimant, I., Meyer, V., Kühl, M. and Kuhl, M.: Fiber-Optic oxygen microsensors, a new tool in aquatic biology, Limnol. Oceanogr., 40(6), 1159–1165, doi:10.4319/lo.1995.40.6.1159, 1995.

Klunder, M. B., Bauch, D., Laan, P., de Baar, H. J. W., van Heuven, S., Ober, S., Baar, H. J. W. De and Heuven, S. Van: Dissolved iron in the Arctic shelf seas and surface waters of the central Arctic Ocean: Impact of Arctic river water and ice-melt, J. Geophys. Res., 117(C1), C01027, doi:10.1029/2011JC007133, 2012.

Korhonen, M., Rudels, B., Marnela, M., Wisotzki, A. and Zhao, J.: Time and space variability of freshwater content, heat content and seasonal ice melt in the Arctic Ocean from 1991 to 2011, Ocean Sci., 9(6), 1015–1055, doi:10.5194/os-9-1015-2013, 2013.

Kraft, A., Nöthig, E.-M., Bauerfeind, E., Wildish, D. J., Pohle, G. W., Bathmann, U. V, Beszczynska-Möller, A. and Klages, M.: First evidence of reproductive success in a southern invader indicates possible community shifts among Arctic zooplankton, Mar. Ecol. Prog. Ser., 493, 291–296, doi:10.3354/meps10507, 2013.

Lalande, C., Bélanger, S. and Fortier, L.: Impact of a decreasing sea ice cover on the vertical export of particulate organic carbon in the northern Laptev Sea, Siberian Arctic Ocean, Geophys. Res. Lett., 36(21), L21604, doi:10.1029/2009GL040570, 2009.

Lalande, C., Nöthig, E.-M., Somavilla, R., Bauerfeind, E., Schevschenko, V., Okolodkov, Y. and Shevshenko, V.: Variability in under-ice export fluxes of biogenic matter in the Arctic Ocean, Global Biogeochem. Cycles, 28, n/a–n/a, doi:10.1002/2013GB004735, 2014.

Laney, S. R., Krishfield, R. a., Toole, J. M., Hammar, T. R., Ashjian, C. J. and Timmermans, M.-L.: Assessing algal biomass and bio-optical distributions in perennially ice-covered polar ocean ecosystems, Polar Sci., 8(2), 73–85, doi:10.1016/j.polar.2013.12.003, 2014.

Langlois, R. J., Hümmer, D. and LaRoche, J.: Abundances and distributions of the dominant nifH phylotypes in the Northern Atlantic Ocean., Appl. Environ. Microbiol., 74(6), 1922–31, doi:10.1128/AEM.01720-07, 2008.

LaRoche, J. and Breitbarth, E.: Importance of the diazotrophs as a source of new nitrogen in the ocean, J. Sea Res., 53(1-2), 67–91, doi:10.1016/j.seares.2004.05.005, 2005.

Lasserre, F. and Pelletier, S.: Polar super seaways? Maritime transport in the Arctic: an analysis of shipowners' intentions, J. Transp. Geogr., 19(6), 1465–1473, doi:10.1016/j.jtrangeo.2011.08.006, 2011.

Lee, S. H., McRoy, C. P. P., Joo, H. M., Gradinger, R., Cui, X., Yun, M. S., Chung, K. H., Choy, E. J., Son, S., Carmack, E. and Whitledge, T. E. TE: Holes in progressively thinning Arctic sea ice lead to new ice algae habitat, Oceanography, 24(3), 302–308, doi:10.5670/oceanog.2011.81, 2011.

Lee, S. H., Whitledge, T. E. and Kang, S.: Carbon uptake rates of sea ice algae and phytoplankton under different light intensities in a landfast sea ice zone, Barrow, Alaska, Arctic, 61(3), 281–291, 2008.

Legendre, L., Horner, R., Ackley, S. F., Dieckmann, G. S., Gulliksen, B., Hoshiai, T., Melnikov, I. A., Reeburgh, W. S., Spindler, M. and Sullivan, C. W.: Ecology of sea ice biota: 2. Global significance, Polar Biol., 12, 429 – 444, doi:10.1007/BF00243113, 1992.

Lehtimaki, J., Moisander, P., Sivonen, K., Kononen, K., Moisander, P. I. A. and Sivonen, K.: Growth, nitrogen fixation and nodularin production by two baltic sea cyanobacteria., Appl. Environ. Microbiol., 63(5), 1647, 1997.

Lehto, N., Glud, R., Nordi, G., Zang, H. and Davison, W.: Anoxic microniches in marine sediments induced by aggregate settlement: Biogeochemical dynamics and implications., Biogeochemistry, doi:10.1007/s10533-014-9967-0, 2014.

Leu, E., Søreide, J. E. E., Hessen, D. O. O., Falk-Petersen, S. and Berge, J.: Consequences of changing sea-ice cover for primary and secondary producers in the European Arctic shelf seas: Timing, quantity, and quality., Prog. Oceanogr., 90(1-4), 18–32, doi:10.1016/j.pocean.2011.02.004, 2011.

Li, W. K. W., McLaughlin, F. A., Lovejoy, C. and Carmack, E. C.: Smallest algae thrive as the Arctic Ocean freshens., Science, 326, 539, doi:10.1126/science.1179798, 2009.

Lund-Hansen, L. C., Hawes, I., Sorrell, B. K. and Nielsen, M. H.: Removal of snow cover inhibits spring growth of Arctic ice algae through physiological and behavioral effects., Polar Biol., 37, 471–481, 2014.

MacDonald, G. M.: Global warming and the Arctic: a new world beyond the reach of the Grinnellian niche?, J. Exp. Biol., 213, 855–861, doi:10.1242/jeb.039511, 2010.

Maestrini, S. Y., Rochet, M., Legendre, L. and Demers, S.: Nutrient limitation of the bottom-ice microalgal biomass (Southeastern Hudson Bay, Canadian Arctic), Limnol. Oceanogr., 31(5), 969–982, 1986.

Markus, T., Stroeve, J. C. and Miller, J.: Recent changes in Arctic sea ice melt onset, freezeup, and melt season length., J. Geophys. Res., 114(C12), C12024, doi:10.1029/2009JC005436, 2009.

Martin, J., Tremblay, J.-É. and Price, N. M.: Nutritive and photosynthetic ecology of subsurface chlorophyll maxima in the Canadian Arctic waters, Biogeosciences Discuss., 9, 6445–6488, doi:10.5194/bgd-9-6445-2012, 2012.

Maslanik, J. A., Fowler, C., Stroeve, J., Drobot, S., Zwally, J., Yi, D. and Emery, W.: A younger, thinner Arctic ice cover: increased potential for rapid, extensive sea-ice loss, Geophys. Res. Lett., 34, L24501, doi:10.1029/2007GL032043, 2007.

Mathis, J. T., Pickart, R. S., Byrne, R. H., McNeil, C. L., Moore, G. W. K., Juranek, L. W., Liu, X., Ma, J., Easley, R. a., Elliot, M. M., Cross, J. N., Reisdorph, S. C., Bahr, F., Morison, J., Lichendorf, T. and Feely, R. a.: Storm-induced upwelling of high pCO_2 waters onto the continental shelf of the western Arctic Ocean and implications for carbonate mineral saturation states, Geophys. Res. Lett., 39, L07606, doi:10.1029/2012GL051574, 2012.

Matrai, P. and Apollonio, S.: New estimates of microalgae production based upon nitrate reductions under sea ice in Canadian shelf seas and the Canada Basin of the Arctic Ocean, Mar. Biol., 160(6), 1297–1309, doi:10.1007/s00227-013-2181-0, 2013.

Matrai, P., Olson, E., Suttles, S., Hill, V. J., Codispoti, L. A., Light, B., Steele, M., Boothbay, E., Hole, W. and Sciences, A.: Synthesis of primary production in the Arctic Ocean: I . Surface waters, Prog. Oceanogr., 110, 93–106, doi:10.1016/j.pocean.2012.11.004, 2013.

McGuire, D. A., Anderson, L. G., Christensen, T. R., Dallimore, S., Guo, L., Hayes, D. J., Heimann, M., Lorenson, T. D., Macdonald, R. W. and Roulet, N.: Sensitivity of the carbon cycle in the Arctic to climate change, Ecol. Monogr., 79(4), 523–555, 2009.

McGuire, D. A., Chapin, F. S., Walsh, J. E. and Wirth, C.: Integrated regional changes in Arctic climate feedbacks: implications for the global climate system, Annu. Rev. Environ. Resour., 31, 61–91, doi:10.1146/annurev.energy.31.020105.100253, 2006.

Melnikov, I. A.: The Arctic sea ice ecosystem, Gordon and Breach Science Publishers, Amsterdam., 1977.

Melnikov, I. and Bondarchuk, L. L.: Ecology of mass accumulations of colonial diatom algae under drifting Arctic ice., Oceanology, 27(2), 233–236, 1987.

Michel, C., Bluhm, B., Gallucci, V., Gaston, A. J., Gordillo, F. J. L., Gradinger, R., Hopcroft, R., Jensen, N., Mustonen, T., Niemi, A. and Nielsen, T. G.: Biodiversity of Arctic marine ecosystems and responses to climate change, Biodiversity, 13(3-4), 200–214, 2012.

Michel, C., Ingram, R. and Harris, L.: Variability in oceanographic and ecological processes in the Canadian Arctic Archipelago, Prog. Oceanogr., 71, 379–401, doi:10.1016/j.pocean.2006.09.006, 2006.

Michel, C., Legendre, L., Demers, S. and Therriault, J.-C.: Photoadaptation of sea-ice microalgae in springtime: photosynthesis and carboxylating enzymes, Mar. Ecol. Prog. Ser., 50, 177–185, 1988.

Miller, G. H., Lehman, S. J., Refsnider, K. a., Southon, J. R. and Zhong, Y.: Unprecedented recent summer warmth in Arctic Canada, Geophys. Res. Lett., 40(21), 5745–5751, doi:10.1002/2013GL057188, 2013.

Mock, T. and Gradinger, R.: Determination of Arctic ice algal production with a new *in situ* incubation technique, Mar. Ecol. Prog. Ser., 177, 15–26, doi:10.3354/meps177015, 1999.

Mohr, W., Grosskopf, T., Wallace, D. W. R. and LaRoche, J.: Methodological underestimation of oceanic nitrogen fixation rates., PLoS One, 5(9), e12583, doi:10.1371/journal.pone.0012583, 2010.

Moisander, P. H., Morrison, A. E., Ward, B. B., Jenkins, B. D. and Zehr, J. P.: Spatial-temporal variability in diazotroph assemblages in Chesapeake Bay using an oligonucleotide *nifH* microarray., Environ. Microbiol., 9(7), 1823–35, doi:10.1111/j.1462-2920.2007.01304.x, 2007.

Moore, C. M., Mills, M. M., Arrigo, K. R., Berman-Frank, I., Bopp, L., Boyd, P. ., Galbraith, E. D., Geider, R. J., Guieu, C., Jaccard, S. L., Jickells, T. D., LaRoche, J., Lenton, T. M., Mahowald, N. M., Marañón, E., Marinov, I., Moore, J. K., Nakatsuka, T., Oschlies, A., Saito, M. A., Thingstad, T. F., Tsuda, A. and Ulloa, O.: Processes and patterns of oceanic nutrient limitation, Nat. Geosci., 6, 701–710, doi:10.1038/ngeo1765, 2013.

Moore, S. E. and Huntington, H. P.: Arctic marine mammals and climate change: impacts and resilience., Ecol. Appl., 18(2), s157–165, 2008.

Mundy, C. J., Ehn, J. K., Barber, D. G. and Michel, C.: Influence of snow cover and algae on the spectral dependence of transmitted irradiance through Arctic landfast first-year sea ice, J. Geophys. Res., 112, C03007, doi:10.1029/2006JC003683, 2007.

Mundy, C., Michel, G., Jens, K. E., Claude, B., Poulin, M., Alou, E., Roy, S., Hop, H., Lessard, S., Papakyriakou, T. N., Barber, D. G. and Stewart, J.: Characteristics of two distinct high-light acclimated algal communities during advanced stages of sea ice melt, Polar Biol., 34, 1869–1886, doi:10.1007/s00300-011-0998-x, 2011.

Nicolaus, M. and Katlein, C.: Mapping radiation transfer through sea ice using a remotely operated vehicle (ROV), Cryosph., 7(3), 763–777, doi:10.5194/tc-7-763-2013, 2013.

Nicolaus, M., Katlein, C., Maslanik, J. and Hendricks, S.: Changes in Arctic sea ice result in increasing light transmittance and absorption, Geophys. Res. Lett., 39(L24501), 1–6, doi:10.1029/2012GL053738, 2012.

Nishino, S., Kikuchi, T., Yamamoto-Kawai, M., Kawaguchi, Y., Hirawake, T. and Itoh, M.: Enhancement/reduction of biological pump depends on ocean circulation in the sea-ice reduction regions of the Arctic Ocean, J. Oceanogr., 67(3), 305–314, doi:10.1007/s10872-011-0030-7, 2011.

Olli, K., Wassmann, P., Reigstad, M., Ratkova, T. N., Arashkevich, E., Pasternak, A., Matrai, P. a., Knulst, J., Tranvik, L., Klais, R. and Jacobsen, A.: The fate of production in the central Arctic Ocean – top–down regulation by zooplankton expatriates?, Prog. Oceanogr., 72, 84–113, doi:10.1016/j.pocean.2006.08.002, 2007.

Pabi, S., van Dijken, G. L. and Arrigo, K. R.: Primary production in the Arctic Ocean, 1998–2006, J. Geophys. Res., 113(C8), C08005, doi:10.1029/2007JC004578, 2008.

Palmer, M. A., Saenz, B. T. and Arrigo, K. R.: Impacts of sea ice retreat, thinning, and melt-pond proliferation on the summer phytoplankton bloom in the Chukchi Sea, Arctic Ocean, Deep Sea Res. Part II Top. Stud. Oceanogr., 1–20, doi:10.1016/j.dsr2.2014.03.016, 2014.

Parkinson, C. L. and Comiso, J. C.: On the 2012 record low Arctic sea ice cover: Combined impact of preconditioning and an August storm, Geophys. Res. Lett., 40, 1356–1361, doi:10.1002/grl.50349, 2013.

Perovich, D. K.: The optical properties of sea ice, Cold Reg. Res. Eng. Lab., Monograph, 1–31, 1996.

Peterson, B. J., Holmes, R. M., McClelland, J. W., Vörösmarty, C. J., Lammers, R. B., Shiklomanov, A. I., Shiklomanov, I. a and Rahmstorf, S.: Increasing river discharge to the Arctic Ocean., Science, 298, 2171–3, doi:10.1126/science.1077445, 2002.

Pfirman, S. L., Colony, R., Niirnberg, D., Eicken, H. and Rigor, I.: Reconstructing the origin and trajectory of drifting Arctic sea ice., J. Geophys. Res., 102(c6), 575–586, 1997.

Piepenburg, D.: Recent research on Arctic benthos: common notions need to be revised, Polar Biol., 28(10), 733–755, doi:10.1007/s00300-005-0013-5, 2005.

Platt, T., Gallegos, C. L. and Harrison, W. G.: Photoinhibition of photosynthesis in natural assemblages of marine phytoplankton., J. Mar. Res., 38, 687–701, 1980.

Platt, T. and Sathyendranath, S.: Modelling primary production, , 1–276, 2007.

Polashenski, C., Perovich, D. and Courville, Z.: The mechanisms of sea ice melt pond formation and evolution, J. Geophys. Res., 117(C01001), 1–23, doi:10.1029/2011JC007231, 2012.

Poltermann, M.: Arctic sea ice as feeding ground for amphipods - food sources and strategies, Polar Biol., 24, 89–96, doi:10.1007/s003000000177, 2001.

Polyakov, I. V., Timokhov, L. a., Alexeev, V. a., Bacon, S., Dmitrenko, I. a., Fortier, L., Frolov, I. E., Gascard, J.-C., Hansen, E., Ivanov, V. V., Laxon, S., Mauritzen, C., Perovich, D., Shimada, K., Simmons, H. L., Sokolov, V. T., Steele, M. and Toole, J.: Arctic Ocean warming contributes to reduced polar ice cap, J. Phys. Oceanogr., 40(12), 2743–2756, doi:10.1175/2010JPO4339.1, 2010.

Polyakov, I. V., Walsh, J. E. and Kwok, R.: Recent changes of Arctic multiyear sea ice coverage and the likely causes, Bull. Am. Meteorol. Soc., 93(2), 145–151, doi:10.1175/BAMS-D-11-00070.1, 2012.

Popova, E. E., Yool, a., Aksenov, Y. and Coward, a. C.: Role of advection in Arctic Ocean lower trophic dynamics: A modeling perspective, J. Geophys. Res. Ocean., 118(3), 1571–1586, doi:10.1002/jgrc.20126, 2013.

Popova, E. E., Yool, A., Aksenov, Y., Coward, A. C. and Anderson, T. R.: Regional variability of acidification in the Arctic: a sea of contrasts, Biogeosciences, 11(2), 293–308, doi:10.5194/bg-11-293-2014, 2014.

Popova, E. E., Yool, A., Coward, A. C., Aksenov, Y. K., Alderson, S. G., de Cuevas, B. a. and Anderson, T. R.: Control of primary production in the Arctic by nutrients and light: insights from

a high resolution ocean general circulation model, Biogeosciences Discuss., 7(4), 5557–5620, doi:10.5194/bgd-7-5557-2010, 2010.

Popova, E. E., Yool, A., Coward, A. C., Dupont, F., Deal, C., Elliott, S., Hunke, E., Jin, M., Steele, M. and Zhang, J.: What controls primary production in the Arctic Ocean? Results from an intercomparison of five general circulation models with biogeochemistry, J. Geophys. Res., 117(C00D12), 1–16, doi:10.1029/2011JC007112, 2012.

Poulin, M., Underwood, G. J. C. and Michel, C.: Sub-ice colonial *Melosira arctica* in Arctic first-year ice, Diatom Res., 29(1), 1–9, doi:10.1080/0269249X.2013.877085, 2014.

Quillfeldt, C. Von, Hegseth, E. N., Sakshaug, E., Johnsen, G. and Syvertsen, E. E.: Ice algae, in Ecosystem Barents Sea, edited by E. Sakshaug, G. Johnsen, and K. M. Kovacs, pp. 285–302, Tapir Aacademic Press, Trondheim, Norway., 2009.

Rabe, B., Karcher, M., Schauer, U., Toole, A. J. M., Krishfield, R. A., Pisarev, S., Kauker, F., Gerdes, R. and Kikuchi, T.: An assessment of Arctic Ocean freshwater content changes from the 1990s to the 2006–2008 period., Deep Sea Res. Part I, 58(2), 173–185, 2011.

Redfield, A. C.: The biological control of chemical factors in the environment, Am. Sci., 46(3), 205–221, 1958.

Reid, P., Johns, D., Edwards, M., Starr, M., Poulins, M. and Snoeijs, P.: A biological consequence of reducing Arctic ice cover: arrival of the Pacific diatom *Neodenticula seminae* in the North Atlantic for the first time in 800 000 years., Glob. Chang. Biol., 13, 1910–1921, 2007.

Reist, J. D., Wrona, F. J., Prowse, T. D., Power, M., Dempson, J. B., Beamish, R. J., King, J. R., Carmichael, T. J. and Sawatzky, C. D.: General effects of climate change on Arctic fishes and fish populations., AMBIO A J. Hum. Environ., 35(7), 370–80, doi:10.1579/0044-7447(2006)35[370:GEOCCO]2.0.CO;2, 2006.

Renner, A. H. H., Gerland, S., Haas, C., Spreen, G., Beckers, J. F., Hansen, E., Nicolaus, M. and Goodwin, H.: Evidence of Arctic sea ice thinning from direct observations, Geophys. Res. Lett., 41, doi:10.1002/2014GL060369, 2014.

Riebesell, U. and Tortell, P. D.: Effects of ocean acidification on pelagic organisms and ecosystems. ., edited by J. Gattuso and L. Hanson, Oxford University Press, Oxford., 2011.

Rösel, A. and Kaleschke, L.: Exceptional melt pond occurrence in the years 2007 and 2011 on the Arctic sea ice revealed from MODIS satellite data, J. Geophys. Res., 117(C05018), 1–8, doi:10.1029/2011JC007869, 2012.

Rösel, A., Kaleschke, L. and Birnbaum, G.: Melt ponds on Arctic sea ice determined from MODIS satellite data using an artificial neural network, Cryosph. Discuss., 5, 2991–3024, doi:10.5194/tcd-5-2991-2011, 2011.

Rothrock, D. A., Yu, Y. and Maykut, G. A.: Thinning of the Arctic sea-ice cover, Geophys. Res. Lett., 26(23), 3469–3472, doi:10.1029/1999GL010863, 1999.

Rudels, B.: The thermohaline circulation of the Arctic Ocean and the Greenland Sea, Philos. Trans. Phys. Sci. Eng., 352(1699), 287–299, 1995.

Rudels, B.: Arctic Ocean circulation and variability – advection and external forcing encounter constraints and local processes, Ocean Sci., 8, 261–286, doi:10.5194/os-8-261-2012, 2012.

Rudels, B., Anderson, L., Eriksson, P., Fahrbach, E., Jakobsson, M., Jones, E. P., Melling, H., Prinsenberg, S., Schauer, U. and Yao, T.: Observations in the ocean, in Arctic climate change: The ACSYS decade and beyond, edited by P. Lemke and H. W. Jacobi, p. 82, Springer Science + Business Media B.V., 2012.

Rudels, B., Jones, E. P., Schauer, U. and Eriksson, P.: Atlantic sources of the Arctic Ocean surface and halocline waters, Polar Res., 23(2), 181–208, doi:10.1111/j.1751-8369.2004.tb00007.x, 2004.

Rysgaard, S., Glud, R. N., Risgaard-Petersen, N. and Dalsgaard, T.: Denitrification and anammox activity in Arctic marine sediments, Limnol. Oceanogr., 49(5), 1493–1502, doi:10.4319/lo.2004.49.5.1493, 2004.

Sakshaug, E. and Slagstad, D.: Light and productivity of phytoplankton in polar marine ecosystems: a physiological view, in Proceedings of the Pro Mare Symposium on Polar Marine Ecology, vol. 1906, edited by E. Sakshaug, C. Hopkins, and N. Oritsland, pp. 69–85, PolarResearch, Trondheim., 1991.

Sakshaug, E., Stein, R. and Macdonald, R. W.: Primary and secondary production in the Arctic Seas., in The Organic Carbon Cycle in the Arctic Ocean, edited by R. Stein and R. W. Macdonald, pp. 57–82, Springer., 2004.

Dos Santos, P. C., Fang, Z., Mason, S. W., Setubal, J. C. and Dixon, R.: Distribution of nitrogen fixation and nitrogenase-like sequences amongst microbial genomes., BMC Genomics, 13, 162, doi:10.1186/1471-2164-13-162, 2012.

Sarmiento, J. L., Highes, T. M. C., Stouffer, R. J. and Manabe, S.: Simulated response of the ocean carbon cycle to anthropogenic climate warming, Nature, 393, 245–249, 1998.

Seuthe, L., Rokkan Iversen, K. and Narcy, F.: Microbial processes in a high-latitude fjord (Kongsfjorden, Svalbard): II. Ciliates and dinoflagellates, Polar Biol., 34(5), 751–766, doi:10.1007/s00300-010-0930-9, 2010.

Shakhova, N., Semiletov, I., Salyuk, A., Yusupov, V., Kosmach, D. and Gustafsson, O.: Extensive methane venting to the atmosphere from sediments of the East Siberian Arctic Shelf., Science, 327, 1246–1250, doi:10.1126/science.1182221, 2010.

Sherr, E. B., Sherr, B. F., Wheeler, P. A. and Thompson, K.: Temporal and spatial variation in stocks of autotrophic and heterotrophic microbes in the upper water column of the central Arctic Ocean, Deep Sea Res. Part I Oceanogr. Res. Pap., 50, 557–571, doi:10.1016/S0967-0637(03)00031-1, 2003.

Slagstad, D., Ellingsen, I. H. H. and Wassmann, P.: Evaluating primary and secondary production in an Arctic Ocean void of summer sea ice: an experimental simulation approach, Prog. Oceanogr., 90(1-4), 117–131, doi:10.1016/j.pocean.2011.02.009, 2011.

Smith, R. E. H. and Herman, A. W.: Productivity of sea ice algae: *In situ* vs. incubator methods, J. Mar. Syst., 2, 97–110, 1991.

Smyth, T. J.: Time series of coccolithophore activity in the Barents Sea, from twenty years of satellite imagery, Geophys. Res. Lett., 31(11), L11302, doi:10.1029/2004GL019735, 2004.

Soltwedel, T., Bauerfeind, Eddy Bergmann, M., Budaeva, N., Hoste, E., Jaeckisch, N., Von Juterzenka, K., Matthiessen, J., Mokievsky, V., Nöthig, E.-M., Quéric, N.-V., Sablotny, B., Sauter, E., Schewe, I., Urban-Malinga, B., Wegner, J., Wlodarska-Kowalczuk, M. and Klages, M.: HAUSGARTEN: Multidisciplinary investigations at a deep-sea, long-term observatory in the Arctic Ocean., Oceanography, 18(3), 46–61, doi:10.5670/oceanog.2005.24, 2005.

Soreide, J., Leu, E., Berge, J., Graeve, M., Falk-Petersen, S. and Søreide, J. E.: Timing of blooms, algal food quality and *Calanus glacialis* reproduction and growth in a changing Arctic., Glob. Chang. Biol., 16, 3154–3163, doi:10.1111/j.1365-2486.2010.02175.x, 2010.

Spilling, K., Tamminen, T., Andersen, T. and Kremp, A.: Nutrient kinetics modeled from time series of substrate depletion and growth: dissolved silicate uptake of Baltic Sea spring diatoms, Mar. Biol., 157(2), 427–436, doi:10.1007/s00227-009-1329-4, 2010.

Steemann Nielsen, E.: The use of radio-active carbon (C^{14}) for measuring organic production in the sea ., J. Cons. Int. Explor. Mer., 18, 117–140, 1952.

Stein, R. and Macdonald, R. W.: The organic carbon cycle in the Arctic Ocean, 1st ed., Springer-Verlag Berlin Heidelberg GmbH., 2004.

Steinacher, M., Joos, F., Fröhlicher, T. L., Plattner, G.-K. and Doney, S. C.: Imminent ocean acidification in the Arctic projected with the NCAR global coupled carbon cycle-climate model, Biogeosciences, 6, 515–533, 2009.

Stroeve, J. C., Serreze, M. C., Holland, M. M., Kay, J. E., Malanik, J. and Barrett, A. P.: The Arctic's rapidly shrinking sea ice cover: a research synthesis, Clim. Change, 110, 1005–1027, doi:10.1007/s10584-011-0101-1, 2012.

Suggett, D. J., Oxborough, K., Baker, N. R., MacIntyre, H. L., Kana, T. M. and Geider, R. J.: Fast repetition rate and pulse amplitude modulation chlorophyll *a* fluorescence measurements for assessment of photosynthetic electron transport in marine phytoplankton, Eur. J. Phycol., 38, 371–384, doi:10.1080/09670260310001612655, 2003.

Syvertsen, E. E.: Ice algae in the Barents Sea: types of assemblages, origin, fate and role in the ice-edge phytoplankton bloom, Proc. Pro Mare Symp. Polar Mar. Ecol., (1961), 277–287, 1991.

Tamelander, T., Reigstad, M., Hop, H. and Ratkova, T.: Ice algal assemblages and vertical export of organic matter from sea ice in the Barents Sea and Nansen Basin (Arctic Ocean), Polar Biol., 32, 1261–1273, doi:10.1007/s00300-009-0622-5, 2009.

Tamelander, T., Reigstad, M., Olli, K., Slagstad, D. and Wassmann, P.: New production regulates export stoichiometry in the ocean., PLoS One, 8(1), e54027, doi:10.1371/journal.pone.0054027, 2013.

Taylor, R. L., Semeniuk, D. M., Payne, C. D., Zhou, J., Tremblay, J.-É., Cullen, J. T. and Maldonado, M. T.: Colimitation by light, nitrate, and iron in the Beaufort Sea in late summer, J. Geophys. Res. Ocean., 118, 3260–3277, doi:10.1002/jgrc.20244, 2013.

Tedesco, L., Vichi, M. and Thomas, D. N.: Process studies on the ecological coupling between sea ice algae and phytoplankton, Ecol. Modell., 226, 120–138, doi:10.1016/j.ecolmodel.2011.11.011, 2012.

Telling, J., Anesio, A. M., Tranter, M., Irvine-Fynn, T., Hodson, A., Butler, C. and Wadham, J.: Nitrogen fixation on Arctic glaciers, Svalbard, J. Geophys. Res., 116, G03039, doi:10.1029/2010JG001632, 2011.

Thomas, D. N. and Dieckmann, G. S.: Sea Ice, Second., edited by D. N. Thomas and G. S. Dieckmann, Wiley-Blackwell, West Sussex., 2010.

Tilman, D., Kilham, S. S. and Kilham, P.: Phytoplankton community ecology: The Role of Limiting Nutrients, Annu. Rev. Ecol. Syst., 13, 349–372, 1982.

Torres-Valdés, S., Tsubouchi, T., Bacon, S., Naveira-Garabato, A. C., Sanders, R., McLaughlin, F. a., Petrie, B., Kattner, G., Azetsu-Scott, K. and Whitledge, T. E.: Export of nutrients from the Arctic Ocean, J. Geophys. Res. Ocean., 118(4), 1625–1644, doi:10.1002/jgrc.20063, 2013.

Tremblay, J.-É. and Gagnon, J.: The effects of irradiance and nutrient supply on the productivity of Arctic waters: a perspective on climate change, in Influence of climate change on the Changing Arctic and sub-arctic conditions, edited by J. Nihoul and A. Kostianoy, pp. 73–93, Springer Science + Business Media B.V., 2009.

Tremblay, J.-É., Simpson, K., Martin, J., Miller, L., Gratton, Y., Barber, D. and Price, N. M.: Vertical stability and the annual dynamics of nutrients and chlorophyll fluorescence in the coastal, southeast Beaufort Sea, J. Geophys. Res., 113(C7), C07S90, doi:10.1029/2007JC004547, 2008.

Turk, K. A., Rees, A. P., Zehr, J. P., Pereira, N., Swift, P., Shelley, R., Lohan, M., Woodward, E. M. S. and Gilbert, J.: Nitrogen fixation and nitrogenase (*nifH*) expression in tropical waters of the eastern North Atlantic., ISME J., 5, 1201–1212, doi:10.1038/ismej.2010.205, 2011.

Vancoppenolle, M., Bopp, L., Madec, G., Dunne, J., Ilyina, T., Halloran, P. R. and Steiner, N.: Future Arctic Ocean primary productivity from CMIP5 simulations: Uncertain outcome, but consistent mechanisms, Global Biogeochem. Cycles, 27, 1–15, doi:10.1002/gbc.20055, 2013.

Vaquer-Sunyer, R., Duarte, C. M., Santiago, R., Wassmann, P. and Reigstad, M.: Experimental evaluation of planktonic respiration response to warming in the European Arctic Sector, Polar Biol., 33, 1661–1671, doi:10.1007/s00300-010-0788-x, 2010.

Vincent, W. F.: Cyanobacterial dominance in the polar regions., in The ecology of cyanobacteria: their diversity in space and time, edited by B. A. Whitton and M. Potts, pp. 321–340, Kluwer Acad., Dordrecht, Netherlands., 2000.

De Vooys, C. G. N.: Primary production in aquatic environments, in The global carbon cycle, edited by B. Bolin, pp. 13, 259, SCOPE., 1979.

Waite, A. M., Thompson, P. a. and Harrison, P. J.: Does energy control the sinking rates of marine diatoms?, Limnol. Oceanogr., 37(3), 468–477, doi:10.4319/lo.1992.37.3.0468, 1992.

Wang, M. and Overland, J. E.: A sea ice free summer Arctic within 30 years: An update from CMIP5 models, Geophys. Res. Lett., 39(L18501), 1–6, doi:10.1029/2012GL052868, 2012.

Ward, B. A., Dutkiewicz, S., Moore, C. M. and Follows, M. J.: Iron, phosphorus, and nitrogen supply ratios define the biogeography of nitrogen fixation, Limnol. Oceanogr., 58(6), 2059–2075, doi:10.4319/lo.2013.58.6.2059, 2013.

Wassmann, P.: Retention versus export food chains: processes controlling sinking loss from marine pelagic systems, Hydrobiologia, 363, 29–57, 1998.

Wassmann, P.: Arctic marine ecosystems in an era of rapid climate change, Prog. Oceanogr., 90(1-4), 1–17, doi:10.1016/j.pocean.2011.02.002, 2011.

Wassmann, P., Bauerfeind, E., Fortier, M., Fukuchi, M., Hargrave, B., Moran, B., Noji, T., Nöthig, E., Olli, K., Peinert, R., Sasaki, H. and Shevchenko, V.: Particulate organic carbon flux to the Arctic Ocean sea floor., in The organic carbon cycle in the Arctic Ocean, edited by R. Stein and R. MacDonald, pp. 101–138, Springer Verlag, Berlin Heidelberg., 2004.

Wassmann, P., Duarte, C. M., Agustí, S. and Sejr, M. K.: Footprints of climate change in the Arctic marine ecosystem, Glob. Chang. Biol., 17(2), 1235–1249, doi:10.1111/j.1365-2486.2010.02311.x, 2011.

Wassmann, P. and Reigstad, M.: Future Arctic Ocean seasonal ice zones and implications for pelagic-benthic coupling., Oceanography, 24(3), 220–231, 2011.

Watanabe, E., Onodera, J., Harada, N., Honda, M. C., Kimoto, K., Kikuchi, T., Nishino, S., Matsuno, K., Yamaguchi, A., Ishida, A. and Kishi, M. J.: Enhanced role of eddies in the Arctic marine biological pump., Nature, 5, 3950, doi:10.1038/ncomms4950, 2014.

Webster, M. A., Rigor, I. G., Nghiem, S. V., Kurtz, N. T., Farrell, S. L., Perovich, D. K. and Sturm, M.: Interdecadal changes in snow depth on Arctic sea ice, J. Geophys. Res. Ocean., n/a–n/a, doi:10.1002/2014JC009985, 2014.

Wegner, C., Hölemann, J. A., Dmitrenko, I., Kirillov, S. and Kassens, H.: Seasonal variations in Arctic sediment dynamics—Evidence from 1-year records in the Laptev Sea (Siberian Arctic), Glob. Planet Chang., 48(1-3), 126–140, 2005.

Westberry, T. K. and Behrenfeld, M. J.: Oceanic net primary production, in Biophysical applications of satellite remote sensing, edited by J. M. Hanes, pp. 205–230, Springer Berlin Heidelberg, Berlin, Heidelberg., 2014.

Wheeler, P. A., Gosselin, M., Sherr, E., Thibault, D., Kirchman, D. L., Benner, R. and Whitledge, T. E.: Active cycling or organic carbon in the central Arctic Ocean, Nature, 380, 697–699, doi:10.1038/380697a0, 1996.

Winkler, L.: Die Bestimmung des in Wasser Gelösten Sauerstoffes., Berichte der Dtsch. Chem. Gesellschaft, 21, 2843–2855, 1888.

Yamamoto-Kawai, M., McLaughlin, F. A., Carmack, E. C., Nishino, S., Shimada, K. and Kurita, N.: Surface freshening of the Canada Basin, 2003–2007: River runoff versus sea ice meltwater., J. Geophys. Res., 114, C00A05, doi:10.1029/2008JC005000, 2009.

Acknowledgements

I would like to thank:

Antje Boetius for giving me the opportunity to work on this fascinating topic and for all her support (also finantial) through the last years. I feel privileged to have taken part in some of the recent Arctic discoveries as part of your team. Thanks for taking me along and encouraging me to improve constantly.

Anya Waite for accepting being the second reviewer last minute and for jumping in with so much enthusiasm and refreshing ideas.

Kai Bischof and Bernhard Fuchs for being part of my defense committee and for all the good advices along the way.

Ilka Peeken, Philipp Assmy and Gerhard Dieckmann for being part of my thesis committee, and for being there for me whenever I had something to ask.

Victor Smetacek for all those enlightening conversations that we have maintained since we know each other. My brain expands every time I talk with you or read one of your papers.

Ronnie Glud for having always time for me and for giving me excellent advice since the beginning.

Eva-Maria Nöthig, Catherine Lalande, Hauke Flores, Estelle Kilias and Kristin Hardge for fruitful discussions at the AWI.

Erika Allhusen and Christiane Uhlig for all those very useful conversations and for help with sampling and much more.

Polarstern captains and crew during my two expeditions to the Arctic. Thanks for bringing us to the North Pole. Thanks as well to all the scientists with whom I shared that wonderful experience. Especially to Kristin Hänselmann, Eva Kirscheman, Heidi Louise Sorensen, Ben Lange, Anique Stecher, Raquel Somavilla, Adam Ulfsbo, Elisabeth Helmke and Ellen Damm.

The Habitat Group for all those nice seminars, lunches and parties. I can hardly imagine a better group to work in. Special thanks to Mirja Meiners, Rafael Stiens, Wiebke Rentzsch, Erika Weiz-Bersch, Volker Asendorf, Axel Nordhausen for their technical support; and Patrick Meyer for designing the photosynthesis versus irradiance incubator.

Christina Bienhold, Marianne Jacob and Josephine Rapp for reading previous versions of this thesis and for keeping me sane through the process of writing.

Janine Felden for all her support with PANGAEA related issues and much more.

Pier Luigi Buttigieg for help with plots, statistics and vital matters in general.

Juliane Wippler, Viola Krukenberg, Petra Pjevac, Liz Robertson, Mira Okshevsky, Julia Schnetzer and Olga Matantseva for being the best girls of the best Marmic Class ever. Special thanks to Amandine Nunes-Jorge and Anna Klindworth for joining this fabulous group of girls.

Dorothee Kottmeier and Katy Hoffmann for coming to Bremen and becoming such an important part of my life.

Hannah Brocke for being a great office mate.

Elmar Prüsse, Stefan Thiele, Ivo Kostadinov, Philipp Hach and Andreas Krupke for being the best MPI boys, not only dancing.

Kendra Turk-Kubo, Mary Hogan, Brandon Carter and all the Zehr Lab in Santa Cruz, California, for making my stay there not only scientifically successful but also a great experience.

Concha Pinedo and Victor de Lorenzo, for being key stones in my path to this degree.

Emilio Marañón for all those helpful discussions and nice chats in Vigo and around the world.

Eva Serrano for being my favorite biologist outside Germany. For sharing your passion for biology with me since the beginning.

Christian Katlein for everything. Because I couldn´t have found a better match for me, both scientifically and personally speaking. Thanks for your patience and for keeping me warm in the cold Arctic.

My family, mama Lola, papi Jose Manuel and little brother Manu for letting me go but giving me always enough reasons to come back. Nada de lo que está aquí escrito habría sido posible sin vuestro apoyo y vuestro cariño en cada paso del camino.

Poster and Oral Presentations

Poster: "Central Arctic primary production and its limiting factors during the sea ice minimum extent record year 2012" AWI PhD Days. Helgoland, Germany. May 2014
Winner Best Poster Award

Oral presentation: "Buoyancy mechanisms and fate of algal aggregates below Arctic sea ice" IGS Sea ice in a changing environment symposium. Hobart, Tasmania. March 2014
Winner Best presentation Award

Oral presentation: "New estimates of primary productivity and its limiting factors in the Central Arctic" GHER Colloquium Primary Productivity in the Oceans. Liege, Belgium. May 2013
Invited speaker

Oral presentation and Poster: "Oxygen controls algal aggregates buoyancy below Arctic sea ice" Marmic Evaluation. May 2013

Oral presentation and Poster: "New estimates of primary productivity and its limiting factors in the Central Arctic" GRS-GRC Polar Marine Science. Ventura, California, USA. March 2013
Winner Poster Award

Poster: "Sea ice impact on Arctic and Antarctic ecosystems" Topic 1. PACES II. AWI Fachbeirat. February 2013

Oral presentation: "Primary Productivity in sea ice and waters of the central Arctic during summer 2011" IPY 2012: From knowledge to action. Montreal, Canada. April 2012

Poster: "Sea ice primary productivity in the Central Arctic Ocean during summer 2011." EGU 2012. Viena, Austria. April 2012

Poster: "Importance of Arctic melt ponds for primary productivity during summer 2011." Marmic Etelsen Retreat. February 2012

Cruise Participations

ARKXXVII/3 "IceArc 2012" RV Polarstern
Eurasian Basin Central Arctic (Tromsø-Bremerhaven) August-October 2012.
Sea Ice Biologist: Ice coring, melt pond and aggregate sampling, radioactive isotope incubations, PE curves, nutrient bioassays, filtration for molecular analysis and microscopy.

ARKXXVI/3 "TransArc 2011" RV Polarstern
Eurasian Basin Central Arctic (Tromsø-Bremerhaven) August-October 2011.
Sea Ice Biologist: Ice coring, filtration, radioactive isotope incubations and microscopy.

Teaching and tutoring

Supervisor Master Thesis "Bacterial diversity in sea ice, melt ponds, water under the ice and aggregates of the Arctic Ocean in summer 2012". Student: Josephine Rapp. September 2013-March 2014

Teaching assistant "Microbial Oceanography" practical course (Prof. Dr. Antje Boetius and Dr. Alban Ramette). MarMic Program. January 2012 & October 2013

Tutor of "Eukaryotic microbial ecology" lectures (Prof. Dr. Victor Smetacek). Marmic Program. May 2011, 2012 and 2014

Supervisor Lab Rotation "Bacterial diversity in arctic algal aggregates" Student: Josephine Rapp. June-July 2013

Supervisor Lab Rotation "Carbon budget of arctic melt pond diatoms" Student: Clara Martínez. June-July 2012

Supervisor Lab Rotation "Primary production in sea-ice algae" Student: Antje Stahl. June-July 2011

Erklärung

Hiermit erkläre ich, Mar Fernández Méndez, dass ich

1. die Arbeit selbstständig verfasst und geschrieben habe,
2. keine anderen als die von mir angegebenen Quellen und Hilfsmittel verwendet habe und
3. die den benutzten Werken wörtlich oder inhaltlich entnommenen Stellen als solche kenntlich gemacht habe und
4. die 3 vorgelegten Exemplare dieser Arbeit in identischer Ausführung abgegeben habe.

Ort, Datum Unterschrift